Unlocking the Total Synthesis of Dragocins A–C: Adventures with Unusual Marine Hybrid Metabolites

A thesis presented

by

Brendyn Paul Smith

to

The Scripps Research Institute Graduate

Program in partial fulfillment of the

requirements
for the degree of
Doctor of Philosophy
in the subject of

Chemistry

for

The Scripps Research Institute
La Jolla, California

February 2024

© Copyright 2024 by Brendyn P. Smith

All rights reserved.

Scripps Research

La Jolla, California
Jupiter, Florida

February 27, 2024

As members of the committee appointed to evaluate the thesis of **Brendyn Smith** we have read his thesis and found it to be acceptable without revision in partial fulfillment of The Scripps Research Institute's requirements for granting of the doctoral degree. Therefore, we the undersigned are satisfied that **Brendyn Smith** has met the requirements for the Doctorate of Philosophy Degree with respect to the written thesis, thesis presentation, and examination by this Committee.

Ryan A. Shenvi, Ph.D., Chair

Phil S. Baran, Ph.D., Advisor

Benjamin F. Cravatt, Ph.D.

Keary M. Engle, Ph.D.

Scott A. Snyder, Ph.D., External Examiner
University of Chicago

Office of Graduate Studies
10550 N. Torrey Pines Rd., TRY 10 • La Jolla, CA 92037 • p (858) 784-8469 • f (858) 784-2802
130 Scripps Way, 3B2 Jupiter, FL 33458 • p (561) 228-2370 • f (561) 228-3073
http://education.scripps.edu

Acknowledgements

Van: I have no words that can describe my gratitude and love for you. From the first time we met, it was very clear to me that you were the one I wanted to spend the rest of my life with. Your hard-working attitude, infectious enthusiasm for life and chemistry, and love for me certainly kept me moving forward during this very difficult and challenging couple of years. I would be beating a dead horse to say that I know we are both so tired of doing long distance (almost three years!) and are relieved to know the end (and the very beginning of our true life together) is literally right around the corner. It's going to be amazing working at Gilead together as process chemist and med chemist, which is really a dream come true for me. I can't wait to see what the future holds and am so excited for the future together!

Family: The past few years has certainly been the most difficult 4-5 years of my life so far. I know I should have reached out more often, especially during the more difficult times, but I know you all realize that it was not because I didn't care about you guys. I'm at a loss for words in my gratitude and love for all of you and am thankful for every moment I get to spend with you all. The good news is that I should have more time (and money to spend) on my hands in the future now that I'll be a corporate man! I love you all and am so proud of everyone in the family.

Phil: It was always my dream to make a natural product in the Baran lab. After almost 10 long years of education and training, I can finally say that I was able to do so. Not only that, but I learned more about myself and chemistry than I ever thought that I would. My experience in the Baran lab will never be forgotten and the skills I've learned here will surely aid me in many ways in my upcoming career as a drug hunter. Thank you for not

only allowing me to work on such a fascinating and challenging project, but also for allowing me to do a summer internship here in 2018, which surely paved the way for me to become a graduate student here.

Alex P: You turned into my little brother in the lab over the past few years. It was a real pleasure to have you around lab and you certainly made the time pass by more quickly. I truly admire your passion for chemistry and science and I think that will take you very far in your career. I will certainly miss everything that we were able to do together, but I'm sure we will be in close touch as time passes. I'm eager to see how your project pans out and I'm confident you'll be able to tackle anything that comes your way!

Nate: Thank you for your incredibly hard work that you put into the project. It was great to collaborate with you over the past year or so, and I realize how lucky I was to have you on the project. I know we didn't see eye to eye sometimes with regards to the project direction, but we always found a way to sort things through quickly and kept things moving forward. I commend you for your willingness to volunteer your time to help the lab out, even if it's not your job. Any company that hires you will be very lucky to have you. I wish you all the best in the future with regards to both your career and relationship with Melanie!

Pranali: I'd be lying if it wasn't a little disappointing that things didn't work out exactly how we had hoped in the Baran lab but I am happy to see you in an environment that leaves you smiling. I hope that all of the things I taught you will continue to aid you in your PhD and future!

Mike M: Your positive attitude and thoughtful nature surely helped me tackle the dragocins much faster than I otherwise would have without you by my side for a year or

so. I'll always cherish the time we got to spend together working on such deceptively simple natural products.

Dongmin: As Phil said in your defense, one way to describe you is "total-synthesis-with-a-smile!" Your uplifting spirit certainly kept me in the game while I was experiencing hardships with the dragocins. I'll miss coming into your office and bugging you!

Cheng: I'll never forget the years that we spent as office mates, giggling over plans to tackle our "next project" or "make some analogues" of our natural products. It was hard to see you go through the difficult times that you had to experience, but I am so glad that you now have what you deserved all along – hopefully peace and a nice paycheck.

Max: Our friendship certainly kept me going throughout grad school. Our seemingly weekly dinners were always something that I looked forward to and quite honestly miss a good deal. It's crazy we never got to play guitar together more than we did – I guess grad school got the best of us. I'll always remember the in-depth discussions we had about life and chemistry and will certainly cherish them for the rest of my life. Also, thanks for paving the way with the online version of Heterocycles! That was a doozy to do all by myself!

Stephen: You certainly stood out to me as a clear leader during your time here in the Baran lab. You seemed to really step up when the lab needed it most during the COVID era, which I have the utmost respect for. I'm glad things seem to be going well for you and your career, I'm sure more exciting things are to come!

Kyle M: You were one of my older brothers during my time in the Baran lab. Being the oldest in my family, I never knew what it was like to have an older brother, and I think you gave me that experience. Thanks for sharing all your wisdom with me and showing me

what it's like to be a great chemist. Your maximiscin project largely inspired my PhD project on the dragocins.

Yuzuru: I know we didn't get to talk or hangout much when I became a grad student here, but I wanted to thank you for being hard on me in the beginning. Not only that, but also for taking me under your wing when I was a visiting student here. I certainly looked up to your incredible skills and tremendous work ethic.

Yi-Yang: I didn't get to know you too well, but I remember you showing me how to run pTLC plates and driving me around sometimes as a visiting student! Thank you!

David P: Another older brother to me in the lab. You always seemed to look at the bright side of things no matter how hard things got (or unfair). It's too bad that Floyd left the institute and I couldn't follow the dual-advisor path that you did, but my PhD turned out better than I had thought. Thanks for always being there and giving support.

Manolis: The wise philosopher and thinker. You were a shining beacon in the Baran lab and I certainly appreciated all the input you gave me not only on my project but for life as well. Your positive attitude was infectious and you certainly brought a lot of greatness to the Baran lab!

Samer: It was always fun joking around with you in the lab. I'll always miss these times and the fun hangouts at Gravity Heights! You really brought a lot to the Baran lab and your legacy lives on in many ways!

Julien: You were an incredible staff scientist. Not only that, but your social nature made you someone that everyone always wanted to be around. I hope all is well with you in Europe!

Molhm: I will certainly miss you a great deal. I know times get tough in the lab sometimes, but you always seem to come out on the other side. Keep paving the way on the projects! I'll always miss messing around in the lab and gossiping about all the latest happenings (haha!).

Gabriele: You always seemed to be in a good mood, which was infectious. I think everyone really liked you in the Baran lab. Your expertise really helped push a lot of the projects forward. Thanks for talking with me towards the end of the project when things were getting tough for me, it made me feel like you sincerely cared!

Philipp: Almost another little brother for me in the lab. I hope things continue to go well for you and that you graduate within a reasonable time frame! It's crazy how fast time flies and I'll miss the Roberto's burrito runs on Fridays!

Byron P: Thanks for pseudo adopting me as a mentee during my time as a visiting student. You were wonderful to talk to and I'll miss our insanely deep conversations…

Tom: Can't wait to join forces at Gilead soon! It's crazy how small the chemistry world is. Your approach to grad school, science, and life in general is certainly one to admire!

Lisa: Thanks for being an incredible office mate. Your incredible work ethic was commendable and I'm glad you are finally enjoying life with Rohan. Also, thanks for shedding light on the difficulties of the SD/SF long distance relationship!

Tamara: The lab would be nothing without you. Your empathetic nature and willingness to take charge makes you a natural leader that the lab is truly lucky to have. I'll miss all our life discussions and being office mates. I wish you all the best!

Kawa: You're an incredibly talented scientist that the lab is truly honored to have had around for as long as they did. Thank you for all of your help along the way and keeping the lab productive! Wishing you the best in your future career!

Alex R: You have gone through a lot and you should be very proud of where you are now. Even if you do not decide to do chemistry in the future, your driven nature will make you successful with whatever you choose to do. Thanks for taking the reigns on some of the group jobs and taking over group meeting!

Anthony: You're a synthetic wizard with brilliant ideas. Keep working hard, mentoring and teaching others, and generating new things to explore. Total synthesis really requires a mind that is working 24/7 and I have no doubt that you will tackle any chemical challenge that comes your way!

Anna, Maithili, and Mahdi: As the upcoming class, it is important to keep asking questions, exposing yourself to new chemistry constantly, brainstorming on a daily basis, and developing a "killer instinct" at the hood. The only bad reaction is one where "you don't know what happened". Run every experiment with the intention of generating a result that will push your project in the right direction – whether it failed or not. Don't be afraid to try new ideas or abandon ones that simply aren't working. At the end of the day, you need to be the one driving the day to day progress on your projects. Keep up the great work!

Sol: Thank you for taking me under your wing when I was a visiting student in 2018. I truly admired your incredible knack for doing science at the highest level. I have you to thank largely for getting me a spot in the Baran lab as a grad student.

Kelly: I know we didn't get to hang out as much as we could have or should have during our PhD's (I guess we can blame COVID in some ways), but it was always a pleasure to

spend time with you outside of lab. You were a lot of fun to have around and certainly helped prop up the social culture of the lab. Things didn't probably go exactly how you wanted in grad school, but I'm glad to know that you will be heading out soon and I look forward to seeing what you do with your career in the future!

Alberto: Your positive nature was infectious. I always loved having you around lab to chat about all sorts of things. It was really fun to hang out with you and Simona (especially towards the end when I had more time on my hands!) and get beers and whatnot. It was a real treat to have you around for the end of the project with the electrochemistry!

Junchen: You are one of the most talented chemists that I know. I still wonder how you finished the portimine project so quickly and left one year before I did! Your skills will take you very far in your career and I wish you all the best!

Christine: Keep growing and staying positive! You have made huge strides in the right direction since you began here, and it's really been a pleasure to watch. Continue to ask questions, read the literature, and develop your skills at the hood. I'm sure you will tackle your project soon and look forward to seeing what's next for you!

John G: The Baran lab is lucky to have you around as a visiting undergraduate. Keep up the tenacity and the hunger and things will go very well for you in grad school and future career.

Nick: I really enjoyed the time that we overlapped in the Baran lab and will certainly miss climbing with you at Mesa Rim!

Kevin R: Mixture between one of my best friends and another older brother. I just loved having you around lab and can't wait to join the ranks at Gilead with you! Enough said ☺

Chi: You were fantastic to have around the lab! You have been sorely missed!

Table of Contents

Acknowledgements……I

Table of Contents……..VIII

List of Figures……X

List of Schemes……...XII

Abbreviations……....XIII

Abstract…….....XVII

Introduction…….....XIX

Chapter 1: Dragocin Introduction, Related Natural Product AB3217-A, and Preliminary Synthetic Studies……...1

1.A. Dragocin Introduction……..2

1.B. Nakata's synthesis of AB3217-A and related work……...4

1.C. Initial studies towards the densely functionalized pyrrolidine – α-functionalization strategies……...6

Chapter 2: [3+2] Cycloaddition approaches……..10

2.A. Investigating vinyl boronic esters as dihydroxyethylene equivalents in an azomethine ylide cycloaddition……..11

2.B. An intramolecular [3+2] strategy……13

Chapter 3: An Enantioselective Pyrrole Dearomatization Sequence Leads to a Failed Intramolecular Glycosylation……17

3.A. Intramolecular glycosylation retrosynthesis and pyrrole dearomatization…..18

3.B. Forward sequence investigations……20

Chapter 4: A Furan-based Approach Backfires: Escapades in Medium-Sized Ring Formation…….28

4.A. Rationale behind this approach and a new pyrrolidine synthesis……..29

4.B. Initial forward sequence and a surprising cyclization result of a dicarbonyl..30

4.C. Breakthrough in an oxygen-based nucleophilic epoxide opening and an undesired 9-membered *endo* isomer in a butenolide-focused approach……..32

Chapter 5: Journey's End: An Emotional Rollercoaster Filled with Triumphs and Tragedies……...36

5.A. Discussion of a new disconnection through an oxidative cyclization…….37

5.B. First successful route towards the 9-membered ring……...39

5.C. Spectacular failure of a demanding C–H oxidation at C4'……...42

5.D. A new C4' strategy via decarboxylation and throughput improvements…….45

5.E. The endgame……...48

5.F. Endgame improvement #1: Electrochemical cyclization/etherification……..52

5.G. Endgame improvement #2: one-step carboxylic acid access and improved Barton decarboxylation

5.H. Preparation of dragocin A through methanolysis of dragocin C and the final route……...71

5.I. Are the dragocins covalently reactive? A stimulating biological consideration……..75

References…….76

Experimental……81

List of Figures

Figure 1.1: Dragocins A–C and related natural product AB3217-A……2

Figure 1.2: Synthon considerations for a C-2 functionalization approach……...6

Figure 1.3: Elimination of lithiated hydroxy pyrrolidines……...7

Figure 1.4: Attempts to leverage triethylborane chemistry…….7

Figure 1.5: Attempt to leverage imine chemistry using hydride transfer chemistry……8

Figure 1.6: An alcohol directed Petasis reaction…….9

Figure 2.1: Cycloaddition logic and Singleton's Diels-Alder precedent……11

Figure 2.2: Hypothetical desired transition state for the [3+2] reaction…….12

Figure 2.3: Intramolecular cycloaddition retrosynthesis……...13

Figure 2.4: Oxidative rearrangement hypothesis……..16

Figure 3.1: Intramolecular glycosylation retrosynthesis……..19

Figure 3.2: A possible chelation model to explain the diastereoselectivity in the 1,2 addition reaction…….22

Figure 4.1: A new furan-based approach towards the dragocins……..29

Figure 5.1: Failed approach summary and the new disconnection via oxidative cyclization……..37

Figure 5.2: Plastic models revealed a promising conformation……37

Figure 5.3: Retrosynthesis for 1st generation oxidative cyclization approach……38

Figure 5.4: Failed late-stage C–H oxidations……44

Figure 5.5: Route towards directing group substrates……45

Figure 5.6: A new C–C bond cleavage strategy……46

Figure 5.7: A new way to generate the key epoxide through epoxidation……47

Figure 5.8: Potential methanolysis of dragocin C to produce dragocin A……51

Figure 5.9: An opportunity for electrochemistry in the cyclization event……52

Figure 5.10: Electrochemical cyclization……..53

Figure 5.11: CV of acyclic precursor……55

Figure 5.12: CV of cyclized desired material……56

Figure 5.13: Overlaid CV of acyclic and cyclized desired compound…….57

Figure 5.14: CV of acyclic, desired, and Boc-pyrrolidine……58

Figure 5.15: CV of acyclic, desired, and *p*-Me-anisole…….59

Figure 5.16: Potential explanation for the oxidative scission product……60

Figure 5.17: CV of undesired stereoisomer……...61

Figure 5.18: CV of desired and undesired isomers……62

Figure 5.19: CV of the HFIP:DMSO mixture (2:1)……..63

Figure 5.20: Screening the conversion of dragocin C to A……73

Figure 5.21: Hypothetical mechanism for the formation of the putative dragocin A isomer…….73

List of Schemes:

Scheme 1.1: Proposed biosynthesis of dragocins A–C……3

Scheme 1.2: Nakata's synthesis of AB3217-A…….5

Scheme 1.3: Syngenta's formal of AB3217-A…….6

Scheme 2.1: An intramolecular cycloaddition with B(pin) functionalized ethylene…….12

Scheme 2.2: Preparation of **2.17**……14

Scheme 2.3: Preparation of **2.20**……14

Scheme 2.4: Convergence of **2.17** and **2.20** and an unexpected rearrangement……15

Scheme 3.1: Racemic route scouting using Ito's dearomatization method…….20

Scheme 3.2: Dearomatization sequence to access 1,2 addition substrate……..21

Scheme 3.3: Route to access **3.20**……..24

Scheme 3.4: Failed intramolecular glycosylation……..26

Scheme 4.1: Initial furan explorations and undesired 6-exo cyclization……31

Scheme 4.2: 2nd generation furan strategy through a butenolide intermediate and undesired cyclization to form an *endo* isomer…….34

Scheme 5.1: 1st successful generation towards the 9-membered ring……40

Scheme 5.2: Improved access to **5.14**……42

Scheme 5.3: Production of **5.20**…….46

Scheme 5.4: Ring opening **5.23** with BzOH……..48

Scheme 5.5: Glycosylation of **5.26** with **5.20** and cyclization with PIFA/CSA……49

Scheme 5.6: Successful endgame through a Barton decarboxylative halogenation……..50

Scheme 5.7: Improved access to acid **5.29**…….71

Scheme 5.8: Improved access to **5.30**……72

Scheme 5.9: Full sequence to the dragocins……74

List of abbreviations:

Å = angstrom

Ac = acetyl

AcOH = acetic acid

aq. = aqueous

br = broad

brsm = based on recovered starting material

t-BuOH – tert butanol

Bz = benzoate

°C = degree celcius

Cbz = carboxy benzyl

cat. = catalytic or catalyst

CSA = camphorsulfonic acid

$CDCl_3$ = chloroform-*d*

DBU = 1,8-diazabicyclo[5.4.0]undec-7-ene

DCC = *N,N'*-Dicyclohexylcarbodiimide

DCE = dichloroethane

DCM = dichloromethane

DDQ = 2,3-dichloro-5,6-dicyano-1,4-benzoquinone

DG = directing group

DMAP = (4-dimethylamino)pyridine

DMF = *N',N'* – dimethylformamide

DMP = Dess-Martin periodinane

DMS = dimethyl sulfide

DMSO = dimethylsulfoxide

Et_3N = triethylamine

ESI = electrospray ionization

Et_2O = diethyl ether

EtOAc = ethyl acetate

hν = UV or light irradiation

g = grams

HAT = hydrogen atom transfer

h = hours

HOTT = S -(1-Oxido-2-pyridinyl)-1,1,3,3-tetramethylthiouronium Hexafluorophosphate

HRMS = high resolution mass spectroscopy

Hz = Hertz

KOH = potassium hydroxide

mA = milliamps

MB = methylene blue

Me = methyl

MeCN (or ACN) = acetonitrile

mg = milligram

M = Molar

Mol = mole

mmol = millimole

NBS = *N*-bromo succinimide

NMO = 4-methylmorpholine *N*-oxide

NMR = nuclear magnetic resonance

OTf = triflate

PDC = pyridinium dichromate

Ph = phenyl

PhH = benzene

PhMe = toluene

PIDA = (diacetoxyiodo)benzene

PIFA = (trifluoroacetoxyiodo) benzene

ppm = parts per million

pTLC = preparative thin layer chromatography

Pyr. = pyridine

quant. = quantitative

rt = room temperature

TBAF = tetra-*n*-butylammonium fluoride

TBSCl = *tert*-Butyldimethylchlorosilane

TMSCl = tetramethyl chlorosilane

TFA = trifluoroacetic acid

TFDO = methyl(trifluoromethyl)dioxirane

TFE = trifluoroethanol

THF = tetrahydrofuran

TLC = thin layer chromatography

TPAP = tetrapropylammonium perruthenate

TsOH = tosic acid

“X” = halogen

Abstract

Natural products that arise from hybrid metabolic pathways offer a unique and exciting opportunity for total synthesis and often result in compelling synthetic campaigns. The dragocin family of natural products represent a peculiar class of these types of secondary metabolites and feature multiple rare or even completely unprecedented structural motifs. Described in this dissertation is a brief background of these intriguing structures along with the strategies that were explored *en route* to these natural products in five separate chapters. Notably, the approaches described herein represent the first reported synthetic forays into these marine-derived compounds and may inform any future work on these structures or related molecules.

Chapter 1 will introduce the dragocins, the synthesis of the only related natural product, AB3217-A, along with preliminary studies towards the preparation of the densely functionalized pyrrolidine found in the dragocins. In chapter 2, [3+2] cycloaddition strategies will be presented, which will feature both azomethine ylide and nitrone synthons along with a discussion of key roadblocks. Chapter 3 will focus on an approach which leveraged an enantioselective pyrrole dearomatization, giving way to the first advanced intermediate which enabled exploration of 9-membered ring formation via an unsuccessful intramolecular glycosylation strategy. In chapter 4, a dearomative furan-based strategy will be presented, which was also unfortunately met with failure. Finally, the first successful approach towards the key 9-membered skeleton and a failed late-stage C–H oxidation strategy will be found in chapter 5. Additionally found in this chapter will be the final successful approach towards these metabolites, which hinged upon a key decarboxylative

chlorination of an intermediate which was constructed from an unprecedented intramolecular electrochemical cyclization/etherification event. A brief discussion of these natural products acting as potential covalently reactive compounds will conclude this dissertation.

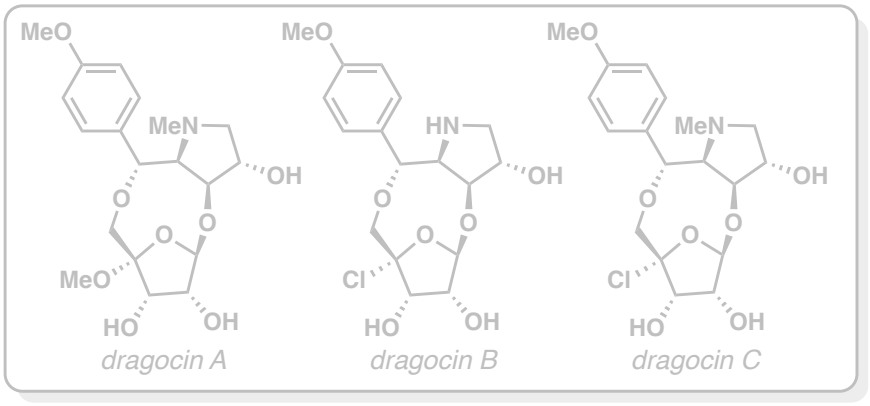
Introduction

"Chemical synthesis is uniquely positioned at the heart of chemistry, the central science, and its impact on our lives and society is all pervasive."
-E.J. Corey

The total synthesis of nature's complex structures continues to be an incredibly colorful and thriving scientific pursuit. It is often that these synthetic campaigns can unravel new and/or useful organic reactivity, shine light upon chemical curiosities and anomalies, and may even enable the first bioactivity studies of a given compound. The experience of a total synthetic pursuit closely resembles, at least in scientific spirit, an astronaut discovering untapped parts of the universe or a biologist discovering a new organism. With that said, as the state of the synthetic field continues to mature at a rapid pace, it is unsurprising to find that many contemporary synthetic campaigns focus on compounds or metabolite classes which have multiple literature precedents. Today, it is becoming increasingly rare to find so-called "one-off" natural product targets which may be completely structurally unprecedented or belong to a metabolite class that contains few synthetic reports in the literature which may act as clues to inform one's studies. These types of compounds represent an opportunity to "freely paint on an open canvas" without any outlines to guide a synthetic creation. While vexing, these pursuits can provide invaluable training for the practicing chemist and may be exceptionally rewarding in that they explore uncharted chemical territory. The dragocin family of natural products belong to a peculiar class of hybrid secondary metabolites that we believe represent these characteristics, which rendered them irresistible focal points for the doctoral work described herein.

Dragocins A–C were isolated off the Caribbean coast near Boca del Drago from a marine cyanobacterium and were found to possess modest cytotoxic activity against human lung cancer cells (H-460).[1] Thus far, the only related natural product to the dragocin family is AB-3217A (**2**) (previously synthesized in 26 steps by Nakata[2]), an anti-mite substance which features a near identical framework but lacks the unique C-4' oxidation found on dragocins A–C. Notably, this C-4' functionalization is unprecedented in the natural product space, with the exception of nucleocidin, a C-4' fluorinated nucleoside.[3] Aside from this unusual feature, the dragocins contain an alluring central 9-membered ring system which consists of a highly oxidized pyrrolidine harboring four contiguous stereocenters and an electron-rich arene, all cemented upon a polar ribose moiety. These structural features made way for a laborious campaign which were met with exhaustive failure and will be described in the ensuing chapters. It is hoped that these failures can shed light on any future campaigns related to the dragocins or any related compounds.

The final successful route features a number of transformations that may find application in other settings, such as: (1) rapid, stereocontrolled entry to polyhydroxylated pyrrolidines through diastereoselective and regioselective reactions, (2) rAP-mediated electrochemical metal-free tosylamide removal, (3) alternative one-pot decarboxylative Barton chlorination procedures, and, most remarkably, (4) oxidative, diastereoselective C–H functionalizing electrochemical cyclization to form a 9-membered ring.



Chapter 1:

Dragocin Introduction, Related Natural Product AB3217-A, and Preliminary Synthetic Studies

1. A. Dragocin introduction

Dragocins A–C (**1.1-1.3**, Figure 1.1) belong to a peculiar hybrid structural class of secondary metabolites.[1] These intriguing molecules were isolated off the Caribbean coast near Boca del Drago from a marine cyanobacterium and were found to possess modest cytotoxic activity against human lung cancer cells (H-460). Thus far, the only related natural product to the dragocin family is AB3217-A[4] (**1.4**) (previously synthesized in 26 steps by Nakata[2]), an anti-mite substance which features a near identical framework, but lacks the unique C-4' oxidation found on dragocins A–C. Notably, this C-4' functionalization is unprecedented in the natural product space, with the exception of nucleocidin,[3] a C-4' fluorinated nucleoside. Aside from this unusual feature, the dragocins contain an alluring central 9-membered ring system which consists of a highly oxidized pyrrolidine harboring four contiguous stereocenters and an electron-rich arene, all cemented upon a polar ribose moiety.

With regards to their biosynthesis, the exact metabolic pathway has not been studied. However, it is proposed by the isolation authors that these remarkable compounds may arise from a mixed biosynthetic pathway that feature modules from non-ribosomal peptide synthetases (NRPS), polyketide synthases (PKS), as well as carbohydrate metabolism.[1]

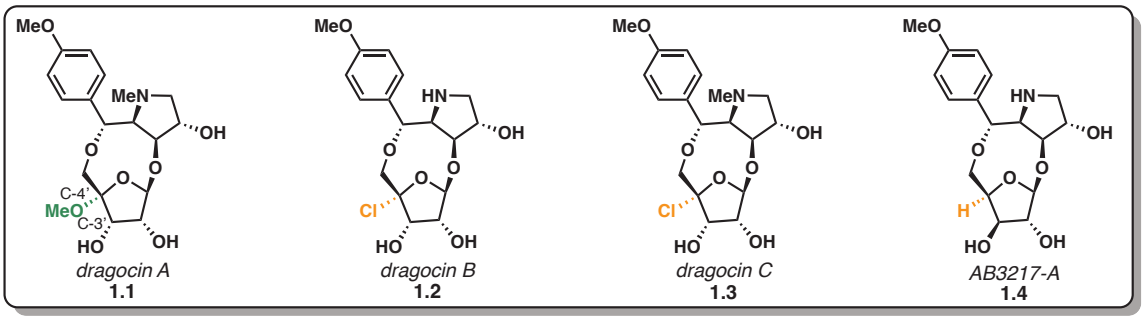
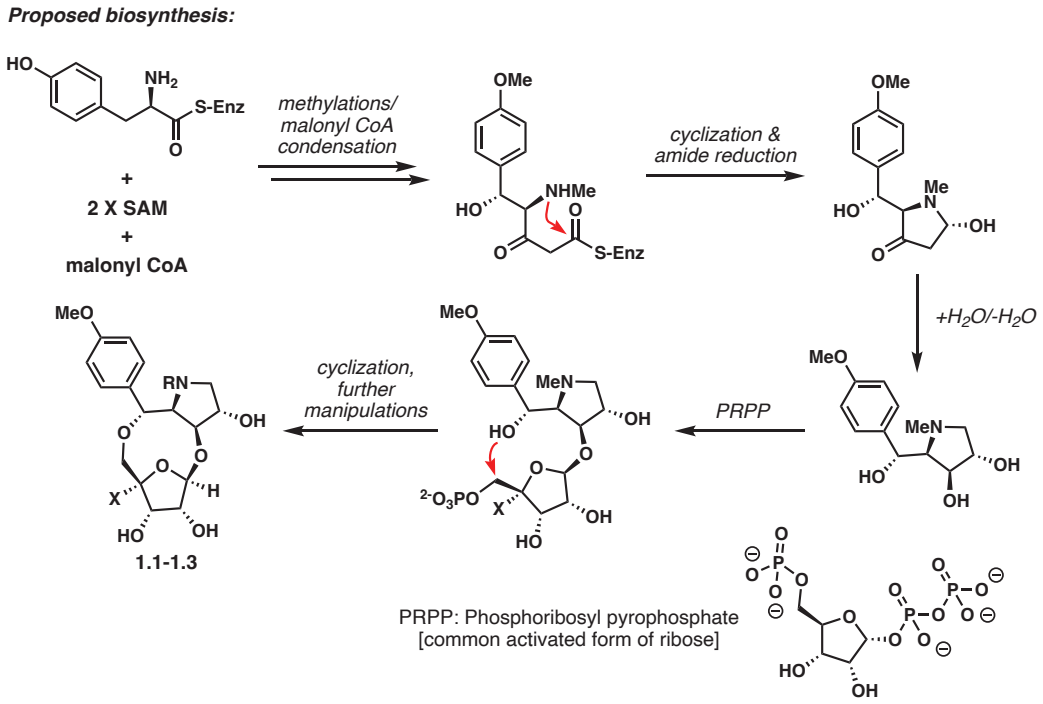


Figure 1.1 Dragocins A–C and related natural product AB3217-A

These assorted pathways arise to give the intriguing core skeleton of the dragocins, with

the installation of the chloride remaining a complete mystery. Given the close structural relationship to AB3217-A, it is possible that either a highly specialized enzyme or marine environment conditions may introduce the C-4' chloride at a late biosynthetic stage – perhaps through radical activation (this postulation guided our failed C–H oxidation approach outlined in chapter 5).



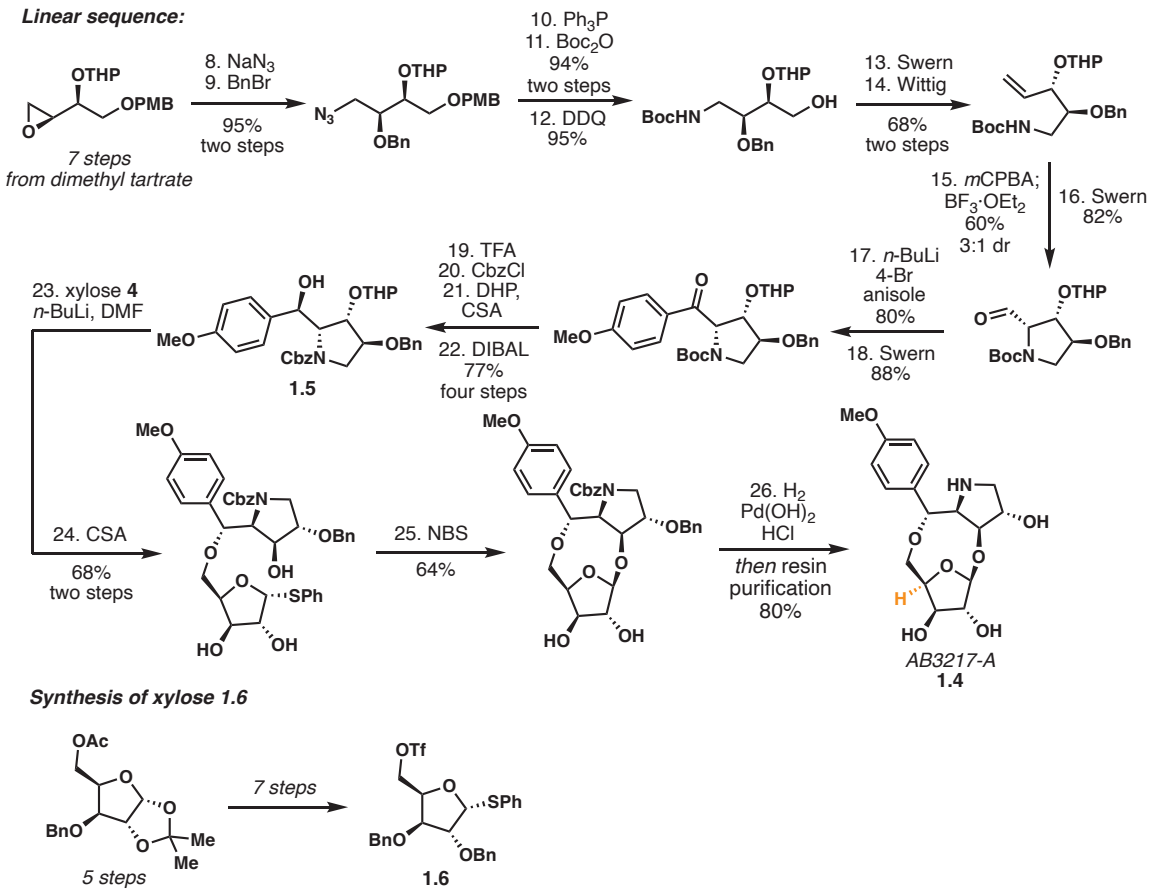
Scheme 1.1 Proposed biosynthesis of dragocins A–C (Gerwick)

As depicted in **Scheme 1.1**, Gerwick and coworkers hypothesize that these compounds arise naturally from a tyrosine residue, followed by redox and cyclization events to forge the key pyrrolidine fragment. Occurring next in their proposal is a glycosylation and S_N2-type reaction with a polyphosphorylated ribose (phosphoribosyl pyrophosphate; PRPP), a common activated form of ribose, to construct the hallmark 9-membered skeleton.[1] As mentioned earlier, the introduction of the C-4' functionality in either the form of -Cl or -OMe remains an enigma, as this specific functionality is unprecedented in the natural product literature. Additionally, the biosynthesis of AB3217-A is also not reported,

rendering any proposals regarding the true origins of these compounds completely speculative. It is interesting to consider why these atypical structures appear to have been nearly forgotten by the chemical community over the past three decades.

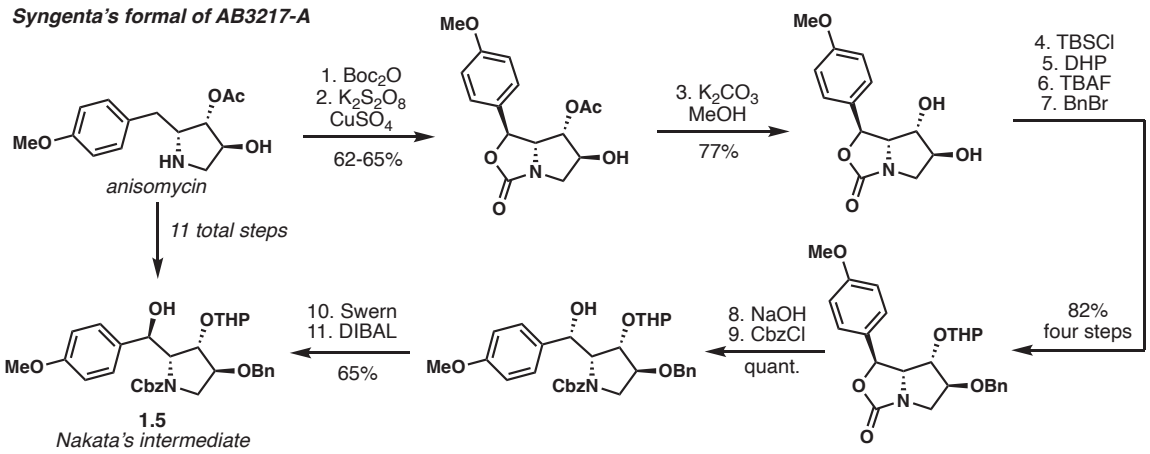
1.B. Nakata's synthesis of AB3217-A and related work

In 1994, Nakata published two identical reports describing the first synthesis of AB3217-A via intermolecular etherification and intramolecular glycosylation.[2] Without providing too much detail, the synthesis can be divided into three key sequences (**Scheme 1.2**). The first, which establishes the longest linear sequence, is the preparation of pyrrolidine **1.5**, which proceeds in 21 steps from dimethyl L-tartrate. A second portion of this report describes the construction of a protected xylose donor **1.6** in 12 total steps. Once Nakata constructs these two fragments, they are unified via an intermolecular S_N2 reaction and subsequently cyclized through an intramolecular glycosylation reaction using standard glycosylation chemistry. Subsequent removal of protecting groups furnished the title material, AB3217-A. While a noteworthy and highly respectable achievement, the route arguably suffered from excessive functional group interconversion and cumbersome protecting group chemistry (which was due to the era this work was completed in and is not necessarily a fair critique). It would be insincere not to give credit to Nakata and coworkers for their pioneering work on these structures, which was frequently referenced throughout the course of the journey towards the dragocins.



Scheme 1.2 Total synthesis of AB3217-A by Nakata and coworkers

Related to this work by Nakata comes a report from Syngenta, a large agricultural company, where they appeared to have had some interest in AB3217-A given its marked anti-mite bioactivity. In this work, Syngenta reports a formal synthesis of AB3217-A, intercepting Nakata's pyrrolidine **1.5** through a benzylic oxidation strategy of anisomycin, an antibiotic compound commonly used in agar (i.e. Martin Lewis agar).[5] This approach proceeds in 11 steps, nearly cutting Nakata's sequence in half (**Scheme 1.3**). However, this report begins with anisomycin, which is an incredibly expensive synthetic starting material ($570/100 mg) and progresses through a >10 step sequence.



Scheme 1.3 Syngenta's formal synthesis of AB3217-A, intercepting Nakata's pyrrolidine **1.5**

While these studies are acknowledged and the utmost respect is given towards the respective authors, the approaches described in these two works (among many others that involve similar pyrrolidine systems) served as benchmarks with which we attempted to improve upon.

1.C. Initial studies towards the densely functionalized pyrrolidine – α-functionalization strategies.

Our initial forays into these natural products attempted to leverage a strategy which involved functionalization at the α-position of the pyrrolidine (C-2) with a compatible benzylic coupling partner. An initial brainstorm led to three disparate synthons to consider: anionic, cationic, and radical synthons (Figure 2).

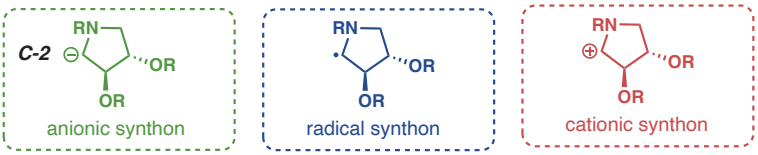


Figure 1.2 Synthon considerations for a C-2 functionalization approach

With regards to the anionic approach, we quickly identified a report from Mordini and coworkers (**Figure 1.3**), where they found that pyrrolidine **1.7** readily underwent

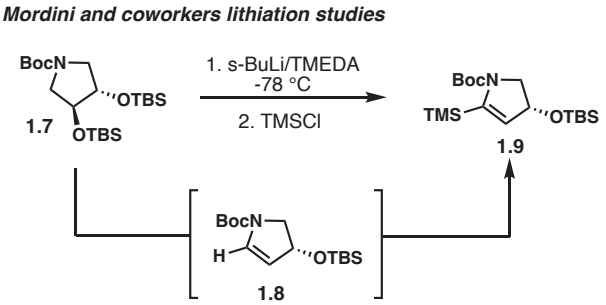


Figure 1.3 Elimination of lithiated hydroxy pyrrolidines by Mordini

elimination to give a dihydropyrrole intermediate **1.8** and subsequent lithiation and silylation to produce **1.9**.[6] Due to these literature findings, we were able to easily rule out a deprotonation strategy given the propensity for these systems to undergo elimination chemistries.

Next, we considered a radical approach. Yoshimitsu and coworkers reported a triethylborane-initiated methodology which couples the α-position of various amines and amides with aldehyde electrophiles,[7] which we envisioned could serve as a suitable platform for preparing a key pyrrolidine fragment. Despite our best efforts on this front, we were unable to detect any desired coupling product upon subjection of pyrrolidine **1.10** to either neat or hexane solutions of triethylborane (**Figure 1.4**). In fact, we observed no consumption of this starting material during any of our attempts, which was perplexing given the aggressive nature of the reaction conditions (even trying up to 100 equiv. of neat

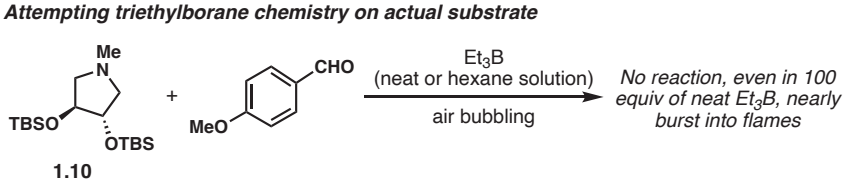


Figure 1.4 Attempts to leverage triethylborane chemistry on a protected hydroxy pyrrolidine

Et_3B!). Control reactions were ran using identical substrates to those reported in the aforementioned paper, confirming that our substrate was unreactive under these conditions – most likely due to the steric encumbrance that the adjacent hydroxyl groups posed.

Reasoning that any further attempts to produce a radical at C-2 of a linchpin pyrrolidine would be difficult due to sterics (and lack of reported methodology to furnish the desired bond between the pyrrolidine and a benzylic fragment to produce a secondary alcohol), it was finally envisaged to produce the desired pyrrolidine fragment(s) through cationic chemistry. These approaches represented the only pyrrolidine synthon that produced the desired bond formation, unfortunately giving us an unfavorable mixture of diastereomers deemed unsatisfactory for synthetic purposes.

The first successful hit towards bond formation was achieved leveraging a protocol from Seidel,[8] which involves the interception of a reactive pyrrolo-imine intermediate with an organometallic nucleophile. Indeed, we were able to smoothly utilize this chemistry to forge the bond between C-2 and a benzylic nucleophile. Unfortunately, these reactions led to inseparable mixtures of **1.12** as diastereomers in low yield from **1.11** (**Figure 1.5**) – slightly favoring the undesired isomer. As previously mentioned, this result was unsuitable

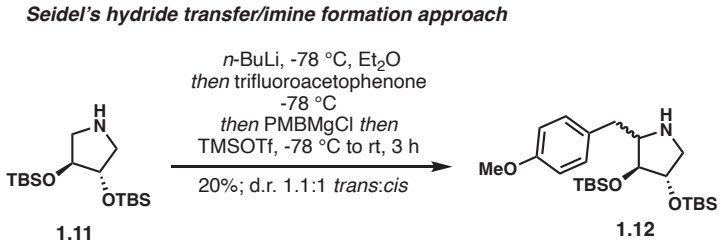


Figure 1.5 Attempt to leverage imine chemistry using hydride transfer chemistry reported by Seidel. A mixture of inseparable diastereomers was obtained.

for material throughput, and a much more efficient solution was desirable at this stage of the project.

Subsequently, we wondered if a compatible nucleophile could be directed in towards the C-2 position of the pyrrolidine, giving a *syn* relationship between the C-3 hydroxy group and resultant C-2 functionalized position. It was encouraging to find a multicomponent Petasis-type reaction from She and coworkers, where a vinyl boronic ester or acid could be directed to react with an adjacent iminium ion formed *in situ* with a protected benzoquinone.[9] Unfortunately, while this reaction seemed quite powerful, it proceeded in only 10% in our hands using **1.13** and **1.14** to give a boronic ester-protected pyrrolidine **1.15**. In addition to the low yield, product **1.15** would require multiple additional manipulations to provide any synthetically useful material.

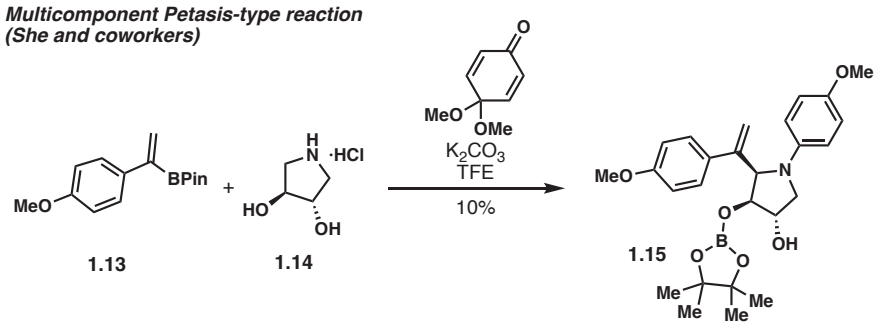
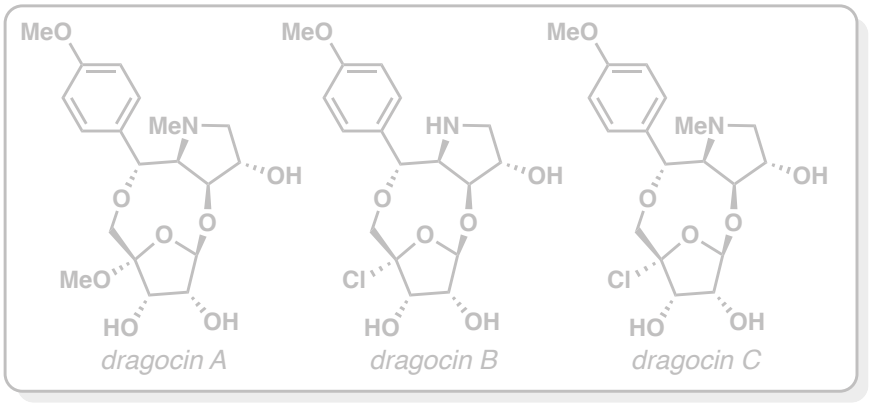


Figure 1.6 An alcohol directed Petasis reaction led to low yields of **5**.



Chapter 2:

[3+2] Cycloaddition Approaches

2.A. Investigating vinyl boronic esters as dihydroxyethylene equivalents in an azomethine ylide cycloaddition

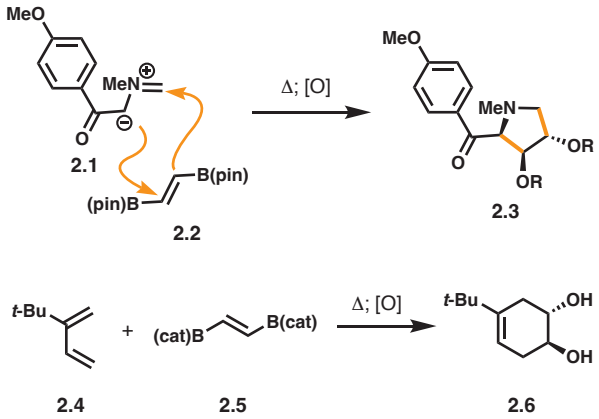
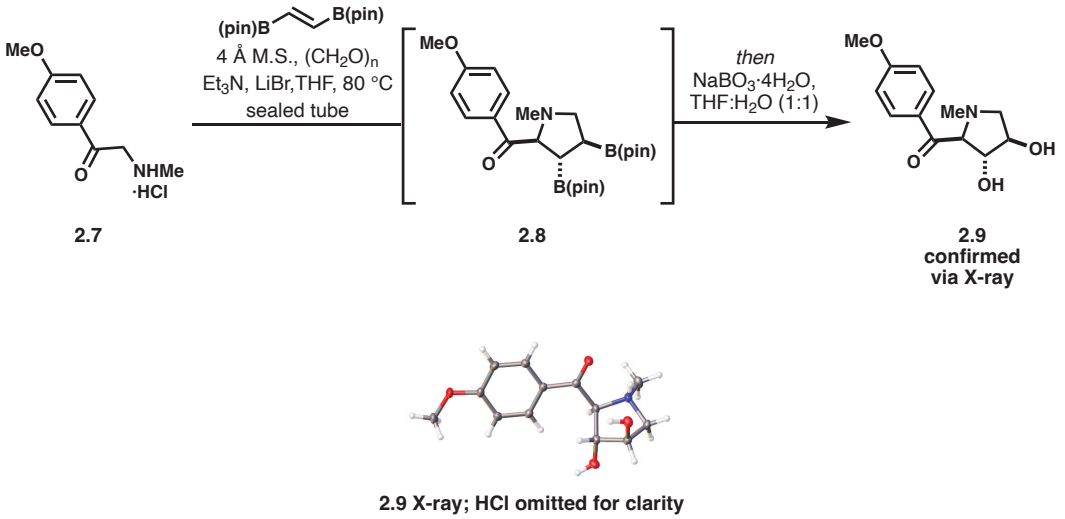


Figure 2.1 Cycloaddition logic and Singleton's Diels-Alder precedent used for inspiration.

In this retrosynthetic iteration (**Figure 2.1**), we wondered if the dihydroxylated pyrrolidine could arise from a cycloaddition involving a stabilized dipole **2.1** and a dihydroxyethylene equivalent dipolarophile such as **2.2** to produce **2.3**. In our initial literature searches for this type of transformation we noticed that there was no precedent for a cycloaddition of this nature. However, we were encouraged to find a report from Singleton which describes utilizing diene **2.4** and vinyl(di)borane **2.5** as a dieneophile in Diels-Alder chemistry.[10] The cycloadduct was then subjected to oxidation to furnish the *trans* dihydroxylated cyclohexane product **2.6**. We envisaged that inspiration could be taken from this report, wherein a similar vinyl(di)borane could be leveraged as a dipolarophile along with an azomethine ylide partner.

After some initial studies, we found that a simple amine **2.7** alongside pinacolborane **2.2** underwent smooth [3+2] cycloaddition with an azomethine ylide formed *in situ* via condensation with formaldehyde at high temperatures. Attempts to isolate cycloadduct **2.8** were challenging and met with failure; an oxidative workup of this intermediate adduct were thus adopted and we were delighted to isolate the desired material upon SiO_2 chromatography. The determination of the relative stereochemistry of racemic **2.9** through

NMR experiments was ambiguous, but X-ray analysis revealed that the wrong C2/C3 isomer was obtained as the *trans* variant (**Scheme 2.1**).



Scheme 2.1 A cycloaddition using a dihydroxyethylene equivalent dipolarophile. Crystal structure of **2.9** revealed the wrong stereochemical outcome of the reaction.

We reasoned that this was likely due to unfavorable steric interactions between dipole **2.1** and dipolarophile **2.2** in the [3+2] transition state (**Figure 2.2**). At this juncture, we wondered if we could not only obtain enantiopure material, but also perhaps alter the relative stereochemical outcome in the reaction through applying enantioselective conditions. Despite our best efforts on this front, reactions proceeded in low yield and less than 5% *ee* when employing various enantioselective cycloaddition strategies (data not shown). While disappointing at this point in the project, we wondered if these studies warranted a tethering strategy, which would involve an intramolecular [3+2] cycloaddition to build not only the pyrrolidine but also the key central 9-membered ring system.

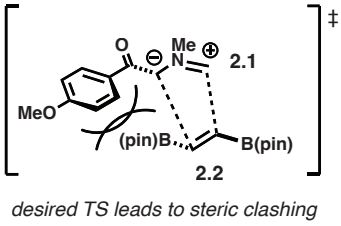


Figure 2.2 Hypothetical desired transition state

2.B. An intramolecular [3+2] strategy

As mentioned previously, the intermolecular cycloaddition studies sparked the investigation of a bold tethering strategy, wherein an unstabilized dipole such as **2.10** could be formed *in situ* upon condensation and decarboxylation with **2.11** to be reacted with a pendant functionality capable of plausibly intercepting the reactive azomethine ylide (**Figure 2.3**).

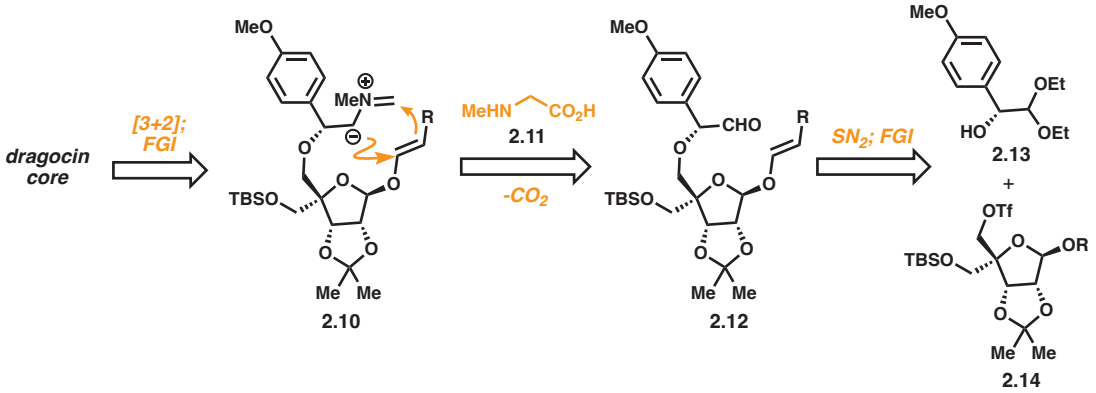
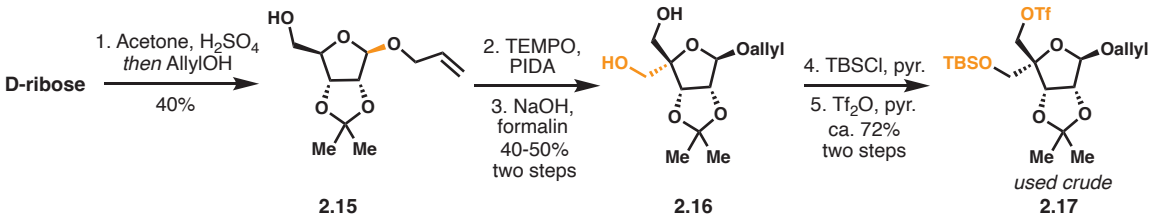


Figure 2.3 Intramolecular cycloaddition approach retrosynthesis

We envisaged that the intramolecular cycloaddition would forge not only the pyrrolidine motif, but also the core ring system. The hypothetical [3+2] adduct could then be further functionalized to the natural products. With this strategy, the key aldehyde **2.12** (azomethine ylide precursor) could be accessed through a short sequence of robust and reliable chemistries beginning with **2.13** and **2.14**. While this approach was ambitious, the relatively short sequence and fact that the project was still in its relative infancy rendered these studies tolerable from a risk-assessment perspective.

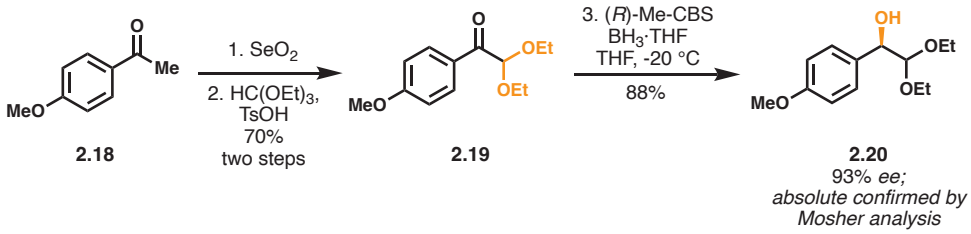
A convergent strategy was employed in order to access the key intermediate aldehyde. Firstly, a functionalized ribose derivative was accessed through a known sequence. Beginning with D-ribose, a one-pot protection sequence enabled access to allyl glycoside

2.15, which was then subjected to an oxidation/Cannizzaro reaction sequence to furnish diol **2.16**. This diol was then regioselectively protected and triflated to give crude electrophile **2.17** for an inevitable S_N2 reaction (**Scheme 2.2**).[11]



Scheme 2.2 Preparation of **2.17**

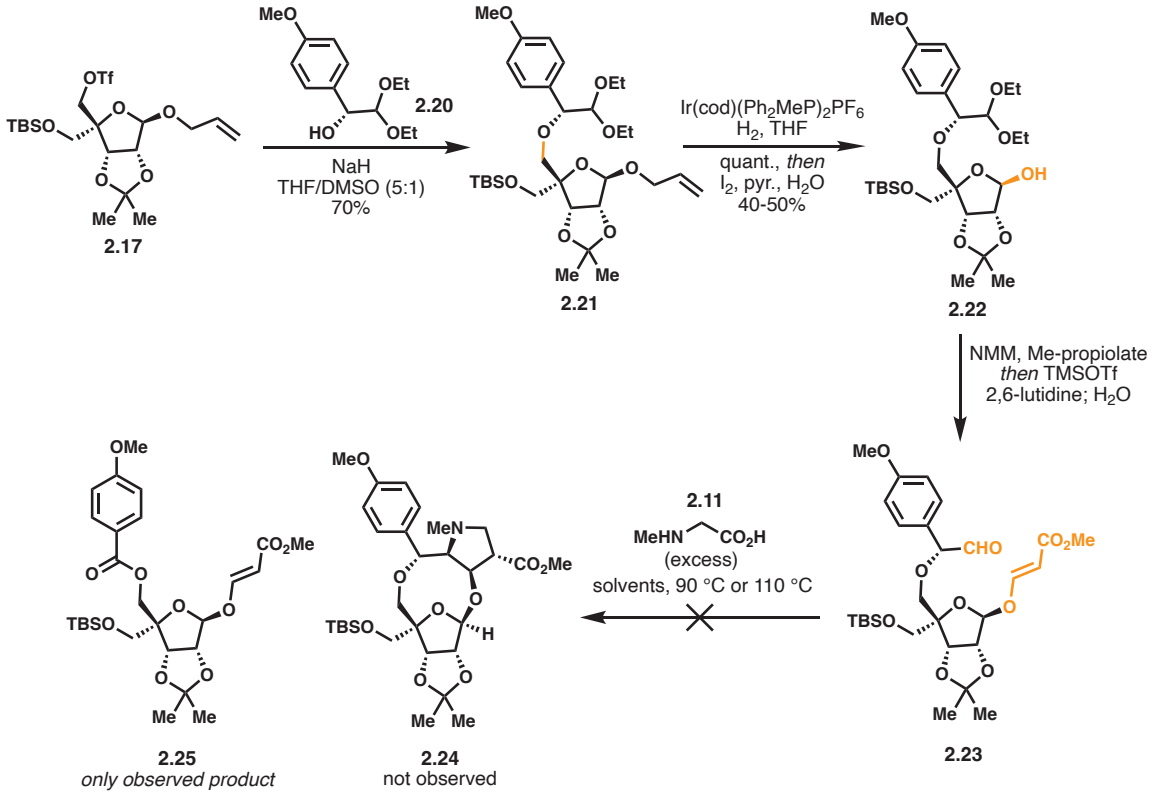
This secondary alcohol was accessed through a three-step sequence involving a SeO_2-mediated α-oxidation of **2.18**, protection to the diethoxy acetal **2.19**,[12] and subsequent CBS reduction to the corresponding chiral alcohol **2.20**. The absolute stereochemistry of this benzylic alcohol was unambiguously assigned through Mosher analysis[13] and was measured to be 93% *ee*.



Scheme 2.3 Preparation of benzylic alcohol **2.20**

With these two partners in hand, a smooth S_N2 reaction was obtained using NaH and a THF/DMSO solvent mixture. At this point, allyl glycoside **2.21** was subject to an iridium-catalyzed isomerization followed by iodine-mediated hydrolysis to give free glycoside **2.22**. This free glycoside then underwent an NMM promoted 1,4-addition with methyl propiolate to give an enol ether as a single isomer. All that was required at this point was to unveil the key aldehyde functionality. After some investigations, it was found that a TMSOTf based system[14] smoothly furnished the desired deprotected material **2.23**. This

step was not as straightforward as we envisioned but was likely met with resistance to the presence of several acid-sensitive functional groups. With key aldehyde **2.23** in hand, we were excited to explore the possibility of engaging this material in such a compelling way. Unfortunately, efforts to form **2.24** were unsuccessful.



Scheme 2.4 Convergent sequence to **2.23** and an unexpected oxidative rearrangement by-product

Upon attempts to condense sarcosine **2.11** (*N*-methyl-glycine) at increased temperatures, we observed a peculiar TLC spot rapidly forming, which did not appear to be in the relative polarity range that we would have expected. When analyzing the resultant mixture, there appeared to be one major product and did not contain a nitrogen atom based on *m/z* data from LCMS analysis. Isolation of this product followed by further NMR-based elucidation revealed that the starting material appeared to undergo a rearrangement that did not involve an intermediary adduct with the condensation partner. After thorough analysis, it was determined that the rearrangement product was benzoate **2.25**. This perplexing result was

surprising and led us to a literature report, where an oxidative rearrangement was described on substructures which had nearly identical functionality to that found on our key system.[15] To be brief, it is hypothesized that this rearrangement occurs through first a tautomerization

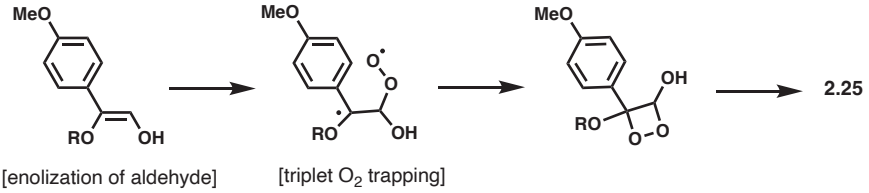
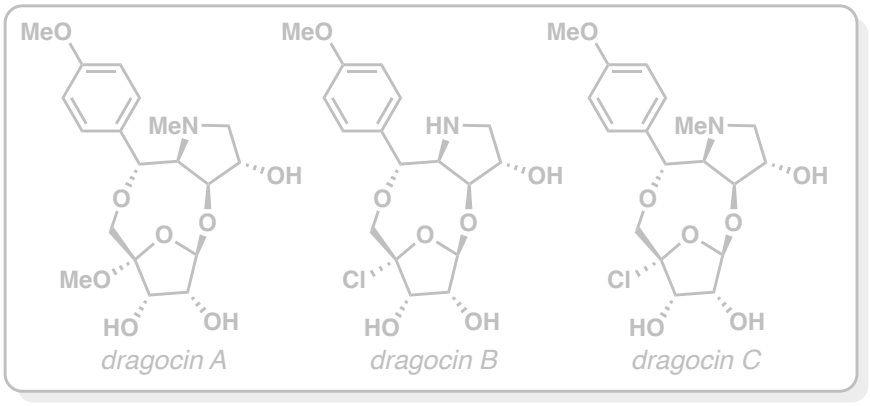


Figure 2.4 Oxidative rearrangement hypothesis to produce **2.25**

of the aldehyde to the corresponding enol, which is subsequently trapped with adventitious singlet oxygen to form a highly stabilized radical, which can collapse and fragment to provide the resultant observed product. This speculation is in line with reports from Hu and coworkers.

To our dismay, we were unable to avoid the rearrangement of this unstable intermediate, despite efforts to exclude oxygen from reaction systems. At this point, our immediate priority became to develop a scalable and stereocontrolled synthesis of a synthetically tractable functionalized pyrrolidine to investigate an apparently less risky cyclization strategy – intramolecular glycosylation. The trials and tribulations of this strategy will be described in the ensuing chapter along with the employment of an enantioselective pyrrole dearomatization sequence to access useful quantities of a properly functionalized pyrrolidine.



Chapter 3:

An Enantioselective Pyrrole Dearomatization Sequence Leads to a Failed Intramolecular Glycosylation

3.A. Intramolecular glycosylation retrosynthesis and pyrrole dearomatization

This approach led us towards what could be regarded as the first pseudo-matured approach towards the dragocins in that the project began to feel more like a synthesis than it ever had before. Scaling and material throughput became more of a consideration, a lot more grit had to be expelled, protecting groups needed to be seriously and tactfully considered, and frustration was starting to make its way into the project picture. The failures that are about to be outlined led to the realization that "wow, this is a lot harder than I thought it was going to be" and "total synthesis doesn't care about your ideas on paper". Towards the end of this saga, my mentality shifted from "bold and provocative first, pragmatic second" to the prioritization of realistically achievable sequences that would reach the end goal in a concise and hopefully clever way.

With regards to the retrosynthesis of this approach, it was envisaged that an intramolecular glycosylation of **3.1** could furnish the core 9-membered ring system, similar to the strategy used by Nakata (**Figure 3.1**).[2] Stereochemistry of this event would be guided by the pre-organization of the system, which can only cyclize to form the desired diastereomer. Further, it was planned that a pyrrole dearomatization of a structure such as **3.3** could pave the way towards an enantio and diastereomerically pure pyrrolidine fragment **3.2** which could be coupled with ribose derivative **3.4** through seemingly simple S_N2 chemistry (it wasn't so simple – nothing ever is in this line of work…no matter how good you think your hands or ideas are).

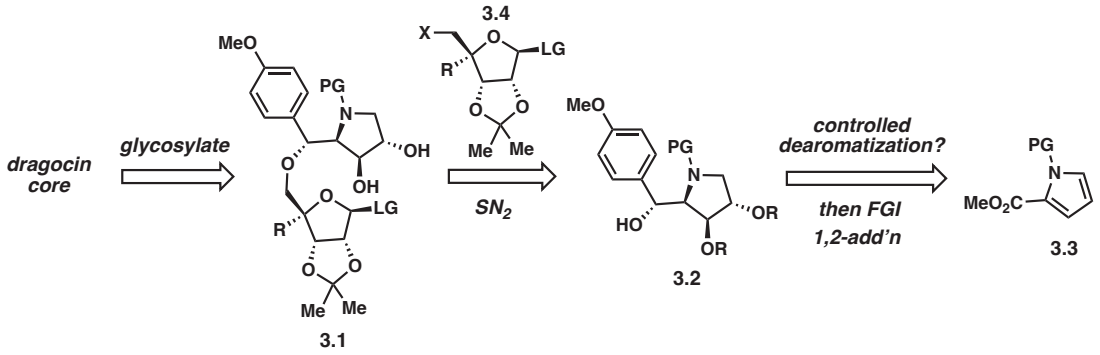
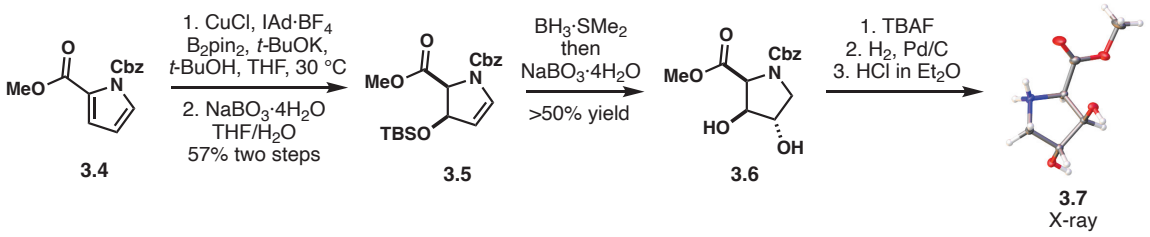


Figure 3.1 Intramolecular glycosylation strategy retrosynthesis

With an initial retrosynthetic analysis laid out, leaning on a convergent strategy of a densely functionalized pyrrolidine and ribose analogue, our initial priority was to identify a way to successfully dearomatize pyrrole **3.3** in a fashion that would allow for exquisite stereocontrol and precise installation of the polar hydroxy groups. Although it seemed far-reaching to achieve such a difficult sequence involving not only a dearomatization, but also difficult stereochemical quandaries, we were delighted and relieved to find a report from Ito and coworkers, which described a borylative dearomatization approach – which also happened to be enantioselective.[16] On top of that, the reaction methodology was reported to furnish the C2/C3 stereochemistry in a *syn* fashion by way of stereoselective protonation on a copper enolate species using a bulky *t*-BuOH proton source. When I found this report, I immediately ran to my only teammate at the time (now Prof. Mike Meanwell, University of Alberta) shaking the article in the air, claiming to have found the answer to the dragocin natural products (it wasn't the answer, unfortunately). After some convincing, we finally made the gear change to leave whatever we were doing and attempt to leverage this chemistry.

3.B. Forward sequence investigations

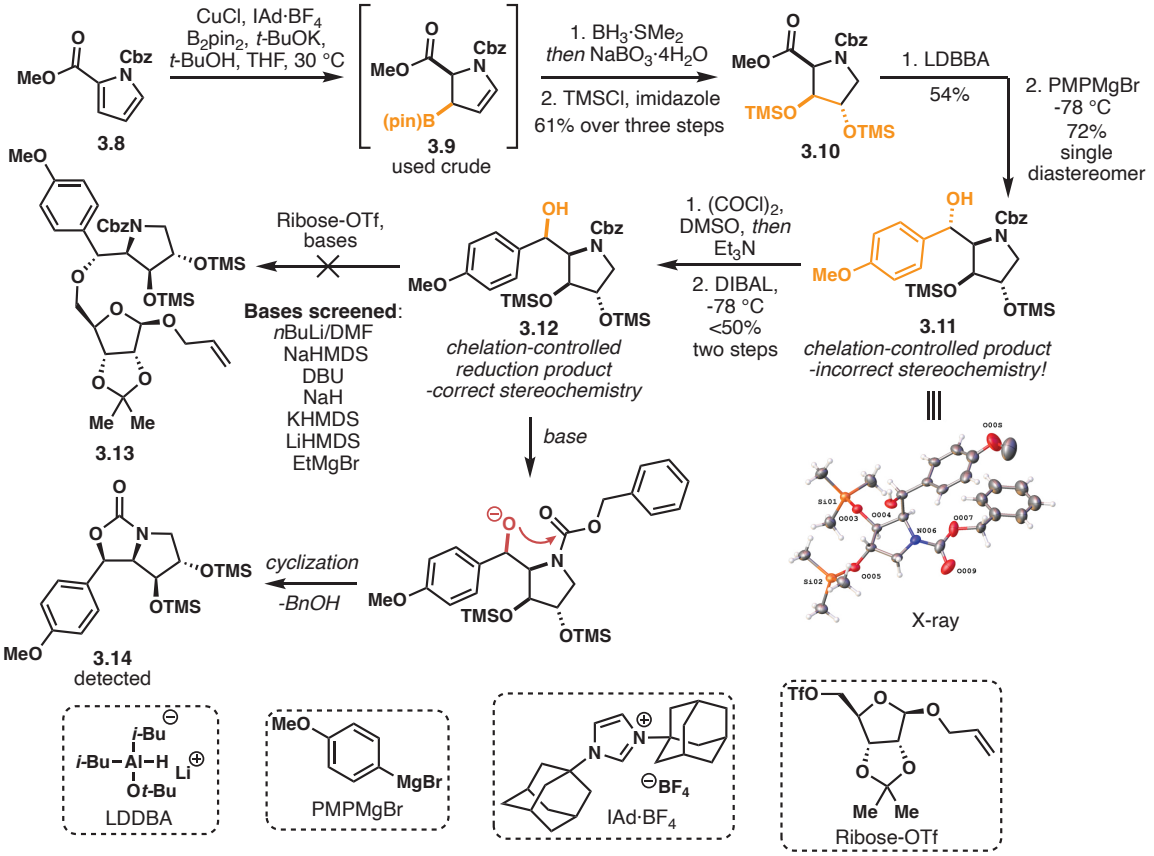
Our initial studies using this approach used a racemic version of Ito's dearomatization reaction. We noticed that the chiral ligand was going to have to be prepped ourselves and given that we were unsure what was going to be required to finish the pyrrolidine synthesis, we decided to move forward with racemic material. So, it was found that Ito's racemic dearomatization proceeded smoothly on **3.4**, which furnished an allylic boronic ester which could be oxidized crude to give an allylic alcohol which appeared to be surprising stable given the *anti* relationship between the ester α proton and the adjacent -OH. It was expected that rearomatization may occur, but this was not observed. This allylic alcohol XX was taken forward to a TBS protection to produce **3.5** and subsequently underwent a hydroboration/oxidation sequence which furnished diol **3.6**. This material was inevitably deprotected and crystallized for X-ray analysis to reveal **3.7**. To our relief at this juncture of the project, the relative stereochemistry of all reactions utilized gave perfect diastereocontrol – securing, for the first time, the stereotriad of the dense pyrrolidine. The "only" thing that we needed to do was introduce an arene *via* a 1,2-addition.



Scheme 3.1 Racemic route scouting leveraging Ito's dearomatization ultimately secured access to the stereotriad

With this proof-of-concept secured, we envisioned the employment of a similar sequence to produce substantial amounts of racemic pyrrolidine material (**Scheme 3.2**). Key to this new sequence would be the strategic hydroboration/oxidation of the allylic boronic ester, requiring only one oxidation step to the diol rather than two separate reactions. Delighted,

it was found that crude intermediary allylic boronic ester **3.9** underwent a smooth and high yielding hydroboration/oxidation[17] to furnish diol **3.10** after TMS protection.



Scheme 3.2 Key dearomatization sequence to explore 1,2 addition chemistry and downstream S_N2 reactions

Initially, we opted for TMS protecting groups, which were facile and straightforward to install and could be prepared on upwards of 20-gram scale. The resultant TMS-protected diol then served as a substrate for reduction to the corresponding aldehyde. After some experimentation it was found that LDBBA,[18] a bulky aluminum-based reducing agent, could provide one-step access to the aldehyde with satisfactory conversion profiles. Next, 1,2-addition reactions were explored using *para*-methoxy magnesium bromide as a nucleophile. Conveniently, this addition reaction proceeded smoothly and in high yield to furnish a single diastereomer. A considerable and incredibly frustrating amount of time was spent attempting to elucidate the relative stereochemistry of this product, as NMR was

futile given the dramatic rotamerism that was observed on this material (along with every single intermediate that was ever produced on this project that contained a carbamate). Finally, although not publishable, a preliminary X-ray report was obtained by the incredible team at the UCSD crystallography facility, revealing that the obtained isomer **3.11** was incorrect. A likely explanation for this outcome is the Cram-chelate model, wherein the Lewis basic Cbz protecting group coordinates and preorganizes the 1,2-addition transition state to yield a "chelation-controlled" product (**Figure 3.2**).[2, 19]

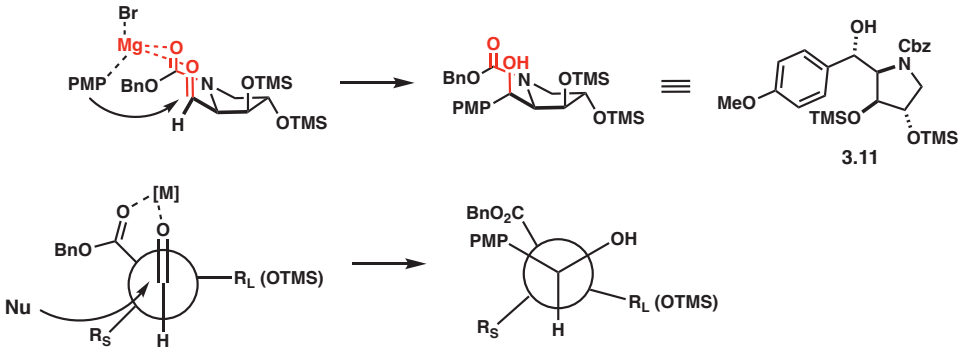


Figure 3.2 A possible Cram-chelate model to explain the selectivity of the 1,2 addition reaction

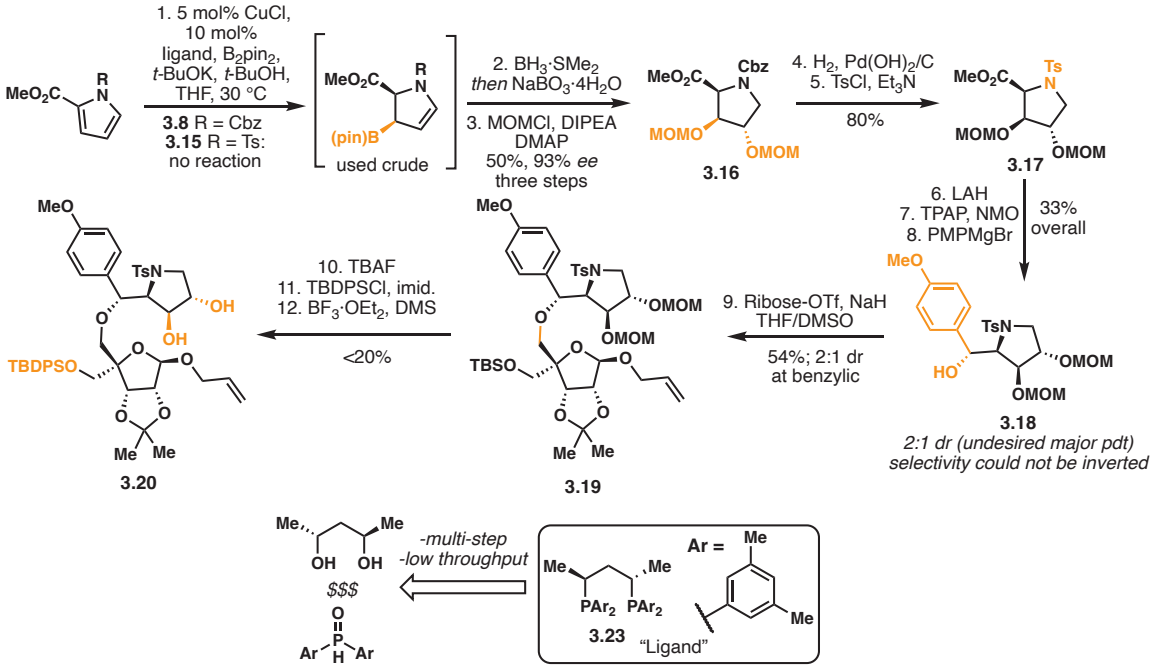
It was reasoned at this point that an oxidation/reduction could affect a formal isomerization of benzylic alcohol **3.11** – while leveraging the propensity for this system to "chelate" organometallic reagents. Thus, **3.11** was oxidized and reduced using a Swern/chelation controlled DIBAL sequence which gave the alternate and desired secondary alcohol **3.12**. With this material in hand, it was decided to attempt alkylation chemistries. Although the material that was accessed at this point was completely racemic, it was deemed worthwhile to investigate the behavior of this compound in subsequent reactions.

Alcohol **3.12** then became the focal point of the project. A series of bases were screened against this intermediate and were then attempted to be coupled to a triflated ribose derivative *via* an S_N2 reaction. Frustratingly, the desired product **3.13** was never obtained.

Instead, we observed the apparent cyclization of the putative alkoxide onto the pendant labile carbamate to give an oxazolidinone by-product (**3.14**),[2, 20] which was observed in crude mixtures. This type of cyclization is well documented and unsurprising – literature searches of alkoxide-based displacement reactions with an adjacent carbamate are nearly nonexistent in the synthetic literature. However, this result was unexpected as Nakata and coworkers reported a very similar S_N2 reaction on a very similar substrate in their total synthesis of AB3217-A. Employment of their conditions (*n*-BuLi, DMF) led to complex mixtures in our hands. With this failure behind, it was anticipated that a simple protecting group swap to a tosyl-amide would solve these issues.

To investigate the simple replacement of Cbz to Ts in this sequence, dearomatization of the parent pyrrole bearing a Ts protecting group was investigated. Unfortunately, these attempts were met with failure as there was no conversion detected when employing **3.15** as a substrate (**Scheme 3.3**). It was at this point in this strategy where the chiral ligand **3.23** was utilized in the dearomatization and was prepared through a cumbersome sequence. Nonetheless, enough ligand was prepared to provide gram-quantities to MOM protected diol **3.16**. MOM protecting groups were employed (instead of TMS) in this iteration to avoid protecting group compatibility issues upon the introduction of a TBS protected ribosyl diol. Following this step was the simple exchange of the Cbz group to a Ts group, which proceeded in a straightforward manner. It was disappointing that Ts-protected pyrrolidine **3.17** behaved poorly in the LDBBA reduction[18] to the corresponding aldehyde. Much higher yields and satisfactory conversions were obtained *via* exhaustive reduction the corresponding alcohol with LAH, followed by re-oxidation back up to the aldehyde.

Next, the 1,2-addition was explored to introduce the arene. Disappointingly, simple Grignard addition into the aldehyde proceeded in low yield to furnish an inseparable mixture diastereomers favoring the undesired isomer in a 2:1 ratio (**3.18**). At this point, a considerable amount of material was pushed forward to the Ts protected variant to investigate the optimization of this reaction. Unfortunately, the selectivity and yield could not be improved. Various common additives were explored which either gave no improvement or produced several byproducts. Boutique conditions were also investigated and were unsuccessful. It was then decided that a 2:1 mixture of diasteromers needed to be pushed forward in order to quickly and rapidly investigate the key ring closing reaction through the proposed intramolecular glycosylation.



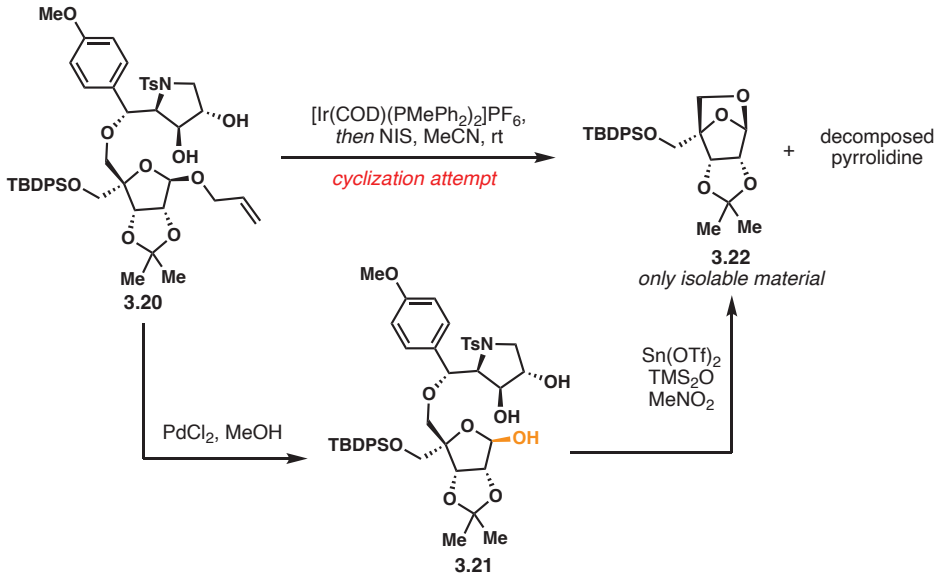
Scheme 3.3 Synthetic route to key intermediate **3.20**

With the frustrating 2:1 mixture of diastereomers in hand, it was a relief to find that **3.18** underwent smooth convergence with a functionalized ribose to give a mixture of separable benzylic diastereomers (**3.19**). At this juncture, the undesired isomer was used as sacrificial material to investigate the removal of the MOM protecting groups. This was an incredibly

discouraging and humbling pursuit (and exemplifies what was meant in the initial paragraph of this chapter section). Exhaustive time was spent attempting to remove the stubborn MOM protecting groups in the presence of multiple labile functionalities. It is not worth the time to explain what all that was done to remove these protecting groups. However, after several weeks of pushing more material forward to investigate this transformation, it was found that the TBS protecting group of **3.19** had to first be removed and replaced with a more robust TBDPS group to enable what inevitably was a low-yielding BF_3-mediated deprotection. This roundabout sequence ultimately resulted in loss of over 80% of the material, which was disappointing due to the incredible labor required to produce this intermediate (chiral ligand preparation was exhaustive, cumbersome, had reproducibility issues, and was expensive). With the little material that remained, it was now time to investigate the key question for this strategy: the intramolecular glycosylation. It is noteworthy at this point to acknowledge that this was the successful strategy employed by Nakata to forge the core ring system found in AB3217-A, which is nearly identical to that found in the dragocins (differs by the C3' ribose stereochemistry).

The stage was now set for the cyclization event. All that needed to occur was the simple isomerization of the allyl glycoside on **3.20** to the corresponding enol followed by subsequent treatment with NIS to promote the glycosylation.[21] Alas, another dead-end was realized. Activation of the enol proceeded rapidly to form a single product as the only obtainable material, identified as the collapsed ribose structure **3.22**. Intuition was suggesting that the wrong tree was being "barked up" and that the substrate was not poised for a successful cyclization event. As drawn, the substrate appears to be positioned

suggestively, allowing one to rationalize that glycosylation could reasonably take place given the apparent proximity of the free alcohol and glycosyl position on a simple 1D drawing. Plastic models suggested otherwise, where the failure of this cyclization can be rationalized by an unfavorable pre-organization of the substrate, placing the pyrrolidine an extensive distance from the reactive anomeric center. Additionally, the electron-rich arene could feasibly assist the departure of the C5' alcohol to attack the putatively formed carbocation intermediate and form the isolated material.



Scheme 3.4 Failed intramolecular glycosylation

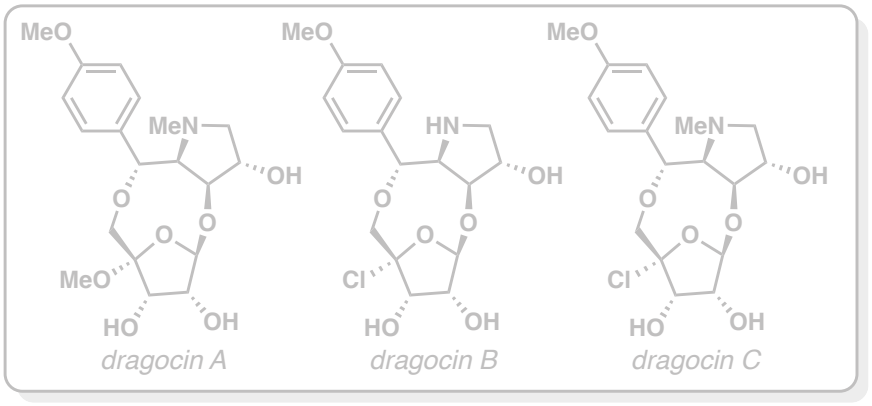
Despite all the reasons why it could be reasoned not to investigate this cyclization further, an alternative substrate was employed which lacked the C4' functionality found on **3.20**. To be short, attempts to cyclize this material were met with utter decomposition and no tractable byproducts were found in the crude mixtures.

Returning to **3.20** and the few milligrams that remained, it was reasoned that the allyl group could be removed to unveil a free glycoside which may behave differently in the cyclization attempts. Deprotection was enabled through the use of $PdCl_2$/MeOH to procure **3.21** and a

Sn-mediated activation[22] was attempted. Dishearteningly, the only observed product from this glycosylation protocol was collapsed ribose byproduct **3.22**. Attempts to activate with acids such as TsOH appeared to give no conversion, even at elevated temperatures. While it seemed desirable to further investigate this strategy by installing different leaving groups, the polyhydroxylated nature of the material made it difficult to investigate the installment of other glycosyl donor groups. This felt like a shot-in-the-dark that had no reasonable chance for success based on these failures and bringing up yet another batch of ligand to produce more material felt virtually useless.

After thoughtful consideration of labor vs. reward and the tremendous failure, it was deemed that a new strategy would be required to access the core ring skeleton. Two key lessons were learned from this approach: 1) while powerful, the dearomatization sequence lends itself to a protecting group juggling event that leads to a mixture of inseparable diastereomers in the end – perhaps a new route needs to be developed. 2) the highly functionalized and protected ribose may have caused problems in the cyclization event – is there a lower oxidation state surrogate that can be employed which circumvents protecting group chemistries and could also address the challenging C4' oxidation?

With these two lessons heavily contemplated, a new strategy was employed towards the dragocins and will be discussed in detail in the next chapter.



Chapter 4:

A Furan-based Approach Backfires: Escapades in Medium-Sized Ring Formation

4.A. Rationale behind this approach and a new pyrrolidine synthesis

As was foreshadowed in the previous chapter, it was reasoned that the presence of multiple protecting groups and functionalities may have caused the failure of the intramolecular glycosylation approach. If it wasn't directly to blame for the failure, it certainly caused extensive material throughput issue that stymied further efforts. Given that the dragocins featured oxidation at the C4' position, it was envisioned that perhaps a furan derivative such as **4.1** could be cyclized and dihydroxylated after oxidation of the parent furan **4.2** (**Figure 4.1**).

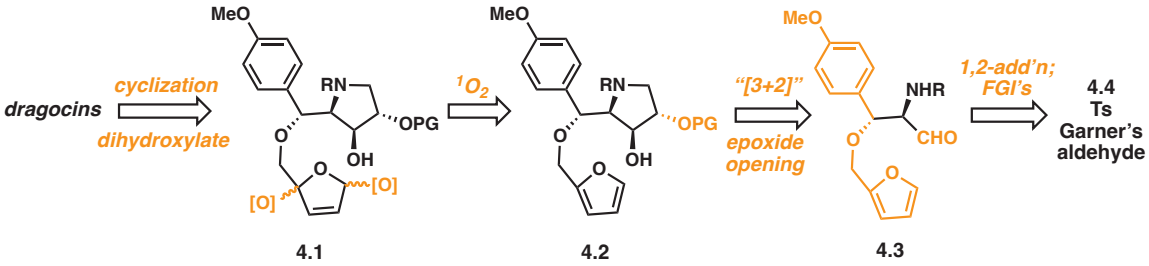


Figure 4.1 A new furan-based approach towards the dragocins

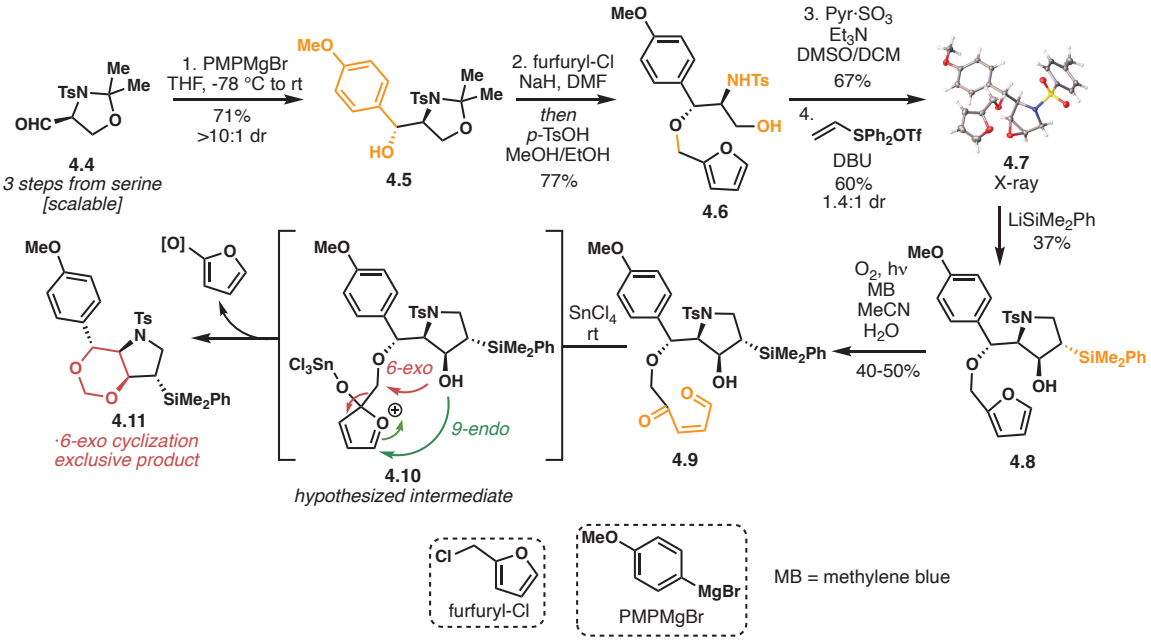
With this general blueprint laid out, a new pyrrolidine synthesis that was compatible with any potential furan-related motifs would be required. At this point, nearly every conceivable reasonable disconnection had been explored to produce a synthetically useful pyrrolidine fragment. After brainstorming for an afternoon, it was realized that this fragment could arrive from an alternative "[3+2]" manner leveraging an amino aldehyde and a reactive ylide to forge the core of the pyrrolidine. Luckily, literature searches revealed that this disconnection has been synthetically explored for pyrrolidines – specifically epoxy-pyrrolidines. However, it's use in total synthesis did not appear to be common. Nonetheless, it was planned that the key epoxy-annulation (initially reported by Aggarwal[23]) could take place on an aldehyde such as **4.3**, which could eventually arrive from a tosylated version of Garner's aldehyde (**4.4**) through a known highly

diastereoselective 1,2-addition.[24] A key epoxy-pyrrolidine could then be ring opened from the more sterically accessible side of the pyrrolidine to furnish material that would ideally be nearly ready to cyclize after the dearomatization event of the furan moiety. The oxidized furan could then be cyclized with the pendant secondary alcohol of the pyrrolidine through various Lewis acid-based conditions. After a final dihydroxylation of the dihydrofuran, the synthesis of the dragocin core with all oxidations in place would be established.

4.B. Initial forward sequence and a surprising cyclization result of a dicarbonyl

As was envisioned in the retrosynthetic analysis, the use of a tosylated version of Garner's aldehyde (**4.4**, **Scheme 4.1**, three simple steps from serine[24-25]) was leveraged to furnish 1,2-addition product **4.5** with >10:1 dr. It was found that this material was quite sensitive to acid and had to be isolated under neutralized basic chromatography conditions and required NMR samples to be prepared in deuterated benzene (as opposed to $CDCl_3$). Regardless, the material was stable to storage and thus large quantities of this material was prepared to enable extensive further studies. Next, **4.5** was engaged in an S_N2 reaction with the reactive furfuryl chloride (prepared from the corresponding alcohol[26]) and deprotected under acidic conditions to furnish amino alcohol **4.6**. Surprisingly, the next oxidation up to the aldehyde was unexpectedly challenging. Canonical Swern[27] or DMP-based[28] conditions resulted in complex mixtures, likely explained by the doubly-benzylic ether flanked with two electron-donating arene systems. Nonetheless, smooth oxidation was observed upon the employment of Parikh-Doering conditions[29] to provide a key amino aldehyde, the material of which would be investigated in the new pyrrolidine disconnection. The ensuing epoxy-annulation[23] [3+2] reaction took place in good yield

with a 1.4:1 ratio of separable epoxide diastereomers. At this juncture, the unambiguous assignment of the two isomers via NMR required X-ray analysis. High-quality crystals were grown, confirming that the slightly favored product was indeed the desired isomer **4.7**. With this material in hand, attention was turned to the ring opening of the epoxide. Initially, various oxygen-based nucleophiles failed to provide any ring-opened product, despite screening various additives and conditions. To be brief, the first condition that provided some sort of clean desired material was the use of a lithiated silane,[30] which was found to ring open the epoxide to give 37% yield of **4.8**. Although the introduction of this specific functionality was not ideal, this reaction enabled the exploration of downstream chemistry. It was deemed that in a worst-case scenario Tamao-Fleming[31] type reactions could be employed to exchange the silane into an alcohol.



Scheme 4.1 Initial furan explorations led to an unexpected 6-exo cyclization product

It was now time to explore the dearomatization reaction of the previously installed furan motif. After some preliminary frontline reactions, it was found that a singlet oxygen promoted reaction provided dicarbonyl **4.9** in moderate isolated yields, with no traces of

the hydrated lactol form. This aldehyde could be isolated with rapid chromatography and was stable in $CDCl_3$ solutions, which was surprising. With this dicarbonyl in hand, it was proposed that an activated intermediate, such as **4.10**, could be formed through Lewis acid treatment. Thus, $SnCl_4$ was employed to form a hypothetical oxonium. Unexpectedly, the reaction proceeded to provide a single major product which had appeared to lose any furan-related functionality, which was perplexing. After isolation and more extensive NMR analysis, the major product was characterized as **4.11**, a peculiar cyclic 6-membered acetal. In hindsight, it was rationalized that this product arises from oxonium **4.10**, but proceeds through a 6-exo mode rather than the desired 9-endo mode.[32] This was unanticipated, but unsurprising upon inspection of all possible side reactions of the putative reactive oxonium. Surely a 9-membered medium ring formation would be difficult with the ability to form a 6-membered ring while rearomatizing a leaving group.

Yet another failed medium-sized ring formation was realized, but a slightly different tactic was employed in the next iteration of this furan-based strategy.

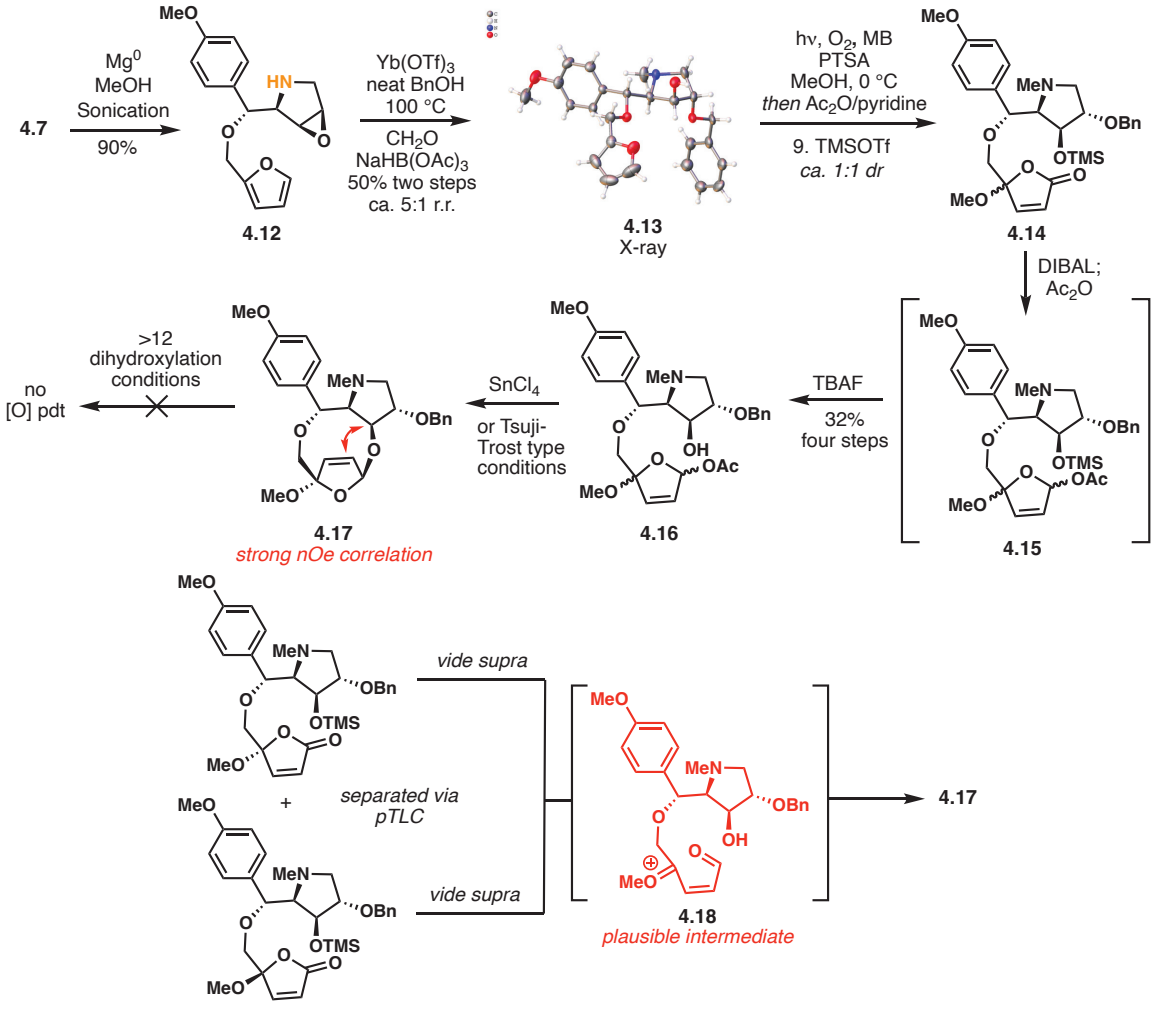
4.C. Breakthrough in an oxygen-based nucleophilic epoxide opening and an undesired 9-membered *endo* isomer in a butenolide-focused approach.

With the failure of the dicarbonyl cyclization behind, a slightly different furan oxidation was planned as shown in **Scheme 4.2** . To be specific, it was envisioned that the furan could be oxidized up to a γ-methoxy butenolide, reduced to the lactol/trapped as the allylic acetate, and activated for cyclization using Tsuji-Trost chemistry[33] or other Lewis acids.

Before the investigation of this furan dearomatization tactic, attention was focused on solving the problem of how to introduce oxygen-based nucleophiles *via* the epoxide ring opening reaction. It was hypothesized that the tosyl protecting group may have caused reactivity issues by complicating the formation of activated (or chelated) epoxide intermediates through steric or electronic deactivation effects. Breakthroughs in reactivity were obtained when the tosyl protecting group was removed prior to activation for ring opening. After some experimentation, it was found that catalytic ytterbium triflate[34] in hot benzyl alcohol conveniently activated **4.12**, providing ring-opened product **4.13** with good regiochemical selectivity and yield after methylation under reductive amination conditions. These isomers were inseparable, but the ratio was deemed synthetically serviceable to investigate the butenolide strategy. It was found that the furan in **4.13** could be dearomatized in methanol with singlet oxygen.[35] The resultant endo-peroxide was then acylated and eliminated to form the desired butenolide **4.14** in a 1:1 diastereomeric mixture after TMS protection. It was hoped that this mixture could be resolved to some degree in the cyclization event through a ring-chain tautomerization-like mechanism (which would soon be the cause of a dead-end). Reduction of the butenolide, *in situ* acetylation of the aluminum alkoxide[36] and removal of the TMS group set the stage another cyclization attempt using **4.16**.

$SnCl_4$ was employed yet again as a Lewis-acid in the initial attempts to cyclize and forge the elusive 9-membered ring. It was encouraging to observe conversion of the starting material to a less polar TLC spot (which was conceivably some sort of cyclized material). Isolation efforts revealed a low yielding product which appeared to have the desired mass

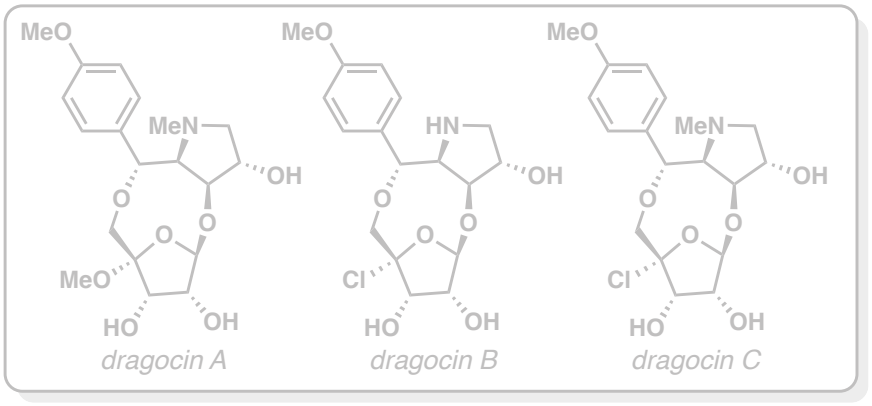
of the target material. Although mass balance was low, it was reasoned that if the cyclized material was correct, the project would be near an end. After extensive and thorough NMR analysis, a smoking-gun nOe correlation was observed that unveiled the true identity of the cyclized material: the undesired *endo* isomer **4.17**. Tedious pTLC separation of the butenolide diastereomers revealed that acyclic methoxy diastereomers funneled to the same product, albeit in low yield. An explanation for this is the formation of ring-chain tautomer-like intermediate **4.18**, which could potentially lead to the formal isomerization/cyclization of both butenolide diastereomers.



Scheme 4.2 Second genearation furan approach via a butenolide intermediate. An undesired *endo* isomer was formed. Separation of the two butenolide diastereomers revealed funneling through **4.18** to produce **4.17**

As a last-ditch attempt to coax the material into cyclizing in the desired fashion, Tsuji-Trost conditions were explored,[33a] including Trost ligands which were hoped to assist diastereoselectivity of the cyclization through match/mismatched transition states. Unfortunately, these attempts were unsuccessful, and the furan strategy had reached a screeching halt. The realization that another generation of exploration would be required was difficult to accept. Luckily, there was one last strategic disconnection that could be leveraged which inevitably led to the successful synthesis of dragocins A–C. However, this ensuing strategy didn't proceed without a grueling and emotional rollercoaster of a fight.

Chapter 5 will discuss this new disconnection, considerations on why it appeared to be promising at its initial planning stage, the failure of a demanding C–H oxidation strategy, and the final successful approach which involved an electrochemical cyclization and decarboxylative chlorination event. Additional details regarding this approach will also be discussed.



Chapter 5:

Journey's End: An Emotional Rollercoaster Filled with Triumphs and Tragedies

5.A. Discussion of a new disconnection through an oxidative cyclization

With the heavy failures that were now left behind, careful consideration of the next approach towards the dragocins needed to be carefully contemplated. Over two years had been now spent on the project and there were several key questions remaining. The pyrrolidine fragment appeared to be a solved problem, leaving the elusive 9-membered ring and the C4' oxidation, which had seen almost no experimental attention at this point.

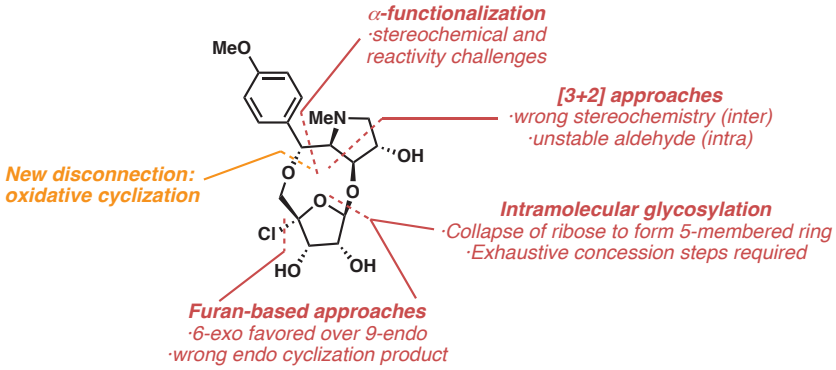


Figure 5.1 Failed approach summary and the new disconnection via an oxidative cyclization

A key realization occurred while building plastic models, which suggested that glycosylation prior to a cyclization event would lock the conformation in such a way that the system appeared to be much more poised to form a 9-membered ring than in the other failed approaches. Restricted rotation about the glycosyl position rendered the C5' alcohol of the sugar within proximity of the benzylic position. If a simple pyrrolidine fragment could be coupled to a properly functionalized ribose component, a cyclization could feasibly be leveraged in some way to construct the core skeleton of the targets. Specifically, the electron rich arene opened up the opportunity for a late-stage oxidative cyclization with the C5' alcohol of the pendant ribose moiety. It was envisaged that multiple modes of benzylic activation could be explored. For example, direct

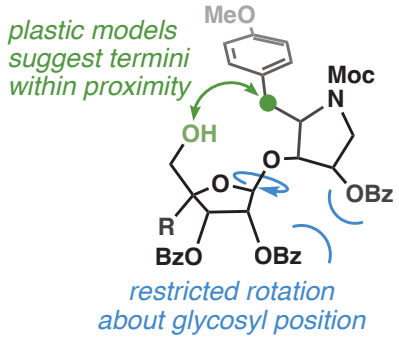


Figure 5.2 Plastic models revealed a promising conformation for the new oxidative cyclization strategy

cyclization with reagents such as DDQ or benzylic bromination followed by an S_N1-type displacement could be explored. Retrosynthetically, the dragocins could be forged through the key oxidative cyclization of **5.1** and C–H oxidation after glycosylation of **5.2** with a simple ribose donor. At this point, it was envisioned that the same epoxy-annulation and epoxide opening chemistry could be leveraged as before. Beginning with **5.4**, the Aggarwal annulation conditions could provide **5.3**, which could be ring opened to furnish **5.2**. Either way, the arene system inspired the consideration of a key quinone-methide type intermediate such as **5.5** that could be intercepted to realize a cyclization event.

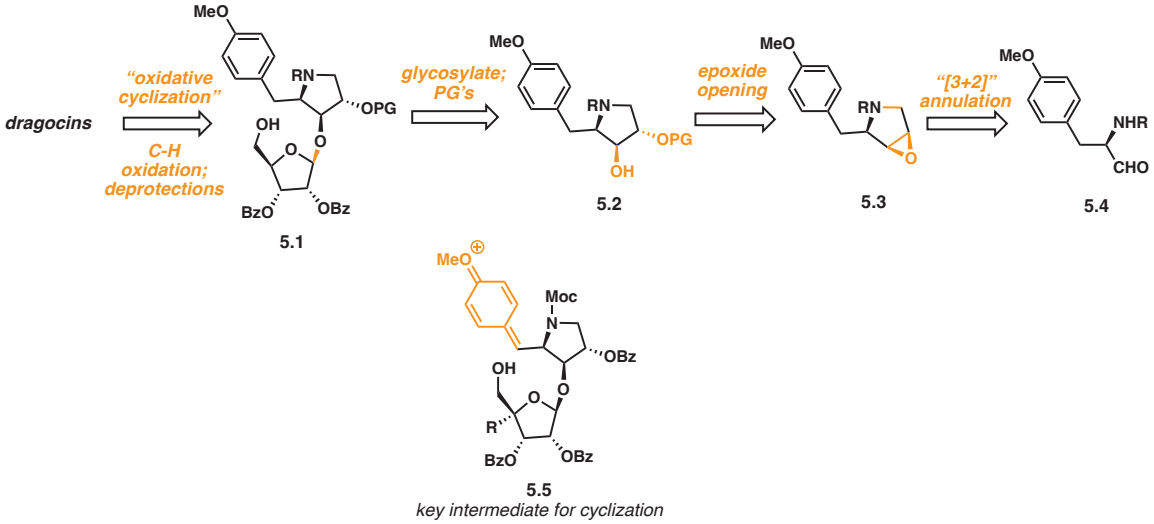


Figure 5.3 Retrosynthetic analysis featuring the new oxidative cyclization disconnection and a late-stage C–H oxidation approach to install the C4' functionality

With regards to the vexing C4' functionalization problem, it was initially planned in this specific iteration to arise from a C–H oxidation of a late-stage intermediate following the cyclization chemistry. Although this proposed functionalization would be incredibly demanding given the nature of the skeleton, it was speculated that the C4' position was uniquely activated given the dragocin's relationship to AB3217-A (which lacks the C4' oxidation and has a hydrogen instead). Perhaps an enzyme was evolved for this type of transformation and/or the C4' hydrogen was unusually primed for C–H abstractions.

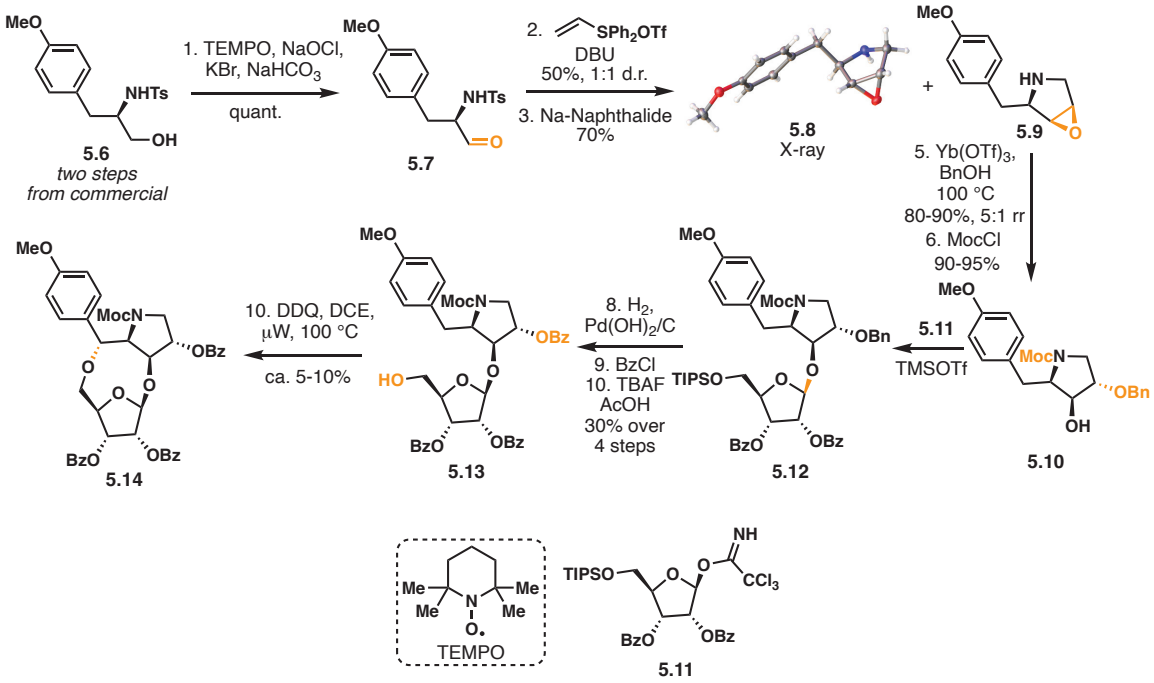
In this strategy, the pyrrolidine was imagined to arise through a nearly identical sequence that was developed in the furan saga. A simple amino alcohol could be accessed, leading way to the epoxy-annulation and ring opening chemistry, ultimately furnishing a properly functionalized pyrrolidine that could be converged *via* glycosylation to a protected ribose derivative.

5.B. First successful route towards the 9-membered ring

As mentioned previously, the route towards the pyrrolidine in this new retrosynthetic iteration towards the 9-membered ring would be straightforward as it would follow the identical blueprint that was utilized in the furan approach.

Unnatural tyrosine analogue **5.6**[37] served as a satisfactory starting point for this new pyrrolidine fragment. A simple tosyl protection of the nitrogen and subsequent borane reduction furnished amino alcohol **5.6** smoothly on decagram scales from a commercial amino acid. With this particular amino alcohol, Parikh-Doering conditions yielded a complex mixture of products. Anelli's conditions,[38] on the other hand, gave smooth conversion to the corresponding aldehyde **5.7** without any traces of racemization. This aldehyde was then subjected to the same epoxy-annulation sequence that was utilized in the prior generation (see chapter 4). However, this time, the reaction proceeded with slightly lower diastereocontrol (**5.8** and **5.9**, 1.1:1 instead of 1.4:1), which made it difficult to comfortably assume the marginally favored product was still the desired epoxide diastereomer. To add to the challenge of unambiguous characterization of the two products,

they were found to be inseparable, which hindered any efforts for X-ray analysis. It was decided to remove the tosyl group, which furnished a tightly separable mixture of epoxy-pyrrolidines that could be crystallized for X-ray. The X-ray crystal structure of the undesired isomer **5.8** was confirmed, and the alternate isomer **5.9** was taken forward into the ring opening chemistry using neat benzyl alcohol and ytterbium triflate at elevated temperatures (see chapter 4). A similar regiochemical ratio of ring opened isomers was observed (ca. 5:1) and was provided in good yield to secure a functionalized stereotriad-containing pyrrolidine **5.10** after Moc protection. A methyl carbamate was chosen as opposed to Boc to avoid any undesired cyclization of the carbamate onto the adjacent hypothetical benzylic carbocation that was planned to be formed (Ts and Cbz was investigated at a very early stage of this approach but no cyclization material was observed upon treatment with DDQ at high temperatures, *vide infra* for DDQ discussion).

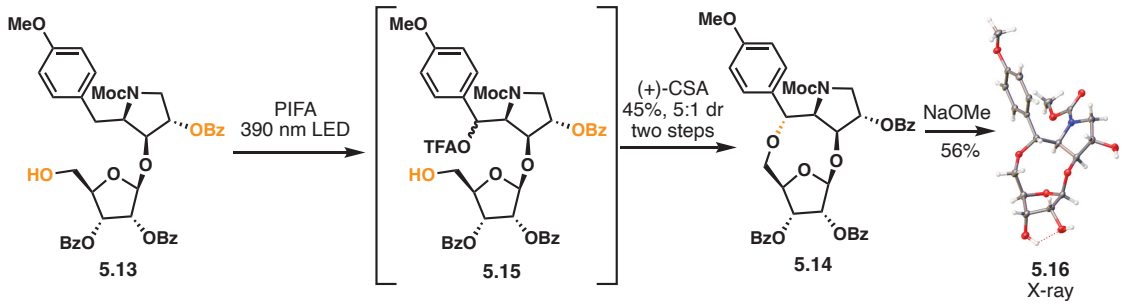


Scheme 5.1 First successful generation towards the key 9-membered ring system using a DDQ cyclization

With pyrrolidine **5.10** in hand, a simple Schmidt glycosylation[39] using ribose **5.11** provided converged material **5.12**, which was then subject to TIPS removal and a protecting group swap. This acyclic precursor (**5.13**) then served as the first-generation substrate for the proof-of-concept of an oxidative cyclization strategy. After some initial experiments, exploring Ts, Cbz, and Moc protecting groups, it was found that the Moc protected variant gave a faint new spot on TLC upon subjection to DDQ[40] at elevated temperatures, which was much less polar than the starting material. UPLC analysis suggested that this new product had the desired mass of our key 9-membered material. Isolation efforts revealed that **5.14** was produced in low yield and with poor conversion profiles. Nonetheless, enough material was isolated on slightly larger scales (ca. 5-10 mg) to begin NMR analysis, which was futile due to the rotamerism of these carbamate containing structures. It was decided that the Moc protecting group should be first removed to enable full characterization. Moc and benzoate removal was achieved using Red-Al at high temperatures, ultimately revealing that for the first time, the desired 9-membered skeleton was produced and with the desired stereochemistry (not shown).

This was an incredibly exciting time that marked the beginning of an exhausting 12-month campaign to bring the project to a sure-fire close. Unfortunately, the DDQ-mediated cyclization was too low yielding to produce enough material to fuel extensive C–H oxidation efforts. Attention was then turned towards developing two-step protocols which would first install a labile benzylic functional group that could be activated and cyclized to form the desired ring. First, NBS mediated conditions[41] were explored but were found to be low yielding due to decomposition of the product and or starting material under the

conditions employed. With the small amount of benzylic bromide starting material that was produced, it was found to be resistant to various forms of activation. With this failure, it was hypothesized that perhaps a benzylic acetate motif could be more easily activated towards ionization. Indeed, it was found that PIFA-mediated conditions[42] smoothly and reproducibly afforded benzylic trifluoroacetate **5.15** as a mixture of diastereomers. This product could be chromatographed and were stable to storage overnight. With this material in hand, it was found that CSA was an effective promotor of cyclization in DCE. Diastereoselectivities in this solvent mixture were serviceable but further optimization was warranted. A screen of various acids and solvent mixtures were explored which revealed ACN and (+)-CSA to be the optimal solvent for both yield and diastereoselectivity. These new conditions were then employed to produce enough **5.14** to fuel sufficient exploration of the impending C–H oxidation. Additionally, debenzoylation of **5.14** provided **5.16**, which unassailably confirmed the structure *via* X-ray analysis. This was a very exciting time in the project.



Scheme 5.2 Improved two-step protocol to generate serviceable quantities of **5.14**

5.C. Spectacular failure of a demanding C–H oxidation at C4'

A discussion of why this approach was considered for such a chemoselectively demanding reaction is warranted. Given the close structural relationship of the dragocins to AB3217-A, which lacks the C4' oxidation, it was hypothesized that this position was uniquely

activated towards C–H abstraction and/or activation pathways and certainly justified an in-depth investigation.

Summarized below in **Figure 5.4** are the attempts to functionalize said position through various means, including radical, dioxirane, photochemical, directing group, and other methods. The failure of these approaches is likely due to the chemoselectivity challenges of the listed substrates. An electron-rich arene, pyrrolidine, multiple activated etheric positions and C–H bonds are all most likely to blame. Additionally, HSQC spectra of compounds such as the ones shown below reveal no substantial difference in ^{13}C NMR shifts, suggesting that there is no clear electronic difference in any of the aliphatic C–H bonds found on these structures.

As a last-ditch attempt, it was decided to send material to Prof. Hans Renata (Rice) to screen either P450's or chlorinase enzymes to see if they could functionalize the desired position. To date, this approach has been unfruitful (data not provided).

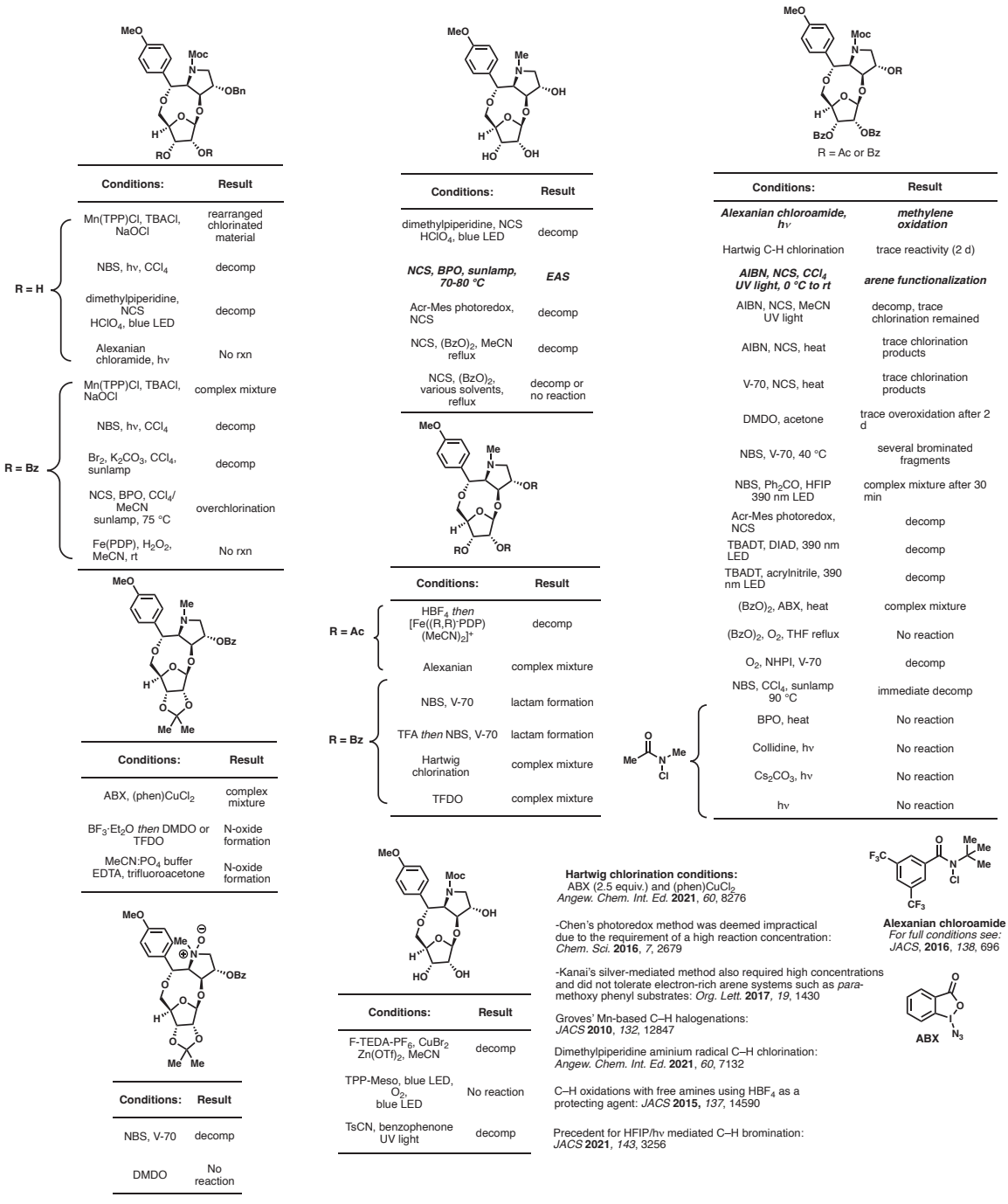


Figure 5.4 Failed late-stage C–H oxidations of various cyclized materials

After nearly 8 months of exhaustive screening, producing various analogues by which to test C–H oxidations and developing a laborious route for installation of directing groups (which was met with failure, see **Figure 5.5**), the decision was made to investigate an alternative strategy to introduce the key C4' oxidation through C–C bond cleavage.

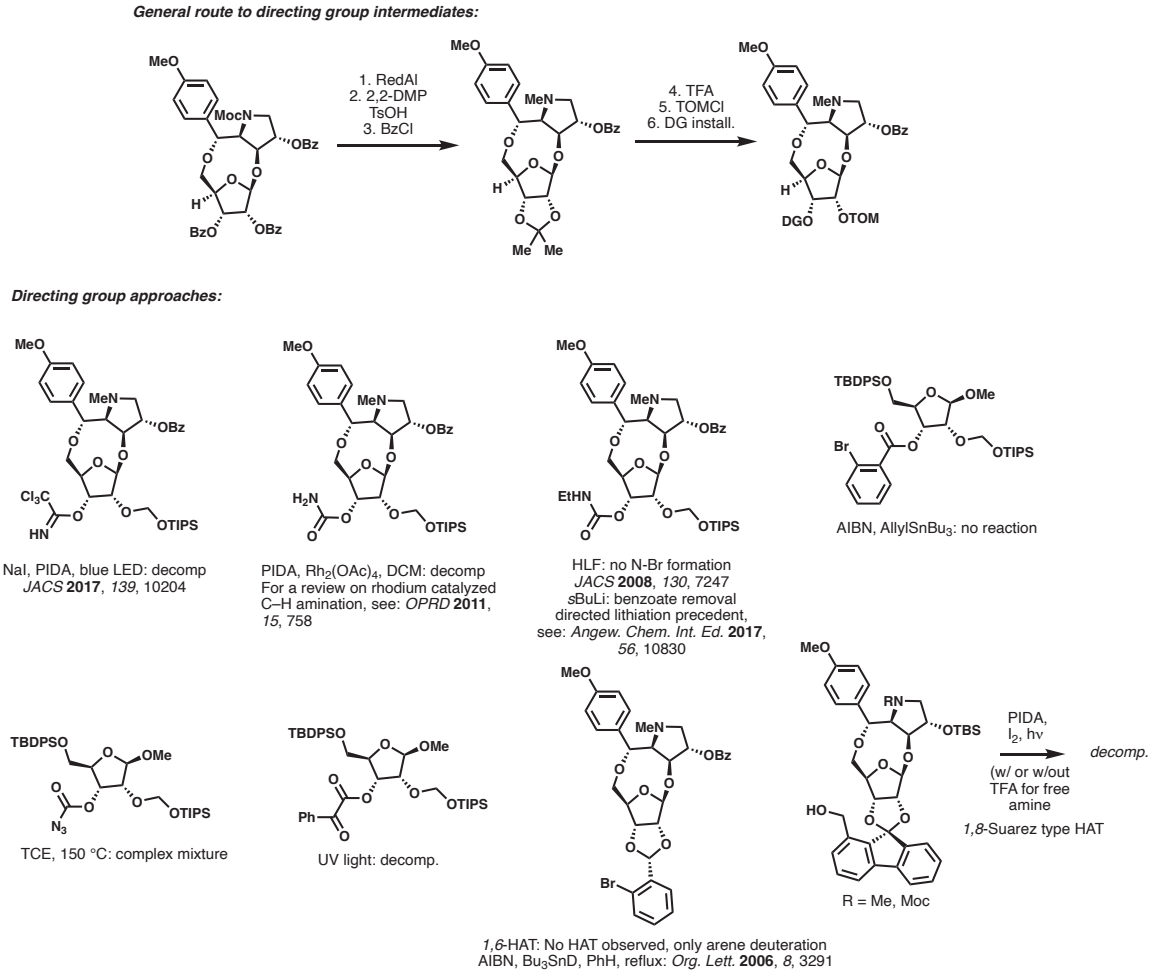


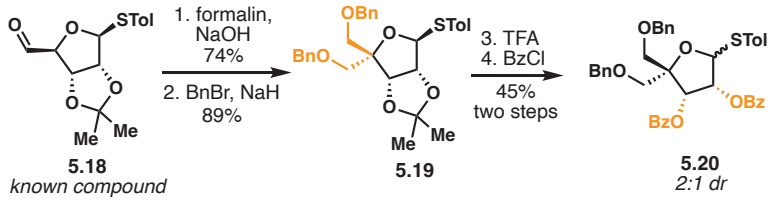
Figure 5.5 Route towards directing group substrates and the failed results

5.D. A new C4' strategy via decarboxylation and throughput improvements

At this juncture, the project was nearing the three-year mark. Frustration was at an all-time high and things became quite morose, believing that these natural products – despite their deceptively simple architecture – were simply unattainable.

There were some bright sides, though. The skeletal framework had been solved, and all that was needed was a peripheral synthetic manipulation. For what would become the final

route towards the dragocins, it was envisioned that ribose **5.20** (**Scheme 5.3,** produced from **5.18** through a Cannizzaro reaction to make **5.19** which was subject to a protecting group swap), importantly containing an oxidized carbon handle for late-stage decarboxylation[43] or other C–C bond cleaving events, could be converged in at the glycosylation stage and subsequently cyclized using the same PIFA/CSA sequence as before. Before the successful endgame is described, several improvements were made to the route to streamline material throughput towards efforts focused on the new key C–C cleavage chemistry.



Scheme 5.3 Production of a new ribose donor **5.20**

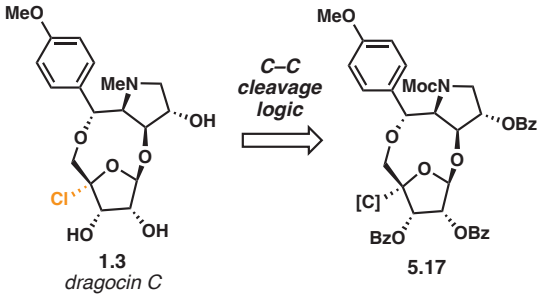


Figure 5.6 A new C–C bond cleavage strategy

Throughput improvement to epoxide 5.23 (**Figure 5.7**) : The first improvement that was made regarded the pesky 1:1 ratio of diastereomers that were formed in the epoxy annulation reaction. Key to the success of the inevitable breakthrough is thanks to Pranali Bedekar, who paved the way on obtaining the results for what is about to be described. Initially, it was hypothesized that various modified annulating reagents could coax the desired diastereomer to be favored. Unfortunately, this was found not to be the case, as this original diphenyl variant proved superior to other substituted arenes (data not shown). Several months of investigation were done on Pranali's end whilst consulting with either Nate or I on the results. Attempts to improve this reaction with said new annulating reagents

proved fruitless, so it was decided that a phosphonium-based annulation[44] could lead to a dihydropyrrole instead of an epoxidized intermediate. This reaction proceeded smoothly to our delight, furnishing **5.21** in good yield. Although this would add a step to the current route, it was imagined that this dihydropyrrole intermediate could be employed as a substrate for a diastereocontolled epoxidation or dihydroxylation event. Several weeks were spent attempting to epoxidize or dihydroxylate **5.21**, which proved futile. Leaning back upon lessons learned in the epoxide ring opening chemistry – where the Ts group was found to interfere with efficient epoxide functionalization – attention was turned to removing the Ts group before attempting to oxidize the olefin. After some investigation, Pranali found literature supporting an ammonium-assisted epoxidation of allylic amines.[45] Cleverly, she hypothesized that a protonated form of **5.22** could potentially lead to a diastereoselective epoxidation process. Indeed, following some initial investigations, it was found that protonation of **5.22** with TsOH followed by epoxidation with peracetic acid smoothly afforded a 4.5:1 crude mixture of epoxide diastereomers (62% isolated of **5.23**) which were found to be separable on SiO_2.

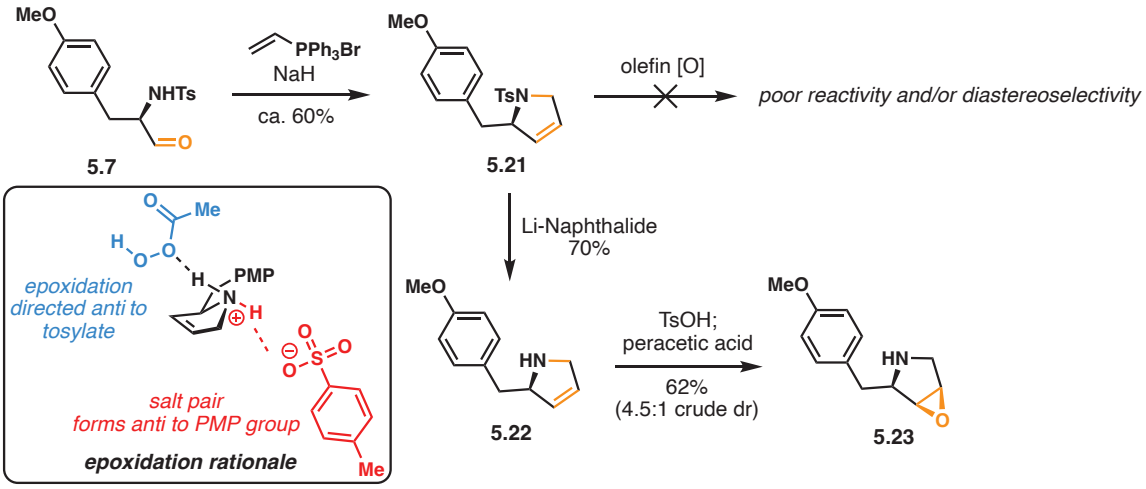
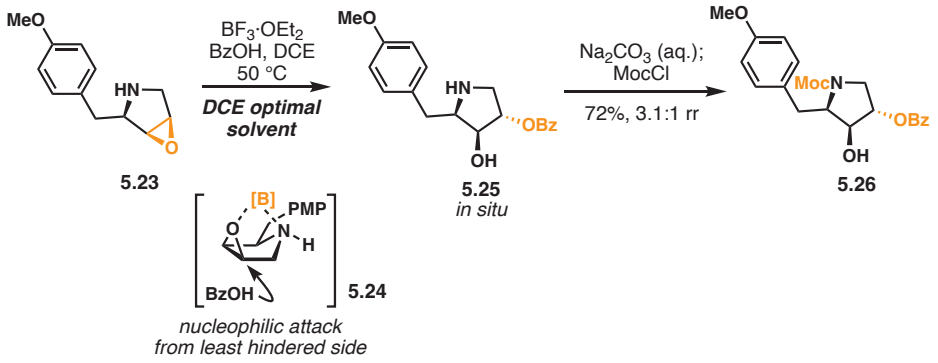


Figure 5.7 A new way to generate the key epoxide intermediate through an olefin epoxidation strategy

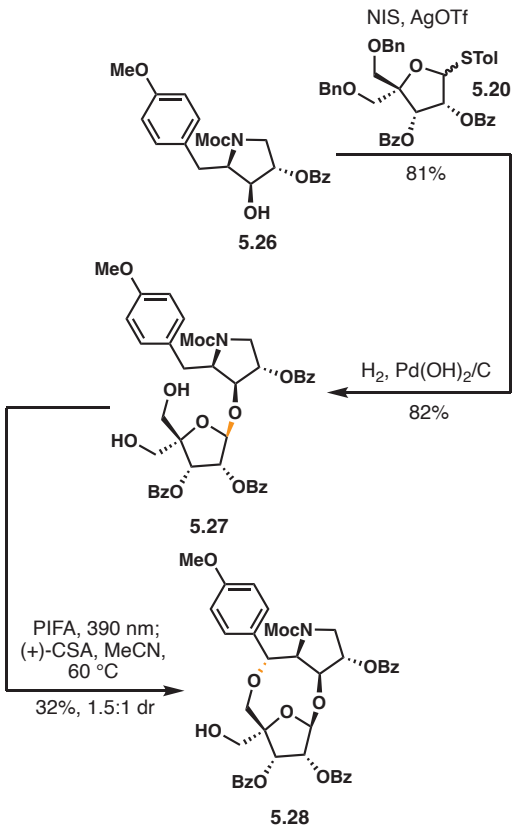
***Epoxide opening with a benzoic acid nucleophile*:** With improved conditions to access epoxide **5.23**, the next focus became avoiding the introduction, removal, and replacement of a benzyl ether by opening the epoxide with benzoic acid nucleophiles as shown in **Scheme 5.6**. This transformation required little attention, as it was quickly found that $BF_3{\cdot}OEt_2$ was an effective promoter of this process utilizing benzoic acid as the opening agent. Good regiochemical ratios and yields were observed for this reaction. Notably, an *in situ* Moc protection was employed to avoid the isolation of an otherwise polar free-amine intermediate. This Moc protection proceeded smoothly with Schotten-Baumann-like conditions after full conversion of the epoxide **5.23** was observed to **5.25**, resulting in a total yield of 78% **5.26** with a 3.1:1 rr of opening products favoring the desired isomer. With an ideal route towards **5.26** secured, the endgame strategy leveraging C–C cleavage was explored.



Scheme 5.4 Ring opening with BzOH using a BF_3 Lewis acid promoter.

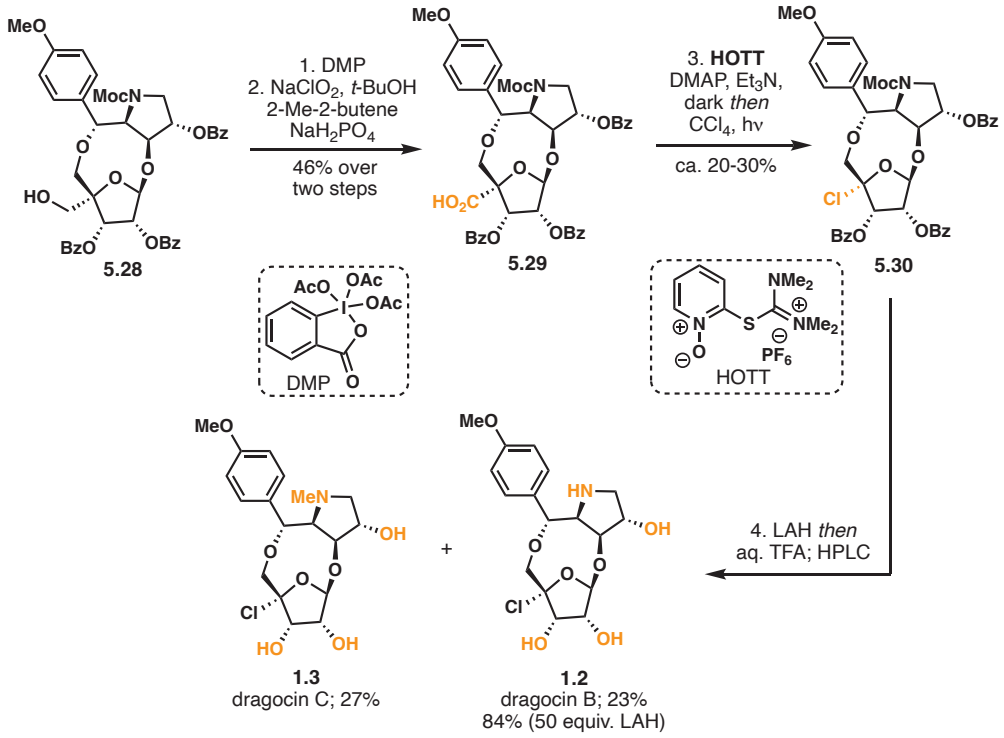
5.E. The endgame

In this chapter subsection, the final strategy for the dragocin natural products will be described. To begin as shown in **Scheme 5.7**, ribose donor **5.20** (four steps from known **5.18**) was subject to activation with NIS/AgOTf,[46] which smoothly coupled with



Scheme 5.5 Glycosylation and cyclization to produce key 9-membered ring for the C–C cleavage approach.

pyrrolidine **5.26** to furnish glycosylated **5.27** in 81% yield as a single diastereomer after benzyl removal, which would serve as starting material for all future cyclization studies. To our relief, it was found that the same PIFA/CSA sequence could be employed to provide cyclized **5.28** in 32% yield with a crude dr of 1.5:1. Although not ideal, this yield was serviceable to begin exploring how a C–C bond cleavage event may take place. It was hypothesized that a decarboxylation may be the most facile C–C bond cleavage to exploit, with an extensive *Chemical Reviews* article describing numerous ways to effect a decarboxylative halogenation.[43] Apparent in this review is the presentation of the Barton decarboxylative halogenation protocol,[47] which is both mild and neutral in nature. Given the recent failure of the exposure of key late-stage materials with aggressive oxidants (see C–H oxidation failures above), it was deemed that Barton's protocol would give the highest chances for success.

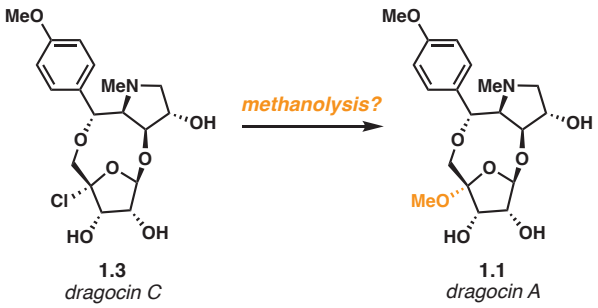


Scheme 5.6 Successful endgame sequence through a Barton decarboxylation approach

In order to investigate a decarboxylative Barton protocol, the oxidation of the free alcohol on **5.28** was required (**Scheme 5.8**). In a first iteration sequence, a simple DMP[28]/Pinnick[48] sequence was employed, which gave acid **5.29** in 46% yield over two steps. With acid **5.29** in hand, the installation of a Barton ester was then explored, which was difficult at first, likely due to the sterically encumbered environment surrounding said acid. Initial attempts featured canonical activation protocols (acyl chloride formation, DCC or CDI activation, etc) and were found to give almost no conversion to the corresponding Barton ester. Literature searches revealed the use of HOTT[49] as a convenient reagent to form particularly hindered Barton esters, especially on carbohydrate derived substrates. This was encouraging, and the utilization of this commercially available reagent provided the first hit towards the activation of acid **5.29** to ester **5.30**. At first, HOTT was simply allowed to react with **5.29** at room temperature in the dark followed by subsequent exposure to light and carbon tetrachloride once sufficient acid conversion was observed. While this provided

5.30 in only ca. 20-30% yield, this reaction successfully installed the incredibly elusive and vexing C4' chloride in quantities suitable for investigating the final global deprotection.

Initially, global deprotection was explored using Red-Al at high temperatures (which was used to produce various C–H oxidation substrates). To our surprise, the chloride appeared to have been exchanged for the Red-Al alkoxide ligand. While initially disappointing, this result indirectly supported the hypothesis that perhaps dragocin C could be converted into dragocin A through a simple solvolysis reaction. More chlorinated material was produced, which enabled the investigation of using LAH as a global deprotection reagent. To our absolute delight, crude NMR analysis of the resultant mixture revealed both dragocins B and C after a TFA workup protocol. Notably, loss of the chloride to a putative elimination-related product was observed when quenching with solutions such as Rochelle's salt. A rapid and acidic quench was crucial to optimal success of this final deprotection to preserve the integrity of the sensitive natural products. Although a triumphant victory over these elusive and deceptively straightforward natural products, this final approach was not up to par with standards – there were still some improvements to be made and one last question to address: how to produce dragocin A, the methoxylated dragocin?



1.3
dragocin C

1.1
dragocin A

Figure 5.8 Potential methanolysis of dragocin C to produce dragocin A

5.F. Endgame improvement #1: Electrochemical cyclization/etherification

After a quick victory lap, attention was turned back on how to further improve the established route. The first step that came to mind was the two-step cyclization using first PIFA and then CSA to cyclize the labile benzylic trifluoracetates. Not only was this a two-step protocol, but it was also low-yielding and proceeded with poor diastereocontrol. Given the presence of the electron-rich arene, it was hypothesized that electrochemical anodic oxidation of the arene may allow for one-step C–H functionalizing cyclization. Alex Pollatos and Dr. Alberto Garrido-Castro are greatfully acknowledged for the gracious assistance regarding the development of this reaction.

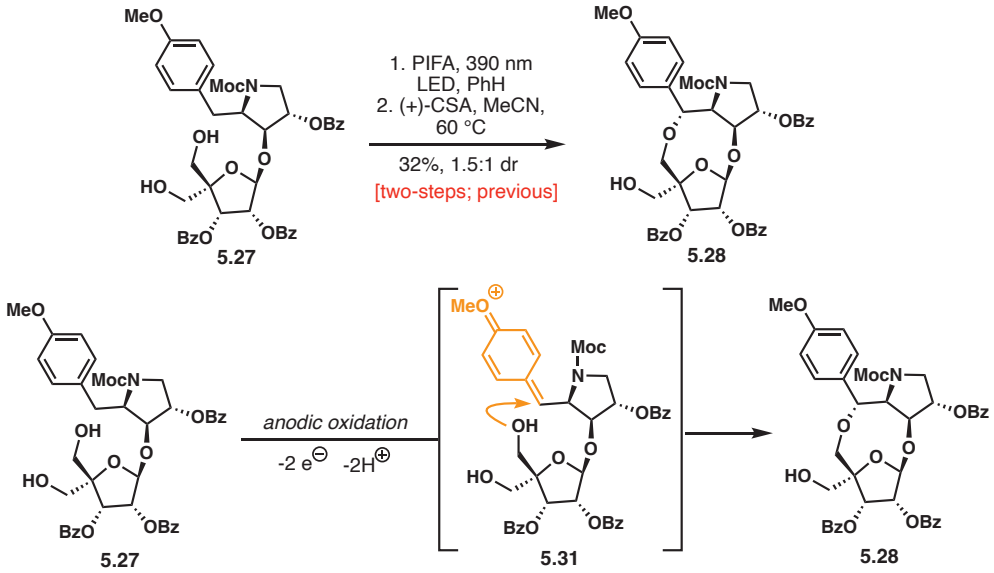


Figure 5.9 An opportunity for electrochemistry in the cyclization event

Ironically, a talented third year in the Baran lab, Alex Pollatos, was working on a related benzylic electrochemical oxidation at the time. It was imagined that his preliminary insights could lead to a cyclization hit using acyclic precursor **5.27**. For a full disclosure of all conditions explored, see **Tables 5.1-5.10**. Although the initial provided conditions ($Me_4N \cdot BF_4$, MeOH, (+)RVC/(–)RVC, 1 mA, 2 F/mol) did not produce any traces of **5.28**,

smooth oxidation to the putative methanol-trapped product was observed. Encouraged by clean reactivity, HFIP was then explored, which gave the first

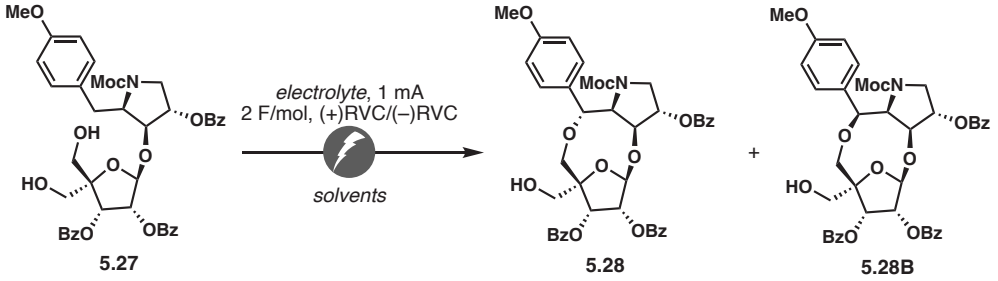


Figure 5.10 Electrochemical cyclization

initial traces of desired cyclized product along with substantial quantities of a benzylic HFIP adduct. Further solvent-based explorations revealed ACN to be an effective co-solvent alongside HFIP in a 1:1 ratio, providing the first double-digit NMR yield of **5.28** along with undesired isomer **5.28B** and anisaldehyde, a product imagined to arise from β-scission pathways. At this juncture, an additional near 100 reactions were investigated changing various parameters such as solvent, temperature, electrode materials, waveform, additives, constant potential, etc. Disappointingly, these studies gave little to no improvement in **5.28** NMR yield, appearing to be a stubborn 10-15% with ca. 1:1 dr. Despite the disappointment, key insights were obtained over the course of these studies. It became apparent that substantial product loss and unfavorable diastereoselectivities were observed at higher conversion profiles. This led to the hypothesis that not only were the product(s) unstable to the oxidation conditions, but that desired isomer **5.28** could be substantially more sensitive towards the anodic oxidation than **5.28B**. At this point, efforts were geared towards "slowing down" the reaction through the addition of sacrificial reductants. A discussion with Baran lab electrochemical expert, Dr. Yu Kawamata, provided key suggestions: perhaps a solvent with a suitable oxidation window[50] could "protect" the starting material from over-oxidation. This hypothesis proved quite fruitful,

leading to the fully optimized conditions. To our relief, NMR yield of **5.28** was doubled upon the introduction of a 10:1 mixture of HFIP:DMSO with minimal by-product formation. Further increasing the relative quantity of DMSO through the employment of a 2:1 HFIP:DMSO mixture gave a similar yield, although this time providing a 4:1 crude dr with substantial recovered starting material (34%). Efforts at this point were geared towards altering other parameters, which ultimately revealed that an unusual fluorosulfate electrolyte gave a notable increase in crude NMR yield (29%, 4.1:1 dr) and even more starting material left over than previous conditions (44%). Yield appeared to be near a local maximum, and thus a cycling protocol was leveraged. On 25 mg scale (2 mA), material was recycled by running the reactions to ca. 50% conversion and resubjecting to another round of electrochemical oxidation conditions. Using an IKA ElectraSyn carousel (6 x 25 mg), a total yield of 44% **5.28** was obtained over two iterative cycles, signifying an improvement over the two-step protocol (32% over two steps). While this was not a substantial increase in yield, the development of this unique electrochemical 9-membered ring formation represented the first of its kind while also reducing total step count. Additionally of note is that 11% starting material remained after the second cycle, which could still be subjected further for throughput purposes.

NOTE: All CV's and corresponding discussions are adapted from XX and were produced with the help of Alexandros Pollatos and Dr. Nathanyal Truax. Credit is gratefully granted to these individuals for producing several of the following figures remaining in this chapter.

Cyclic Voltammogram Studies

Cyclic Voltammogram of Acyclic Precursor 5.27

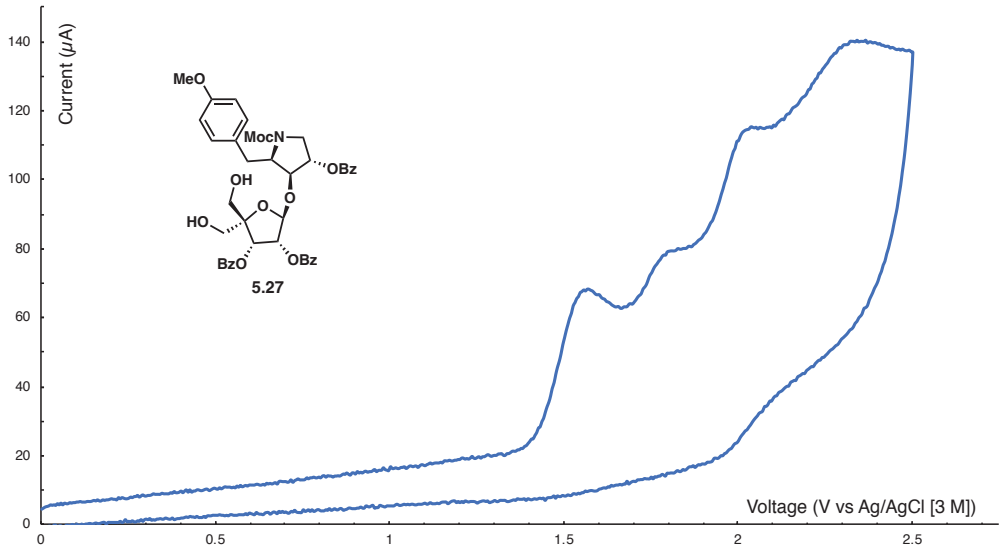


Figure 5.11 Cyclic Voltammogram of Acyclic Precursor **5.27**

A cyclic voltammogram of acyclic precursor **5.27**(5.0 mg, 0.006 mmol) was recorded in the presence of $Me_4N•BF_4$ (0.3 mmol, 0.1 M) in 3 mL of HFIP:MeCN (1:1). A 3 mm GC disk electrode was used as the working electrode, 3 M Ag/AgCl was used as a reference, and platinum was used as the counter electrode. The CV was recorded under argon from 0-2.5 V with a scan rate of 50 mV/s.

Cyclic Voltammogram of Macrocycle 5.28

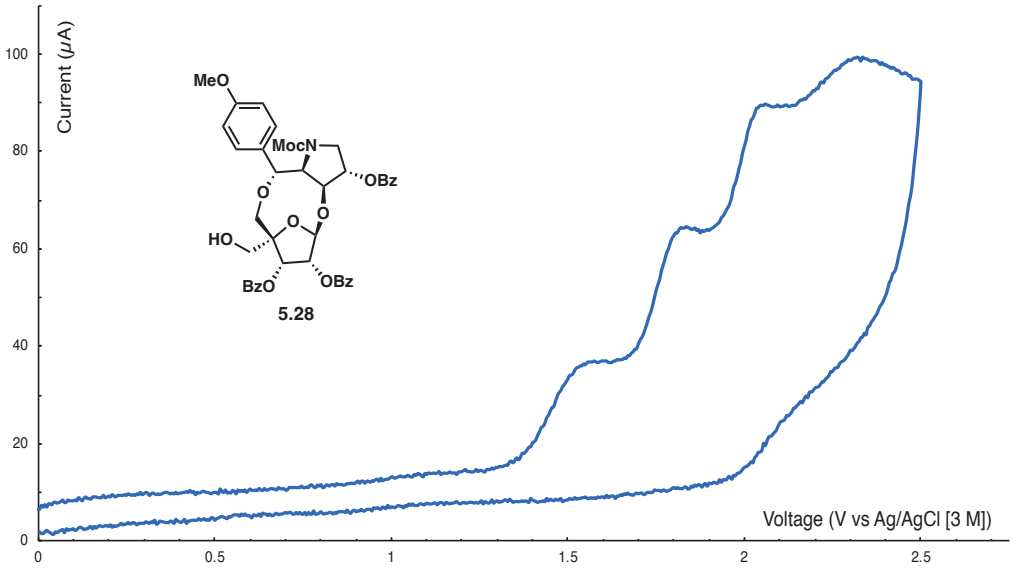


Figure 5.12 CV of 5.28

A cyclic voltammogram of desired macrocycle **5.28** (4.5 mg, 0.006 mmol) was recorded in the presence of $Me_4N•BF_4$ (0.3 mmol, 0.1 M) in 3 mL of HFIP:MeCN (1:1). A 3 mm GC disk electrode was used as the working electrode, 3 M Ag/AgCl was used as a reference, and platinum was used as the counter electrode. The CV was recorded under argon from 0-2.5 V with a scan rate of 50 mV/s.

Cyclic Voltammogram of Acyclic Precursor 5.27 overlaid with CV of Macrocycle 5.28

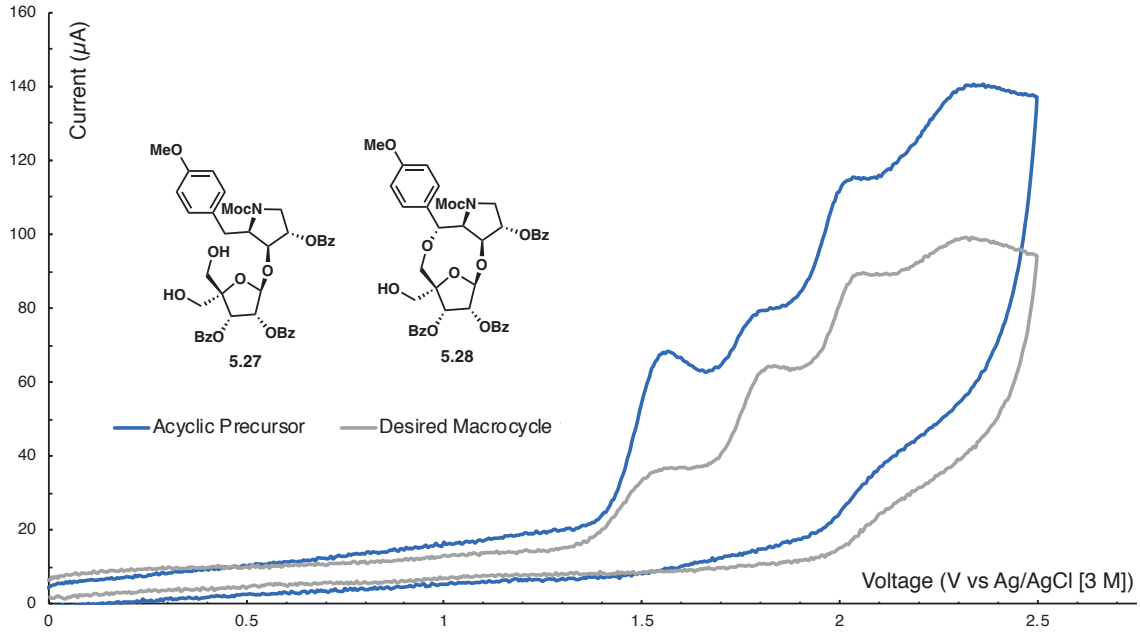


Figure 5.13 Overlaid CV of 5.27 and 5.28

Discussion of Figures 5.11-5.13

On the basis of these CVs it was determined that the onset of first oxidation wave for the acyclic diol **5.27** and desired macrocycle 5.28 are quite similar, occurring at approximately 1.56 V and 1.55 V respectively. Given the difference in current response for this first oxidation wave (68 vs 37 μA respectively), we posited that the transformation would still be feasible, but may require halting at lowered conversion.

It was also imagined that the seemingly sluggish oxidation wave of the desired macrocycle **5.28** might imply a kinetic preference for oxidation of the acyclic diol **5.27**. Such kinetic preferences have been exploited for chemoselective electrochemical transformations by using rapid alternating polarity (rAP). We therefore reasoned that alternating the polarity

may allow for differentiation of **5.27** and **5.28** during the reaction course. Unfortunately, the hypothesis was not validated in practice, and it was found that rAP conditions offered little to no advantage over direct current electrolysis. It is possible this can be attributed to the decreased faradaic efficiency of rAP, which is often pronounced on small scale in our hands.

Cyclic Voltammogram of Acyclic Precursor 5.27, Macrocycle 5.28, and Boc-Pyrrolidine Overlaid

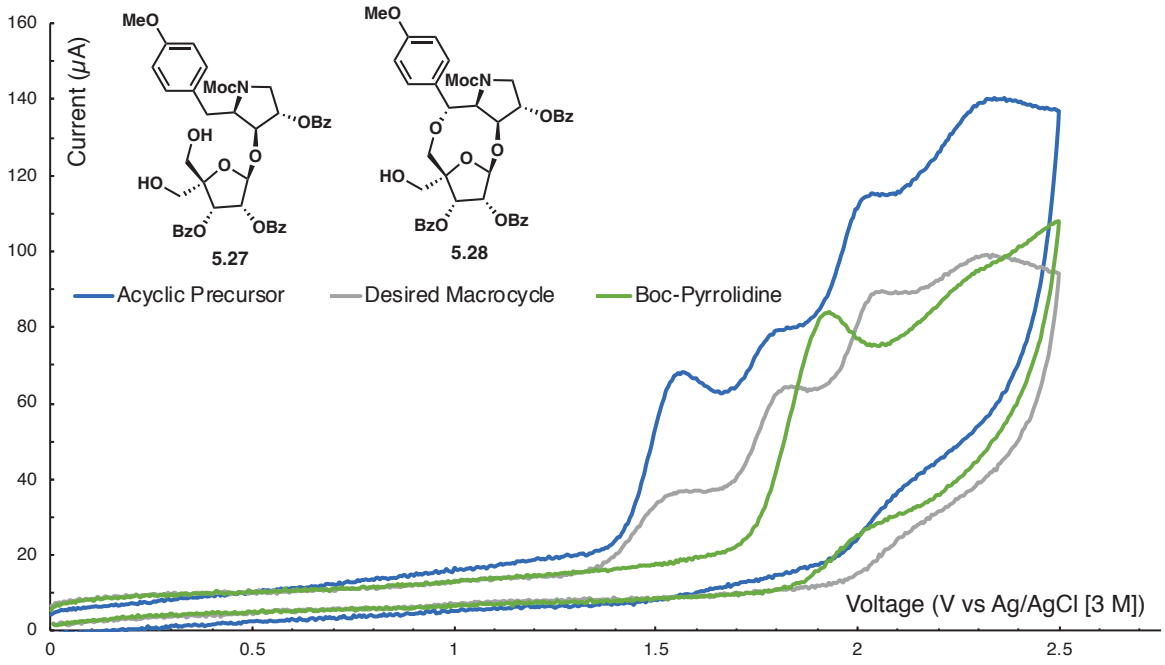


Figure 5.14 Cyclic Voltammogram of Acyclic Precursor **5.27**, Macrocycle **5.28**, and Boc-Pyrrolidine Overlaid

CVs of **5.27** and **5.28** overlaid with cyclic voltammogram of Boc-pyrrolidine (0.01 mmol) recorded in the presence of $Me_4N•BF_4$ (0.3 mmol, 0.1 M) in 3 mL of HFIP:MeCN (1:1). A 3 mm GC disk electrode was used as the working electrode, 3 M Ag/AgCl was used as a

reference, and platinum was used as the counter electrode. The CV was recorded under argon from 0-2.5 V with a scan rate of 50 mV/s.

Cyclic Voltammogram of Acyclic Precursor 5.27, Macrocycle 5.28, and *p*-Me-Anisole Overlaid

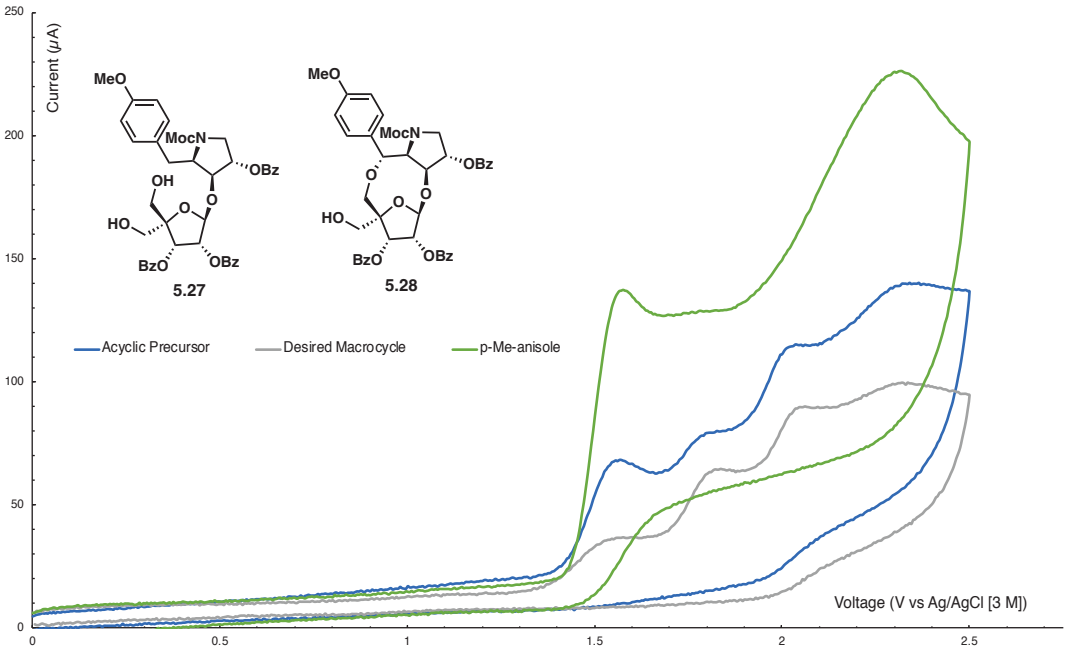


Figure 5.15 Cyclic Voltammogram of Acyclic Precursor **5.27**, Macrocycle **5.28**, and *p*-Me-Anisole Overlaid

CVs of **5.27** and **5.28** overlaid with cyclic voltammogram of *p*-Me-anisole (0.01 mmol) recorded in the presence of $Me_4N•BF_4$ (0.3 mmol, 0.1 M) in 3 mL of HFIP:MeCN (1:1). A 3 mm GC disk electrode was used as the working electrode, 3 M Ag/AgCl was used as a reference, and platinum was used as the counter electrode. The CV was recorded under argon from 0-2.5 V with a scan rate of 50 mV/s.

Discussion of Figures 5.14-5.15

During the course of optimization studies two key problems were identified as detrimental to yield: non-productive oxidative byproducts and overoxidation (see next section for discussion). With regard to non-productive byproducts, *p*-anisaldehyde as well as the putative scission product (*vide infra*) appeared to be major, arising from either oxidation of **5.27** or overoxidation of **5.28**. The structures of these compounds were derived from LCMS analysis and were not isolated.

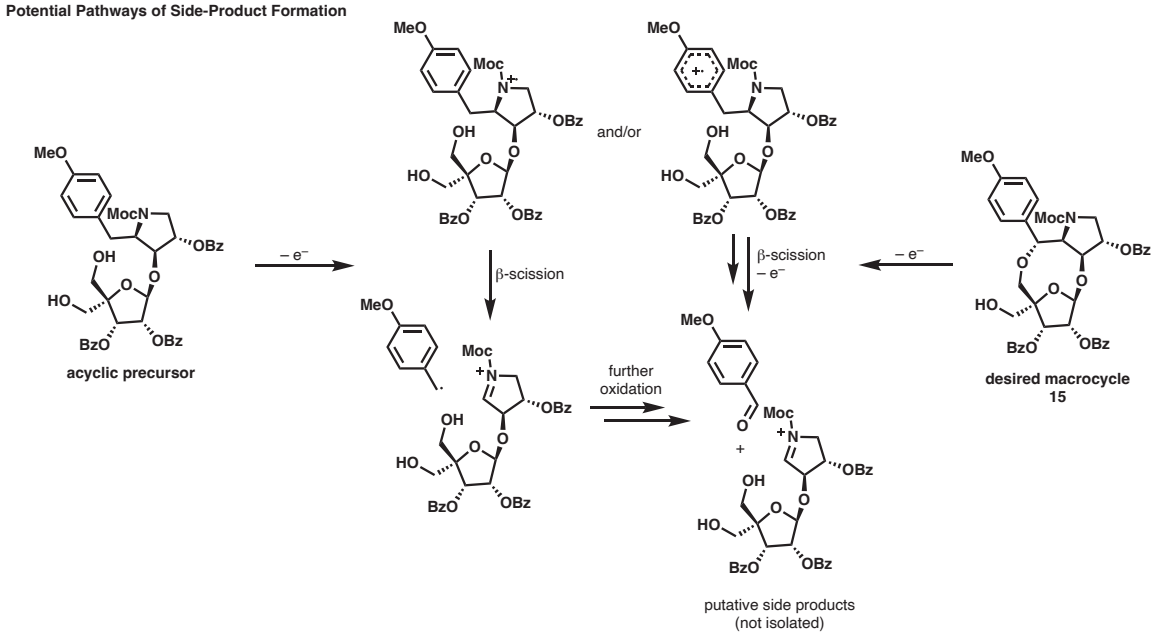


Figure 5.16 Potential explanation for the formation of para-anisaldehyde through oxidative scisssion

These byproducts could be formed by either arene oxidation or a Shono-type oxidation of the pyrrolidine. To this end, CVs of truncated systems (Boc-pyrrolidine and *p*-Me-anisole) were obtained and compared to the CV profiles of **5.27** and **5.28**. We could thereby indirectly assign the first oxidative wave of both **5.27** and **5.28** as arising from arene

oxidation and the second wave as arising from a Shono-type process. The source of the two oxidative waves with the highest potential remain ambiguous.

Hopeful to eliminate the formation of the aforementioned side products and improve the reaction profile, we attempted to saturate the system with either arene or Shono-type acceptors. Once again, these efforts did result in significant improvements to the reaction.

Cyclic Voltammogram of Undesired Macrocycle 5.28B

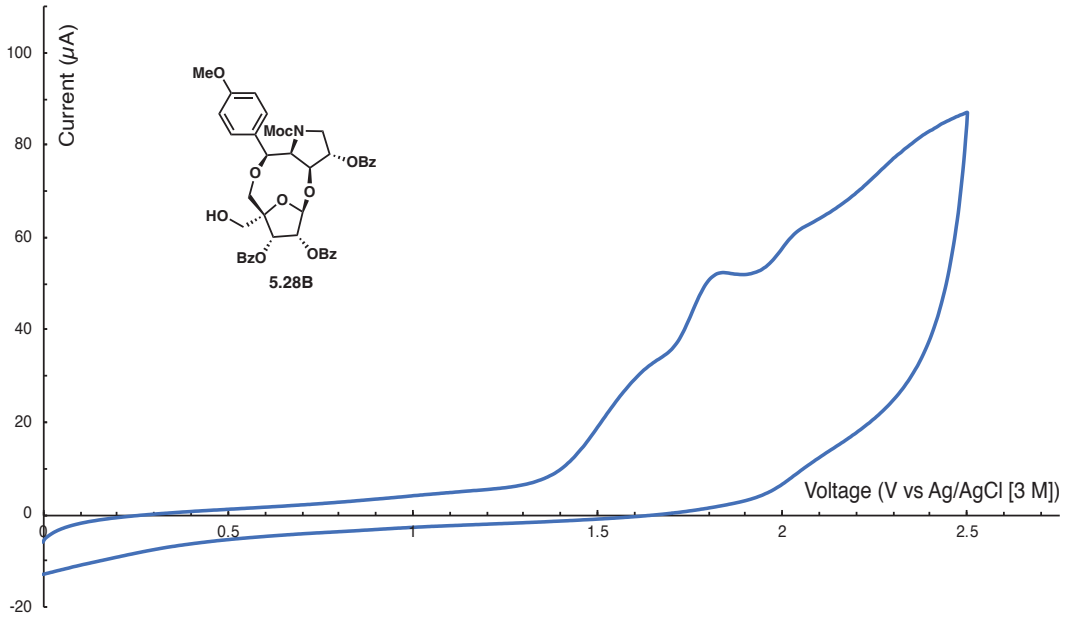


Figure 5.17 Cyclic voltammogram of undesired **5.28B**

A cyclic voltammogram of undesired macrocycle **5.28B** (5.6 mg, 0.0075 mmol) was recorded in the presence of $Me_4N•BF_4$ (0.3 mmol, 0.1 M) in 3 mL of HFIP:MeCN (1:1). A 3 mm GC disk electrode was used as the working electrode, 3 M Ag/AgCl was used as a

reference, and platinum was used as the counter electrode. The CV was recorded under argon from 0-2.5 V with a scan rate of 50 mV/s.

Cyclic Voltammogram of Desired Macrocycle 5.28 overlaid with CV of Undesired Macrocycle 5.28B

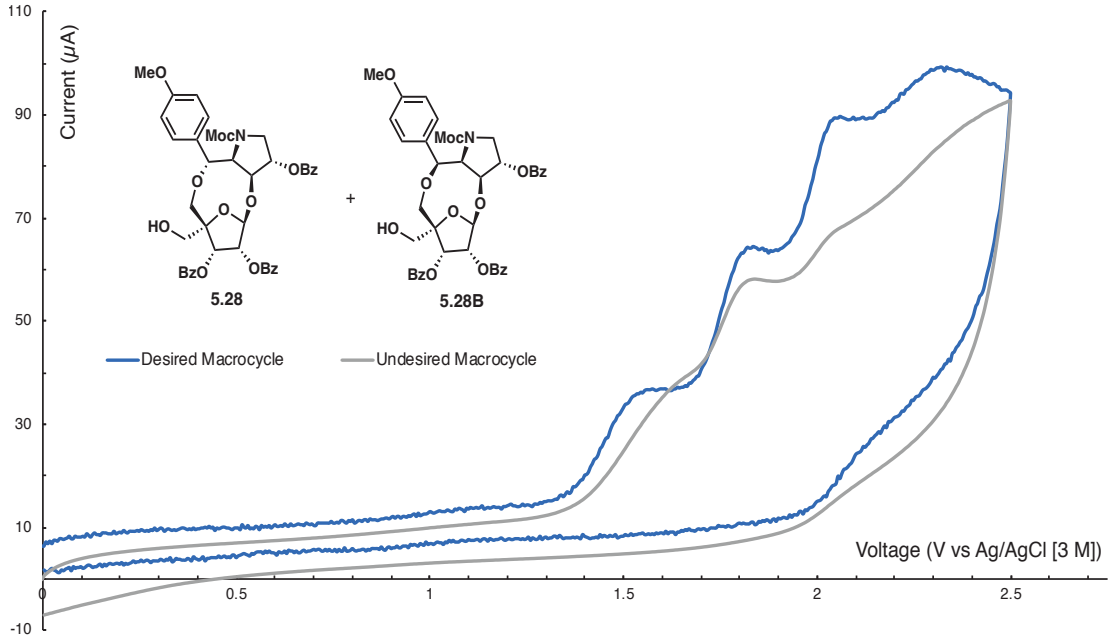


Figure 5.18 CV of **5.28** and **5.28B**

Reproduction of title compounds' CVs overlaid for comparison. Note: in the CV of undesired macrocycle, **5.28B** the current values have been normalized by adjusting the y-intercept to a value of 0 for a more direct comparison of the voltammograms.

Cyclic Voltammogram of HFIP:DMSO (2:1) solvent mixture

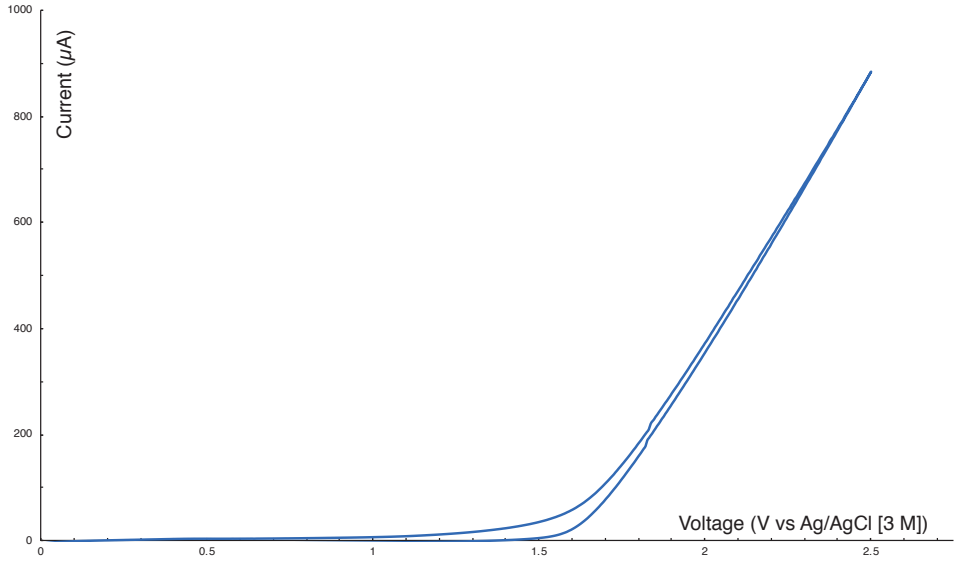


Figure 5.19 CV of the HFIP:DMSO mixture (2:1)

A cyclic voltammogram of HFIP:DMSO (2:1) 3 mL was recorded in the presence of $Et_4N•SO_3F$ (0.3 mmol, 0.1 M). A 3 mm GC disk electrode was used as the working electrode, 3 M Ag/AgCl was used as a reference, and platinum was used as the counter electrode. The CV was recorded under argon with a scan rate of 50 mV/s.

Discussion of Figures 5.17-5.19

As noted in the main text, it was found that the dr of the reaction at lower conversions was high (ca. 5.5:1), but dropped to favor the undesired **5.28B.** above ca. 50% conversion, with concomitant formation of the aforementioned oxidative byproducts that seemed to account for the loss of **5.28**. We wondered if the desired **5.28** was selectively decomposing under the reaction conditions. **Figures 5.18-5.19** indicate that the first oxidative wave for the undesired **5.28B** is significantly less pronounced than that of desired macrocycle **5.28**. This

seems to account for the requirement for halting the reaction at ca. 50% conversion to maintain the inherent dr.

Figure 5.19 shows the solvent oxidation window of the 2:1 HFIP:DMSO mixture employed in the optimized conditions. The onset of oxidation beginning at approx. 1.50 V may account for the observed ‘protective’ effect of this solvent-electrolyte combination, resulting in less overoxidation and oxidative byproduct formation.

Table 5.1 Solvent screen

Entry	Scale (mg)	Electrodes	Solvent	Current (mA)	F/mol	Electrolyte	Base/ Additive	PDT (15)	SI-16	CHO	SM (14)	Mass recovery	BRSM
1	5	RVC/RVC	10:1 HFIP/DMF	1	2	$Me_4N•BF_4$	-	17	34	3	8	62	18
2	5	RVC/RVC	10:1 HFIP/DMA	1	2	$Me_4N•BF_4$	-	14	32	trace	9	55	15
3	5	RVC/RVC	1:1 DCM/HFIP	1	2	$Me_4N•BF_4$	-	5	25	4	16	59	6
4	5	RVC/RVC	10:1 HFIP/NMP	1	2	$Me_4N•BF_4$	-	13	24	4	nd	41	13
5	5	RVC/RVC	1:1 DCE/HFIP	1	2	$Me_4N•BF_4$	-	4	19	3	22	48 (+HFIP adduct)	5
6	5	RVC/RVC	10:1 HFIP/DMSO	1	2	$Me_4N•BF_4$	-	20	27	5	9	61	22
7	5	RVC/RVC	10:1 HFIP/MeCN	1	2	$Me_4N•BF_4$	-	4	16	9	9	38	4
8	5	RVC/RVC	10:1 HFIP/sulfalone	1	2	$Me_4N•BF_4$	-	14	20	6	trace	40	14
9	5	RVC/RVC	1:1 MeCN/HFIP	1	3	$Me_4N•BF_4$	-	10	16	22	16	64	12
10	5	RVC/RVC	10:1 MeCN/TFA	1	2	$Me_4N•BF_4$	-	8	14	11	8	41	9
11	5	RVC/RVC	10:1 MeCN/HFIP	1	2	$Me_4N•BF_4$	-	13	17	9	30	69	19
12	5	RVC/RVC	MeCN (10 eq HFIP)	1	2	$Me_4N•BF_4$	-	5	10	11	23	49	6
13	5	RVC/RVC	MeCN	1	2	$Me_4N•BF_4$	-	3	6	10	14	33	3
14	5	RVC/RVC	3:1 DCM/MeCN	1	2	$Me_4N•BF_4$		3	3	7	24	37	4
15	25	RVC/RVC	1:1 MeCN/HFIP	3	2	$Me_4N•BF_4$	-	14	14	5	27	60	19
16	5	RVC/RVC	2:1 MeCN/HFIP	1	2	$Me_4N•BF_4$	-	9	8	12	46	75	17
17	5	RVC/RVC	1:1 MeCN/HFIP	1	2	$Me_4N•BF_4$	-	15	10	7	29	61	21
18	5	RVC/RVC	2:1 HFIP/DMSO	1	2	$Me_4N•BF_4$	-	18	4.5	trace	34	57	27
19	5	RVC/RVC	8:2:1 HFIP/MeCN/DMSO	1	2	$Me_4N•BF_4$	-	21	11	4	13	49	24
20	5	RVC/RVC	3:1 HFIP/DMSO	1	2	$Me_4N•BF_4$	-	21	8	trace	21	50	27
21	5	RVC/RVC	4:1 HFIP/DMSO	1	2	$Me_4N•BF_4$	-	26	14	4	25	69	35
22	5	RVC/RVC	1:1 MeCN/IPA	1	2	$Me_4N•BF_4$	-	-	-	-	67	71 (+ trace IPA adduct)	-

23	5	RVC/RVC	10:1 HFIP/methylphenylsulfoxide	1	2	$Me_4N•BF_4$	-	-	-	nd	77	77	-
27	5	RVC/RVC	1:1 MeCN/MeOH	1	2	$Me_4N•BF_4$	-	trace (LC)	trace (LC)	11	20	31 (+ MeOH adduct)	
28	5	RVC/RVC	1:1:1 MeCN/HFIP/DMSO	1	2	$Me_4N•BF_4$	-	trace (LC)	trace (LC)		mostly sm by LC		-
29	5	RVC/RVC	1:1 MeCN/DMSO	1	2	$Me_4N•BF_4$	-	trace (LC)	trace (LC)		mostly sm by LC		-

Table 5.2 Base screen

Entry	Scale (mg)	Electrodes	Solvent	Current (mA)	F/mol	Electrolyte	Base/Additive (equiv)	PDT (15)	SI-16	CHO	SM (14)	Mass recovery	BRSM
30	5	RVC/RVC	1:1 MeCN/HFIP	1	2	$Me_4N•BF_4$	Collidine (1)	16	26	trace	11	53	18
31	5	RVC/RVC	1:1 MeCN/HFIP	1	2	$Me_4N•BF_4$	Collidine (3)	4	trace	6	41	51	7
32	5	RVC/RVC	1:1 MeCN/HFIP	1	2	$Me_4N•BF_4$	K_2CO_3 (3)	2.5	trace	4	29	36	4
33	5	RVC/RVC	1:1 MeCN/HFIP	1	2	$Me_4N•BF_4$	TMAOH (3)	-	-	19	-	19	0
34	5	RVC/RVC	1:1 MeCN/HFIP	1	2	$Me_4N•BF_4$	NaOAc (3)	4.5	trace	6	38	49	7
35	5	RVC/RVC	1:1 MeCN/HFIP	1	2	$Me_4N•BF_4$	DBU (3)	-	-	14	-	14	0

Table 5.3 rAP screen

Entry	Scale (mg)	Electrodes	Solvent	Current (mA)	Pulse (ms)	F/mol	Electrolyte	PDT (15)	SI-16	CHO	SM (14)	Mass recovery	BRSM
36	5	RVC/RVC	1:1 MeCN/HFIP	1	100	6	$Me_4N•BF_4$	no rxn					
37	5	RVC/RVC	1:1 MeCN/HFIP	3	100	6	$Me_4N•BF_4$	no rxn					
38	5	RVC/RVC	1:1 MeCN/HFIP	3	150	6	$Me_4N•BF_4$	3	2	11	35	51	5
39	5	RVC/RVC	1:1 MeCN/HFIP	3	250	6	$Me_4N•BF_4$	3	trace	9	30	42	4

Table 5.4 Constant potential

Entry	Scale (mg)	Electrodes	Solvent	Current (mA)	F/mol	Electrolyte	Base/ Additive	PDT (15)	SI-16	CHO	SM (14)	Mass recovery	BRSM
41	5	RVC/RVC	1:1 MeCN/HFIP	nd (+1.5V constant)	~16 total	$Me_4N•BF_4$	-	decomp	nd	nd	nd	nd	

Table 5.5 Current screen

Entry	Scale (mg)	Electrodes	Solvent	Current (mA)	F/mol	Electrolyte	Base/ Additive	PDT (15)	SI-16	CHO	SM (14)	Mass recovery	BRSM
42	5	RVC/RVC	1:1 MeCN/HFIP	0.3	2	$Me_4N•BF_4$	-	3	2	10	46	61	6
43	5	RVC/RVC	1:1 MeCN/HFIP	3	2	$Me_4N•BF_4$	-	9	9	10	30	58	13
44	5	RVC/RVC	1:1 MeCN/HFIP	10	2	$Me_4N•BF_4$	-	10	7	3	29	49	14

Table 5.6 Total charge

Entry	Scale (mg)	Electrodes	Solvent	Current (mA)	F/mol	Electrolyte	Base/ Additive	PDT (15)	SI-16	CHO	SM (14)	Mass recovery	BRSM
44	5	RVC/RVC	2:1HFIP/DMSO	1	3	$Et_4N•FSO_3$	-	30	8.7	2.7	25	66.4	40
45	5	RVC/RVC	2:1HFIP/DMSO	1	3	$BMIMPF_6$	-	30	9	5.7	14	58.7	35
46	5	RVC/RVC	10:1 HFIP/DMSO	1	0.45	$Me_4N•BF_4$	-	10	6	trace	58	74	24
47	5	RVC/RVC	10:1 HFIP/DMSO	1	1.52	$Me_4N•BF_4$	-	17	18	trace	13	48	20
48	5	RVC/RVC	10:1 HFIP/DMSO	1	1.06	$Me_4N•BF_4$	-	19	12	3	28	62	26
49	5	RVC/RVC	10:1 HFIP/DMA	2	4	$Me_4N•BF_4$	-	-	6	11	-	17	0
50	5	RVC/RVC	2:1 HFIP/DMA	2	3	$Me_4N•BF_4$	-	26	10	2	29	67	37
51	5	RVC/RVC	2:1 HFIP/DMA	2	4	$Me_4N•BF_4$	-	12	3	4	-	19	12

52	5	RVC/RVC	4:1 HFIP/ DMA	2	3	$Me_4N•BF_4$	-	17	13	4	-	34	17

Table 5.7 Electrodes

Entry	Scale (mg)	Electrodes	Solvent	Current (mA)	F/mol	Electrolyte	Base/ Additive	PDT (15)	SI-16	CHO	SM (14)	Mass recovery	BRSM
53	5	(+)Pt/(–)RVC	1:1 MeCN/HFIP	1	2	$Me_4N•BF_4$	-	-	-	-	-	0	0
54	5	(+)RVC/(–)Pt	1:1 MeCN/HFIP	0.5	2	$Me_4N•BF_4$	-	-	-	-	-	0	0
55	5	(+)RVC/(–)Pt	1:1 MeCN/HFIP	1	2	$Me_4N•BF_4$	-	7	14	14	15	50	8
56	5	(+)RVC/(–)Pt	1:1 MeCN/HFIP	3	2	$Me_4N•BF_4$		10	11	8	21	50	13
57	5	(+)RVC/(–)Pt	2:1HFIP/ DMSO	1	2	$Me_4N•BF_4$		20	10	7	30	67	29

Table 5.8 Electrolytes

Entry	Scale (mg)	Electrodes	Solvent	Current (pulse T)	F/mol	Electrolyte	Base/ Additive	PDT (15)	SI-16	CHO	SM (14)	Mass recovery	BRSM
59	5	RVC/RVC	1:1 MeCN/ HFIP	1	2	pyr•TFA		-	-	8	62	70	0
60	5	RVC/RVC	1:1 MeCN/ HFIP	1	2	TMACSA		trace	19	3	33	55	1
61	5	RVC/RVC	1:1 MeCN/ HFIP	1	2	$NaPF_6$		5	4	11	40	60	8
62	5	RVC/RVC	1:1 MeCN/ HFIP	1	2	$LiBF_4$		5	15	6	24	50	7
63	5	RVC/RVC	1:1 MeCN/ HFIP	1	2	$TBABF_4$		7	13	14	19	53	9
64	5	RVC/RVC	1:1 MeCN/ HFIP	1	2	$MgClO_4$		7	8	9	38	62	11
65	5	RVC/RVC	1:1 MeCN/ HFIP	1	2	TBAOAc		8	3	4	45	60	15
66	5	RVC/RVC	1:1 MeCN/ HFIP	1	2	$TBAPF_6$		15	16	8	28	67	21
67	5	RVC/RVC	1:1 MeCN/	1	2	$TBAClO_4$		-	10	10	-	20	

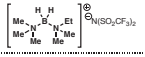
			HFIP										
68	5	RVC/RVC	2:1HFIP/ DMSO	1	2	$BMIMBBF_4$		22	5	3.4	37	67.4	35
69	5	RVC/RVC	2:1HFIP/ DMSO	1	2	$BMIMPF_6$		29	8	2	45	84	53
70	5	RVC/RVC	2:1HFIP/ DMSO	1	2	$Et_4N•FSO_3$		29	7	2	44	82	52
71	5	RVC/RVC	2:1HFIP/ DMSO	1	2			28	8	3	32	71	41
72	5	RVC/RVC	2:1HFIP/ DMSO	1	2	$BMIMNO_3$		14	2	6	45	67	25
74	5	RVC/RVC	1:1 MeCN/ HFIP	1	2	$LiSbF_6$	-	traces	traces		mostly sm (LCMS)	nd	
75	5	RVC/RVC	2:1HFIP/ DMSO	1	2	KF	-	6	3	trace	38	47	
76	5	RVC/RVC	2:1HFIP/ DMSO	1	2	$BMIMPF_6$ + $Et_4N•FSO_3$	-	22	6	2	27	57	

Table 5.9 Additives

Entry	Scale (mg)	Electrodes	Solvent	Current (pulse T)	F/mol	Electrolyte	Additive (equiv)	PDT (15)	SI-16	CHO	SM (14)	Mass recovery	BRSM
77	5	RVC/RVC	1:1 MeCN/HFIP	1	2	$Me_4N•BF_4$	$AgBF_4$	-	7	14	26	47	0
78	5	RVC/RVC	1:1 MeCN/HFIP	1	2	$Me_4N•BF_4$	DMS	-	-	-	88	88	0
79	5	RVC/RVC	1:1 MeCN/HFIP	1	2	$Me_4N•BF_4$	IPA	3	3	21	24	51	4
80	5	RVC/RVC	1:1 MeCN/HFIP	1	8	$Me_4N•BF_4$	anisole (5)	7	6	11	17	41	8
81	5	RVC/RVC	1:1 MeCN/HFIP	1	2	$Me_4N•BF_4$	anisole (5)	10	3	3	53	69	21
82	5	RVC/RVC	1:1 MeCN/HFIP	1	2	$Me_4N•BF_4$	THF	14	12	10	22	58	18
83	5	RVC/RVC	1:1 MeCN/HFIP	1	2	$Me_4N•BF_4$	NBoc Pyrrolidine	15	13	12	26	66	20
84	5	RVC/RVC	1:1 MeCN/HFIP	1	2	$Me_4N•BF_4$	DMSO (200)	18	11	9	27	65	25
85	5	RVC/RVC	1:1 MeCN/HFIP	1	2	$Me_4N•BF_4$	DMSO (100)	8	8	8	16	40	10

86	5	RVC/RVC	1:1 MeCN/HFIP	1	2	$Me_4N•BF_4$	DMSO (400)	15	8	7	26	56	20
87	5	RVC/RVC	10:1 HFIP/ DMSO	1	2	$Me_4N•BF_4$	Pivalic Acid TMAOH	7	6	9	32	54	10

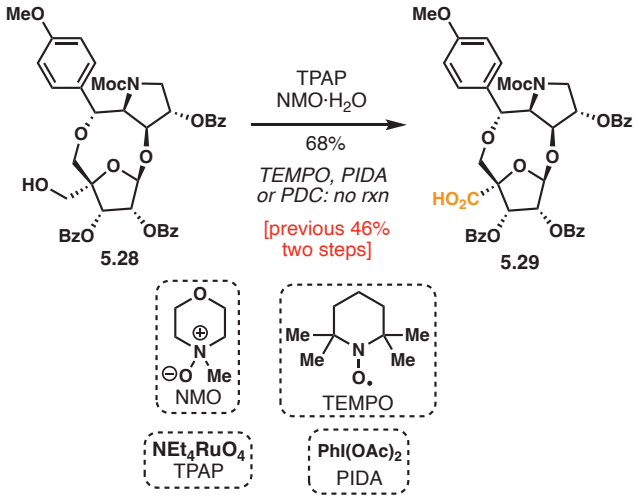
Table 5.10 Temperature

Entry	Scale (mg)	Electrodes	Solvent	Current (pulse T)	F/mol	Electrolyte	Temp (°C)	PDT (15)	SI-16	CHO	SM (14)	Mass recovery	BRSM
88	5	RVC/RVC	1:1 MeCN/HFIP	1	2	$Me_4N•BF_4$	0	12	7	8	30	57	17
89	5	RVC/RVC	1:1 MeCN/HFIP	1	2	$Me_4N•BF_4$	40	10	14	13	34	71	15

5.G. Endgame improvement #2: one-step carboxylic acid access and improved Barton decarboxylation

All that remained to achieve a satisfactory synthetic route to the dragocins was to truncate the free-alcohol oxidation to form carboxylic acid **5.29** and to improve the reproducibility and yield of the Barton decarboxylative halogenation.

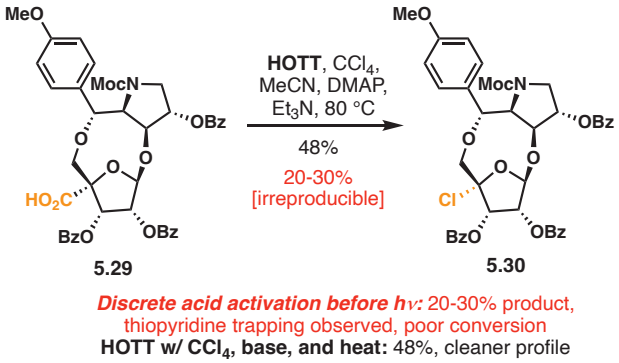
To be brief, the free alcohol oxidation was simply achieved using Ley-Griffith (TPAP, $NMO{\cdot}H_2O$) conditions[51] to give acid **5.29** in 68% yield. Surprisingly, the employment of PDC/DMF[52] or TEMPO/PIDA gave no reaction on this system. Recall that previously this transformation was achieved in two steps with a DMP/Pinnick sequence (**Scheme 5.9**)



Scheme 5.7 Improved acid access

Attention was then turned to the key decarboxylative chlorination event, which had proceeded in a modest 20-30% yield with varying degrees of reproducibility. The primary cause of reproducibility was not in the actual light-initiated chlorination step itself but in the *in situ* activation to form the Barton ester, which varied from ca. 30% conversion to 95% conversion as indicated with UPLC analysis. It was hypothesized that simply heating HOTT with XX in a mixture of ACN and CCl_4 (ACN for solubility) with Et_3N and DMAP as bases could improve the result of this transformation. It was reasoned that the high

temperature (while excluding light), could not only assist the Barton ester formation but also accelerate the decarboxylation process. Gratifyingly, this hypothesis proved fruitful, reproducibly achieving 48% isolated yield of the chlorinated product **5.30** as shown in **Scheme 5.10**.

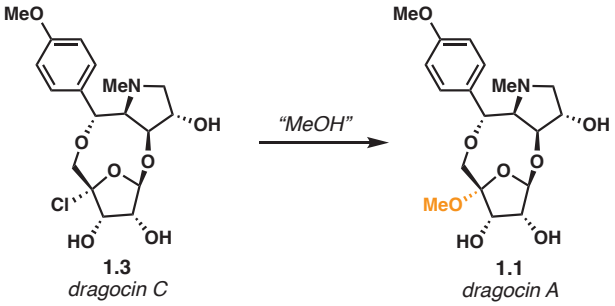


Scheme 5.8 Improved Barton decarboxylation with HOTT and heat

The optimization of this reaction marked the end of the optimization campaign and only one key question remained: dragocin A.

5.H. Preparation of dragocin A through methanolysis of dragocin C and the final route

From the outset of the project, it was reasoned that dragocin A could in fact be a mere artifact of isolation, resulting from methanolysis of dragocin C. In order to replicate this in a synthetically useful way, several methanol-based conditions were investigated, summarized in **Figure 5.22**. As seen in the provided table, full conversion of dragocin C was observed in hot methanol with a key AgOTf additive as a halide scavenger,[53] obtaining 51% yield of dragocin A after HPLC isolation. As the progress of the reaction was tracked through UPLC, a notable isomer was observed which contained the same mass as dragocin A. Although the structure was not fully elucidated, it is speculated that this isomer is **5.31** or a related structure, which could feasibly be produced through C1' attack of dragocin C.



conditions	result
MeOH, rt	no reaction
MeOH, reflux	traces
MeONa	-Cl product (structure not elucidated)
MeOH, TFA, several days	no reaction
MeOH, AgOTf, reflux, overnight	***full conversion, dragocin A detected (51%)***

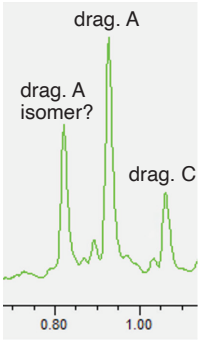


Figure 5.20 Screening the transformation of dragocin C to A

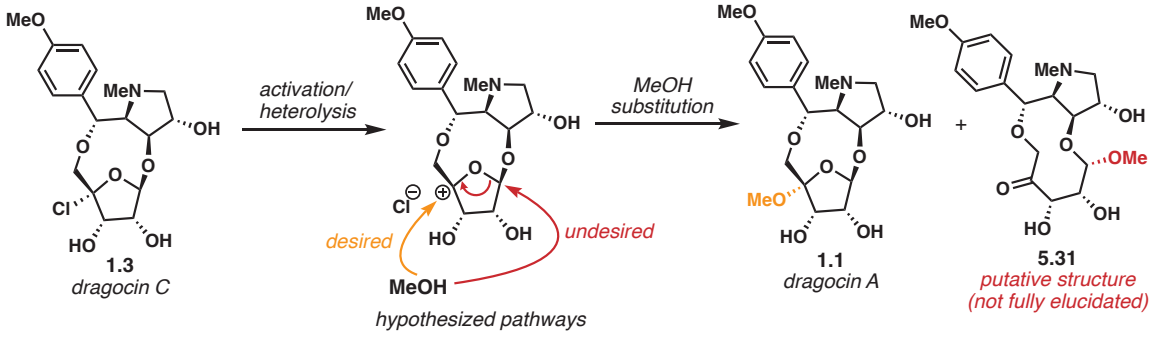
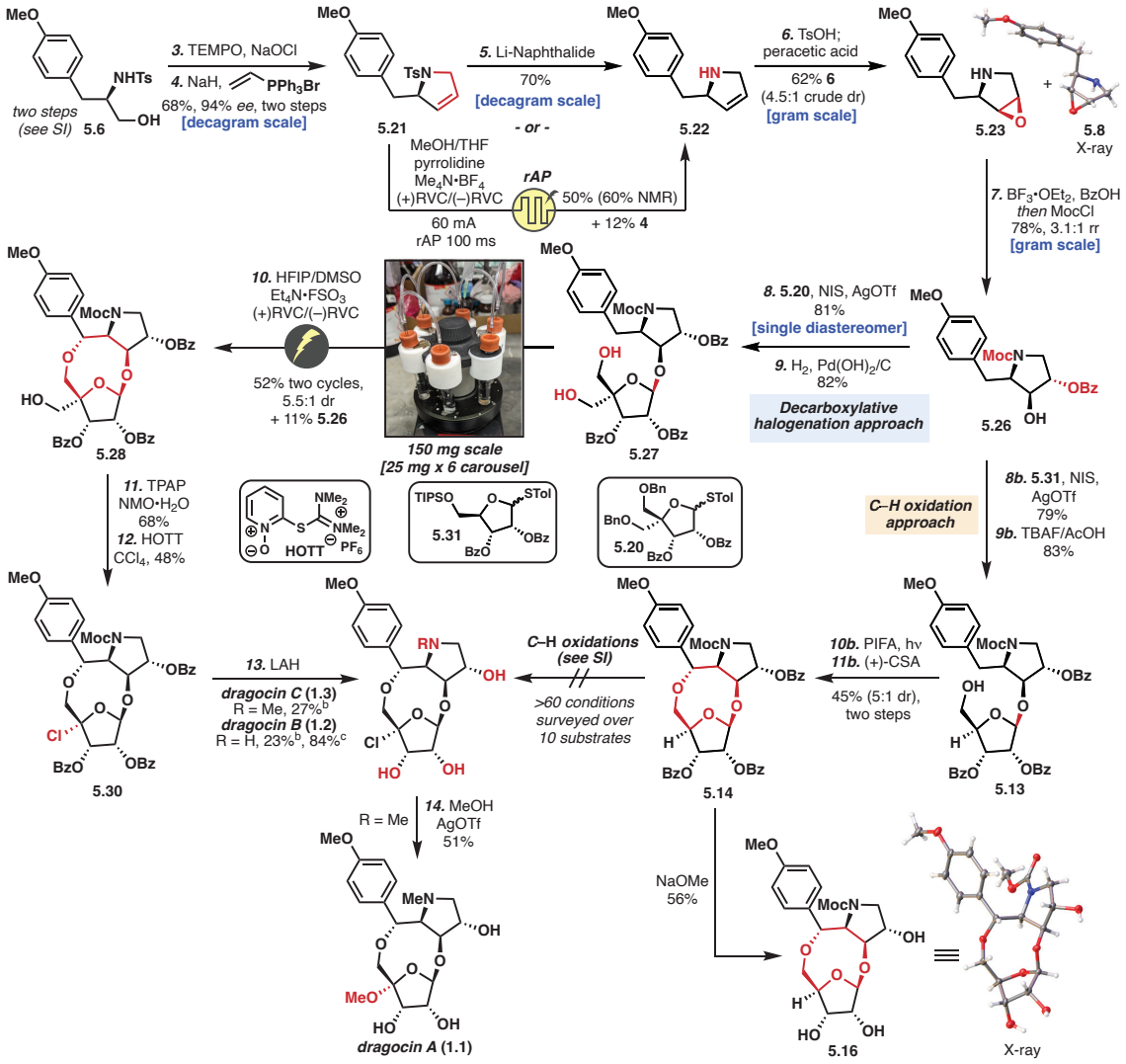


Figure 5.21 Hypothetical mechanism for the formation of putative ring-opened isomer of dragocin A

This was an unanticipated but stimulating result in that it could indirectly suggest how biological nucleophiles may interact with these fascinating natural products. With all three dragocins fully prepared, this concluded the project, where the entire sequence is provided below.



Scheme 5.9 Total synthesis of dragocins A–C

5.I. Are the dragocins covalently reactive? A stimulating biological consideration

It was hypothesized from the beginning of the project that these natural products may be covalently reactive[54] with biological nucleophiles. Hints that would point to this (without having any synthetic information) would be the fact that dragocin A is isolated along with dragocin C and B. If, in fact, dragocin A was an artifact of isolation – perhaps a product of sitting in methanolic solutions for prolonged periods – it is feasible that nucleophilic amino acid residues could seemingly react in a similar fashion.

For a long time, it was incredibly tempting to compare the C4' oxidized architecture found on the dragocins to the C4' abasic lesions found on DNA or RNA,[55] which have been found to react with nitrogenous nucleophiles and invoked in the chemical modification of DNA.[56] Further, while not readily explored in the synthetic literature, these types of substructures have been leveraged in the chemical biology and nucleotide literature as bioconjugation agents.[56-57] Although the exact mechanism may not be the same, it is alluring to consider the possibility that the dragocins may react with nucleophiles in a similar fashion. For example, putative product 5.31 (see **Figure 5.21**), could suggest that biological nucleophiles may be able to attack the supposed electrophilic ribose moiety from either C4' or C1'; if a nitrogenous nucleophile is invoked, the structure could collapse to form an aza-ribose analogue of dragocin. It is intriguing to consider why nature decided to modify the C4' position, perhaps it could have been for these purposes. If any of this is true, it would represent a first-of-its-kind covalent mechanism as a sort of damaged DNA/RNA mimic.

While not experimentally validated, it is worthwhile to leave record of this consideration – particularly due to the observation that dragocin C can be converted to dragocin A (while aggressive conditions were leveraged, it is important to note this reaction was employed for preparative synthetic purposes). I hope that further studies are done on these interesting natural products in the future and that light may be shed upon these musings.

References

(1) Choi, H.; Engene, N.; Byrum, T.; Hwang, S.; Oh, D. C.; Gerwick, W. H. Dragocins A-D, Structurally Intriguing Cytotoxic Metabolites from a Panamanian Marine Cyanobacterium. *Org. Lett.* **2019**, *21*, 266-270. DOI: 10.1021/acs.orglett.8b03712

(2) (a) Nakata, M.; Tamai, T.; Kamio, T.; Kinoshita, M.; Tatsuta, K. The Total Synthesis of AB3217-A, a Novel Antimite Substance, Via Intermolecular Etherification and Intramolecular Glycosylation. *Bull. Chem. Soc. Jpn* **1994**, *67*, 3057-3066. DOI: DOI 10.1246/bcsj.67.3057. (b) Nakata, M.; Tamai, T.; Kamio, T.; Kinoshita, M.; Tatsuta, K. Total Synthesis of AB3217-A, a Novel Antimite Substance, Via Intramolecular Glycosylation. *Tetrahedron Lett.* **1994**, *35*, 3099-3102. DOI: Doi 10.1016/S0040-4039(00)76839-0

(3) Thomas, S. O.; Singleton, V. L.; Lowery, J. A.; Sharpe, R. W.; Pruess, L. M.; Porter, J. N.; Mowat, J. H.; Bohonos, N. Nucleocidin, a new antibiotic with activity against Trypanosomes. *Antibiot. Annu.* **1956**, 716-721.

(4) Kanbe, K.; Mimura, Y.; Tamamura, T.; Yatagai, S.; Sato, Y.; Takahashi, A.; Sato, K.; Naganawa, H.; Nakamura, H.; Takeuchi, T.; et al. AB3217-A, a novel anti-mite substance produced by a strain of Streptomyces platensis. *J. Antibiot.* **1992**, *45*, 458-464. DOI: 10.7164/antibiotics.45.458

(5) Toueg, J.; Godfrey, C. R. A.; Wibley, J. E. Formal Synthesis of AB3217-A from Anisomycin Using a Directed Benzylic Oxidation. *Synlett* **2010**, 2721-2724. DOI: 10.1055/s-0030-1259010

(6) Mordini, A.; Valacchi, M.; Epiroti, F.; Reginato, G.; Cicchi, S.; Goti, A. Studies on the Lithiation of Hydroxypyrrolidines: Synthesis of Polyhydroxylated Pyrrolidines via Chiral Enecarbamates. *Synlett* **2011**, 235-240. DOI: 10.1055/s-0030-1259307

(7) Yoshimitsu, T.; Arano, Y.; Nagaoka, H. Radical hydroxyalkylation of C-H bond adjacent to nitrogen of tertiary amides, ureas, and amines. *J. Am. Chem. Soc.* **2005**, *127*, 11610-11611. DOI: 10.1021/ja053855q

(8) Paul, A.; Seidel, D. α-Functionalization of Cyclic Secondary Amines: Lewis Acid Promoted Addition of Organometallics to Transient Imines. *J. Am. Chem. Soc.* **2019**, *141*, 8778-8782. DOI: 10.1021/jacs.9b04325

(9) Yi, C. B.; She, Z. Y.; Cheng, Y. F.; Qu, J. Redox-Neutral alpha-C-H Functionalization of Pyrrolidin-3-ol. *Org. Lett.* **2018**, *20*, 668-671. DOI: 10.1021/acs.orglett.7b03807

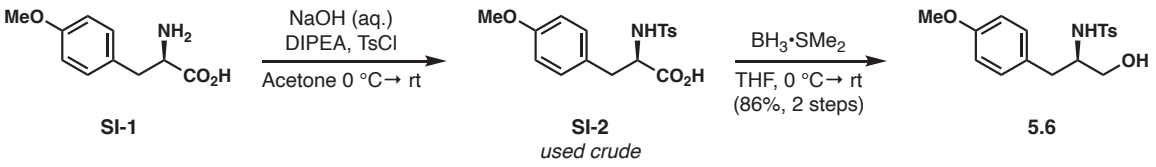
(10) Singleton, D. A.; Redman, A. M. Vinylboranes as Trans-Dihydroxyethylene Equivalents for Diels-Alder Reactions. *Tetrahedron Lett.* **1994**, *35*, 509-512. DOI: Doi 10.1016/S0040-4039(00)75824-2
(11) Fukushima, K.; Ishikawa, Y.; Sakai, R.; Oikawa, M. A monocyclic neodysiherbaine analog: Synthesis and evaluation. *Bioorg. Med. Chem. Lett.* **2016**, *26*, 5164-5167. DOI: 10.1016/j.bmcl.2016.09.074
(12) Chen, F.; Wang, Y.; Ai, J.; Zhan, Z. S.; Lv, Y. C.; Liang, Z. J.; Luo, C.; Mei, D. S.; Geng, M. Y.; Duan, W. H. O-Linked Triazolotriazines: Potent and Selective c-Met Inhibitors. *Chem. Med. Chem.* **2012**, *7*, 1276-1285. DOI: 10.1002/cmdc.201200145
(13) Hoye, T. R.; Jeffrey, C. S.; Shao, F. Mosher ester analysis for the determination of absolute configuration of stereogenic (chiral) carbinol carbons. *Nat. Protoc.* **2007**, *2*, 2451-2458. DOI: 10.1038/nprot.2007.354
(14) Fujioka, H.; Sawama, Y.; Murata, N.; Okitsu, T.; Kubo, O.; Matsuda, S.; Kita, Y. Unexpected highly chemoselective deprotection of the acetals from aldehydes and not ketones: TESOTf-2,6-lutidine combination. *J. Am. Chem. Soc.* **2004**, *126*, 11800-11801. DOI: 10.1021/ja046103p
(15) Hu, B.; Li, Y. F.; Li, Z. J.; Meng, X. B. Aniline mediated oxidative C-C bond cleavage of α-alkoxy aldehydes in air and a model reaction for the synthesis of α-(D)-amino acid derivatives. *Org. Bio. Chem.* **2013**, *11*, 4138-4141. DOI: 10.1039/c3ob40685g
(16) Hayama, K.; Kojima, R.; Kubota, K.; Ito, H. Synthesis of Chiral N-Heterocyclic Allylboronates via the Enantioselective Borylative Dearomatization of Pyrroles. *Org. Lett.* **2020**, *22*, 739-744. DOI: 10.1021/acs.orglett.9b04581
(17) Demartino, G.; Decaprariis, P.; Abignente, E.; Rimoli, M. G. New Synthetic Method for 4-Hydroxyproline. *J. Het. Chem.* **1990**, *27*, 507-509. DOI: DOI 10.1002/jhet.5570270306
(18) Kim, M. S.; Choi, Y. M.; An, D. K. Lithium diisobutylbutoxyaluminum hydride, a new and efficient reducing agent for the conversion of esters to aldehydes. *Tetrahedron Lett.* **2007**, *48*, 5061-5064. DOI: 10.1016/j.tetlet.2007.05.091
(19) Gryko, D.; Urbánczyk-Lipkowska, Z.; Jurczak, J. Diastereoselective addition of vinylmagnesium halides to variously N-mono- and N,N-diprotected L-alaninals. *Tetrahedron: Asymmetry* **1997**, *8*, 4059-4067. DOI: Doi 10.1016/S0957-4166(97)00558-2
(20) Yoo, S. E.; Lee, S. H. A Total Synthesis of (-)-Alpha-Kainic Acid Involving a Pauson-Khand Reaction as the Key Step. *J. Org. Chem.* **1994**, *59*, 6968-6972. DOI: DOI 10.1021/jo00102a021
(21) Wang, P.; Haldar, P.; Wang, Y.; Hu, H. Simple glycosylation reaction of allyl glycosides. *J. Org. Chem.* **2007**, *72*, 5870-5873. DOI: 10.1021/jo070512x
(22) Mukaiyama, T.; Matsubara, K.; Hora, M. An Efficient Glycosylation Reaction of 1-Hydroxy Sugars with Various Nucleophiles Using a Catalytic Amount of Activator and Hexamethyldisiloxane. *Synthesis* **1994**, 1368-1373.
(23) Unthank, M. G.; Tavassoli, B.; Aggarwal, V. K. Epoxy-annulations by reactions of alpha-amido ketones with vinyl sulfonium salts. Reagent versus substrate control and kinetic resolution. *Org. Lett.* **2008**, *10*, 1501-1504. DOI: 10.1021/ol800318h
(24) Nolen, E. G.; Cao, Y. M.; Lewis, B. D.; Powers, M. H.; Thompson, A. W.; Bennett, J. M. Stereoselective Synthesis of (4S,5S)-5-Vinyloxazolidin-2-one-4-carboxylate as a beta-Vinylserine Synthetic Equivalent by Vinyl Grignard Addition to an N-Tosyl Version of Garner's Aldehyde. *Synlett* **2021**, *32*, 601-604. DOI: 10.1055/a-1308-0370

(25) Donohoe, T. J.; Wheelhouse, K. M. R.; Lindsay-Scott, P. J.; Glossop, P. A.; Nash, I. A.; Parker, J. S. Pyridine-N-oxide as a mild reoxidant which transforms osmium-catalyzed oxidative cyclization. *Angew. Chem. Int. Ed.* **2008**, *47*, 2872-2875. DOI: 10.1002/anie.200705425
(26) Yan, Y. H.; Li, W.; Chen, W.; Li, C.; Zhu, K. R.; Deng, J.; Dai, Q. Q.; Yang, L. L.; Wang, Z.; Li, G. B. Structure-guided optimization of 1H-imidazole-2-carboxylic acid derivatives affording potent VIM-Type metallo-beta-lactamase inhibitors. *Eur. J. Med. Chem.* **2022**, *228*, 113965. DOI: 10.1016/j.ejmech.2021.113965
(27) Omura, K.; Swern, D. Oxidation of Alcohols by Activated Dimethyl-Sulfoxide - Preparative, Steric and Mechanistic Study. *Tetrahedron* **1978**, *34*, 1651-1660. DOI: Doi 10.1016/0040-4020(78)80197-5
(28) Dess, D. B.; Martin, J. C. Readily Accessible 12-I-5 Oxidant for the Conversion of Primary and Secondary Alcohols to Aldehydes and Ketones. *J. Org. Chem.* **1983**, *48*, 4155-4156. DOI: DOI 10.1021/jo00170a070
(29) Parikh, J. R.; Doering, W. V. E. Sulfur Trioxide in Oxidation of Alcohols by Dimethyl Sulfoxide. *J. Am. Chem. Soc.* **1967**, *89*, 5505-&. DOI: DOI 10.1021/ja00997a067
(30) Shen, R. C.; Corey, E. J. Studies of the stereochemistry of [2+2]-photocycloaddition reactions of 2-cyclohexenones with olefins. *Org. Lett.* **2007**, *9*, 1057-1059. DOI: 10.1021/ol063092r
(31) Fleming, I.; Henning, R.; Plaut, H. The Phenyldimethylsilyl Group as a Masked Form of the Hydroxy Group. *J. Chem. Soc. Chem. Comm.* **1984**, 29-31. DOI: DOI 10.1039/c39840000029
(32) Baldwin, J. E. Rules for Ring-Closure. *J. Chem. Soc. Chem. Comm.* **1976**, 734-736. DOI: DOI 10.1039/c39760000734.
(33) (a) Sengoku, T.; Xu, S.; Ogura, K.; Emori, Y.; Kitada, K.; Uemura, D.; Arimoto, H. Total synthesis of the antibiotic kendomycin: a macrocyclization using the Tsuji-Trost etherification. *Angew. Chem. Int. Ed.* **2014**, *53*, 4213-4216. DOI: 10.1002/anie.201400305. (b) Sofiadis, M.; Xu, D.; Rodriguez, A. J.; Nissl, B.; Clementson, S.; Petersen, N. N.; Baran, P. S. Convergent Total Synthesis of (-)-Cyclopamine. *J. Am. Chem. Soc.* **2023**, *145*, 21760-21765. DOI: 10.1021/jacs.3c09085.
(34) Miller, D. J.; Bashir-Uddin Surfraz, M.; Akhtar, M.; Gani, D.; Allemann, R. K. Removal of the phosphate group in mechanism-based inhibitors of inositol monophosphatase leads to unusual inhibitory activity. *Org. Biomol. Chem.* **2004**, *2*, 671-688. DOI: 10.1039/b312808c
(35) Pérez, M.; Canoa, P.; Gómez, G.; Terán, C.; Fall, Y. The furan approach to oxacycles:: synthesis of medium-size 2,3-disubstituted oxacycles. *Tetrahedron Lett.* **2004**, *45*, 5207-5209. DOI: 10.1016/j.tetlet.2004.05.035
(36) Hegedus, L. S.; Geisler, L.; Riches, A. G.; Salman, S. S.; Umbricht, G. De novo synthesis of 4′-ethoxy nucleoside analogues. *J. Org. Chem.* **2002**, *67*, 7649-7655. DOI: 10.1021/jo020151f
(37) Craig, D.; Spreadbury, S. R. J.; White, A. J. P. Synthesis and hetero-Diels-Alder reactions of enantiomerically pure dihydro-1H-azepines. *Chem. Comm.* **2020**, *56*, 9803-9806. DOI: 10.1039/d0cc04413j
(38) Anelli, P. L.; Biffi, C.; Montanari, F.; Quici, S. Fast and Selective Oxidation of Primary Alcohols to Aldehydes or to Carboxylic-Acids and of Secondary Alcohols to Ketones

Mediated by Oxoammonium Salts under 2-Phase Conditions. *J. Org. Chem.* **1987**, *52*, 2559-2562.
(39) Schmidt, R. R.; Toepfer, A. Glycosylimidates .50. Glycosylation with Highly Reactive Glycosyl Donors - Efficiency of the Inverse Procedure. *Tetrahedron Lett.* **1991**, *32*, 3353-3356. DOI: Doi 10.1016/S0040-4039(00)92704-7
(40) Rogano, F.; Rüedi, P. The Biomimetic Synthesis and Final Structure Determination of (+)- and (-)-Centrolobine, Naturally Occurring Diarylheptanoid 2,6-Disubstituted Tetrahydro-2-pyrans. *Helv. Chim. Acta.* **2010**, *93*, 1281-1298. DOI: DOI 10.1002/hlca.201000096
(41) Shen, Y.; Li, L.; Xiao, X.; Yang, S.; Hua, Y.; Wang, Y.; Zhang, Y. W.; Zhang, Y. Site-Specific Photochemical Desaturation Enables Divergent Syntheses of Illicium Sesquiterpenes. *J. Am. Chem. Soc.* **2021**, *143*, 3256-3263. DOI: 10.1021/jacs.1c00525
(42) Sakamoto, R.; Inada, T.; Selvakumar, S.; Moteki, S. A.; Maruoka, K. Efficient photolytic C-H bond functionalization of alkylbenzene with hypervalent iodine(III) reagent. *Chem. Comm.* **2016**, *52*, 3758-3761. DOI: 10.1039/c5cc07647a
(43) Varenikov, A.; Shapiro, E.; Gandelman, M. Decarboxylative Halogenation of Organic Compounds. *Chem. Rev.* **2021**, *121*, 412-484. DOI: 10.1021/acs.chemrev.0c00813
(44) Burley, I.; Hewson, A. T. Enantiospecific Synthesis of 3-Pyrrolines - a Route to Novel Polyhydroxylated Pyrrolidines. *Tetrahedron Lett.* **1994**, *35*, 7099-7102. DOI: Doi 10.1016/0040-4039(94)88236-3
(45) Aggarwal, V. K.; Fang, G. Y. Highly regioselective and diastereoselective epoxidation of allylic amines with Oxone. *Chem. Comm.* **2005**, 3448-3450. DOI: 10.1039/b503516c
(46) Das, R.; Mukhopadhyay, B. Chemical O-Glycosylations: An Overview. *Chemistry Open* **2016**, *5*, 401-433. DOI: 10.1002/open.201600043
(47) Barton, D. H. R.; Crich, D.; Motherwell, W. B. A Practical Alternative to the Hunsdiecker Reaction. *Tetrahedron Lett.* **1983**, *24*, 4979-4982. DOI: Doi 10.1016/S0040-4039(01)99826-0
(48) Lindgren, B. O.; Nilsson, T. Preparation of Carboxylic-Acids from Aldehydes (Including Hydroxylated Benzaldehydes) by Oxidation with Chlorite. *Acta. Chem. Scand.* **1973**, *27*, 888-890. DOI: DOI 10.3891/acta.chem.scand.27-0888
(49) Garner, P.; Anderson, J. T.; Dey, S.; Youngs, W. J.; Galat, K. S-(1-Oxido-2-pyridinyl)-1,1,3,3-tetramethylthiouronium Hexafluorophosphate. A New Reagent for Preparing Hindered Barton Esters. *J. Org. Chem.* **1998**, *63*, 5732-5733. DOI: 10.1021/jo980870n
(50) Schotten, C.; Nicholls, T. P.; Bourne, R. A.; Kapur, N.; Nguyen, B. N.; Willans, C. E. Making electrochemistry easily accessible to the synthetic chemist. *Green Chem.* **2020**, *22*, 3358-3375. DOI: 10.1039/d0gc01247e
(51) Schmidt, A. K. C.; Stark, C. B. W. TPAP-Catalyzed Direct Oxidation of Primary Alcohols to Carboxylic Acids through Stabilized Aldehyde Hydrates. *Org. Lett.* **2011**, *13*, 4164-4167. DOI: 10.1021/ol2014335
(52) Corey, E. J.; Schmidt, G. Useful Procedures for the Oxidation of Alcohols Involving Pyridinium Dichromate in Aprotic Media. *Tetrahedron Lett.* **1979**, 399-402.
(53) Mondal, A.; van Gemmeren, M. Silver-Free C-H Activation: Strategic Approaches towards Realizing the Full Potential of C-H Activation in Sustainable Organic Synthesis. *Angew. Chem. Int. Ed.* **2022**, *61*. DOI: 10.1002/anie.202210825

(54) Lagoutte, R.; Patouret, R.; Winssinger, N. Covalent inhibitors: an opportunity for rational target selectivity. *Curr. Opin. Chem. Biol.* **2017**, *39*, 54-63. DOI: 10.1016/j.cbpa.2017.05.008
(55) Chowdhury, G.; Guengerich, F. P. Tandem Mass Spectrometry-Based Detection of C4 '-Oxidized Abasic Sites at Specific Positions in DNA Fragments. *Chem. Res. Tox.* **2009**, *22*, 1310-1319. DOI: 10.1021/tx900115z
(56) Yang, B.; Jinnouchi, A.; Suemune, H.; Aso, M. Difluoro-C4'-oxidized abasic site for efficient amine modification in biological systems. *Org. Lett.* **2012**, *14*, 5852-5855. DOI: 10.1021/ol302703m
(57) (a) Yang, B.; Jinnouchi, A.; Usui, K.; Katayama, T.; Fujii, M.; Suemune, H.; Aso, M. Bioconjugation of Oligodeoxynucleotides Carrying 1,4-Dicarbonyl Groups via Reductive Amination with Lysine Residues. *Bioconjugate Chem.* **2015**, *26*, 1830-1838. DOI: 10.1021/acs.bioconjchem.5b00361. (b) Yuhas, S. C.; Laverty, D. J.; Lee, H.; Majumdar, A.; Greenberg, M. M. Selective Inhibition of DNA Polymerase beta by a Covalent Inhibitor. *J. Am. Chem. Soc.* **2021**, *143*, 8099-8107. DOI: 10.1021/jacs.1c02453

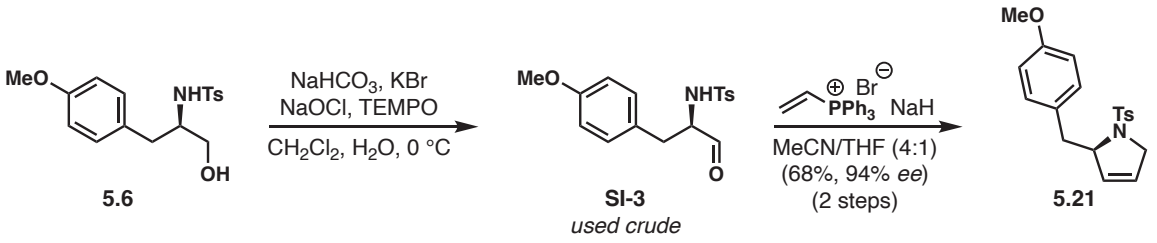
Experimental Details



Compound SI-2 - tosyl protected amino acid: Tosyl protected amino acid **SI-2** was synthesized following a modified procedure of White and co-workers. A 2 L round bottomed flask was charged with (*R*)-OMe-Tyr (100 g, 512 mol, 1.0 equiv). The solid was dissolved in Acetone (255 mL) and DIPEA (94 mL, 540 mmol, 1.05 equiv) was added followed by aq. NaOH (2 M, 256 mL, 512 mmol, 1.0 equiv). The resulting biphasic mixture was cooled to 0 °C and TsCl (102.9 g, 540 mmol, 1.05 equiv) was added in a single portion. The reaction was stirred while slowly warming to ambient temperature. After stirring for 18 h, the reaction mixture was transferred to a separatory funnel and was extracted with Et_2O (3 x ~200 mL). The combined organic layers were then extracted with 2 M aq. NaOH (200 mL) and the combined aqueous layers were carefully acidified to pH ~1 using concentrated HCl (~ 45 mL) and were subsequently extracted with EtOAc (3 x 300 mL). The combined EtOAc extracts were washed with brine, dried over Na_2SO_4, filtered, and concentrated *in vacuo* to yield tosyl protected methyl tyrosine **SI-2** as a light-yellow foam. This material was taken on to the borane reduction assuming 100% yield.

Compound 5.6 - tosyl protected amino alcohol: A 3 L round bottomed flask containing crude tosyl protected methyl tyrosine **SI-2** (512 mmol, 1.0 equiv, assumed full conversion in the previous step) was equipped with an addition funnel and the entire apparatus was evacuated and refilled with argon (3x). The yellow foam was dissolved in THF (340 mL)

and the clear light-yellow solution was cooled to 0 °C. A cannula was used to charge the addition funnel with BH_3•DMS (2 M in THF, 765 mL, 1.53 mol, 3.0 equiv) which was then added dropwise over ~ 1 h at 0 °C. After complete addition the reaction was stirred for an additional 30 min at 0 °C at which point the 0 °C bath was removed and the reaction was stirred at ambient temperature. After stirring at ambient temperature for 36 hours, trace starting acid **SI-2** remained, thus additional BH_3•DMS (2 M in THF, 191 mL, 0.383 mol, 0.75 equiv) was added dropwise via the addition funnel over ~ 30 min at ambient temperature. After stirring an additional 48 h at ambient temperature, full conversion was noted by TLC. The reaction mixture was then cooled to 0 °C before adding 2 M NaOH (960 mL) slowly via the attached addition funnel, stopping the addition when gas evolution became too vigorous. Complete addition of the 2 M NaOH solution took ~ 1 h. After complete addition the reaction was warmed to ambient temperature and was stirred for an additional hour. The mixture was transferred to a separatory funnel using EtOAc to ensure quantitative transfer. The aqueous layer was extracted with EtOAc (4 x 400 mL) and the combined organic layers were washed with brine, dried over $MgSO_4$, filtered and concentrated *in vacuo*. The crude material was purified by dry column vacuum chromatography (6-inch diameter sintered glass funnel, 5.5 inches tall of Merck Silica Gel 60 (15-40 μm), dry loaded in CH_2Cl_2 using SiliaFlash silica gel, 40-63 μm) eluting 0 → 70% EtOAc in hexanes (10% increments, 1 L each) followed by 80% EtOAc in hexanes until all product was eluted (2 L) to yield tosyl protected amino alcohol **5.6** (147 g, 510 mmol, 86% yield over 2 steps) as a taffy like sticky yellow oil which became an off white solid over prolonged storage in the fridge.



Compound SI-3 - tosyl amino aldehyde: A 3 L, 3 necked round bottomed flask was charged with solid amino alcohol **5.6** (14.48 g, 43.17 mmol, 1.0 equiv). Under air, the white solid was dissolved in CH_2Cl_2 (720 mL) and sat. aq. $NaHCO_3$ (360 mL) maintaining stirring at 560 rpm utilizing an overhead stirrer (*Note: insufficient mixing of the biphasic reaction mixture results in sluggish and irreproducible oxidation. On large scale magnetic stirring was inadequate*). The biphasic mixture was then cooled to 0 °C prior to the addition of solid KBr (5.14 g, 43.2 mmol, 1.0 equiv) and TEMPO (338 mg, 2.16 mmol, 5 mol %). NaOCl (0.66 M (aq) 131 mL, 86.3 mmol, 2.0 equiv) was then added dropwise over 1 h via addition funnel while maintaining a temperature of 0 °C. After stirring for an additional 1 h, TLC indicated full consumption of amino alcohol **3**, thus, the reaction was quenched at 0 °C by dropwise addition of sat. aq. $Na_2S_2O_3$ (~ 280 mL) over ~ 15 min via addition funnel. The material was then transferred to an addition funnel rinsing with CH_2Cl_2 to ensure quantitative transfer. The aqueous layer was extracted with CH_2Cl_2 (3 x ~ 250 mL) and the combined organic layers were washed with brine, dried over $MgSO_4$, filtered, and concentrated via rotovap to yield crude amino aldehyde **SI-3** as an orange oil. The oil was dissolved in minimal PhMe (~ 10 mL) and concentrated to azeotropically remove water (3x).

Compound 5.21 - tosyl dihydropyrrole: The round bottomed flask containing azeotropically dried crude aldehyde **SI-3** was equipped with a magnetic stir bar and was

evacuated and refilled with Argon (3x). The orange oil was dissolved in MeCN (344 mL) and THF (86 mL) which resulted in a clear, light orange solution. At ambient temperature, Solid NaH (60 wt% dispersion in oil, 1.9 g, 47.5 mmol, 1.1 equiv) was added in a single portion, immediately followed by vinyl triphenyl phosphonium bromide (17.55 g, 47.52 mmol, 1.1 equiv) resulting in a light brown/orange opaque mixture. After stirring for 1 h at ambient temperature, TLC indicated complete consumption of starting aldehyde. Excess NaH was carefully quench by dropwise addition of IPA (until no H_2 (g) evolution was noted) before transferring the mixture to a separatory funnel, rinsing with EtOAc to ensure quantitative transfer. The mixture was treated with 1 M aq HCl (~ 200 mL) which resulted in a clear light brown/orange solution which was extracted with EtOAc (4 x ~ 150 mL). The combined organic layers were washed with brine, dried over Na_2SO_4, filtered, and concentrated *in vacuo* to yield an orange/brown oil. The crude oil was purified by flash chromatography (3 inch diameter column, ~ 5 inches of silica, dry loaded) eluting 0 → 45% EtOAc in hexanes (15% increments, 2 L each), to yield dihydropyrrole **5.21** as a light yellow/orange opaque oil (10.07 g, 29.32 mmol, 68% yield).

Physical state: Light yellow/orange opaque oil

TLC: R_f = 0.29 (1:4 EtOAc:hexanes, UV active; stains blue with Seebach's stain)

^{1}H NMR (600 MHz, $CDCl_3$): δ 7.73 (d, *J* = 8.3 Hz, 2H), 7.30 (d, *J* = 8.1 Hz, 2H), 7.14 (d, *J* = 8.6 Hz, 2H), 6.82 (d, *J* = 8.6 Hz, 2H), 5.51 (dq, *J* = 5.4, 1.8 Hz, 1H), 5.48 (dq, *J* = 6.3, 2.0 Hz, 1H), 4.60 (dddq, *J* = 9.2, 5.4, 3.7, 1.9 Hz, 1H), 4.02 (dq, *J* = 14.9, 2.1 Hz, 1H), 3.92

(ddt, J = 14.8, 5.4, 1.9 Hz, 1H), 3.78 (s, 3H), 3.19 (dd, J = 13.4, 3.5 Hz, 1H), 2.91 (dd, J = 13.3, 8.4 Hz, 1H), 2.41 (s, 3H).

^{13}C NMR (151 MHz, $CDCl_3$): δ 158.3, 143.6, 134.9, 131.0, 129.9, 129.4, 129.4, 127.5, 125.2, 113.7, 68.7, 55.8, 55.3, 42.3, 21.6.

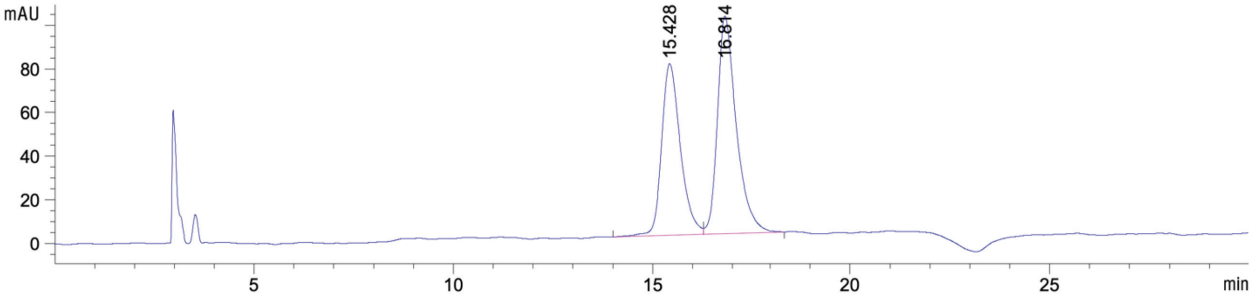
HRMS (ESI-TOF) m/z: calc'd for $C_{19}H_{21}NO_3S$ $[M + H]^+$ 344.1315, found 344.1315.

Optical rotation: $[a]_D^{25}$ –182.9° (c 1.63, $CHCl_3$)

Chiral HPLC traces:

The analysis was performed on an Agilent Technologies 1220 Infifnity II LC HPLC using a CHIRACEL® OD-H column (5 µm particle size, 4.6 x 250 mm) under isocratic conditions (1 mL/min, 5% IPA/hexanes) at 23 °C. The enantiomers were detected by UV light (228 nm). Racemic material was prepared by mixing *O*-Methyl-L-tyrosine and *O*-Methyl-L-tyrosine 1:1 wt/wt and repeating the chemistry described above.

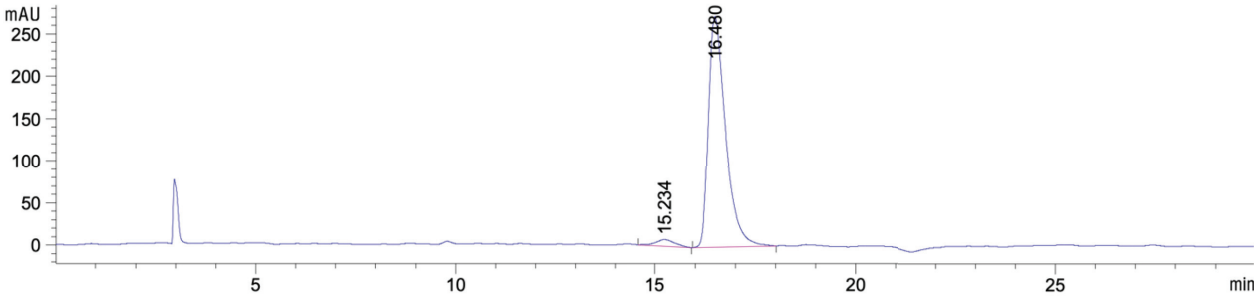
Racemic:



Signal 2: DAD1 C, Sig=228,4 Ref=off

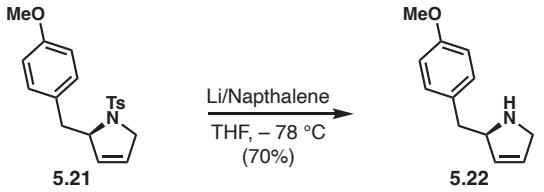
Peak #	RetTime [min]	Type	Width [min]	Area [mAU*s]	Height [mAU]	Area %
1	15.428	BV	0.4995	2586.37793	78.69109	44.0296
2	16.814	VB	0.4906	3287.80786	99.72923	55.9704

Optically Active (prepared using O-Methyl-D-tyrosine):



Signal 2: DAD1 C, Sig=228,4 Ref=off

Peak #	RetTime [min]	Type	Width [min]	Area [mAU*s]	Height [mAU]	Area %
1	15.234	BB	0.4763	254.80708	7.69556	3.0464
2	16.480	BB	0.4487	8109.30615	272.86038	96.9536

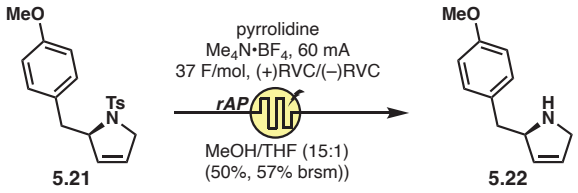


Compound 5.22 - detosylated dihydropyrrole:

Preparation of ~ 1 M Li/Napthalene in THF: A flame dried 250 mL round bottomed flask was charged with naphthalene (19.2 g, 150 mmol, 1.0 equiv). The flask was equipped with a septum and was evacuated and refilled with Argon (3x). The naphthalene was then dissolved in THF (150 mL) and solid Li° granules (1.25 g, 180 mmol, 1.2 equiv) were added. The mixture was sonicated for 45 minutes during which time the clear colorless mixture became a dark blue/green opaque color.

Tosyl Deprotection: A 1 L round bottomed flask containing tosyl protected dihydropyrrole **5.21** (10.1 g, 29.3 mmol, 1.0 equiv) was equipped with a magnetic stir bar and an oven dried graduated addition funnel. The entire apparatus was evacuated and refilled with argon (3x) before dissolving the yellow oil in THF (230 mL) and cooling the solution to –78 °C. Freshly prepared Li/Napthalene solution (see prep above, 1.0 M, 120 mL, 120 mmol, 4.1 equiv) was transferred via cannula to the addition funnel which was used to add the Li/Napthalene solution dropwise over ~ 30 minutes to the –78 °C stirred solution of dihydropyrrole **5.21** which turned to a dark green/blue as addition completed. After complete addition of the Li/Napthalene solution, the reaction was stirred at –78 °C until complete consumption of tosylated dihydropyrrole was noted by TLC (typically 3 hours). Upon completion, excess Li/Napthalene was quenched by dropwise addition of MeOH at –78 °C until the dark blue/green color no longer persisted and the reaction returned to a

clear light-yellow color (typically ~ 1 mL required). sat. aq. $NaHCO_3$ (100 mL) was slowly added, and the reaction was allowed to warm to ambient temperature. The bulk of the THF was then removed via rotovap before transferring the mixture into a separatory funnel using 3:1 $CHCl_3$:IPA (~ 200 mL). The aqueous layer was then extracted with 3:1 $CHCl_3$:IPA (6 x 50 mL). *Note: this compound has a high affinity for the aqueous layer. Relative quantity of desired product in the aqueous layer was monitored by UPLCMS. Further extractions were completed as necessary.* The combined organic layers were washed with brine, dried over Na_2SO_4, filtered, and concentrated *in vacuo* to yield a yellow crude oil. The oil was purified by flash chromatography (3 inch diameter column, ~ 5 inches of silica, dry loaded) eluting 2 L CH_2Cl_2, 5 → 15 % MeOH in CH_2Cl_2 (5% increments, 1 L each) and finally 20% MeOH in CH_2Cl_2 (until all product had eluted) to yield dihydropyrrole **5.22** (3.86 g, 20.4 mmol, 70% yield) as a clear, light-yellow viscous oil.



rAP Tosyl Deprotection: A 20 mL ElectraSyn vial equipped with a stir bar was charged with tosyl protected dihydropyrrole **5.21** (172 mg, 0.5 mmol, 1.0 equiv) and $Me_4N•BF_4$ (258 mg, 1.6 mmol, ca. 0.1 M). The compounds were dissolved in MeOH (15.0 mL) and THF (1.0 mL) before adding pyrrolidine (0.41 mL, 4.9 mmol, 9.8 equiv) resulting in a clear light yellow solution. Next, and ElectraSyn cap with RVC anode and RVC cathode affixed was placed on the vial and the vial subsequently sparged by a constant stream of Argon for 3 min. *Note: Electrodes were cut from 80 ppi RVC block using a hollow 3 mL syringe to make a 3 mL volume electrode.* After sparging, the vial was placed onto an ElectraSyn and

subjected to the programmed electrolysis (constant current, 60 mA, rAP (100 ms), 37 F/mol, stir rate 1000 rpm). From ~8 F/mol to 28 F/mol the reaction was a dark green color which became a clear orange/red color upon completion of the programmed electrolysis. The cap was then removed, and the electrodes were rinsed with EtOAc (2 mL each). The combined washings were filtered through a Kimtech wipe and reaction mixture was concentrated *in vacuo*. Crude NMR with CH_2Br_2 as an internal standard revealed 60% amine **5** and 14% remaining starting material **5.21**. The crude brown oil was then dissolved in MeCN and directly subjected to reversed-phase MPLC (C18 50 g gold) eluting 10% to 45% MeCN:H_2O over 30 min to afford detosylated dihydropyrrole **5.22** (46.9 mg, 0.248 mmol, 50% yield. The gradient was then pushed from 45% MeCN in H_2O to 100% MeCN over the next 5 minutes, holding at 100% MeCN until starting tosylate **5.21** (20.5 mg, 0.059 mmol, 12% RSM) eluted which upon concentration resulted in a light-yellow film.

Physical state: Clear, light yellow viscous oil

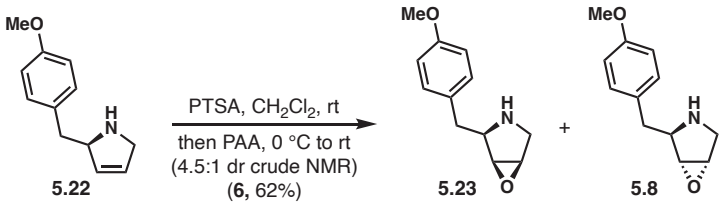
TLC: R_f = 0.2 (10% MeOH in CH_2Cl_2, faintly UV active; stains green with Seebach's stain)

^{1}H NMR (600 MHz, $CDCl_3$): δ 7.12 (d, *J* = 8.1 Hz, 2H), 6.83 (d, *J* = 8.3 Hz, 2H), 5.83-5.87 (m, 1H), 5.75-5.79 (m, 1H), 4.19 (bs, 1H), 3.79 (s, 3H), 3.66-3.77 (m, 2H), 2.67-2.75 (m, 2H), 1.92 (s, 1H).

^{13}C NMR (151 MHz, $CDCl_3$): δ 158.2, 132.2, 131.4, 130.2 (2), 128.9, 113.9 (2), 67.0, 55.4, 53.7, 42.6.

HRMS (ESI-TOF) m/z: calc'd for $C_{12}H_{15}NO$ $[M + H]^+$ 190.1227, found 190.1226.

Optical rotation: $[a]_D^{25}$ –97.5° (c 1.00, $CHCl_3$)



Compounds 6 & 7 - Pyrrolidine epoxides: A 25 mL round bottomed flask was charged with pyrrolidine **5.22** (1.00 g, 5.28 mmol, 1.0 equiv) and PTSA•H_2O (1.00 g, 5.26 mmol, 1.0 equiv). The flask was equipped with a septum and was evacuated and refilled with argon (3x) before dissolving the mixture in CH_2Cl_2 (5.3 mL) at ambient temperature. After stirring the mixture for 1 h, the clear light-yellow solution was cooled to 0 °C and peracetic acid (2.20 mL, 10.6 mmol, 2.0 equiv) was added dropwise over ~ 5 mins. The reaction was stirred an additional 10 minutes at 0 °C at which point the 0 °C bath was removed and the reaction was continued at ambient temperature. After stirring for an additional 23 h UPLC indicated 90 to 95% conversion thus the solution was cooled to 0 °C and was quenched by the slow addition of Na_2SO_3 (~ 2 mL). *Note: It was found that leaving the reaction for longer than 24 hours to push to full conversion resulted in drastically lower yields.* The solution was then adjusted to pH 10-12 by the addition of aq. KOH (2 M, ~ 15 mL). The biphasic mixture was transferred to a separatory funnel, rinsing with CH_2Cl_2 to ensure quantitative transfer. The aqueous layer was extracted with 3:1 $CHCl_3$ (7 x 10 mL) periodically checking the contents of the aqueous layer by UPLC to ensure all amine had been successfully extracted. The combined organic layers were washed with brine, dried over Na_2SO_4, filtered, and concentrated *in vacuo*. Crude NMR revealed a 4.5:1.0 ratio of desired epoxide **5.23** to undesired epoxide **5.8**. The crude material was purified by flash chromatography (1.5 inch column, ~ 5 inches silica, wet loaded in CH_2Cl_2.) eluting 0 → 7.5% IPA in EtOAc containing 1% aq. NH_4OH (2.5% increments, 500 mL each) to provide

desired epoxide **5.23** (671 mg, 3.27 mmol, 62% yield) as a colorless amorphous solid. These conditions led to ~200 mg of a mixture of undesired epoxide **5.8** and an unidentified byproduct**.** It was later found that this mixture could be repurified by reverse phase MPLC (50 g gold C18) eluting 0 → 55% ACN in H_2O to gain access to an analytically pure sample **7** for complete characterization**.**

*Data for syn-epoxide **5.23**:*

Physical state: colorless amorphous solid

Melting point: 57 – 59 °C

TLC: R_f = 0.34 (10% MeOH in CH_2Cl_2, faintly UV active; stains green with Seebach's stain)

^{1}H NMR (600 MHz, $CDCl_3$): δ 7.18 (d, *J* = 8.6 Hz, 2H), 6.85 (d, *J* = 8.6 Hz, 2H), 3.79 (s, 3H), 3.53 (d, *J* = 2.8 Hz, 1H), 3.35 (d, *J* = 2.9 Hz, 1H), 3.16 (d, *J* = 13.5 Hz, 1H), 3.11 (dd, *J* = 8.7, 5.8 Hz, 1H), 2.89 (dd, *J* = 13.4, 5.8 Hz, 1H), 2.79 – 2.68 (m, 2H), 1.59 (bs, 1H).

^{13}C NMR (151 MHz, $CDCl_3$): δ 158.4, 130.7, 130.1 (2), 114.1 (2), 61.1, 57.3, 56.5, 55.4, 48.44, 35.9.

HRMS (ESI-TOF) m/z: calc'd for $C_{12}H_{15}NO_2$ $[M + H]^+$ 206.1176, found 206.1175.

Optical rotation: $[a]_D^{25}$ –26.0° (*c* 0.86, $CHCl_3$)

*Data for anti-epoxide **5.8**:*

Physical state: Off-white crystalline solid

Melting point: 92 – 94 °C

TLC: R_f = 0.38 (10% MeOH in CH_2Cl_2, faintly UV active; stains green with Seebach's stain)

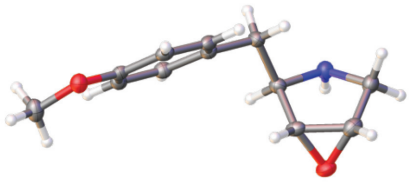
^{1}H NMR (600 MHz, $CDCl_3$): δ 7.14 (d, *J* = 8.1 Hz, 2H), 6.84 (d, *J* = 8.1 Hz, 2H), 3.79 (s, 3H), 3.54 (bs, 1H), 3.45 – 3.39 (m, 2H), 3.06 (d, *J* = 13.4 Hz, 1H), 2.70 (d, *J* = 13.4 Hz, 1H), 2.60 (dd, *J* = 14.0, 7.3 Hz, 1H), 2.53 (dd, *J* = 13.9, 7.4 Hz, 1H), 1.92 (bs, 1H).

^{13}C NMR (151 MHz, $CDCl_3$): δ 158.3, 130.8, 130.2 (2), 114.0 (2), 59.8, 58.8, 55.9, 55.4, 46.4, 36.8.

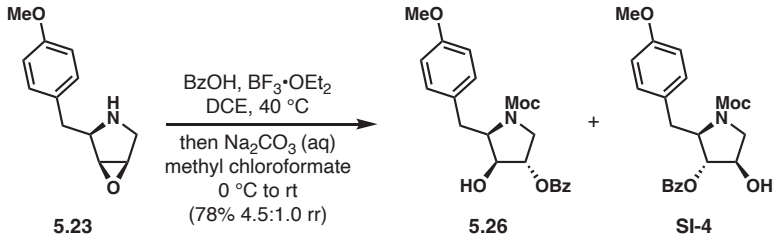
HRMS (ESI-TOF) m/z: calc'd for $C_{12}H_{15}NO_2$ $[M + H]^+$ 206.1176, found 206.1183.

Optical rotation: $[a]_D^{25}$ 4.2° (*c* 1.00, $CHCl_3$)

X-ray crystallography structure:



(See **X-Ray Crystallography Data** section for full report)



5.23 5.26 SI-4

Compounds 8 & SI-4 - Moc pyrrolidine alcohols: A 100 mL round bottomed flask was charged with syn-epoxide **5.23** (1.12 g, 5.46 mmol, 1.0 equiv) and benzoic acid (1.34 g, 10.9 mmol, 2.0 equiv). The mixture was azeotropically dried using PhMe (3x), backfilling with Argon in between each solvent removal. After the final backfill with Argon, the mixture was dissolved in DCE (25 mL) and BF_3•OEt_2 (1.15 mL, 9.28 mmol, 1.7 equiv) was added dropwise at ambient temperature. The reaction flask was then placed in a preheated 40 °C oil bath and was stirred at that temperature until full consumption of starting syn epoxide was noted by UPLC (typically 16 to 24 h). The now cloudy brown mixture was cooled to 0 °C prior to the addition of aq. Na_2CO_3 (1.0 M, 27 mL, 27 mmol, 4.9 equiv) followed by methyl chloroformate (1.05 mL, 13.7 mmol, 2.5 equiv) which turned the reaction cloudy and pink in color. The reaction was stirred at 0 °C until full conversion to the Moc protected amine was noted by UPLC (typically 2 to 4 h). The biphasic mixture was transferred to a separatory funnel rinsing with CH_2Cl_2 to ensure quantitative transfer. The aqueous layer was extracted with CH_2Cl_2 (4 x 10 mL), and the combined organic layers were washed with brine, dried over Na_2SO_4, filtered, and concentrated to yield a brown oil. The oil was purified by flash chromatography (1.5 inch diameter column, ~ 5 inches of silica, dry loaded) eluting 0 → 35% EtOAc in hexanes (5% increments, 500 mL each) to yield desired alcohol **5.26** (1.25 g, 3.24 mmol, 59% yield) as a white foam, and a 1.0:3.0 mixture of **5.26:SI-4** (409 mg, 1.06 mmol, 19% yield) as a white foam for a total yield of 78%, 3.1:1.0 rr. For characterization of the undesired

regioisomer and recovery of the desired regioisomer, the mixture was resubjected to silica gel chromatography.

*Data for desired benzoate **5.25**:*

Physical state: White foam

Melting point: 40 – 41 °C

TLC: R_f = 0.35 (40% EtOAc in hexanes, UV active; stains blue with Seebach's stain)

^{1}H NMR (600 MHz, $CDCl_3$): δ 7.94 (d, *J* = 7.8 Hz, 2H), 7.57 (t, *J* = 7.4 Hz, 1H), 7.42 (t, *J* = 7.7 Hz, 2H), 7.31 – 7.15 (m, 2H), 6.82 (d, *J* = 8.5 Hz, 2H), 5.00 (bs, 1H), 4.37 – 4.20 (m, 2H), 3.77 (s, 3H), 3.75 – 3.60 (m, 5H), 3.49 – 3.33 (m, 1H), 3.11 – 2.93 (m, 2H).

^{13}C NMR (151 MHz, $CDCl_3$): δ 167.3 and 166.6 (1C, rotamers), 158.3, 156.0, 133.7, 130.9, 130.6, 129.9, 129.3, 128.6, 78.6 and 78.1 (1C, rotamers), 75.7 and 74.3 (1C, rotamers), 62.2 and 61.6 (1C, rotamers), 55.3, 52.7, 49.8 and 49.3 (1C, rotamers), 33.2 and 32.1 (1C, rotamers).

HRMS (ESI-TOF) m/z: calc'd for $C_{21}H_{23}NO_6$ $[M + H]^+$ 386.1598, found 386.1601.

Optical rotation: $[a]_D^{25}$ 8.8° (*c* 1.0, $CHCl_3$)

*Data for undesired benzoate **SI-4**:*

Physical state: White foam

Melting point: 52 – 53 °C

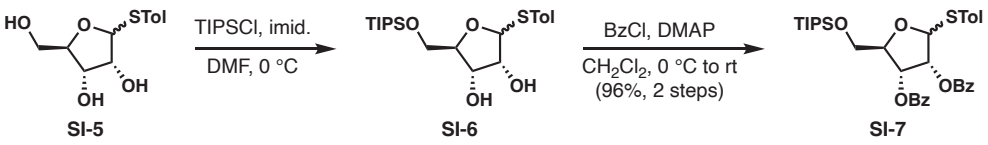
TLC: R_f = 0.27 (40% EtOAc in hexanes, UV active; stains blue with Seebach's stain)

^{1}H NMR (600 MHz, $CDCl_3$): δ 7.86 (brs, 2H), 7.55 (t, *J* = 7.5 Hz, 1H), 7.39 (t, *J* = 7.7 Hz, 2H), 7.19 (brs, *J* = 8.7 Hz, 2H), 6.81 (d, *J* = 7.1 Hz, 2H), 5.09 (d, *J* = 13.9 Hz, 1H), 4.36 (s, 1H), 4.27 and 4.18 (two brs, 1H, rotamers) 4.01 and 3.89 (two brs, 1H, rotamers), 3.82 – 3.66 (m, 6H), 3.51 – 3.12 (m, 3H), 3.06 – 2.96 (m, 1H).

^{13}C NMR (151 MHz, $CDCl_3$): δ 166.8 and 166.5 (1C, rotamers), 158.4, 155.6, 133.7, 130.7 (br), 129.9, 129.6, 129.2, 128.5, 114.2, 82.8 and 82.2 (1C rotamers), 74.3 and 73.8 (1C, rotamers), 63.9, 55.3, 52.7 and 52.2 (1C rotamers), 37.4 and 36.5 (1C, rotamers).

HRMS (ESI-TOF) m/z: calc'd for $C_{21}H_{23}NO_6$ $[M + H]^+$ 386.1598, found 386.1606.

Optical rotation: $[a]_D^{25}$ 27.4° (*c* 1.0, $CHCl_3$)



Compound SI-6 - TIPS diol ribose: A flame dried 50 mL round bottomed flask was charged with triol **SI-5** (2.5 g, 9.8 mmol, 1.0 equiv, 4:1 mixture of anomers) and imidazole (1.33 g, 19.5 mmol, 2.0 equiv). The flask was equipped with a septum and was evacuated and refilled with argon (3x). The solids were dissolved in DMF (9.8 mL) and the resulting clear colorless solution was cooled to 0 °C before adding TIPSCl (2.3 mL, 10.7 mmol, 1.1 equiv) dropwise over ~ 2 min. After stirring for 30 minutes the 0 °C bath was removed and the reaction was stirred at ambient temperature for 21 h at which point full conversion was noted by TLC. The reaction was quenched by the addition of sat. aq. NH_4Cl (~ 10 mL). The biphasic mixture was transferred to a separatory funnel rinsing with EtOAc (~ 50 mL) to ensure quantitative transfer. The organic layer was then treated sequentially with 1 M aq. HCl (2 x 20 mL), sat. aq. $NaHCO_3$ (20 mL), 10% aq. LiCl (20 mL), and brine (2 x 10 mL). The organic layer was then dried over Na_2SO_4, filtered, and concentrated *in vacuo* to yield crude TIPS protected ribose **SI-6** (3.93 g, 9.52 mmol, 98% yield) as a clear colorless oil which was used directly in the next step.

Compound SI-7 - protected ribose: A 100 mL round bottomed flask containing crude TIPS protected ribose **SI-5** (3.93 g, 9.52 mmol, 1.0 equiv) was equipped with a septum and was evacuated and refilled with argon (3x). The oil was dissolved in CH_2Cl_2 (19 mL) prior to the addition of DMAP (3.49 g, 28.6 mmol, 3.0 equiv). The resulting clear colorless solution was cooled to 0 °C and BzCl (2.65 mL, 22.9 mmol, 2.4 equiv) was added dropwise over ~ 2 minutes. After stirring for 1 h the 0 °C bath was removed and the reaction was

stirred at ambient temperature for an additional 2 h at which point the reaction was complete as judged by TLC. The solution was cooled to 0 °C and was quenched by the addition of 1 M aq. HCl (~ 10 mL). The biphasic mixture was transferred to a separatory funnel rinsing with CH_2Cl_2 to ensure quantitative transfer. The aqueous layer was extracted with CH_2Cl_2 (2 x 15 mL) and the combined organic layers were treated with sat. aq. $NaHCO_3$ (~20 mL), washed with brine, dried over Na_2SO_4, filtered, and concentrated *in vacuo* to yield a clear light-yellow oil. The crude oil was purified by flash chromatography eluting 0 → 10% Et_2O in CH_2Cl_2 to yield fully protected ribose **SI-7** (4.68 g, 9.40 mmol, 96% over 2 steps, 4:1 ratio of anomers)

Reported as a 4:1 mixture of inconsequential anomers:

Physical state: Clear colorless oil

TLC: R_f = 0.73 (30% EtOAc in hexanes, UV active; stains with PAA & Seebach's stain's stain)

Major Diastereomer (likely β-anomer)

^{1}H NMR (600 MHz, $CDCl_3$): δ 7.96 – 7.90 (m, 4H), 7.52 (t, *J* = 7.5 Hz, 2H), 7.48 (d, *J* = 7.9 Hz, 2H), 7.38 – 7.33 (m, 4H), 7.15 (d, *J* = 7.7 Hz, 2H), 5.72 (d, *J* = 5.3, 3.4 Hz, 1H), 5.61 (dd, *J* = 6.6, 5.2 Hz, 1H), 5.52 (d, *J* = 6.5 Hz, 1H), 4.38 (q, *J* = 4.0 Hz, 1H), 3.96 (dd, *J* = 10.8, 4.0 Hz, 1H), 3.80 (dd, *J* = 10.8, 4.6 Hz, 1H), 2.34 (s, 3H), 1.19 – 1.07 (m, 21H).

Minor Diastereomer (likely α-anomer)

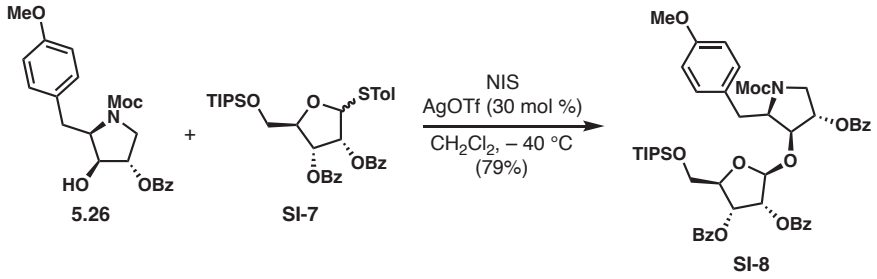
^{1}H NMR (600 MHz, $CDCl_3$): δ 8.14 (d, *J* = 7.4 Hz, 2H), 7.98 (d, *J* = 7.7 Hz, 2H), 7.57 (t, *J* = 7.4 Hz, 1H), 7.54-7.50 (obscure, 1H), 7.46 – 7.41 (m, 4H), 7.34-7.33 (obscure, 2H) 7.10 (d, *J* = 7.8 Hz, 2H), 6.03 (d, *J* = 6.0 Hz, 1H), 5.84 (dd, *J* = 6.0, 3.2 Hz, 1H), 5.76 – 5.73 (obscure, 1H), 4.57 (q, *J* = 2.9 Hz, 1H), 4.08 (dd, *J* = 11.1, 2.9 Hz, 1H), 4.00 (dd, *J* = 11.1, 2.8 Hz, 1H), 2.32 (s, 3H), 1.19 – 1.07 (obscure, 21H).

Mixture of diastereomers

^{13}C NMR (151 MHz, $CDCl_3$): δ 165.9, 165.5, 165.3, 165.2, 138.4, 137.5, 133.8, 133.4, 133.39, 133.37, 132.43, 131.5, 130.13, 130.07, 129.95, 129.91, 129.85, 129.8, 129.7, 129.6, 129.42, 129.38, 129.0, 128.6, 128.52, 128.47, 128.45, 91.1, 88.5, 84.3, 83.0, 74.7, 74.0, 73.0, 72.2, 64.0, 63.5, 21.3, 21.2, 18.16, 18.15, 18.12, 18.09, 12.1.

HRMS (ESI-TOF) m/z: calc'd for $C_{35}H_{44}O_6SSi$ $[M + Na]^+$ 643.2520, found 643.2528.

Optical rotation: $[a]_D^{25}$ -33.6° (*c* 1.0, $CHCl_3$)



Compound SI-7 - glycosylated TIPS ether: A flame dried 50 mL round bottomed flask was charged with pyrrolidine **5.26** (105 mg, 0.273 mmol, 1.0 equiv), TIPS protected ribose **SI-7** (267 mg, 0.536 mmol, 2.0 equiv) and 4 Å MS (500 mg). The flask was evacuated and refilled with argon (3x) before suspending/dissolving the mixture in CH_2Cl_2 (5.2 mL). The white/colorless mixture was cooled to – 40 °C prior to the addition of solid NIS (116 mg, 0.519 mmol, 2.0 equiv) followed by AgOTf (20 mg, 0.078 mmol, 30 mol %) as solids. Over the next 30 minutes, the mixture turned to a deep red/brown color. After 1 h, TLC indicated full consumption of starting pyrrolidine. At – 40 °C the reaction was quenched by the addition of Et_3N (0.1 mL) which caused the reaction to go from dark red/brown to a yellow/orange color. The mixture was filtered through celite into a separatory funnel containing sat. aq. $NaHCO_3$ (~2.5 mL). The organic layer was then treated with sat. aq. $Na_2S_2O_3$ (5 mL) and the combined aqueous layers were extracted with CH_2Cl_2 (3 x 5 mL). The combined organic layers were washed with brine, dried over Na_2SO_4, filtered, and concentrated via RotoVap. The clear light yellow crude oil was purified by flash chromatography (1 inch diameter column, ~ 5 inches of silica, dry loaded) eluting 2% Et_2O in CH_2Cl_2 until all product had eluted to yield glycosylated TIPS ether **SI-8** (190 mg, 0.215 mmol, 79% yield) as a white foam. An analytical sample of the material was obtained by PTLC (5% Et_2O in DCM).

Physical state: White foam

Melting point: 54 – 56 °C

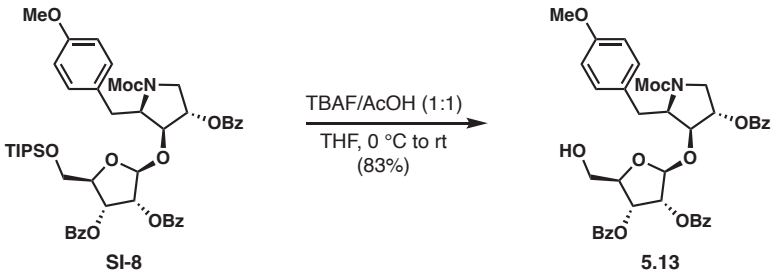
TLC: R_f = 0.28 (30% EtOAc in hexanes, UV active; stains blue with Seebach's stain)

^{1}H NMR (600 MHz, $CDCl_3$): δ 7.99 – 7.85 (m, 6H), 7.55 – 7.49 (m, 3H), 7.41 – 7.27 (m, 7H), 7.17 (br s, 1H), 6.83 (d, *J* = 8.2 Hz, 2H), 5.68 – 5.62 (m, 2H), 5.60 (d, *J* = 2.6 Hz, 1H), 5.20 – 5.05 (m, 1H), 4.59 (br d, *J* = 47.0 Hz, 1H), 4.46 (q, *J* = 4.6 Hz, 1H), 4.36 (br s, 1H), 3.92 (br s, 2H), 3.86 – 3.54 (m, 7H), 3.45 (br s, 1H), 3.24 – 2.81 (m, 2H), 1.07 (d, *J* = 6.9 Hz, 21H).

^{13}C NMR (151 MHz, $CDCl_3$): δ 165.9, 165.5, 165.3, 158.3, 155.7, 133.5, 133.4, 131.1 and 131.0 (1C, rotamers), 130.4, 130.3, 129.9, 129.84, 129.81, 129.5, 129.4, 129.3, 128.6, 128.5, 113.9 (2), 105.2 and 105.0 (1C, rotamers), 83.1, 79.9 and 79.1 (1C, rotamers), 75.8, 72.7, 65.0, 60.7 and 59.9 (1C, rotamers), 55.3, 52.6, 49.4 and 49.0 (1C, rotamers), 34.2 and 32.6 (1C, rotamers), 18.1 (6), 12.1 (3).

HRMS (ESI-TOF) m/z: calc'd for $C_{49}H_{59}NO_{12}Si$ $[M + Na]^+$ 904.3698, found 904.3697.

Optical rotation: $[a]_D^{25}$ 16.6° (*c* 1.0, $CHCl_3$)



Compound 5.13 - glycosylated alcohol: A 13 x 100 mm culture tube containing TIPS protected ether **SI-8** (120 mg, 0.135 mmol, 1.0 equiv) was equipped with a magnetic stir bar and was evacuated and refilled with argon (3x). The white foam was dissolved in THF and the resulting clear colorless solution was cooled to 0 °C. A freshly prepared ~1:1 stock solution of TBAF/AcOH (~0.95 M in THF, 0.71 mL, 0.68 mmol, 5 equiv) was added dropwise over ~2 min. *Note: stock solution was prepared by dissolving 57 µL of AcOH in 1 mL of 1.0 M TBAF in THF*. The now clear light-yellow solution was stirred at 0 °C for 10 minutes before removing the 0 °C bath and allowing the reaction to stir at ambient temperature. After stirring for 3 d, the starting material was mostly consumed by UPLC and TLC. Sat. aq. NH_4Cl and 2 drops of DI H_2O were added. The aqueous layer was extracted with EtOAc (4 x 1 mL). The combined organics were dried over Na_2SO_4, filtered, and concentrated *in vacuo* to yield a crude light-yellow oil. The oil was purified by flash chromatography (3/4 inch column, ~5 inches silica, wet loaded in CH_2Cl_2) eluting 0 → 30% EtOAc in hexanes (10% increments, 100 mL each) to yield the target alcohol **5.13** (81.2 mg, 0.112 mmol, 83% yield) as a white foam.

Physical state: White foam

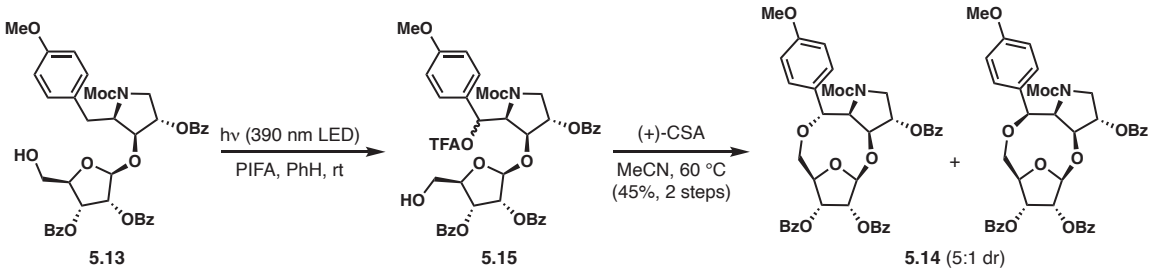
TLC: R_f = 0.53 (30% EtOAc in CH_2Cl_2, UV active; stains blue with Seebach's stain)

^{1}H NMR (600 MHz, $CDCl_3$): δ 7.98 – 7.92 (m, 4H), 7.88 (d, *J* = 7.7 Hz, 2H), 7.59 – 7.49 (m, 3H), 7.42 – 7.36 (m, 4H), 7.34 (t, *J* = 7.7 Hz, 2H), 7.29 (br s, 1H), 7.20 (br s, 1H), 6.87 (d, *J* = 8.7 Hz, 2H), 5.63 (d, *J* = 4.5 Hz, 1H), 5.57 – 5.53 (m, 2H), 5.24 (br s, 1H), 4.71 – 4.52 (m, 1H), 4.48 – 4.36 (m, 2H), 3.89 – 3.50 (m, 10H), 3.32 – 2.89 (m, 2H), 2.17 – 2.02 (m, 1H).

^{13}C NMR (151 MHz, $CDCl_3$): δ 166.0, 165.9, 165.3, 158.4, 155.7, 133.7, 133.6, 130.7, 130.5, 129.93, 129.89, 129.87, 129.4, 129.2, 129.1, 128.6, 128.6, 114.0 (2), 104.5, 82.7, 79.4 and 78.5 (1C rotamers), 76.1, 75.6, 71.7, 63.0, 60.4 and 59.7 (1C rotamers), 55.4, 52.7, 49.3 and 49.0 (1C, rotamers), 34.3 and 32.9 (1C, rotamers).

HRMS (ESI-TOF) m/z: calc'd for $C_{40}H_{39}NO_{12}$ $[M + Na]^+$ 748.2364, found 748.2361.

Optical rotation: $[a]_D^{25}$ 16.7° (*c* 1.0, $CHCl_3$)



5.13 **5.15** **5.14** (5:1 dr)

Compound 5.15 - benzylic TFA: A round bottomed flask containing acyclic alcohol **10** (1.10 g, 1.52 mmol, 1.0 equiv) was charged with PIFA (783 mg, 1.82 mmol, 1.2 equiv). The flask was equipped with a septum and was evacuated and refilled with argon (3x) before dissolving the mixture in anhydrous benzene (43 mL). The clear colorless solution was irradiated with purple LED (Kessil PR160L-390 nm at 100% intensity), blowing air on the flask to keep the solution at ambient temperature. When full consumption of starting material was noted by TLC (typically 40 to 70 min) irradiation was halted and the solvent was removed via rotovap at ≤ 30 °C. The light-yellow oil was quickly passed through a plug of silica eluting with 50% EtOAc in hexanes to yield benzylic TFA **5.15** (1.22 g, 1.45 mmol, 95%, 1:1 dr) as a white foam.

Compound 5.14 - protected deschloro-dragocin: Benzylic TFA **5.15** was split into two round bottomed flask one containing (RB A, 613 mg, 0.732 mmol, 1.0 equiv) and the other (RB B, 602 mg, 0.719 mmol, 1.0 equiv). Each flask was also charged with (+)-CSA (RB A, 192 mg, 0.825 mmol, 1.13 equiv) and (RB B, 186 mg, 0.801, 1.13 mmol) respectively before equipping them with a septum. Minimal toluene was added to each flask and then removed *in vacuo* (3x) to azeotropically dry the mixture, backfilling with argon. The mixtures were then dissolved in MeCN (RB A, 93 mL) and (RB B, 91 mL) and each was placed in a preheated 60 °C oil bath. After full consumption of benzylic TFA **5.15** was

noted by TLC (typically 4 to 6 hours) the solution was cooled to ambient temperature and Et_3N (2 mL) was added to each flask resulting in a change from a clear dark yellow/orange to a clear light-yellow solution. The bulk of the MeCN was removed via rotovap and the mixtures were combined in the same separatory funnel, rinsing with CH_2Cl_2 to ensure quantitative transfer. The material was treated with sat. aq. $NaHCO_3$ (25 mL) and the resulting aqueous layer was extracted with CH_2Cl_2 (3 x 15 mL). The combined organic layers were washed with brine, dried over Na_2SO_4, filtered, and concentrated *in vacuo*. The crude material was purified by flash chromatography eluting 20% → 33% EtOAc in heaxanes to yield an inseparable mixture of 9-membered ring benzylic diastereomers **11** (500 mg, 0.691 mmol, 45% yield 5:1 dr over 2 steps) as a white foam.

Reported as a 5:1 mixture favoring the desired diastereomer

Physical state: White foam

TLC: R_f = 0.18 (30% EtOAc in CH_2Cl_2, UV active; stains blue with Seebach's stain)

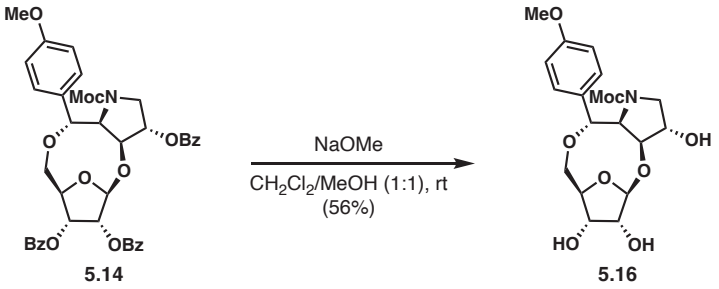
Due to the 5:1 mixture of diastereomers and rotamers the minor and major diastereomers could not be separately assigned, thus the integrations and peak picking was completed and reported exactly as shown in the NMR in a single line listing resulting in reported integrals as fractions. Peaks that are distinguishable will be reported as from the 'minor' or 'major' compound.

^{1}H NMR (600 MHz, $CDCl_3$): δ 8.05 (minor, d, *J* = 7.3 Hz, 0.5H), 8.03 – 7.99 (major, m, 4H), 7.93 (minor, d, *J* = 7.5 Hz, 0.5H), 7.86 – 7.80 (m, 2.3H), 7.61 – 7.29 (m, 11H), 7.29 – 7.24 (m, 3H), 6.96 (minor, d, *J* = 8.9 Hz, 0.4H), 6.88 (major, d, *J* = 8.5 Hz, 2H), 6.27 (minor, t, *J* = 5.4 Hz, 0.2H), 5.91 (minor, d, *J* = 5.7 Hz, 0.2H), 5.82 – 5.71 (m, 2H), 5.59 (major, br s, 1H), 5.51 (major, q, *J* = 5.9 Hz, 1H), 5.45 (minor, s, 0.2H), 5.16 – 4.83 (m, 1H), 4.79 – 4.43 (m, 4H), 4.39 – 3.95 (m, 2H), 3.91 – 2.92 (m, 11.3H). (46.6, 9.6)

^{13}C NMR (151 MHz, $CDCl_3$): δ 166.3, 165.9, 165.8, 165.7, 165.4, 165.3, 159.9, 159.4, 155.6, 133.63, 133.59, 133.56, 133.5, 133.38, 133.35, 130.02, 130.00, 129.95, 129.82, 129.79, 129.51, 129.47, 129.5, 129.4, 129.23, 129.15, 128.61, 128.59, 128.51, 128.45, 114.0, 113.3, 107.1, 106.7, 84.7, 82.8, 80.7, 75.8, 72.6, 67.5, 57.8, 55.5, 55.4, 53.0, 52.6, 48.6, 48.1.

HRMS (ESI-TOF) m/z: calc'd for $C_{40}H_{37}NO_{12}$ $[M + H]^+$ 724.2389, found 724.2372.

Optical rotation: $[a]_D^{25}$ 15.9° (*c* 1.0, $CHCl_3$)



Compound 5.16 - Moc protected deschloro dragocin: A 13 x 100 mm culture tube containing a 5:1 diastereomeric mixture of tris benzoate **5.14** (12.0 mg, 0.017 mmol, 1.0 equiv) was evacuated and refilled with Argon (3x). The film was then dissolved in CH_2Cl_2 (0.28 mL) prior to the addition of a freshly prepared stock solution of NaOMe in MeoH (1.9 mg/mL solution, used 0.28 mL, 0.53 mg, 0.0098 mmol, 0.58 equiv) dropwise at ambient temperature. After stirring for 14 h at ambient temperature all three benzoates had been removed according the UPLC analysis. The solution was quench at ambient temperature by the addition of 1 M aq. HCl (10 μL) and the solvent was removed *in vacuo* to yield a clear colorless film. The film was purified by preparative TLC eluting with 5% MeOH/$CHCl_3$ providing desired triol **5.16** (3.8 mg, 0.0092 mmol, 56% yield) as a clear colorless film.

Physical state: Colorless film that could be crystalized by slow evaporation from MeOH

Melting point: insufficient crystals to obtain melting point

TLC: R_f = 0.15 (5% MeOH in $CHCl_3$, UV active; stains blue with Seebach's stain)

^{1}H NMR (600 MHz, $CDCl_3$): ^{1}H NMR (600 MHz, $CDCl_3$) δ 7.18 (br s, 2H), 6.82 (d, *J* = 8.3 Hz, 2H), 5.25 (s, 1H), 4.99 – 4.53 (m, 1H), 4.52 – 4.19 (m, 5H), 4.10 (br s, 1H), 3.99 (br s, 1H), 3.84 – 3.62 (m, 4H), 3.55 – 3.07 (m, 8H).

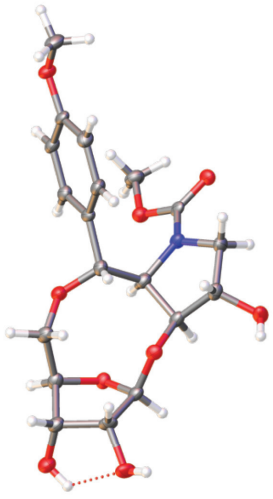
Over extended periods of time the material precipitated out of $CDCl_3$ so 4 drops d_4-methanol was added to solubilize the compound for ^{13}C NMR & HSQC experiments.

^{13}C NMR (151 MHz, $CDCl_3$ / MeOD): δ 159.0, 155.6, 132.2, 128.9 and 128.1 (2C, rotamers), 112.9 (2), 110.3, 85.1, 83.9, 83.3, 76.1, 71.9, 71.6, 71.4, 63.2, 55.3, 52.1, 48.6.

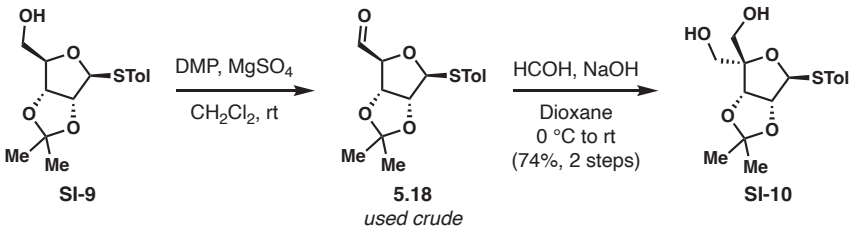
HRMS (ESI-TOF) m/z: calc'd for $C_{19}H_{25}NO_9$ $[M + H]^+$ 412.1602, found 412.1609

Optical rotation: $[a]_D^{25}$ 5.0° (*c* 0.36, MeOH)

X-ray crystallography structure:



(See **X-Ray Crystallography Data** section for full report)



Compound SI-10 - Ribose diol: Following a known procedure, compound **SI-9** (10.8 g, 36.4 mmol, 1.00 equiv) was added to a flame-dried round-bottomed flask charged with a stir bar and $MgSO_4$ (2.45 g). The reaction flask was then evacuated and placed under an argon atmosphere with a balloon. Anhydrous DCM (245 mL) was then added followed by DMP (16.1 g, 38.0 mmol, 1.04 equiv) in one portion and the reaction mixture was allowed to stir at room temperature until TLC revealed full consumption of starting material (ca. 1 h). Once the reaction was deemed complete, the reaction was filtered over a short pad of celite and the filtrate was washed with a 1:1 sat'd $NaHCO_3$/ sat'd $Na_2S_2O_3$ mixture (2 x 150 mL) and then H_2O (1 x 150 mL). This resulting crude mixture was then dried with Na_2SO_4, filtered, and evaporated *in vacuo* to reveal the crude aldehyde, whose ^1H NMR agreed with the literature report.

The crude aldehyde from above **5.18** (assumed quantitative for stoichiometry, 36.4 mmol) was then dissolved in 1,4-Dioxane (132 mL) in a round-bottomed flask charged with a stir bar. The flask was cooled to 0 °C with an ice water bath followed by the addition of an aqueous formaldehyde solution (37% wt. in H_2O, 26.4 mL, 325 mmol, 8.92 equiv) and aq. NaOH (2 M, 65.0 mL, 130 mmol, 3.57 equiv). The reaction was allowed to slowly warm to room temperature over 16 h, where then TLC analysis revealed full conversion of the aldehyde starting material. The reaction flask was cooled once again to 0 °C and 10% aq. AcOH (200 mL) was then added to quench any excess NaOH. 1,4-Dioxane was then

removed *in vacuo* and the remaining crude material was taken up in DCM (250 mL) and washed with H_2O (3 x 150 mL). The resultant organic mixture was dried with Na_2SO_4, filtered, and evaporated *in vacuo* to give the crude diol. Flash column chromatography of the crude material (4:1 then 2:1 then 1:1 hexanes/ethyl acetate) provided the desired product **5.19** (8.80 g, 27.0 mmol, 74% over two steps).

Physical state: colorless viscous syrup that solidified upon storage at low temperature.

m.p.: 85-87 °C

TLC: R_f = 0.25 (1:1 hexanes/ethyl acetate, UV, stains blue with Seebach's stain)

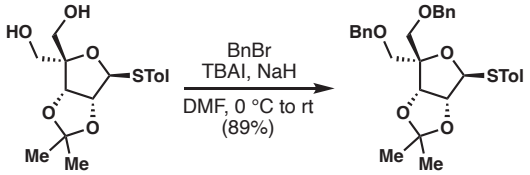
^{1}H NMR (600 MHz, $CDCl_3$) δ 7.39 (d, *J* = 8.1 Hz, 2H), 7.14 (d, *J* = 8.2 Hz, 2H), 5.53 (d, *J* = 2.6 Hz, 1H), 4.83 (dd, *J* = 6.3, 2.6 Hz, 1H), 4.77 (d, *J* = 6.2 Hz, 1H), 3.84 (d, *J* = 12.2 Hz, 1H), 3.80 (d, *J* = 12.0 Hz, 2H), 3.70 (d, *J* = 11.6 Hz, 1H), 2.50 (s, 1H, OH), 2.33 (s, 3H), 1.53 (s, 3H), 1.35 (s, 3H).

^{13}C NMR (151 MHz, $CDCl_3$) δ 138.4, 132.6, 130.2, 129.3, 113.9, 92.6, 90.1, 86.6, 82.8, 64.9, 63.3, 26.5, 24.9, 21.3.

HRMS (ESI-TOF) m/z: calc'd for $C_{16}H_{22}O_5S$ $[M + Na]^+$ 349.1080, found 349.1091.

Optical rotation: : $[a]_D^{25}$ –137.6° (*c* 1.00, $CHCl_3$)

Ref for prep: Kandasamy, J.; Atia-Glikin, D.; Belakhov, V.; Baasov, T. *Med. Chem. Commun.* **2011**, *2*, 165-171



SI-10 **5.19**

Compound 5.19 - Benzyl protected diol: To a flame-dried, round-bottomed flask containing a magnetic stir bar was added **SI-10** (8.80 g, 27.0 mmol, 1.0 equiv) and TBAI (290 mg, 0.78 mmol, 3 mol %). Next, the flask was backfilled with argon, before dissolving the mixture in DMF (57 mL). The resulting solution was allowed to cool to 0 °C with an ice water bath with stirring. After sufficient cooling, NaH (60% mineral oil suspension, 3.08 g, 77.0 mmol, 2.85 equiv) was added in three separate portions to avoid any vigorous H_2 evolution and was allowed to stir for 15 minutes. After this time, neat benzyl bromide (7.0 mL, 54.0 mmol, 2.2 equiv) was added dropwise while stirring the reaction at 0 °C. Once benzyl bromide addition was complete, the reaction was allowed to warm to room temperature. When the reaction was complete (ca. 4 h), MeOH (~5 mL) was added at 0 °C to quench excess NaH. The quenched mixture was then warmed to room temperature and diluted with Et_2O (250 mL) and extracted with H_2O (3 x 150 mL). The remaining organics were then washed with LiCl (100 mL) and then brine (100 mL). The organic layer was then dried with Na_2SO_4, filtered, and concentrated *in vacuo* to give the crude, which was then purified via flash column chromatography (20:1 to 10:1 hexanes/ethyl acetate) to provide the title compound, **5.19** (12.1 g, 23.9 mmol 89% yield).

Physical state: colorless viscous syrup that solidified upon storage at low temperature.

m.p.: 70-72 °C

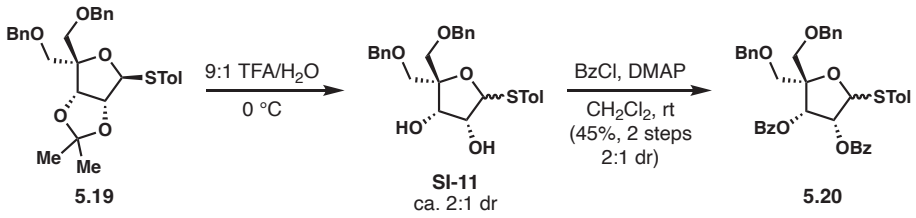
TLC: R_f = 0.56 (4:1 hexanes/ethyl acetate, UV, stains blue with Seebach's stain)

^{1}H NMR (600 MHz, $CDCl_3$) δ 7.40 (d, *J* = 8.2 Hz, 2H), 7.35 – 7.24 (m, 10H), 7.09 – 7.07 (d, *J* = 7.7 Hz, 2H), 5.42 (d, *J* = 2.8 Hz, 1H), 4.84 (dd, *J* = 6.0, 2.8 Hz, 1H), 4.74 (d, *J* = 6.0 Hz, 1H), 4.64 (d, *J* = 12.2 Hz, 1H), 4.61 (d, *J* = 11.9 Hz, 1H), 4.55 (d, *J* = 12.0 Hz, 1H), 4.52 (d, *J* = 12.2 Hz, 1H), 3.87 (d, *J* = 9.7 Hz, 1H), 3.80 (d, *J* = 10.2 Hz, 1H), 3.72 (d, *J* = 9.7 Hz, 1H), 3.64 (d, *J* = 10.1 Hz, 1H), 2.31 (s, 3H), 1.46 (s, 3H), 1.31 (s, 3H).

^{13}C NMR ^{13}C NMR (151 MHz, $CDCl_3$) δ 138.6, 138.3, 137.5, 132.4, 131.2, 129.8, 128.44, 128.37, 127.9, 127.8, 127.7, 127.6, 113.4, 93.7, 89.1, 87.0, 83.1, 73.8, 73.7, 71.0, 69.4, 26.9, 25.4, 21.2.

HRMS (ESI-TOF) m/z: calc'd for $C_{30}H_{34}O_5S$ $[M + Na]^+$ 529.2019, found 529.2018.

Optical rotation: : $[a]_D^{25}$ –89.0° (*c* 1.00, $CHCl_3$)



Compound 5.20 - Benzoyl protected glycosyl donor: A round bottomed flask containing a magnetic stir bar was charged with **5.19** (12.1 g, 23.9 mmol, 1.0 equiv). The flask was pre-cooled to ca. 0 °C with an ice water bath. Once sufficiently cooled, a fresh 9:1 TFA/H_2O solution was added in one portion down the chilled sides of the flask with a graduated cylinder. To obtain desirable stirring and solubilization of the substrate on gram scales, the flask had to be manually agitated with swirling. After around 20 minutes of stirring at 0 °C, LCMS analysis revealed full conversion of starting acetonide to the desired diol **SI-11**. At this time, the aqueous TFA was removed via rotovap with the water bath kept at ambient temperature. To remove excess water, the mixture was azeotroped with toluene (3 x 100 mL) to provide crude diol **SI-11**, which was used without any further purification. *Note: due to the acidic conditions required for removal of the acetonide, we observed inadvertent epimerization of the thioglycoside to a ca. 2:1 anomeric mixture.)*

A round bottomed flask containing crude diol **SI-11** (see above, assumed quantitative conversion, 23.9 mmol) was equipped with a stir bar. DMAP (8.75 g, 71.6 mmol, 3.0 equiv) was added followed by CH_2Cl_2 (251 mL). Neat benzoyl chloride (5.69 mL, 49.0 mmol, 2.05 equiv) was then added dropwise to the stirring reaction mixture. The resulting mixture was then allowed to stir overnight at room temperature. At this point, H_2O (150 mL) was added, and the mixture was stirred vigorously for 10 minutes. The layers were then separated and the aqueous layer was extracted further with CH_2Cl_2 (2 x 150 mL). The

organic layers were then dried with Na_2SO_4, filtered, and concentrated *in vacuo* to give the crude, which was purified by flash column chromatography (dry loaded, 20:1 to 10:1 hexanes/ethyl acetate) to give the title product **5.20** as a ca. 2:1 mixture of anomeric diastereomers (7.3 g, 10.8 mmol, 45% over two steps).

Physical state: viscous light-yellow syrup

TLC: R_f = 0.35 (4:1 hexanes/ethyl acetate, UV, stains blue with Seebach's stain)

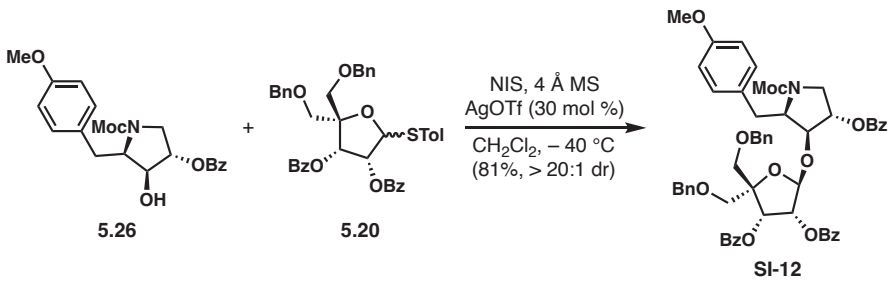
^{1}H NMR ^{1}H NMR (600 MHz, $CDCl_3$) δ 8.18 (d, *J* = 6.8 Hz, 1H), 7.87 (d, *J* = 8.2 Hz, 2.5H), 7.84 (d, *J* = 6.9 Hz, 2H), 7.60 (tt, *J* = 7.4, 1.3 Hz, 0.5H), 7.54 (tt, *J* = 7.5, 1.3 Hz, 1H), 7.52 – 7.45 (m, 5H), 7.42 (d, *J* = 7.9 Hz, 1H), 7.37 – 7.32 (m, 9H), 7.31 – 7.26 (m, 5H), 7.23 – 7.20 (m, 4H), 7.18 – 7.13 (m, 3H), 7.10 (d, *J* = 7.8 Hz, 3H), 6.14 (d, *J* = 5.4 Hz, 0.5H), 6.07 (d, *J* = 6.2 Hz, 0.5H), 5.91 – 5.78 (m, 1.5H), 5.80 (dd, *J* = 6.7, 5.3 Hz, 1H), 5.56 (d, *J* = 6.7 Hz, 1H), 4.62 (s, 1H), 4.60 (d, *J* = 12.3 Hz, 1H), 4.57 (d, *J* = 12.2 Hz, 1H), 4.51 (d, *J* = 12.1 Hz, 1H), 4.47 (d, *J* = 12.0 Hz, 0.5zH), 4.42 (d, *J* = 12.1 Hz, 1H), 4.39 (d, *J* = 12.0 Hz, 0.5H), 4.03 (d, *J* = 9.8 Hz, 0.5H), 3.90 (d, *J* = 10.3 Hz, 0.5H), 3.86 (d, *J* = 9.7 Hz, 0.5H), 3.81 (dd, *J* = 9.9, 2.9 Hz, 2H), 3.76 (d, *J* = 9.8 Hz, 1H), 3.70 (d, *J* = 10.3 Hz, 0.5H), 3.62 (d, *J* = 9.9 Hz, 1H), 2.33 (s, 1.5H), 2.31 (s, 3H).

^{13}C NMR (151 MHz, $CDCl_3$) δ ^{13}C NMR (151 MHz, $CDCl_3$) δ 165.4, 165.2, 165.0, 165.0, 138.4, 138.2, 138.00, 137.98, 137.9, 137.6, 133.9, 133.4, 133.33, 133.32, 132.5, 131.6, 130.2, 130.0, 129.88, 129.86, 129.84, 129.81, 129.7, 129.6, 129.4, 129.3, 128.7, 128.6,

128.51, 128.46, 128.40, 128.35, 127.8, 127.72, 127.67, 127.63, 127.62, 91.1, 88.2, 86.7, 86.6, 74.7, 74.0, 73.88, 73.85, 73.7, 73.6, 73.4, 73.0, 72.9, 72.0, 70.6, 69.5, 21.3, 21.2. (seven total arene carbons are overlapping in the arene region between ca. 139 ppm and 127 ppm)

HRMS (ESI-TOF) m/z: calc'd for $C_{41}H_{38}O_7S$ $[M + Na]^+$ 679.2230, found 679.2209

Optical rotation: $[a]_D^{25}$ +2.80° (*c* 1.00, $CHCl_3$)



Compound SI-12 Glycosylation product: To a flame-dried round-bottomed flask containing a stir bar was added pyrrolidine **5.26** (400 mg, 1.04 mmol, (1.0 equiv), donor **5.20** (1.05 g, 1.56 mmol, 1.5 equiv), and freshly activated 4 Å MS (2.1 g) before the flask was evacuated and backfilled with an argon balloon. CH_2Cl_2 (20.8 mL) was then added to create a light-yellow slurry after stirring for a few moments. This mixture was cooled to – 40 °C using an MeCN/dry ice bath over 5 minutes. Once sufficient cooling was obtained, NIS (351 mg, 1.56 mmol, 1.5 equiv) was added in one portion followed shortly by AgOTf (80 mg, 0.31 mmol, 30 mol %). The reaction was allowed to continue stirring at – 40 °C for approximately 2 h, at which point UPLC (and TLC) indicated full conversion of the pyrrolidine starting material (dark red color was observed). When the reaction was deemed complete, Et_3N (approximately 1 mL) was added at – 40 °C, which resulted in a color change to yellow. The reaction mixture was removed from the cooling bath and allowed to warm to room temperature over 5 min. Then, the reaction slurry was filtered to remove the molecular sieves and the resultant filtrate was diluted with CH_2Cl_2 (50 mL) and washed twice with a 1:1 mixture of sat'd $NaHCO_3/Na_2S_2O_3$ (50 mL x 2) to give a light-yellow organic phase. The aqueous layer was extracted once more with CH_2Cl_2 (50 mL) to ensure full recovery and the combined organics were dried over Na_2SO_4, filtered, and evaporated *in vacuo* to give the crude, which was purified by flash column chromatography eluting

10% → 40% EtOAc in hexanes (10% gradient increments) to furnish **SI-12** (789 mg, 0.842 mmol, 81% yield) as a single diastereomer.

Physical state: off-white to light yellow foam

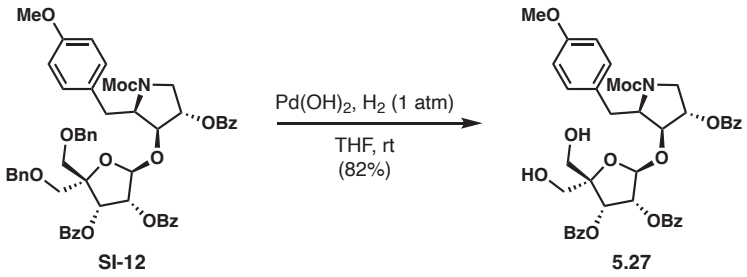
TLC: R_f = 0.33 (1.5:1 hexanes/ethyl acetate, UV, stains blue with Seebach's stain)

^{1}H NMR (600 MHz, $CDCl_3$) δ 7.92 (d, *J* = 7.7 Hz, 2H), 7.84 (d, *J* = 7.6 Hz, 2H), 7.77 (d, *J* = 7.7 Hz, 2H), 7.55 – 7.47 (m, 3H), 7.35 – 7.26 (m, 9H), 7.26 – 7.10 (m, 9H), 6.81 (d, *J* = 8.6 Hz, 2H), 5.86 (s, 1H), 5.78 (dd, *J* = 5.4, 2.4 Hz, 1H), 5.60 (d, *J* = 2.3 Hz, 1H), 5.08 (s, 1H), 4.66 – 4.50 (m, 3H), 4.54 (d, *J* = 12.1 Hz, 1H), 4.45 (d, *J* = 12.1 Hz, 1H), 4.35 – 4.24 (m, 1H), 3.86 (d, *J* = 9.9 Hz, 1H), 3.82 (d, *J* = 9.9 Hz, 1H), 3.80 – 3.52 (m, 9H), 3.39 (m, 1H), 3.05 and 2.80 (rotameric, 2H).

^{13}C NMR (151 MHz, $CDCl_3$) δ 165.9, 165.1, 165.0, 158.3, 155.6, 138.1, 138.0, 133.4, 133.3, 131.1, 131.0, 130.5, 130.4, 129.8, 129.5, 129.2, 128.5, 128.4, 127.71, 127.66, 114.0, 104.9 and 104.6 (1C, rotamers), 86.1, 79.5 and 78.6 (1C, rotamers), 76.2 and 75.8 (1C, rotamers), 73.9, 73.8, 73.7, 72.2, 69.9, 60.4 and 59.7 (1C, rotamers), 55.3, 52.6, 49.2 and 48.9 (1C, rotamers), 34.2 and 32.9 (1C, rotamers). 7 total carbons are overlapping in the arene region. All other non-aromatic carbons can be accounted for.

HRMS (ESI-TOF) m/z: calc'd for $C_{55}H_{53}NO_{13}$ $[M + Na]^+$ 958.3409, found 958.3405

Optical rotation: $[a]_D^{25}$ +18.7° (c 0.7, $CHCl_3$)



SI-12 5.27

Compound 5.27 - glycosylated diol: A round-bottomed flask containing a stir bar was charged with glycosylation product (410 mg, 0.44 mmol, 1.0 equiv). The flask was equipped with a septum, evacuated and backfilled with an argon balloon twice before adding $Pd(OH)_2/C$ (20 wt %, 618 mg, 0.88 mmol, 2.0 equiv) and THF (4.4 mL). A hydrogen balloon was installed via an 18G needle and the atmosphere was allowed to equilibrate to ca. 1 atm H_2 by allowing hydrogen to flow through the vessel for approximately 1 min (flow was initiated by inserting an 18G exit needle into the septum). After ~ 30 min, UPLC analysis revealed full conversion to desired diol. At this point, the septum was removed and a gentle stream of argon was passed over the top of the solution to ensure a hydrogen-free environment. Then, the solution was filtered over a small pad of celite and washed with CH_2Cl_2 (3 x 10 mL) and the resulting colorless solution was concentrated *in vacuo*. The resulting crude material was purified by flash column chromatography eluting 60% EtOAc in hexanes to give **5.27** as a white foam (273 mg, 0.631 mmol, 82% yield).

Physical state: White foam

Melting point: 95-96 °C

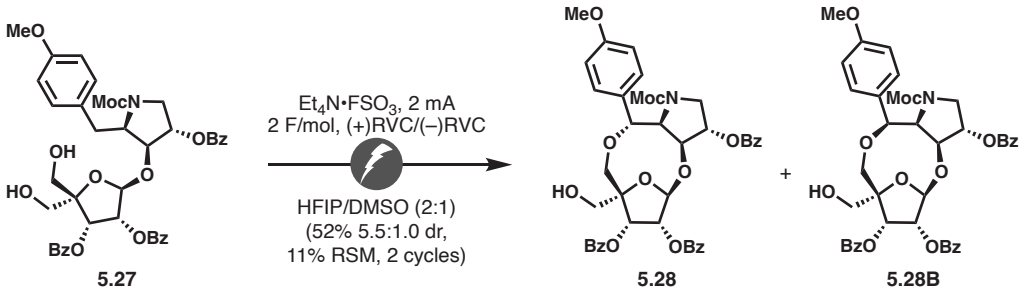
TLC: R_f = 0.23 (50% EtOAc in hexanes, UV active; stains blue with Seebach's stain)

^{1}H NMR (600 MHz, $CDCl_3$): δ 7.96 (d, *J* = 7.7 Hz, 2H), 7.88 (d, *J* = 7.7 Hz, 4H), 7.58 – 7.50 (m, 3H), 7.41 – 7.31 (m, 6H), 7.29 (br s, 1H), 7.22 (br s, 1H), 6.90 (d, *J* = 8.6 Hz, 2H), 5.70 (d, *J* = 5.3 Hz, 1H), 5.65 (d, *J* = 5.5 Hz, 1H), 5.57 (s, 1H), 5.27 (br s, 1H), 4.73 – 4.57 (m, 1H), 4.49 – 4.33 (m, 1H), 3.99 (dd, *J* = 11.9, 5.5 Hz, 1H), 3.89 (dd, *J* = 12.0, 7.8 Hz, 2H), 3.79 (s, 3H), 3.77 – 3.41 (m, 6H), 3.21 and 2.95 (two br s, 1H, rotamers), 3.04 (dd, *J* = 13.9, 8.3 Hz, 1H), 2.45 – 2.27 (m, 1H, -OH), 2.19 (s, 1H, -OH).

^{13}C NMR (151 MHz, $CDCl_3$): δ 166.0, 165.7, 165.2, 158.4, 155.6, 133.8, 133.7, 133.6, 130.7 (2), 130.4, 129.9, 129.7, 129.3, 129.0, 128.7, 128.6, 114.1 (2), 103.8, 103.8, 86.7, 79.1 and 78.2 (1C, rotamers), 76.4, 75.7, 73.5, 65.7, 63.4, 60.0 and 59.5 (1C, rotamers), 55.4, 52.8, 49.0, 34.7 and 33.5 (1C, rotamers).

HRMS (ESI-TOF) m/z: calc'd for $C_{41}H_{41}NO_{13}$ $[M + Na]^+$ 756.2651, found 756.2662.

Optical rotation: $[a]_D^{25}$ 16.8 ° (*c* 1.0, $CHCl_3$)



Compounds 5.28 & 5.28B - cyclized primary alcohols: Six 5 mL ElectraSyn vials were charged with diol **5.27**(25 mg, 0.033 mmol, 1.0 equiv, each) and Et_4N•FSO_3 (80 mg, 0.1

M to solvent, each). The mixtures were then dissolved in a premade solution of HFIP/DMSO (2:1, 3.5 mL, each). *Note: mixing HFIP and DMSO was found to be exothermic and was done prior to addition to avoid decomposing the starting materials.* The ElectraSyn vials were then equipped with two electrodes each (RVC, 8 mm wide, 50 mm length, 1 mm thickness) and sealed. The mixture was then sparged with Argon (10 mins). The vials were set up on an ElectraSyn carousel and were electrolyzed in parallel under DC conditions (electrolysis parameters: constant current: 2 mA, amount of charge: 2 F/mol). After reaction completion the cap was removed, and the electrodes were rinsed with EtOAc into a 100 mL round bottomed flask. Each vial was added to the same round bottomed flask, rinsing with EtOAc to ensure quantitative transfer, and the bulk of the HFIP and EtOAc were removed via rotovap before transferring the remaining solution to a separatory funnel, again rinsing with EtOAc (~50 mL) to ensure quantitative transfer. DI H_2O (~50 mL) was added to the separatory funnel and the funnel was shaken vigorously. The aqueous layer was then extracted with EtOAc (3 x 15 mL) and the combined organic layers were washed with brine (4 x 10 mL), dried over Na_2SO_4, filtered, and concentrated *in vacuo*. The resulting oil was purified by flash chromatography (1 inch column, ~ 5 inches of silica, dry loaded) eluting 0 → 80% EtOAc in hexanes (10% increments, 150 mL each) to yield the desired alcohol **5.28** (53.6 mg, 0.071 mmol, 35% yield) as a white foam and a mixture of undesired alcohol **5.28B** and remaining starting diol **5.27** (60 mg). The mixed material was subjected to a second purification utilizing a reverse phase MPLC (50 g gold C18) eluting 10 → 80% MeCN in H_2O providing recovered diol (40.6 mg, 27% yield RSM) as a white foam as well as undesired 9-membered ring (9.2 mg, 0.012 mmol, 6% yield).

The recovered diol **5.27** was split into two 5 mL ElectraSyn vials (20.3 mg each, 0.027 mmol each, 1.0 equiv). The vials were also charged $Et_4N•FSO_3$ (80 mg each, 0.1 M to solvent, each). The mixtures were then dissolved in a premade solution of HFIP/DMSO (2:1, 3.5 mL each) and both ElectraSyn vials were equipped with two electrodes (RVC, 8 mm wide, 50 mm length, 1 mm thickness) and sealed. The mixtures were then sparged with Argon (10 mins), set up on an ElectraSyn carousel, and electrolyzed in parallel under DC conditions (electrolysis parameters: constant current: 2 mA, amount of charge: 2 F/mol). After reaction completion the cap was removed, and the electrodes were rinsed with EtOAc into 50 mL round bottomed flask. The two reactions were also added to the round bottomed flask rinsing with EtOAc to ensure quantitative transfer. The bulk of the HFIP and EtOAc was removed via rotovap and the resulting solution was transferred to a separatory funnel rinsing with EtOAc (~ 20 mL) to ensure quantitative transfer. DI H_2O (~20 mL) was added to the separatory funnel and the funnel was shaken vigorously. The aqueous layer was then extracted with EtOAc (3 x 10 mL) and the combined organic layers were washed with brine (4 x 10 mL), dried over Na_2SO_4, filtered, and concentrated *in vacuo*. The mixture was purified by flash chromatography(1/2 inch column, ~5 inches silica, dry loaded) eluted 0 → 80% EtOAc in hexanes (10% increments, 50 mL each) to yield the desired 9-membered ring **5.28**(12.0 mg, 0.016 mmol, 30% yield) and 20 mg of 5:1 molar NMR mixture of starting diol **5.27** (16.6 mg, 0.022 mmol, 41% yield RSM) and undesired 9-membered ring **5.28B** (3.3 mg, 0.0044 mmol, 8% yield).

The above two cycles result in overall recovery of desired 9-membered ring **5.28** (65.6 mg, 0.087 mmol, 44%), undesired 9-membered ring **5.28B** (12.5 mg, 0.017 mmol, 8%) and

recovered diol **14** (16.6 mg, 0.022 mmol, 11% yield RSM) for 52% yield 5.5:1 dr over 2 cycles or 59% 5.5:1 brsm over 2 cycles.

Example of the carousel setup for the first cycle (left two images) and second cycle (right image):



See the section on electrochemical cyclization optimization for more details on this reaction.

Data for desired 9-membered diastereomer:

Physical state: White foam

TLC: R_f = 0.45 (60% EtOAc in hexanes, UV active; stains blue with Seebach's stain)

^{1}H NMR (600 MHz, $CDCl_3$): δ 8.01 (d, *J* = 7.7 Hz, 2H), 7.95 (d, *J* = 7.3 Hz, 2H), 7.85 (d, *J* = 7.3 Hz, 2H), 7.60 – 7.53 (m, 2H), 7.50 (t, *J* = 7.4 Hz, 1H), 7.44 (t, *J* = 7.6 Hz, 2H), 7.41 – 7.27 (m, 6H), 6.87 (d, *J* = 8.2 Hz, 2H), 5.87 (br s, 1H), 5.82 (d, *J* = 5.4 Hz, 1H), 5.61 (br s, 1H), 5.50 (br s, 1H), 4.78 – 4.47 (m, 3H), 4.28 (br s, 1H), 3.99 (dd, *J* = 11.8, 5.4 Hz, 1H), 3.80 (s, 3H), 3.79 – 3.55 (m, 4H), 3.28 (br s, 3H), 2.19 (br s, 1H).

^{13}C NMR (151 MHz, $CDCl_3$): ^{13}C NMR (151 MHz, $CDCl_3$) δ 166.3, 165.7, 165.1, 159.4, 155.6, 133.7, 133.6, 131.6, 129.9, 129.9, 129.9, 129.5, 129.0, 128.9, 128.6, 128.6, 113.3 (2), 105.6, 86.9, 82.7, 80.7, 76.3, 74.2, 71.0 and 68.6 (1C rotamers), 63.1, 60.6, 55.4, 52.6, 48.6.

HRMS (ESI-TOF) m/z: calc'd for $C_{41}H_{39}NO_{13}$ $[M + H]^+$ 754.2494, found 754.2498.

Optical rotation: $[a]_D^{25}$ 19.7° (*c* 1.0, $CHCl_3$)

Data for undesired 9-membered ring:

Physical state: white foam

TLC: R_f = 0.30 (60% EtOAc in hexanes, UV active; stains blue with Seebach's stain)

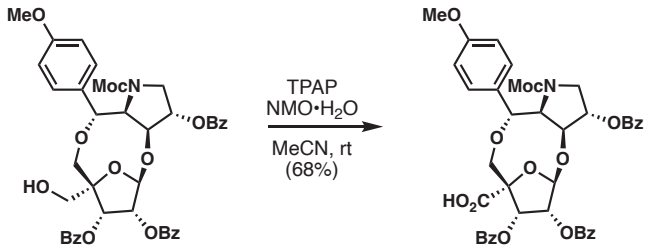
^{1}H NMR (600 MHz, $CDCl_3$): δ 8.02 (d, *J* = 7.0 Hz, 2H), 7.92 (d, *J* = 7.5 Hz, 2H), 7.83 (d, *J* = 7.4 Hz, 2H), 7.59 (t, *J* = 7.4 Hz, 1H), 7.56 – 7.47 (m, 2H), 7.47 – 7.36 (m, 6H), 7.30 (t,

J = 7.9 Hz, 2H), 6.96 (d, *J* = 8.7 Hz, 2H), 6.49 (d, *J* = 5.5 Hz, 1H), 5.96 (d, *J* = 5.5 Hz, 1H), 5.43 (s, 1H), 5.16 – 4.81 (m, 2H), 4.72 (br s, 1H), 4.35 (t, *J* = 8.2 Hz, 1H), 4.22 – 3.99 (m, 3H), 3.91 – 3.70 (m, 7H), 3.14 – 2.92 (m, 2H), 2.07 (br s, 1H, -OH).

^{13}C NMR (151 MHz, $CDCl_3$): δ 165.9, 165.2, 165.1, 159.9, 155.2, 133.8, 133.6, 133.4, 130.8 and 130.5 (1C rotamers), 129.9, 129.8, 129.6, 129.5, 129.3, 129.3, 129.0, 128.8, 128.7, 128.6, 128.5, 114.0 (2), 105.5, 88.3, 81.9 and 81.3 (1C rotamers), 80.6 and 79.6 (1C, rotamers), 75.6, 74.9 and 74.1 (1C, rotamers), 72.0, 69.1, 63.8, 57.8, 55.5, 53.0, 48.0.

HRMS (ESI-TOF) m/z: calc'd for $C_{41}H_{39}NO_{13}$ $[M + H]^+$ 754.2494, found 754.2502.

Optical rotation: $[a]_D^{25}$ 30.4° (*c* 1.0, $CHCl_3$)



5.28 5.29

Compound 5.29 - Carboxylic acid: A 13 x 100 mm culture tube containing a magnetic stir bar was charged with primary alcohol **5.28** (45 mg, 0.06 mmol, 1.0 equiv) followed by NMO•H_2O (81 mg, 0.6 mmol, 10.0 equiv). The mixture was dissolved in MeCN (0.6 mL) under air before adding TPAP (2.1 mg, 0.006 mmol, 0.1 equiv) in a single portion at room temperature. The reaction was allowed to stir for ca. 45 minutes at which point UPLC analysis revealed full conversion to the desired acid. Isopropanol (ca. 0.5 mL) was added to quench any excess reagent and the reaction mixture was concentrated *in vacuo* to reveal a dark brown/black crude mixture. The crude was then purified via PTLC (eluting with 1% AcOH, 2% MeOH, 97% EtOAc) to provide carboxylic acid (31 mg, 0.04 mmol, 68% yield).

Physical state: colorless film

TLC: R_f = 0.36 (1% AcOH, 2% MeOH, 97% EA; UV active, stains blue with Seebach's stain)

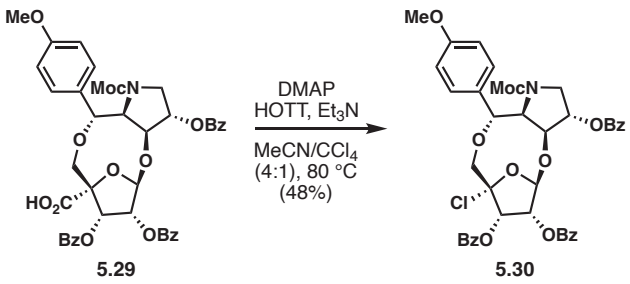
^{1}H NMR (600 MHz, $CDCl_3$) δ 8.01 (d, *J* = 7.6 Hz, 2H), 7.88 (s, 2H), 7.81 (d, *J* = 7.7 Hz, 2H), 7.58 (t, *J* = 7.4 Hz, 1H), 7.52 (s, 1H), 7.44 (t, *J* = 7.7 Hz, 3H), 7.37-7.21 (m, 6H), 6.85

(d, J = 8.1 Hz, 2H), 6.12 – 5.93 (m, 1H), 5.89 (d, J = 5.3 Hz, 1H), 5.72 (s, 1H), 5.50 (s, 1H), 4.85 – 4.21 (m, 4H), 3.97 (s, 1H), 3.79 (s, 3H), 3.68 (m, 2H), 3.30 (s, 3H).

^{13}C NMR (150 MHz, $CDCl_3$) δ 168.8, 166.3, 164.9, 159.6, 155.5, 133.8, 133.7, 131.0, 130.0, 129.9, 129.8, 129.3, 128.64, 128.60, 128.5, 113.4, 106.6, 88.0, 83.3, 81.3, 76.1, 74.4, 71.9, 62.6, 55.4, 52.7, 48.5. (5 carbons are overlapping in the arene region; carboxylic acid carbon is not visible due to rotameric signal broadening)

HRMS (ESI-TOF) m/z: calc'd for $C_{41}H_{37}NO_{14}$ $[M + H]^+$ 768.2287, found 768.2289

Optical rotation: $[a]_D^{25}$ +20.0° (c 0.2, $CHCl_3$)



5.29 5.30

Compound 5.30 - protected dragocins B and C: A flame-dried 13 x 100 mm culture tube was charged with acid **5.29** (12.1 mg, 0.016 mmol, 1.0 equiv) which was azeotropically dried with benzene (3 x 1 mL) to ensure a moisture-free environment. Next, a stir bar and HOTT (23.4 mg, 0.063 mmol, 4.0 equiv) were added and the reaction vessel before evacuating and refilling with an argon balloon (3x). At this point, the overhead hood lights were turned off and the tube was wrapped with aluminum foil. Degassed carbon tetrachloride (sparged with an argon balloon while sonicating for 20 minutes, 2.4 mL) was then added to create a suspension of the starting material and the HOTT reagent. Finally, 300 µL of a freshly prepared stock solution of *DMAP (1.6 mg) and Et_3N (34.7 µL) in MeCN (1.2 mL,* sparged, *vide supra*) was added. The septum cap was quickly replaced with a septum-free screw cap and was sealed with Teflon before the reaction tube was lowered into a pre-heated oil bath (80 °C) while being shielded from light. After ca. 1 h, UPLC analysis revealed >90% conversion of the acid starting material to a single major peak corresponding to tertiary chloride **5.30**. The reaction tube was then removed from the oil bath and the lights were turned back on to unveil a dark orange solution which was concentrated *in vacuo* to give the crude mixture, which was then purified via PTLC (1:1 hexanes/ethyl acetate) to provide the title chlorinated compound **5.30** (5.8 mg, 0.0077 mmol, 48%) as a clear colorless film.

Physical state: colorless film

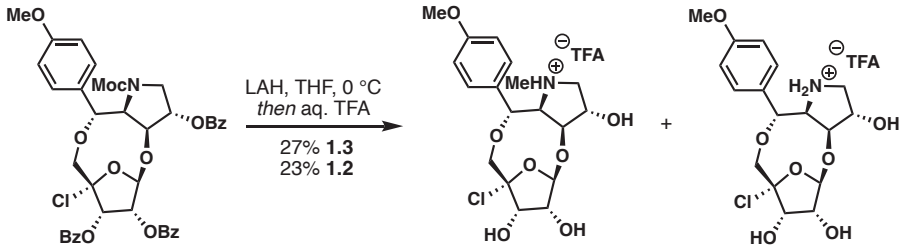
TLC: R_f = 0.50 (1:1 hexanes/ethyl acetate; UV active, stains blue with Seebach's stain)

^{1}H NMR (600 MHz, $CDCl_3$) δ 8.17 (d, *J* = 7.3 Hz, 2H), 8.05 (d, *J* = 7.6 Hz, 2H), 7.85 (d, *J* = 7.3 Hz, 2H), 7.63 (t, *J* = 7.5 Hz, 1H), 7.59 (t, *J* = 7.3 Hz, 1H), 7.54 – 7.43 (m, 6H), 7.26 (m, obsc., 3H), 6.91 (d, *J* = 8.1 Hz, 2H), 6.24 (d, *J* = 4.6 Hz, 1H), 5.83 (d, *J* = 4.6 Hz, 1H), 5.67 – 5.57 (m, 2H), 4.94 (s, 1H), 4.45 (s, 1H), 4.07 (s, 1H), 3.86 – 3.80 (m, obsc., 1H) 3.82 (s, 3H), 3.75 – 3.59 (m, 1H), 3.49 (s, 3H). (2 total proton integrations are not present due to rotameric signal broadening, see spectra)

^{13}C NMR (151 MHz, $CDCl_3$) δ 166.4, 165.4, 165.1, 159.9, 155.4, 133.8, 133.7, 133.6, 130.4, 130.3, 130.04, 130.02, 129.9, 129.3, 129.2, 128.82, 128.79, 128.6, 128.5, 113.7, 104.3, 104.1, 81.5, 78.5, 76.3, 74.1, 72.3, 69.5 and 67.9 (1C, rotamers), 58.4 and 56.7 (1C, rotamers), 55.4, 52.8, 48.2.

HRMS (ESI-TOF) m/z: calc'd for $C_{40}H_{36}ClNO_{12}$ $[M + H]^+$ 758.1999, found 758.2001

Optical rotation: $[a]_D^{25}$ +28.0° (*c* 0.1, $CHCl_3$)



5.30 **1.3** (dragocin C) **1.2** (dragocin B)

Dragocin C (1.3): A flame-dried reaction tube was charged with chlorinated compound **5.30** (3.3 mg, 0.044 mmol, 1.0 equiv) and azeotroped with benzene (3 x 1 mL) to remove any residual moisture. Next, a stir bar was added, and the reaction vessel was evacuated and backfilled 3x with an argon balloon and THF (0.248 mL) was added. The dissolved material was then cooled to 0 °C with an ice water bath and stirred. Once sufficient cooling was obtained, LAH (1.0 M THF solution, 79 mL, 0.079 mmol, 18.0 equiv) was added dropwise and the reaction was allowed to continue stirring until full conversion was achieved (around 2 h). After this point in time, UPLC analysis revealed full conversion of the starting material to dragocin B and dragocin C as the major product peaks in a ca. 1:1 ratio. To quench the reaction, a fresh 0.1 M aq. TFA solution was prepared and was added dropwise to the mixture at 0 °C (3.16 mL, 0.316 mmol, 72.0 equiv). ***Note: inadvertent loss of the chloride was observed when the reaction was quenched under basic conditions, i.e. sat'd aqueous solution of Rochelle's salt (sodium potassium tartrate). An acidic workup was critical for optimal success of this sequence and minimal loss of the desired material.*** Finally, the quenched mixture was exhaustively extracted with a 3:1 $CHCl_3$:IPA mixture, making sure to check the aqueous layer via UPLC for any remaining product that may have not been fully extracted. The combined organics were dried with Na_2SO_4, filtered, and evaporated *in vacuo* to give a yellow crude mixture, which was purified via semi-preparative reverse phase HPLC (Phenomenex Luna 5 µm C18 100 Å 250 x 10 mm)

eluting with 10% to 50% ACN/H_2O over 15 min). The collected fractions were lyophilized to provide dragocin C TFA salt (10.3 min, 0.6 mg, 27%) as well as ca. 80% pure dragocin B TFA salt (9.25 min, 0.5 mg, 23%) as colorless oils.

Dragocin C TFA salt:

Physical state: colorless oil

^{1}H NMR (600 MHz, MeOD) δ 7.49 (d, *J* = 8.3 Hz, 2H), 7.04 (d, *J* = 8.6 Hz, 2H), 5.38 (s, 1H), 4.83 – 4.81 (m, 1H), 4.77 (d, *J* = 4.3 Hz, 1H), 4.69 (d, *J* = 9.6 Hz, 1H), 4.37 (d, *J* = 2.7 Hz, 1H), 4.12 (d, *J* = 4.3 Hz, 1H), 4.07 (dd, *J* = 9.7, 2.2 Hz, 1H), 4.00 (d, *J* = 13.7 Hz, 1H), 3.97 (dd, *J* = 13.1, 3.2 Hz, 1H), 3.88 (d, *J* = 13.6 Hz, 1H), 3.83 (s, 3H), 3.17 (d, *J* = 12.7 Hz, 1H), 2.41 (s, 3H).

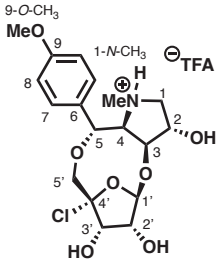
^{13}C NMR (150 MHz, MeOD) δ 162.5, 131.0 (2), 129.6, 115.7 (2), 107.7, 106.0, 80.8, 79.0, 77.3, 76.4, 75.4, 74.6, 72.9, 65.2, 55.9, 45.3.

^{19}F NMR (376 MHz, MeOD) δ – 79.6.

HRMS (ESI-TOF) m/z: calc'd for $C_{18}H_{24}ClNO_7$ $[M + H]^+$ 402.1314, found 402.1316.

Optical rotation: Synthetic: $[a]_D^{25}$ -12.0° (c 0.05, MeOH) Literature: $[a]_D^{25}$ -26.7° (c 0.3, MeOH)

Comparison Table for Dragocin C•TFA Salt



Skeletal numbering system for dragocin C TFA salt

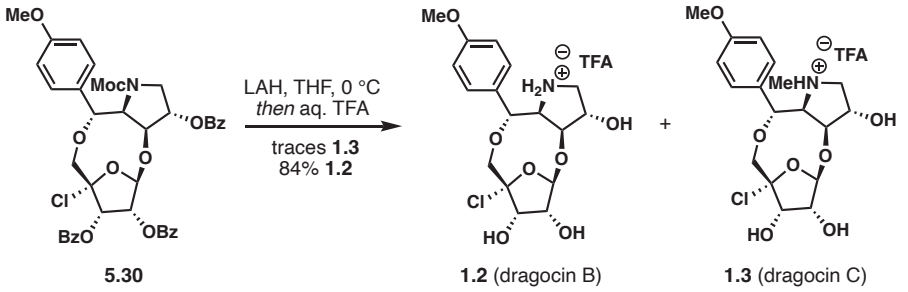
Tabulated data for Natural and Synthetic Dragocin C (^{1}H NMR, ppm)

position	Natural (500 MHz, MeOD)	Synthetic (600 MHz, MeOD)	D ppm
1a	3.97, dd, (*J* = 12.5, 3.3 Hz)	3.97, dd (*J* = 13.1, 3.2 Hz)	-
1b	3.17 d, (*J* = 12.5 Hz)	3.17 d (*J* = 12.7 Hz)	-
2	4.36, brd (*J* = 3.3 Hz)	4.37, d (*J* = 2.7 Hz)	0.01
3	4.82, m	4.83, m	0.01
4	4.06, dd (*J* = 10.0, 3.0 Hz)	4.07, dd (*J* = 9.7, 2.2 Hz)	0.01
5	4.70, d (*J* = 10.0 Hz)	4.69, d (*J* = 9.6 Hz)	0.01
6	-	-	-
7	7.49, d (*J* = 8.3 Hz)	7.49, d (*J* = 8.3 Hz)	-
8	7.04, d (*J* = 8.3 Hz)	7.04, d (*J* = 8.6 Hz)	-
9	-	-	-
1-*N*-CH3	2.41, s	2.41, s	-
9-*O*-CH3	3.83, s	3.83, s	-
1’	5.38, s	5.38, s	-
2’	4.11, d (*J* = 4.1 Hz)	4.12, d (*J* = 4.3 Hz)	0.01
3’	4.77, d (*J* = 4.1 Hz)	4.77, d (*J* = 4.3 Hz)	-
4’	-	-	-
5’a	4.00, d (*J* = 13.4 Hz)	4.00, d (*J* = 13.7 Hz)	-
5’b	3.88, d (*J* = 13.4 Hz)	3.88, d (*J* = 13.6 Hz)	-

Tabulated data for Natural and Synthetic Dragocin C (^{13}C NMR, ppm)

position	Natural	Synthetic	D ppm
1	65.2	65.2	-
2	72.8	72.9	0.1
3	80.7	80.8	0.1
4	76.4	76.4	-
5	77.1	77.3	0.2
6	129.4	129.6	0.2
7	131.0	131.0	-
8	115.7	115.7	-

9	162.5	162.5	-
1-N-CH3	45.2	45.3	0.1
9-O-CH3	55.7	55.9	0.2
1’	106.0	106.0	-
2’	74.6	74.6	-
3’	78.8	79.0	0.2
4’	107.7	107.6	0.1
5’	75.3	75.4	0.1



5.30 **1.2** (dragocin B) **1.3** (dragocin C)

Dragocin B (1.2): To obtain samples of dragocin B that were free of co-eluting impurities, the procedure reported above for dragocin C was adopted with the following alterations: Two separate flame-dried reaction tubes were each charged with chlorinated compound 16 (1.0 mg, 0.0013 mmol, 1.0 equiv.) and azeotroped with benzene (3 x 1 mL) to remove any residual moisture. Next, a stir bar was added, and the reaction vessels were each evacuated and backfilled 3x with an argon balloon and THF (0.1 mL) was added to the tubes. The dissolved material was then cooled to 0 °C with an ice water bath and stirred. Once sufficient cooling was obtained, LAH (1.0 M THF solution, 65 mL, 0.065 mmol, 50.0 equiv) was added dropwise and the reactions were allowed to continue stirring for 2 h at this temperature. After this point in time, UPLC analysis revealed full conversion of the starting material to dragocin B as the major product peak as well as traces of dragocin C. To quench the reactions, a fresh 0.3 M aq. TFA solution was prepared and was added quickly to the mixtures at 0 °C (0.89 mL for each reaction tube). Finally, the quenched mixtures were exhaustively extracted with a 3:1 $CHCl_3$:IPA mixture, making sure to check the aqueous layer via UPLC for any remaining product that may have not been fully extracted. The combined organics were dried with Na_2SO_4, filtered, and evaporated *in vacuo* to give a yellow crude mixture, which was purified via semi-preparative reverse phase HPLC (Phenomenex Luna 5 μm C18 100 Å 250 x 10 mm) eluting with 10% to 34% ACN/H_2O over 15 min). The collected fractions were lyophilized to provide dragocin B

TFA salt as a colorless oil, which was spectroscopically pure by NMR analysis (retention time 11.5 min, 1.1 mg, 84%).

Dragocin B TFA salt:

Physical state: colorless oil

^{1}H NMR (600 MHz, MeOD) δ 7.44 (d, *J* = 8.6 Hz, 2H), 7.01 (d, *J* = 8.6 Hz, 2H), 5.39 (s, 1H), 4.81 (d, *J* = 4.3 Hz, 1H), 4.69 (d, *J* = 3.6 Hz, 1H), 4.65 (d, *J* = 10.0 Hz, 1H), 4.40 (d, *J* = 3.9 Hz, 1H), 4.13 (d, *J* = 4.2 Hz, 1H), 4.10 (dd, *J* = 10.0, 3.6 Hz, 1H), 4.04 (d, *J* = 13.6 Hz, 1H), 3.91 (d, *J* = 13.6 Hz, 1H), 3.82 (s, 3H), 3.54 (dd, *J* = 12.5, 4.0 Hz, 1H), 3.16 (d, *J* = 12.4 Hz, 1H).

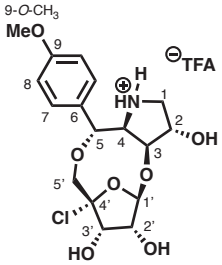
^{13}C NMR (150 MHz, MeOD) δ 162.3, 130.4 (2), 130.0, 115.6 (2), 107.9, 106.2, 79.6, 79.1, 77.5, 75.6, 74.6, 73.5, 66.7, 55.8, 53.5.

^{19}F NMR (376 MHz, MeOD) – 79.6.

HRMS (ESI-TOF) m/z: calc'd for $C_{17}H_{22}ClNO_7$ $[M + H]^+$ 388.1163, found 388.1171.

Optical rotation: Synthetic: $[a]_D^{25}$ -16.7° (c 0.3, MeOH), Literature: $[a]_D^{25}$ –22.2° (c 0.3, MeOH)

Comparison Table for Dragocin B•TFA Salt



Skeletal numbering system for dragocin B TFA salt

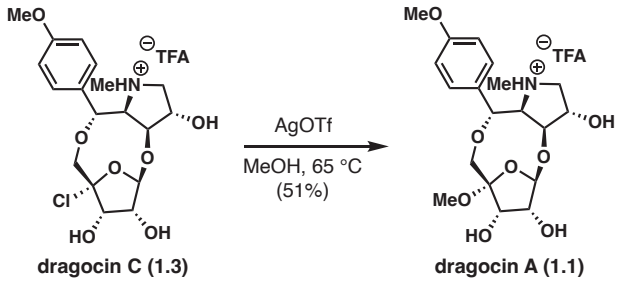
Tabulated data for Natural and Synthetic Dragocin B (^{1}H NMR, ppm)

position	Natural (500 MHz, MeOD)	Synthetic (600 MHz, MeOD)	D ppm
1a	3.55, brd (*J* = 10.2 Hz)	3.54, dd (*J* = 12.5, 4.0 Hz)	0.01
1b	3.14, d (*J* = 10.2 Hz)	3.16, d (*J* = 12.4 Hz)	0.02
2	4.39, brs	4.40, d (*J* = 3.9 Hz)	0.01
3	4.67, obsc.	4.69, d (*J* = 3.6 Hz)	0.02
4	4.09, brd (*J* = 8.5 Hz)	4.10, dd (*J* = 10.0, 3.6 Hz)	0.01
5	4.68, obsc.	4.65, d (*J* = 10.0 Hz)	0.01
6	-	-	-
7	7.44, d (*J* = 8.5 Hz)	7.44, d (*J* = 8.6 Hz)	-
8	6.99, d (*J* = 8.5 Hz)	7.01, d (*J* = 8.6 Hz)	0.02
9	-	-	-
9-*O*-CH3	3.80, s	3.82, s	0.02
1’	5.37, s	5.39, s	0.01
2’	4.14, brs	4.13, d (*J* = 4.2 Hz)	0.01
3’	4.83, obsc.	4.81, d (*J* = 4.3 Hz)	0.02
4’	-	-	-
5’a	4.03, d (*J* = 13.6 Hz)	4.04, d (*J* = 13.6 Hz)	0.01
5’b	3.88, d (*J* = 13.6 Hz)	3.91, d (*J* = 13.6 Hz)	0.03

Tabulated data for Natural and Synthetic Dragocin B (^{13}C NMR, ppm)

position	Natural (projected from 2D, 1D not provided in original isolation report)	Synthetic	D ppm
1	53.8	53.5	0.3
2	73.9	73.5	0.4
3	80.0	79.6	0.4
4	67.3	66.7	0.4
5	78.0	77.5	0.5
6	129.8	130.0	0.2
7	130.9	130.4	0.5

8	116.1	115.6	0.5
9	162.8	162.3	0.5
9-O-CH3	56.6	55.8	0.8
1’	106.8	106.2	0.6
2’	75.0	74.6	0.4
3’	79.7	79.1	0.6
4’	109.0	107.9	1.1
5’	76.0	75.6	0.4



dragocin C (1.3) dragocin A (1.1)

Dragocin A (1A): To a flame-dried culture tube containing a stir bar and dragocin C TFA salt (1.0 mg, 0.0019 mmol, 1.0 equiv) under argon was added methanol (0.25 mL) and a stock solution of AgOTf in methanol (0.19 M, 10 mL, 0.0019 mmol, 1.0 equiv). The resulting solution was heated to 65 °C after sealing the tube with a screw cap and parafilm. After 18 h, UPLC analysis revealed full conversion of dragocin C. The solvent was evaporated to give a crude mixture, which was purified via semi-preparative reverse phase HPLC (Phenomenex Luna 5 µm C18 100 Å 250 x 10 mm) eluting with 10% to 42% ACN/H_2O over 20 min). The collected fractions were lyophilized to provide dragocin A TFA salt as a colorless oil (retention time 10.75 min, 0.5 mg, 51%).

Physical state: colorless film

^{1}H NMR (600 MHz, MeOD) δ 7.48 (d, *J* = 8.5 Hz, 2H), 7.03 (d, *J* = 8.7 Hz, 2H), 5.27 (s, 1H), 4.83 (obscure, 1H, HSQC) 4.56 (d, *J* = 9.9 Hz, 1H), 4.51 (d, *J* = 4.6 Hz, 1H), 4.36 (d, *J* = 2.8 Hz, 1H), 4.09 (d, *J* = 4.9 Hz, 1H), 4.03 (dd, *J* = 9.8, 3.4 Hz, 1H), 3.97 (dd, *J* = 12.6, 3.4 Hz, 1H), 3.83 (s, 3H), 3.70 (d, *J* = 13.8 Hz, 1H), 3.65 (d, *J* = 13.7 Hz, 1H), 3.39 (s, 3H), 3.16 (d, *J* = 12.8 Hz, 1H), 2.36 (s, 3H).

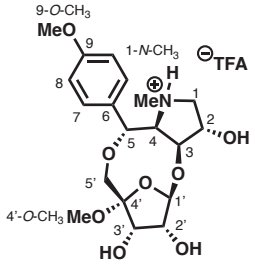
^{13}C NMR (151 MHz, MeOD) δ 162.4, 130.7 (2), 115.7 (2), 105.5, 105.1, 80.4, 79.2, 77.8, 76.6, 74.7, 73.1, 70.6, 65.3, 55.9, 50.5, 49.9, 45.5.

^{19}F NMR (376 MHz, MeOD) δ – 79.59.

HRMS (ESI-TOF) m/z: calc'd for $C_{19}H_{27}NO_8$ $[M + H]^+$ 398.1809, found 398.1808.

Optical rotation: Synthetic: $[a]_D^{25}$ –22.2° (c 0.018, MeOH) Literature: $[a]_D^{25}$ –28.3° (c 0.3, MeOH)

Comparison Table for Dragocin A•TFA Salt



Skeletal numbering system for dragocin A TFA salt

Tabulated data for Natural and Synthetic Dragocin A (^{1}H NMR)

position	Natural (500 MHz, MeOD)	Synthetic (600 MHz, MeOD)	D ppm
1a	3.97, dd (*J* = 12.8, 3.3)	3.97, dd (*J* = 12.6, 3.4)	-
1b	3.17, d (*J* = 12.8)	3.16, d (*J* = 12.8)	0.01
2	4.36, brd (*J* = 3.3)	4.36, d (*J* = 2.8)	-
3	4.84, m	4.83, obsc (see HSQC)	0.01
4	4.04, dd (*J* = 10.0, 3.6)	4.03, dd (*J* = 9.8, 3.4)	0.01
5	4.55, d (*J* = 10.0)	4.56, d (*J* = 9.9 Hz)	0.01
6	-	-	-
7	7.47, d (*J* = 8.3)	7.48 (*J* = 8.5 Hz)	0.01
8	7.03, d (*J* = 8.3)	7.03 (*J* = 8.7 Hz)	-
9	-	-	-
1-*N*-CH3	2.36, s	2.36, s	-
9-*O*-CH3	3.82, s	3.83, s	0.01
1’	5.27, s	5.27, s	-
2’	4.08, d (*J* = 4.5)	4.09, d (*J* = 4.9 Hz)	0.01
3’	4.50, d (*J* = 4.5)	4.51, d (*J* = 4.6 Hz)	0.01
4’	-	-	-
5’a	3.70, d (*J* = 13.8)	3.70, d (*J* = 13.8 Hz)	-
5’b	3.64, d (*J* = 13.8)	3.65, d (*J* = 13.7 Hz)	0.01
4’-*O*-Me	3.38, s	3.39, s	0.01

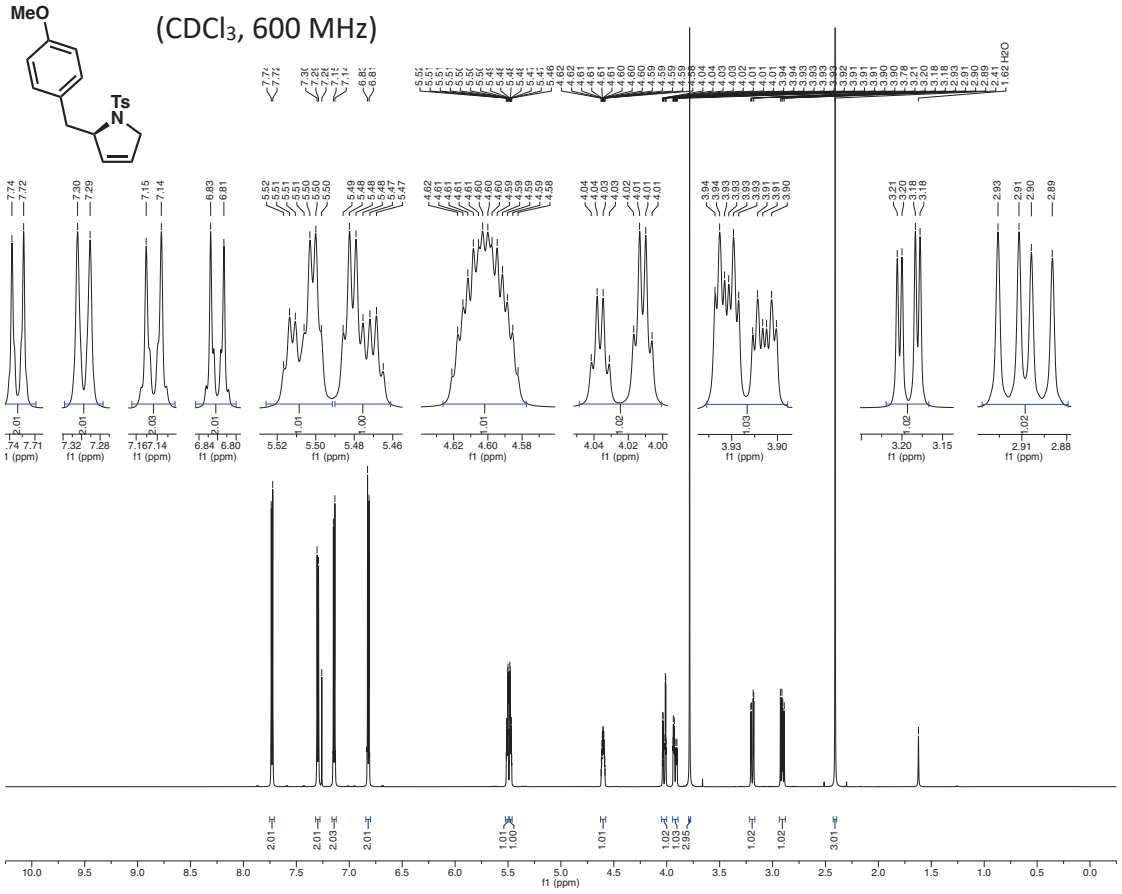
Tabulated data for Natural and Synthetic Dragocin A (^{13}C NMR)

position	Natural	Synthetic	D ppm
1	65.1	65.3	0.2
2	73.0	73.1	0.1
3	80.1	80.4	0.3
4	76.4	76.6	0.2
5	77.6	77.8	0.2
6	131.1	131.0 (HMBC)	0.1
7	130.8	130.7	0.1
8	115.7	115.6	0.1
9	162.9	162.4	0.5
1-N-CH3	45.6	45.5	0.1

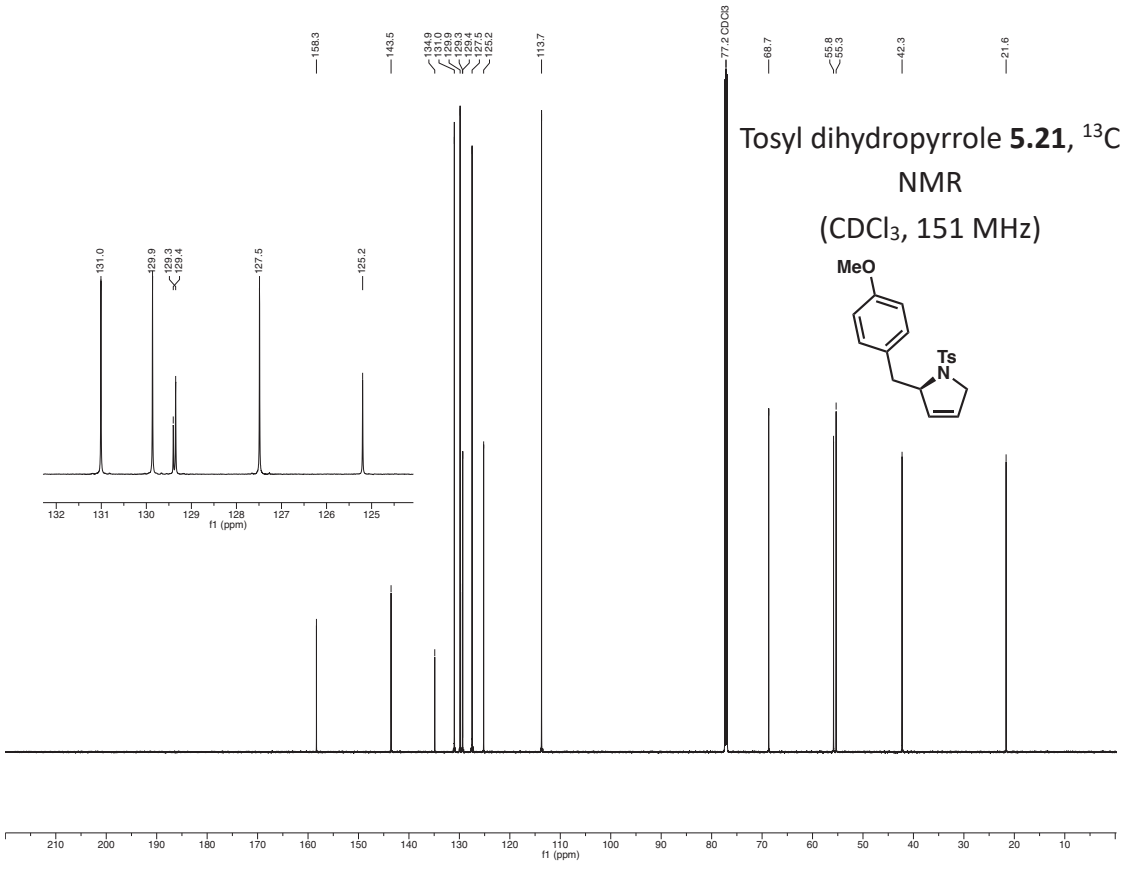
9-O-CH3	55.5	55.9	0.4
1’	105.0	105.1	0.1
2’	74.7	74.7	-
3’	79.7	79.2	0.5
4’	106.0	105.5	0.5
5’	70.3	70.6	0.3
4’-*O*-Me	50.3	50.5	0.2

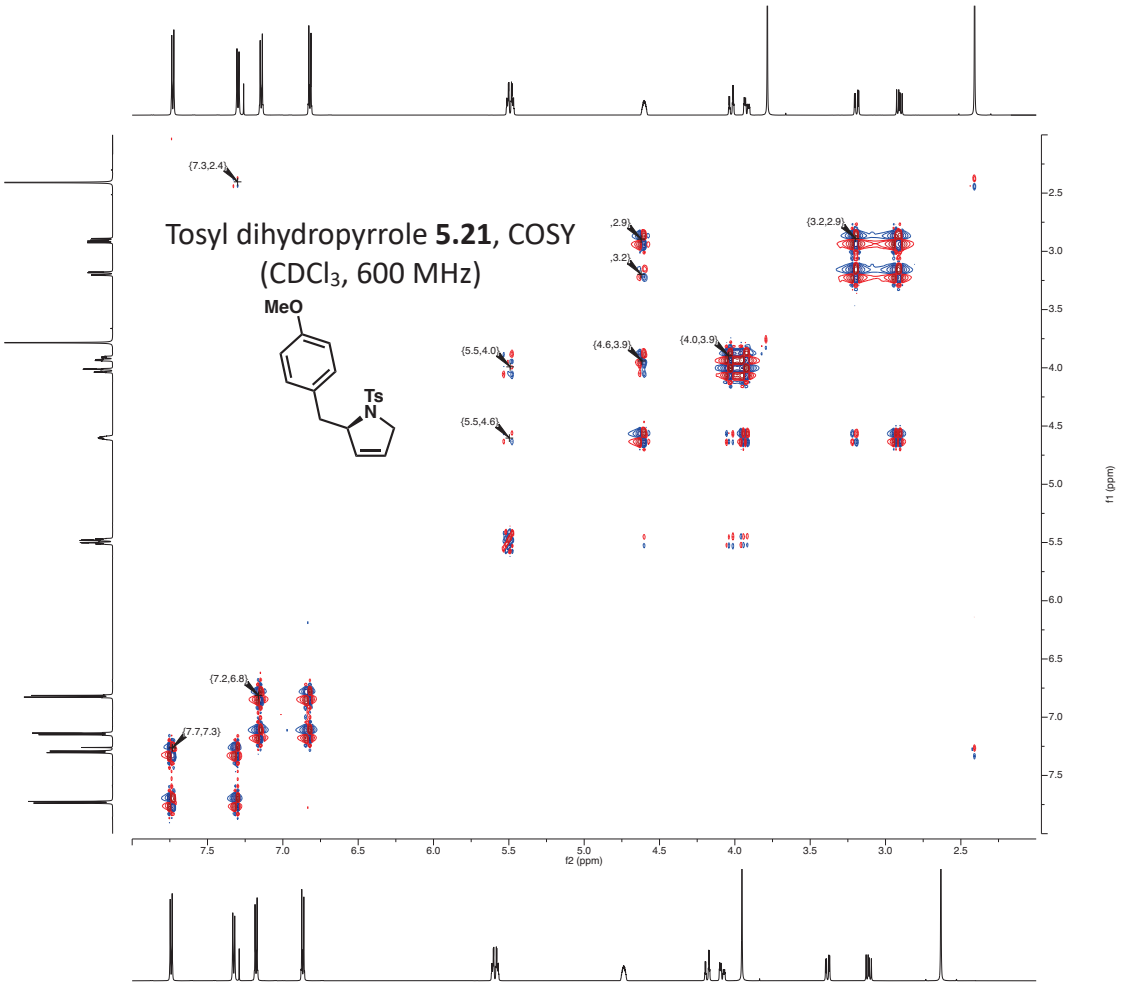
NMR Spectra

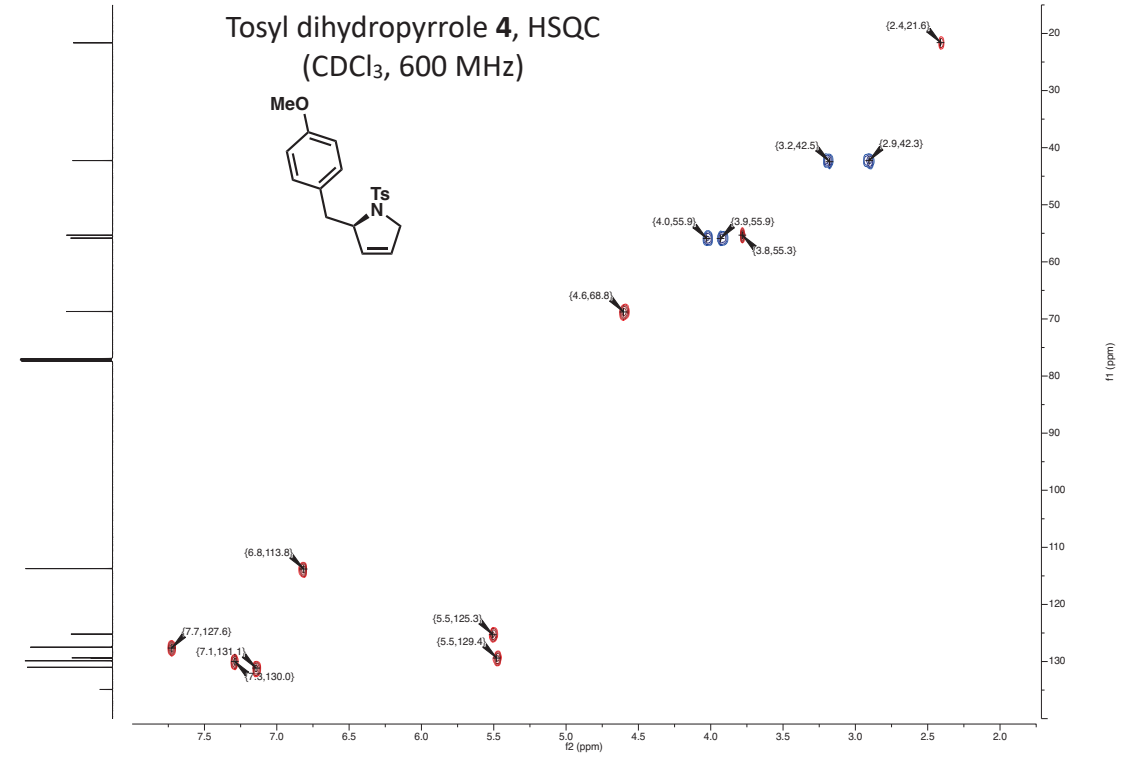
Tosyl dihydropyrrole **5.21**, ^{1}H NMR ($CDCl_3$, 600 MHz)



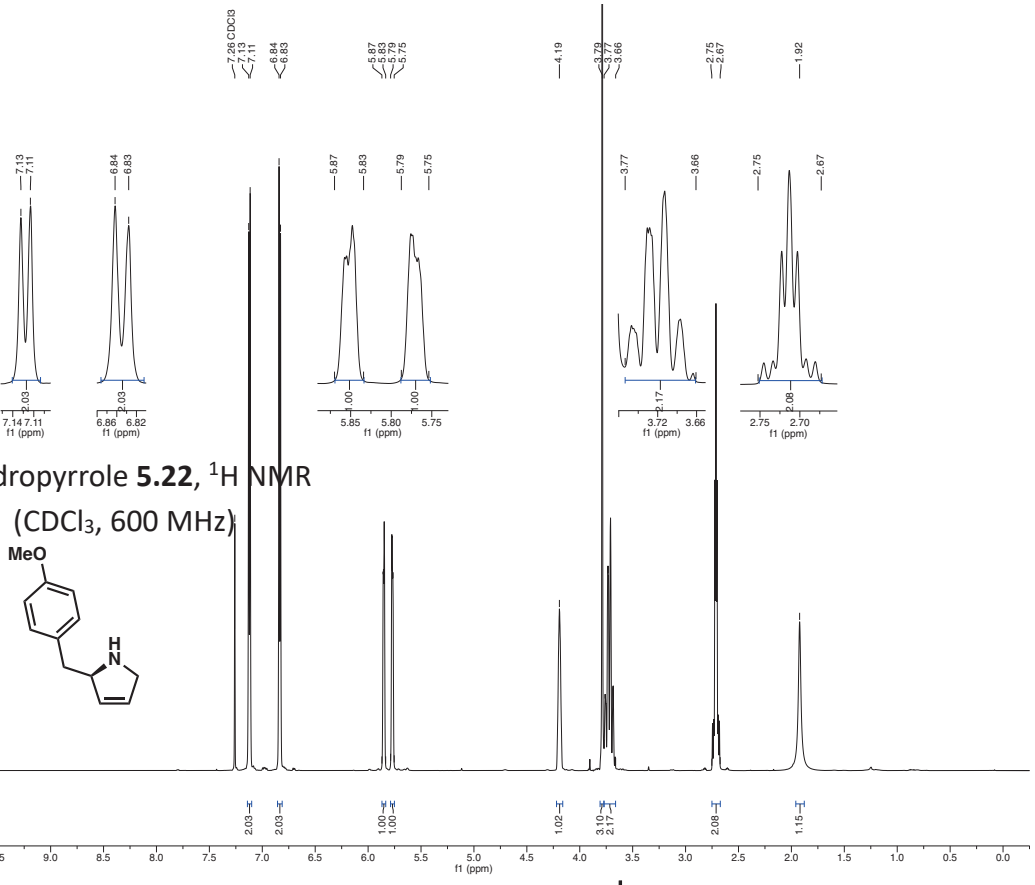
Tosyl dihydropyrrole **5.21**, ^{13}C NMR ($CDCl_3$, 151 MHz)



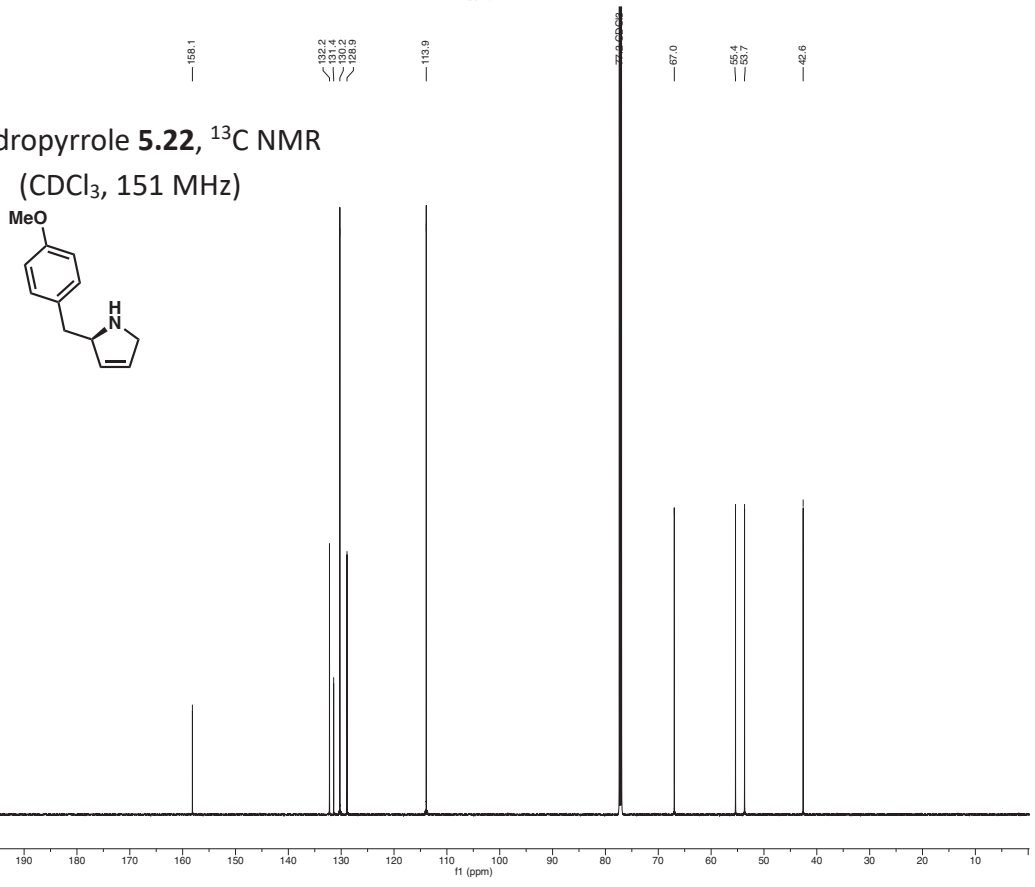

Tosyl dihydropyrrole **5.21**, COSY
(CDCl3, 600 MHz)
MeO
Ts
N
{7.3,2.4}
{5.5,4.0}
{4.6,3.9}
{4.0,3.9}
{3.2,2.9}
{5.5,4.6}
{7.2,6.8}
{7.7,7.3}
f2 (ppm)
f1 (ppm)

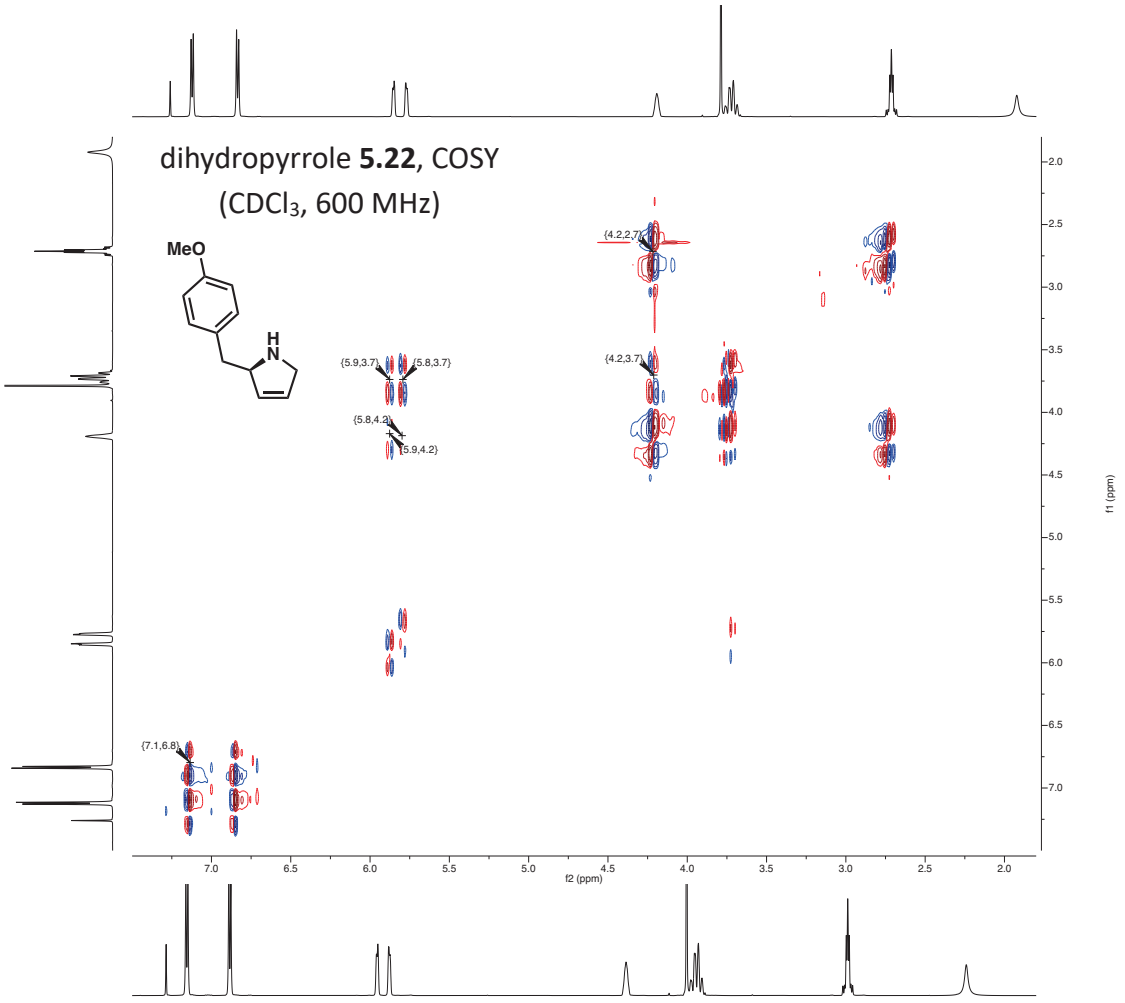

Tosyl dihydropyrrole **4**, HSQC
(CDCl3, 600 MHz)
MeO
Ts
N
{2.4,21.6}
{3.2,42.5}
{2.9,42.3}
{4.0,55.9}
{3.9,55.9}
{3.8,55.3}
{4.6,68.8}
{6.8,113.8}
{7.7,127.6}
{7.1,131.1}
{7.3,130.0}
{5.5,125.3}
{5.5,129.4}
f2 (ppm)
f1 (ppm)

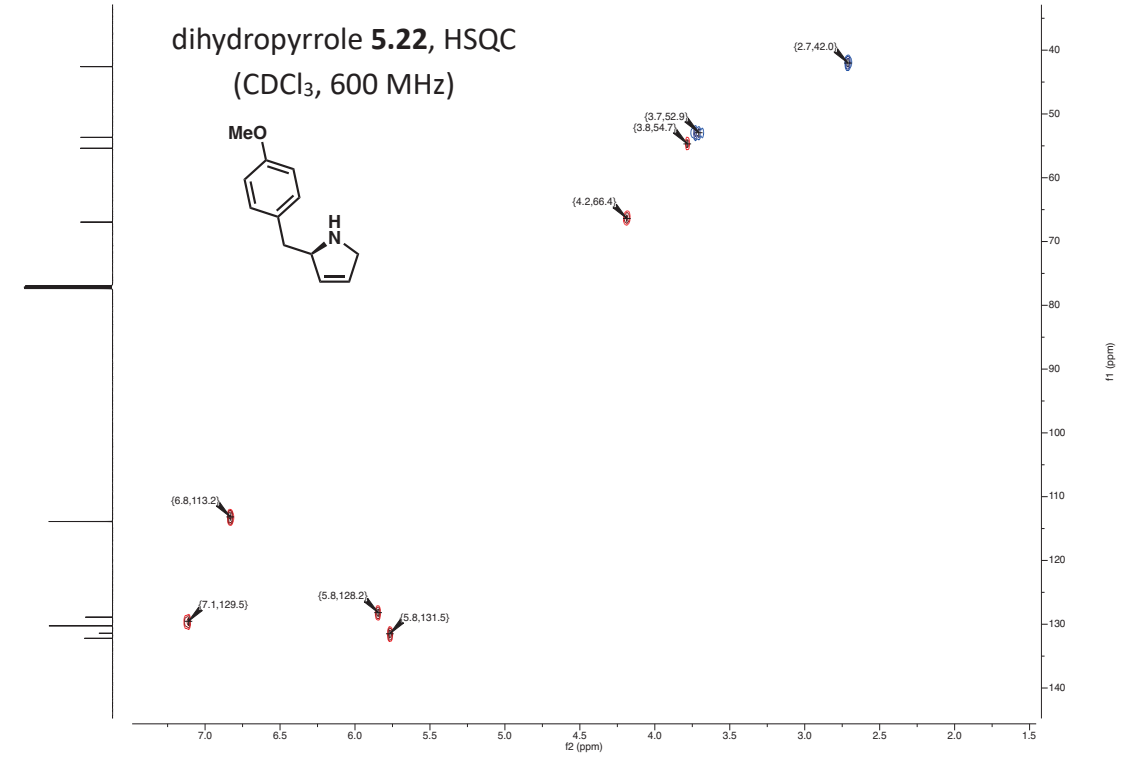
dihydropyrrole **5.22**, ^{1}H NMR ($CDCl_3$, 600 MHz)



dihydropyrrole **5.22**, ^{13}C NMR ($CDCl_3$, 151 MHz)

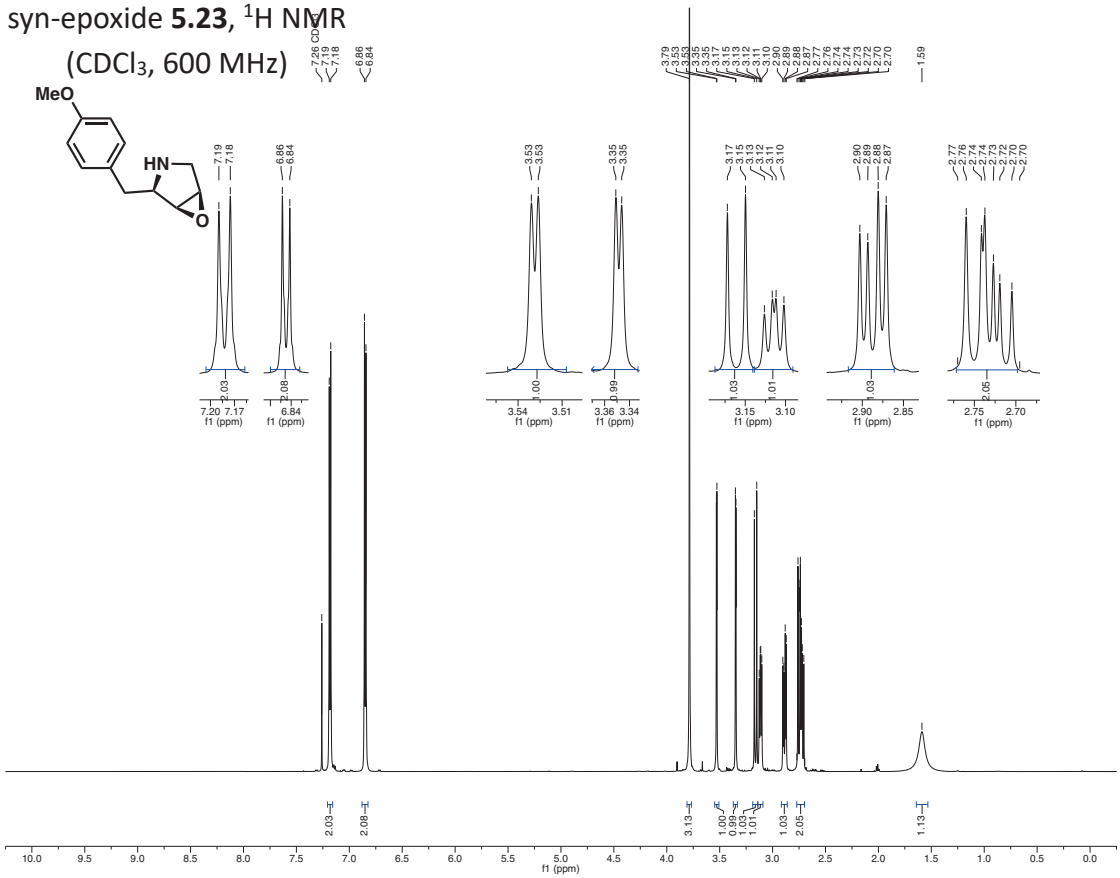



dihydropyrrole **5.22**, COSY
($CDCl_3$, 600 MHz)
MeO
H
N
{5.9,3.7}
{5.8,3.7}
{5.8,4.2}
{5.9,4.2}
{4.2,2.7}
{4.2,3.7}
{7.1,6.8}
f2 (ppm)
f1 (ppm)

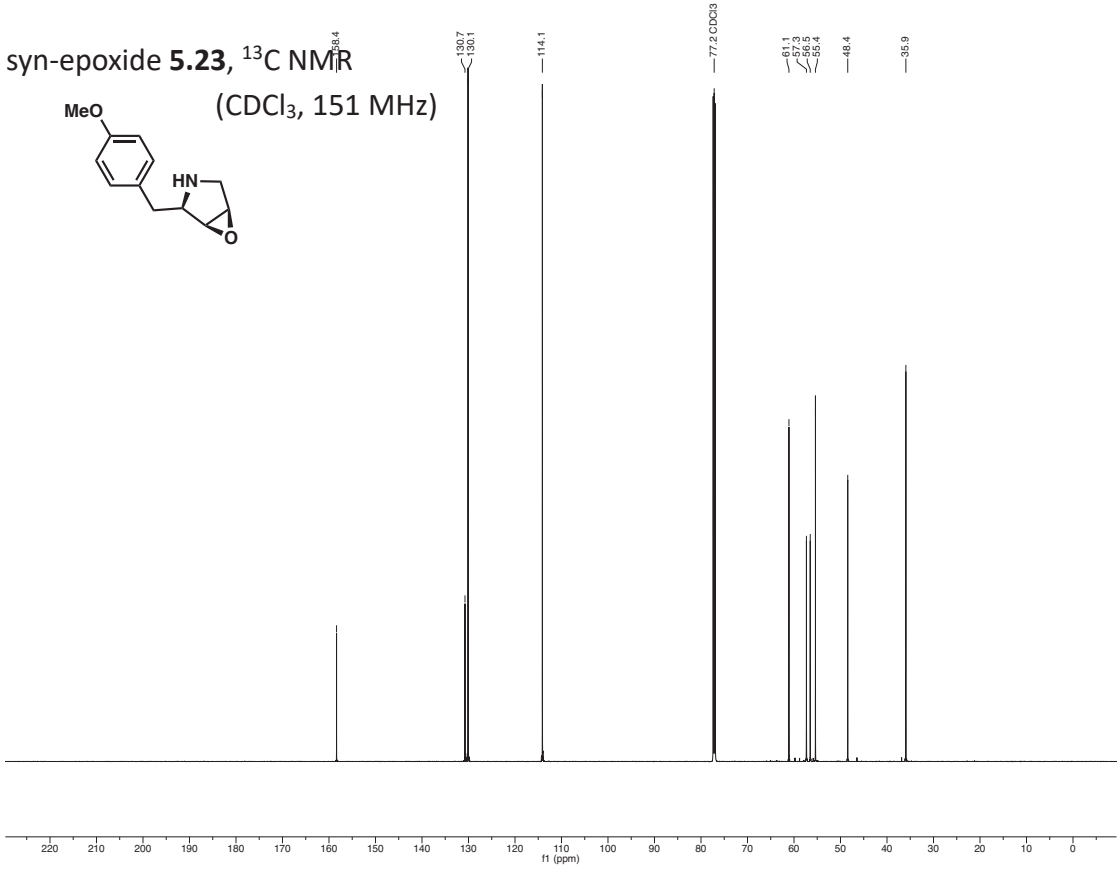

dihydropyrrole **5.22**, HSQC
($CDCl_3$, 600 MHz)
MeO
H
N
{2.7,42.0}
{3.7,52.9}
{3.8,54.7}
{4.2,66.4}
{6.8,113.2}
{7.1,129.5}
{5.8,128.2}
{5.8,131.5}
f2 (ppm)
f1 (ppm)

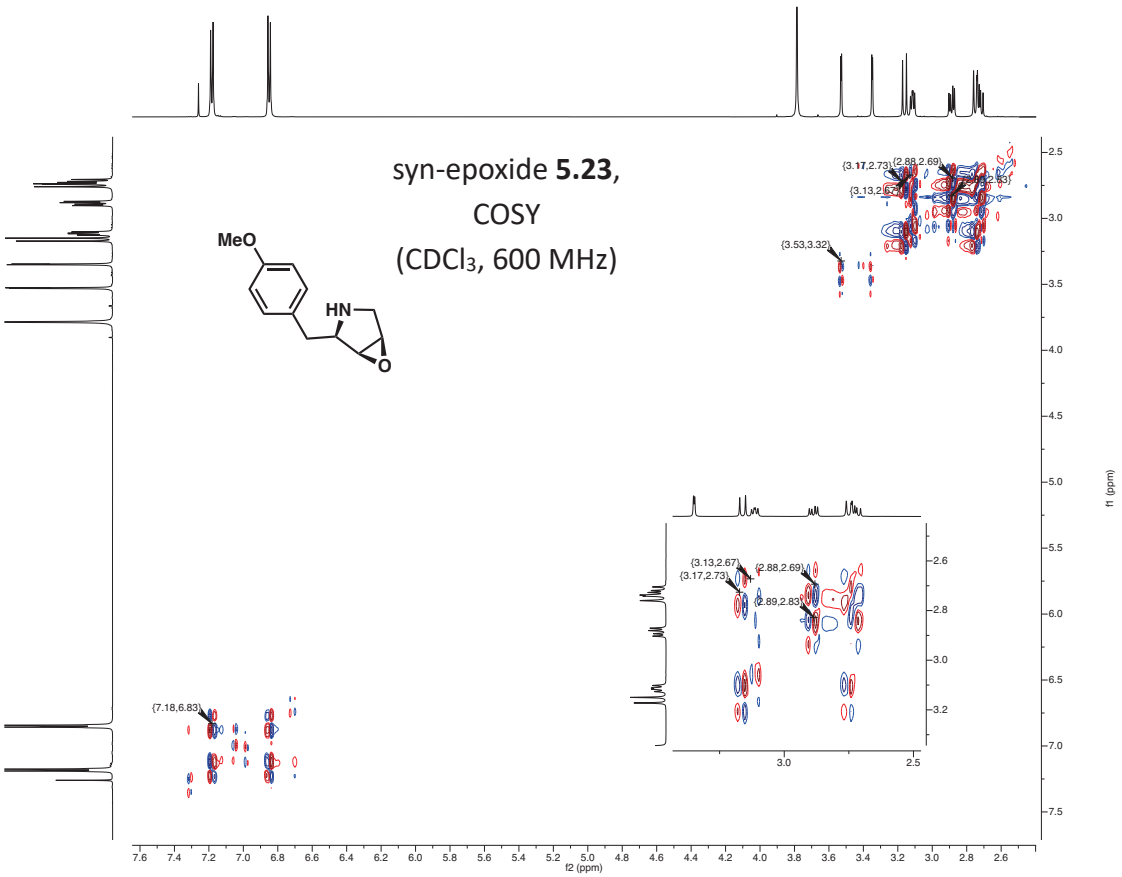
t

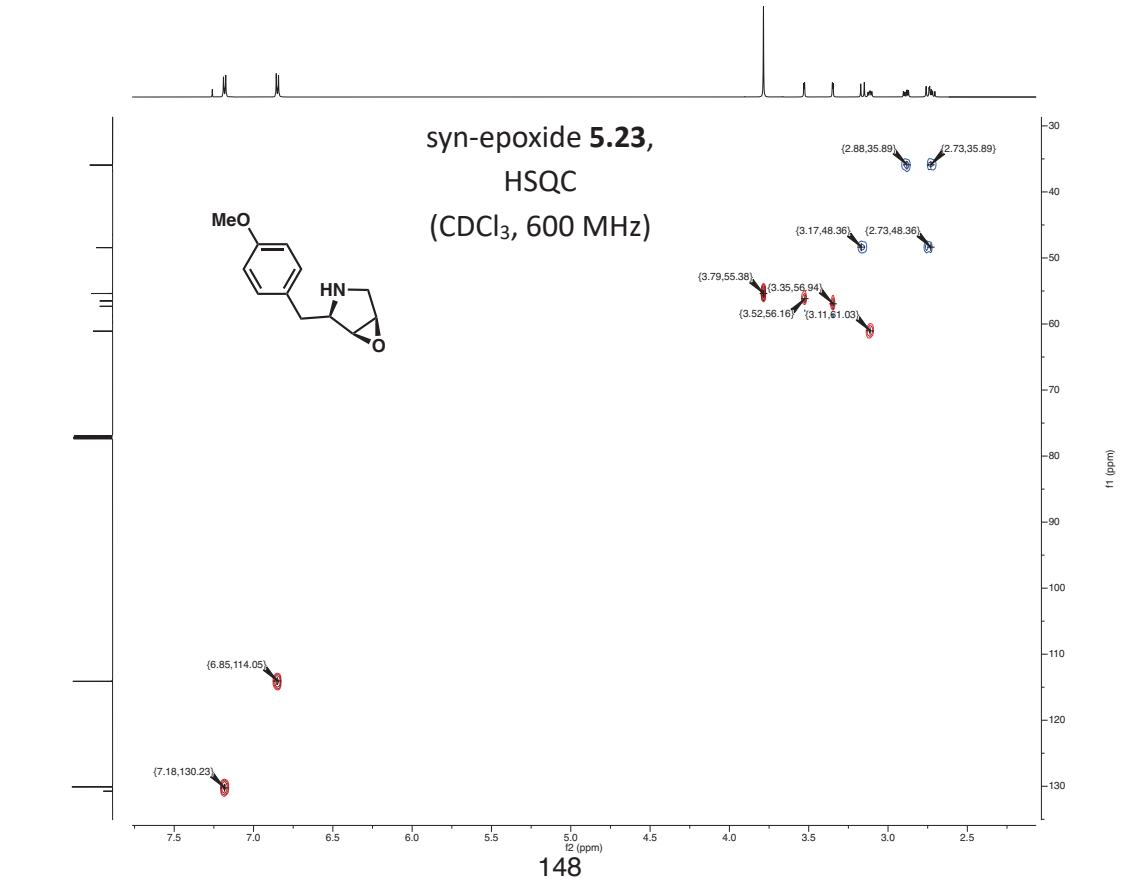
syn-epoxide **5.23**, ^{1}H NMR ($CDCl_3$, 600 MHz)



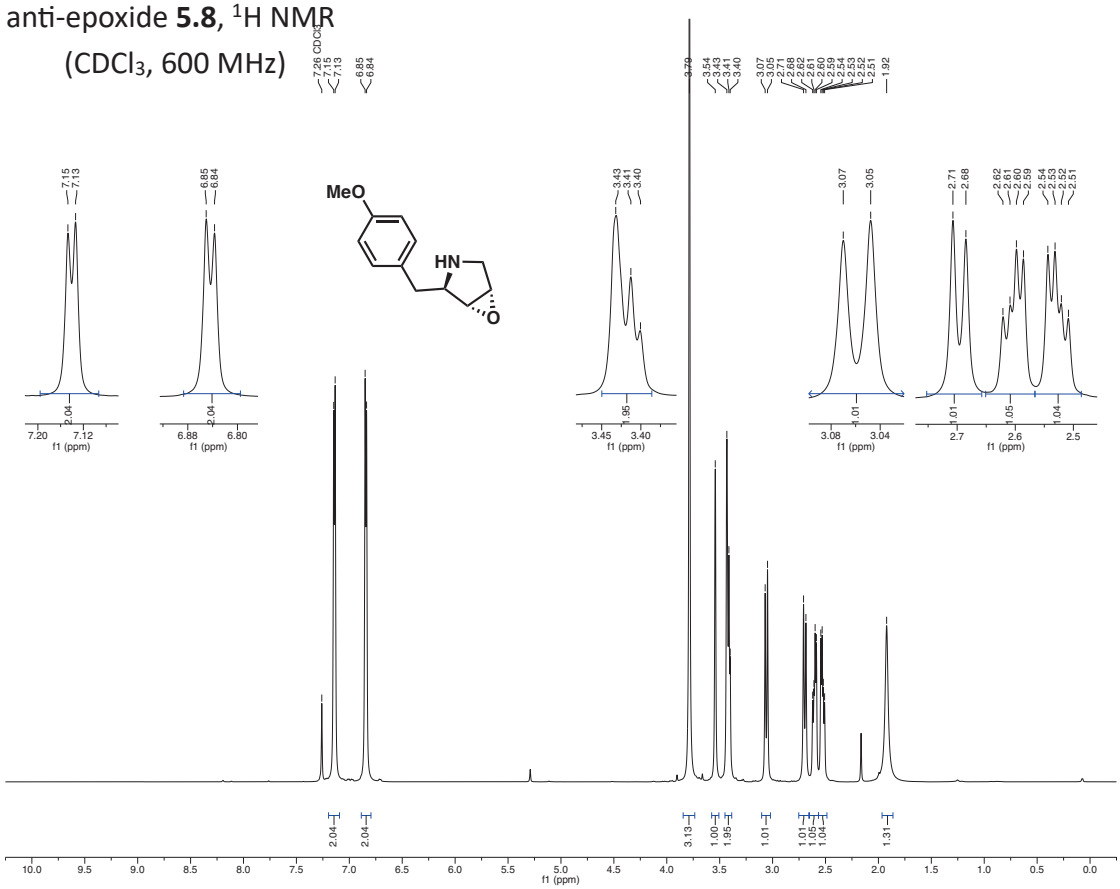
syn-epoxide **5.23**, ^{13}C NMR ($CDCl_3$, 151 MHz)



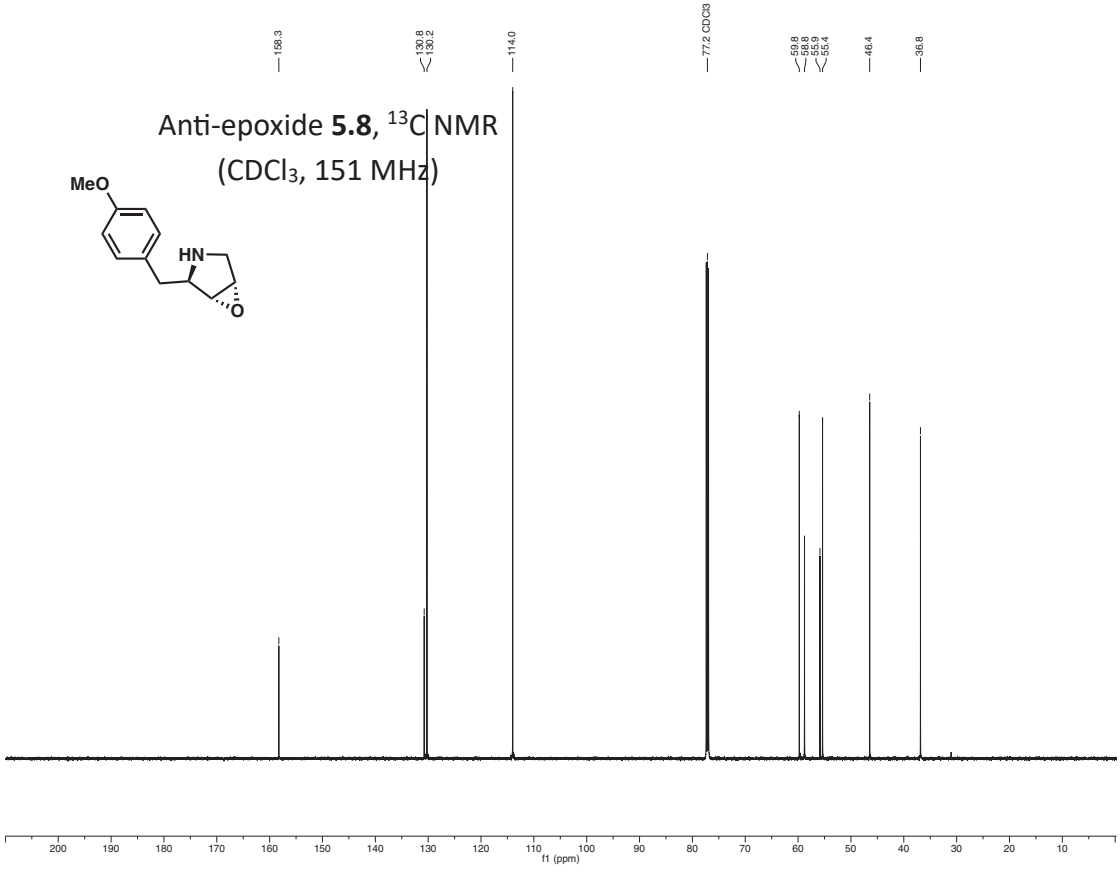

syn-epoxide **5.23**,
COSY
($CDCl_3$, 600 MHz)
MeO
HN
O
{3.53,3.32}
{7.18,6.83}
{3.13,2.67}
{3.17,2.73}
{2.88,2.69}
{2.89,2.83}
f2 (ppm)
f1 (ppm)

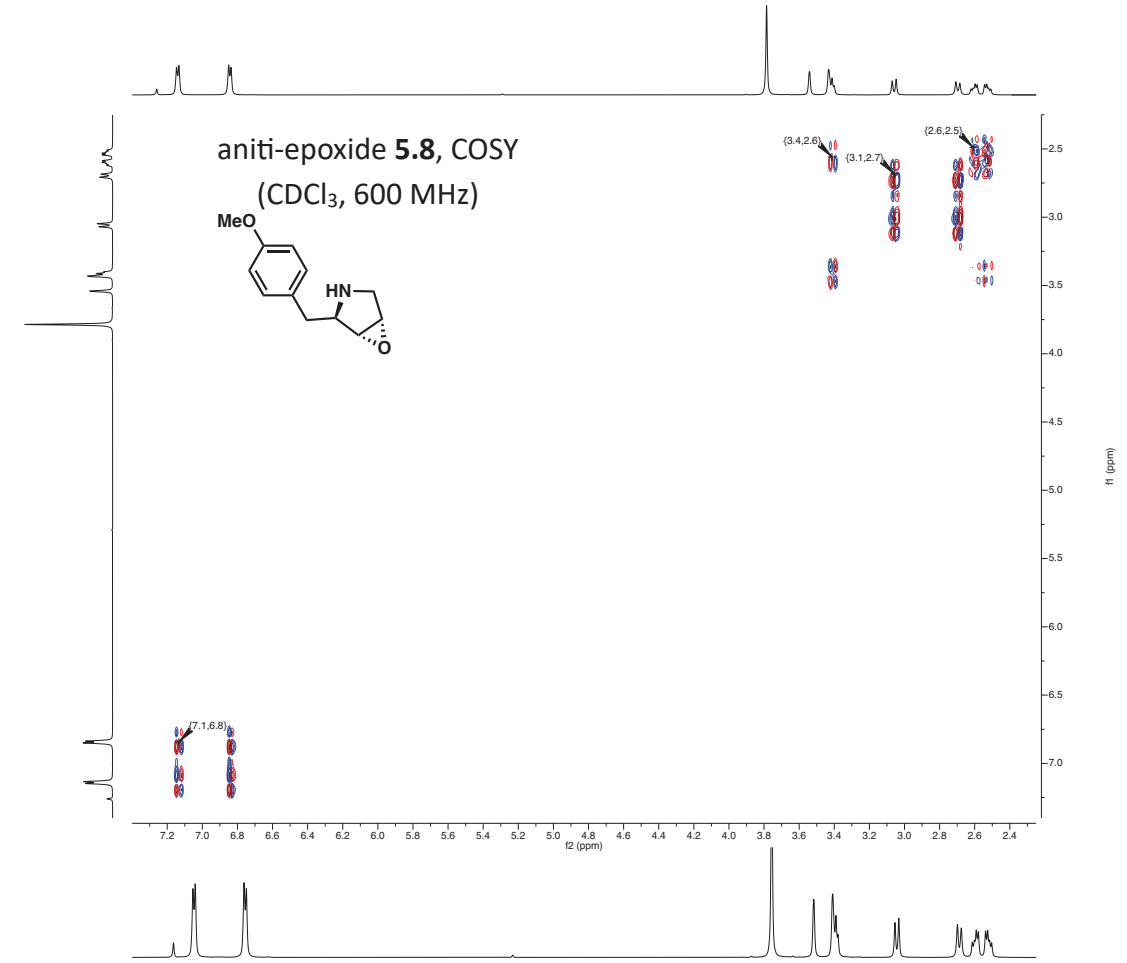

syn-epoxide **5.23**,
HSQC
($CDCl_3$, 600 MHz)
MeO
HN
O
{2.88,35.89}
{2.73,35.89}
{3.17,48.36}
{2.73,48.36}
{3.79,55.38}
{3.35,56.94}
{3.52,56.16}
{3.11,61.03}
{6.85,114.05}
{7.18,130.23}
f2 (ppm)
f1 (ppm)

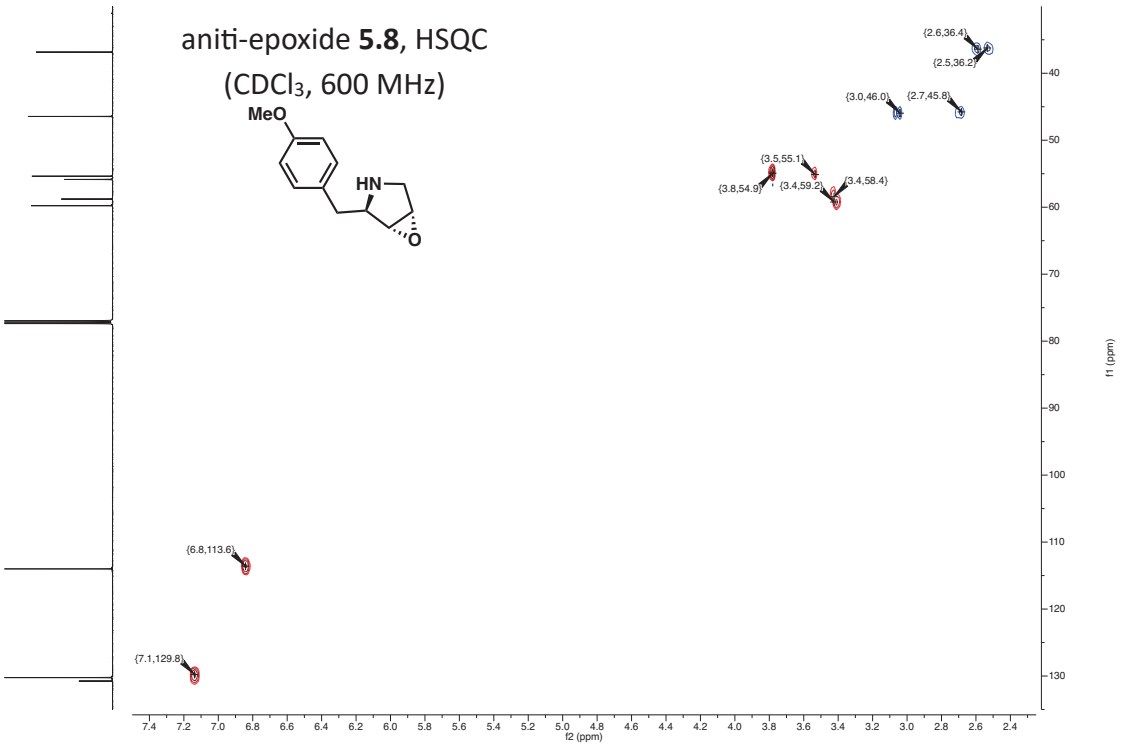
anti-epoxide **5.8**, ^{1}H NMR
($CDCl_3$, 600 MHz)



Anti-epoxide **5.8**, ^{13}C NMR
($CDCl_3$, 151 MHz)

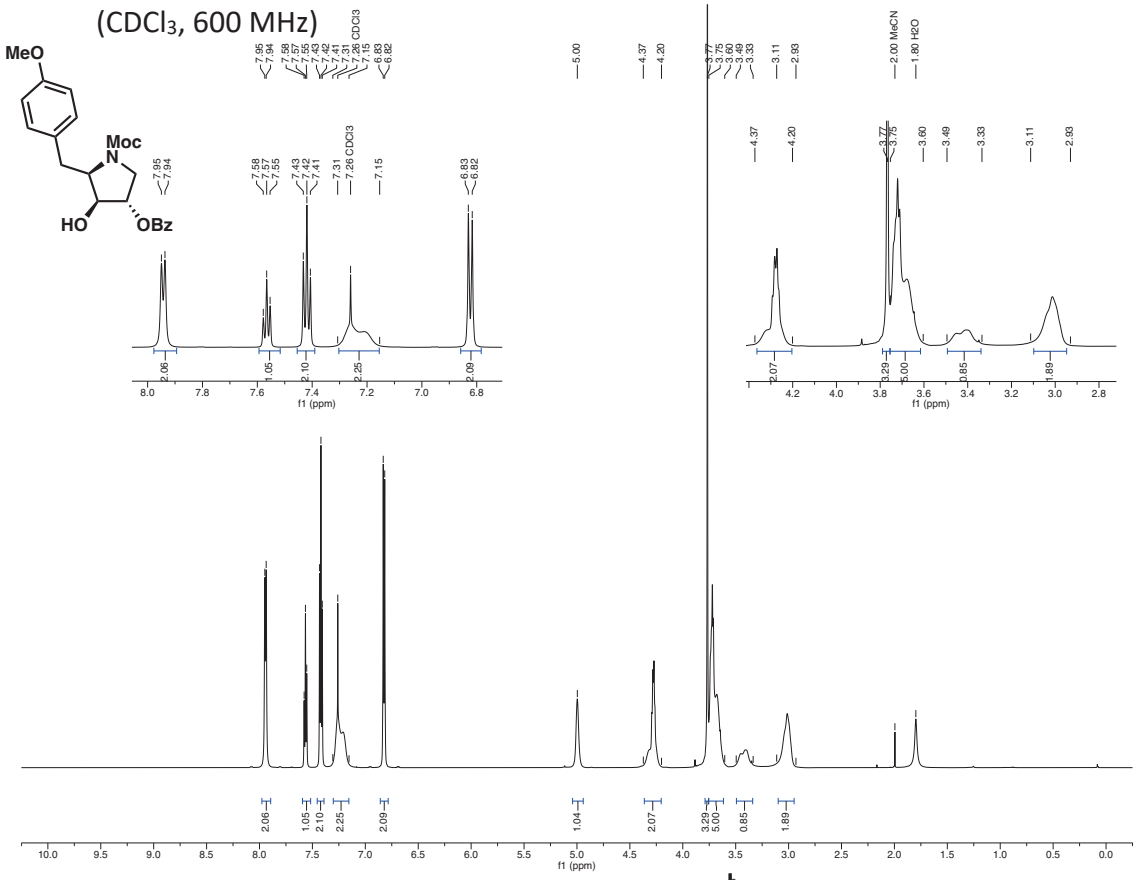



aniti-epoxide **5.8**, COSY
(CDCl3, 600 MHz)
MeO
HN
O
{3.4,2.6}
{3.1,2.7}
{2.6,2.5}
{7.1,6.8}
f2 (ppm)
f1 (ppm)


aniti-epoxide **5.8**, HSQC
(CDCl3, 600 MHz)
MeO
HN
O
{2.6,36.4}
{2.5,36.2}
{3.0,46.0}
{2.7,45.8}
{3.5,55.1}
{3.8,54.9}
{3.4,59.2}
{3.4,58.4}
{6.8,113.6}
{7.1,129.8}
f2 (ppm)
f1 (ppm)

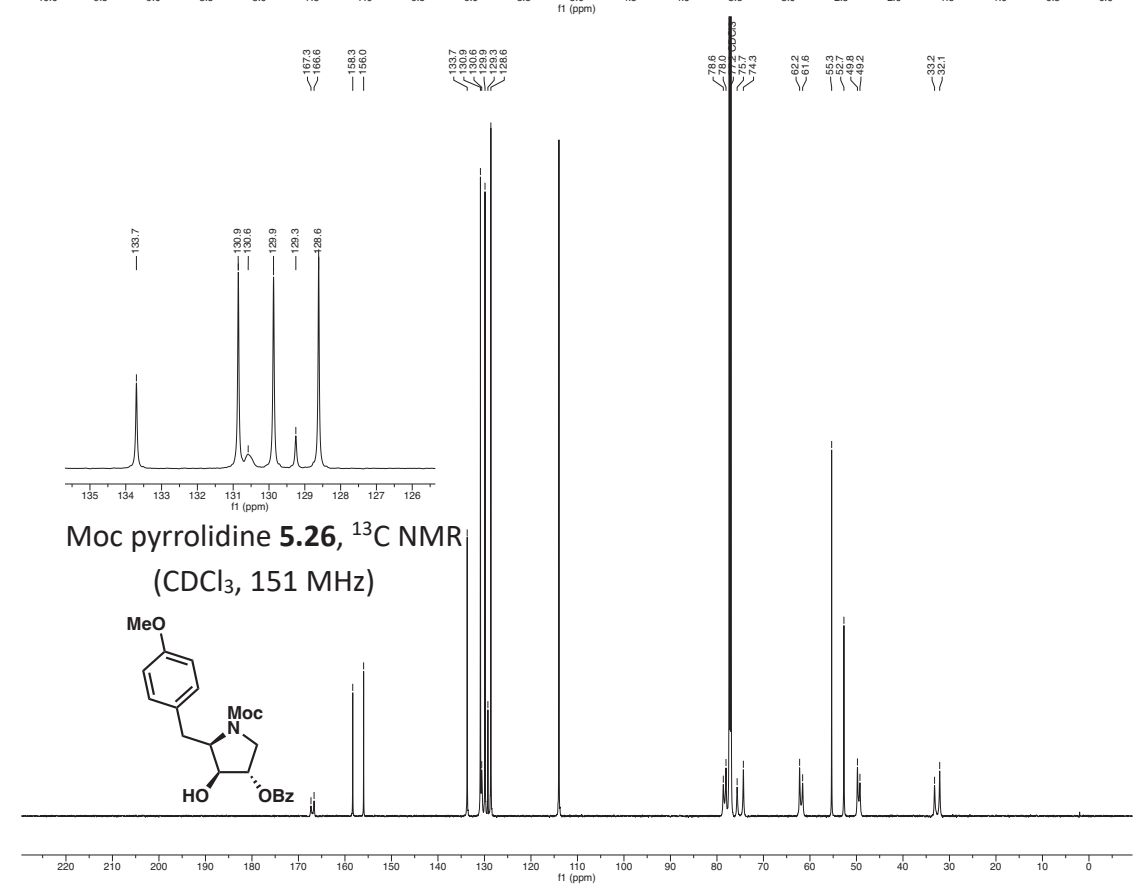
Moc pyrrolidine **5.26**, ^{1}H NMR

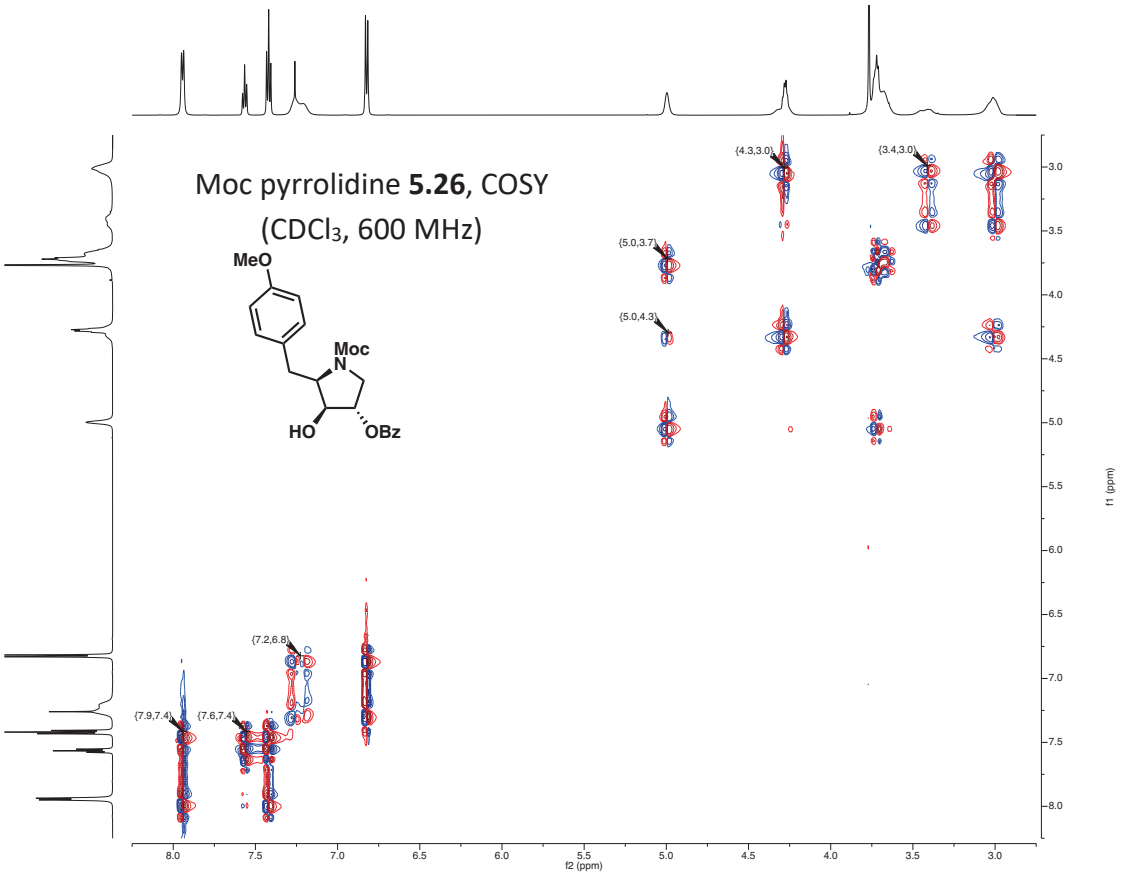
($CDCl_3$, 600 MHz)

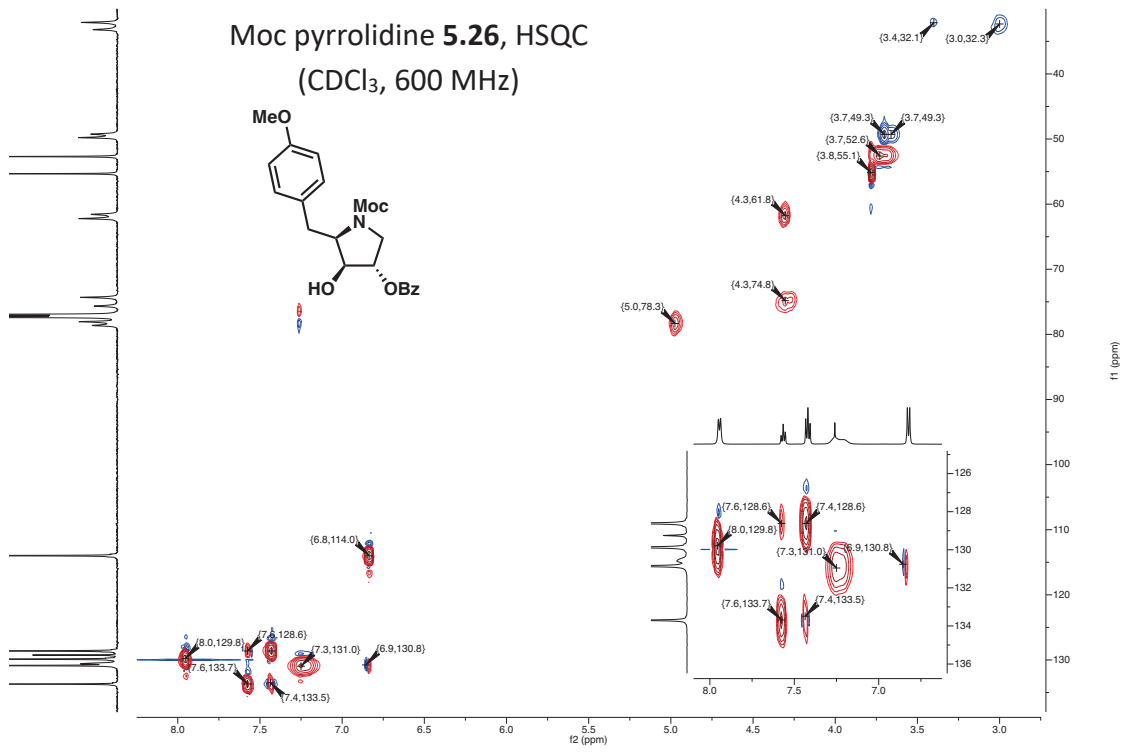


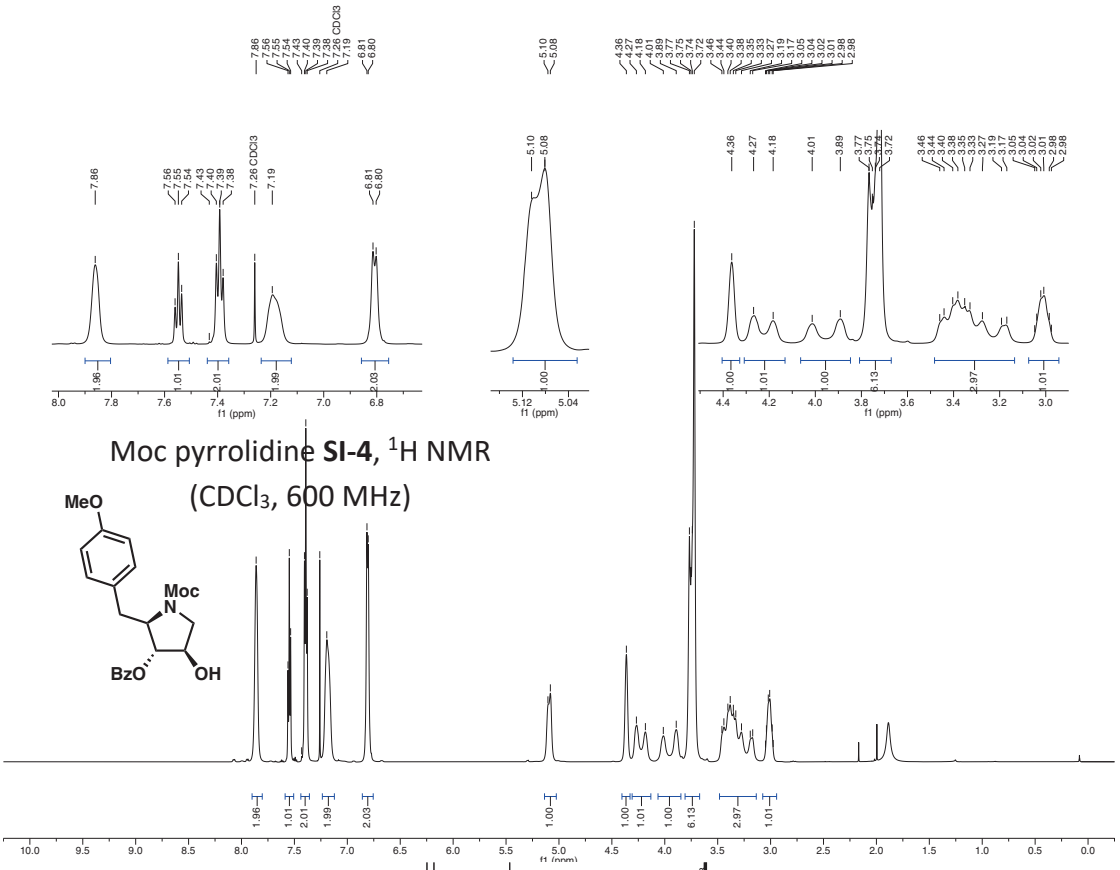
Moc pyrrolidine **5.26**, ^{13}C NMR

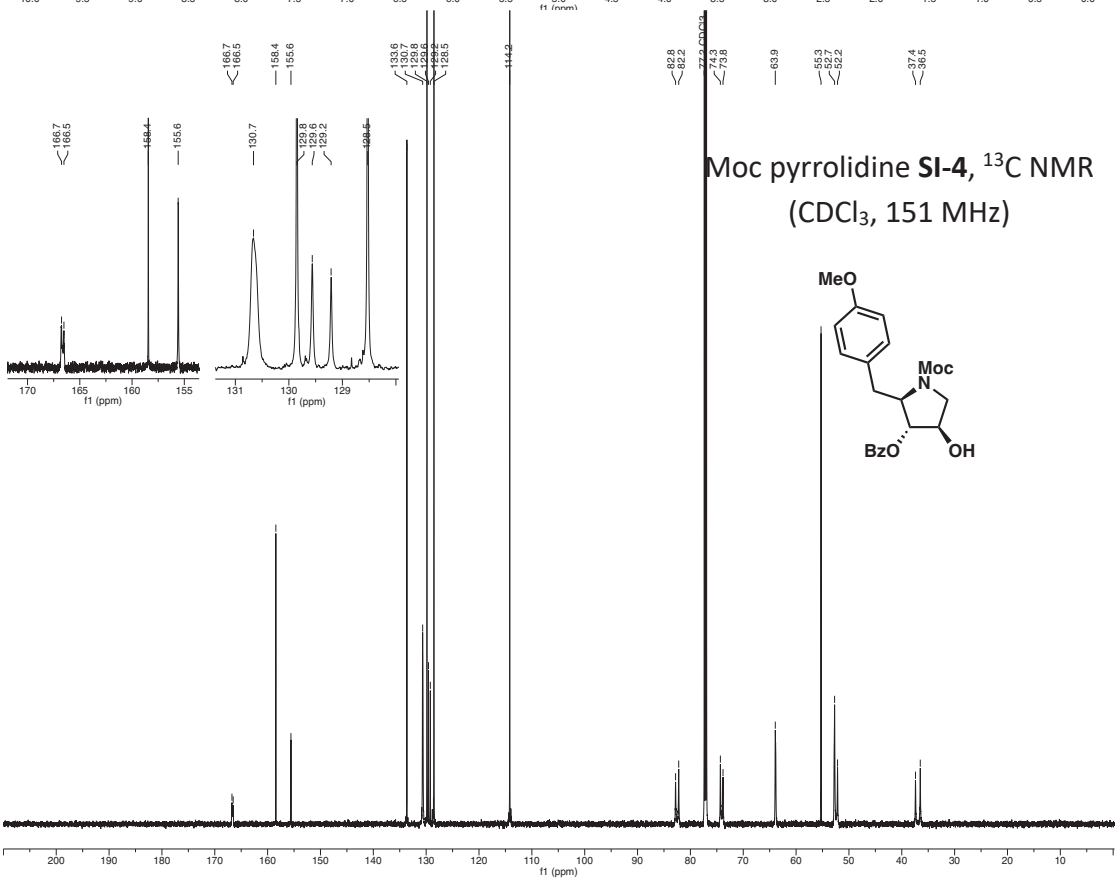
($CDCl_3$, 151 MHz)

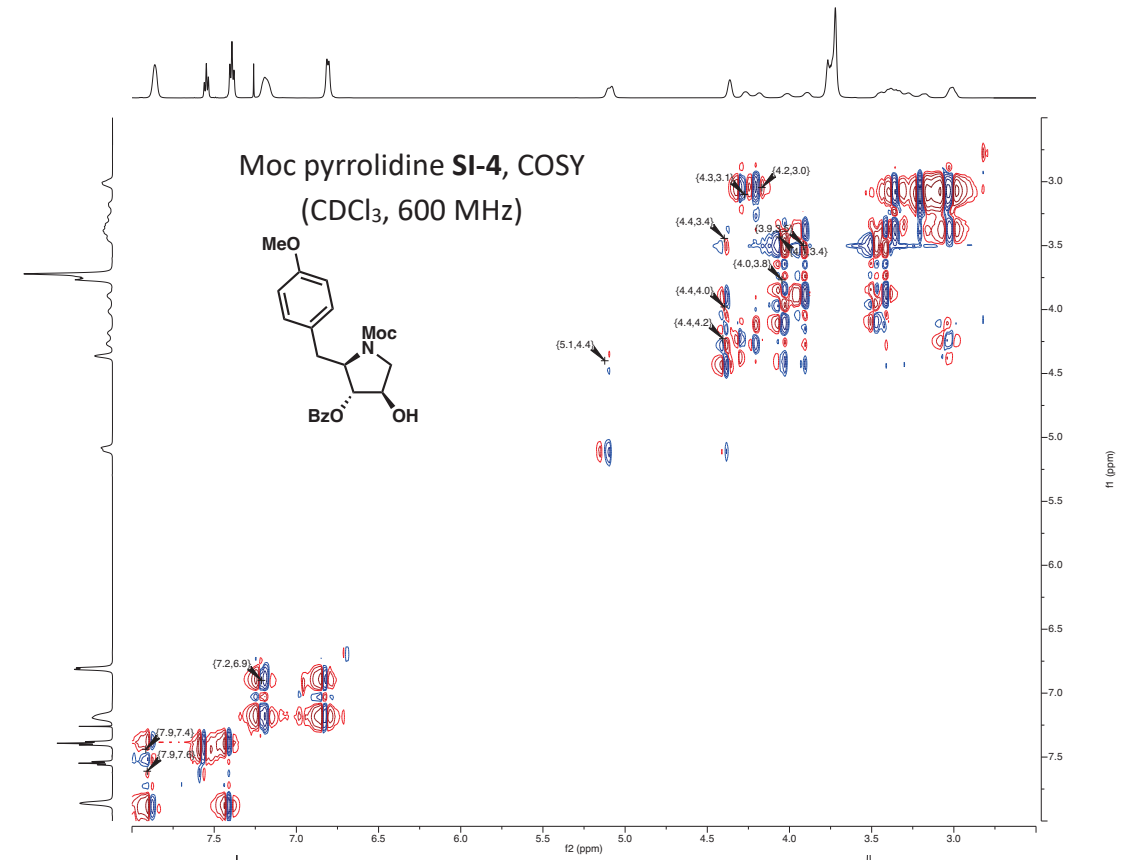


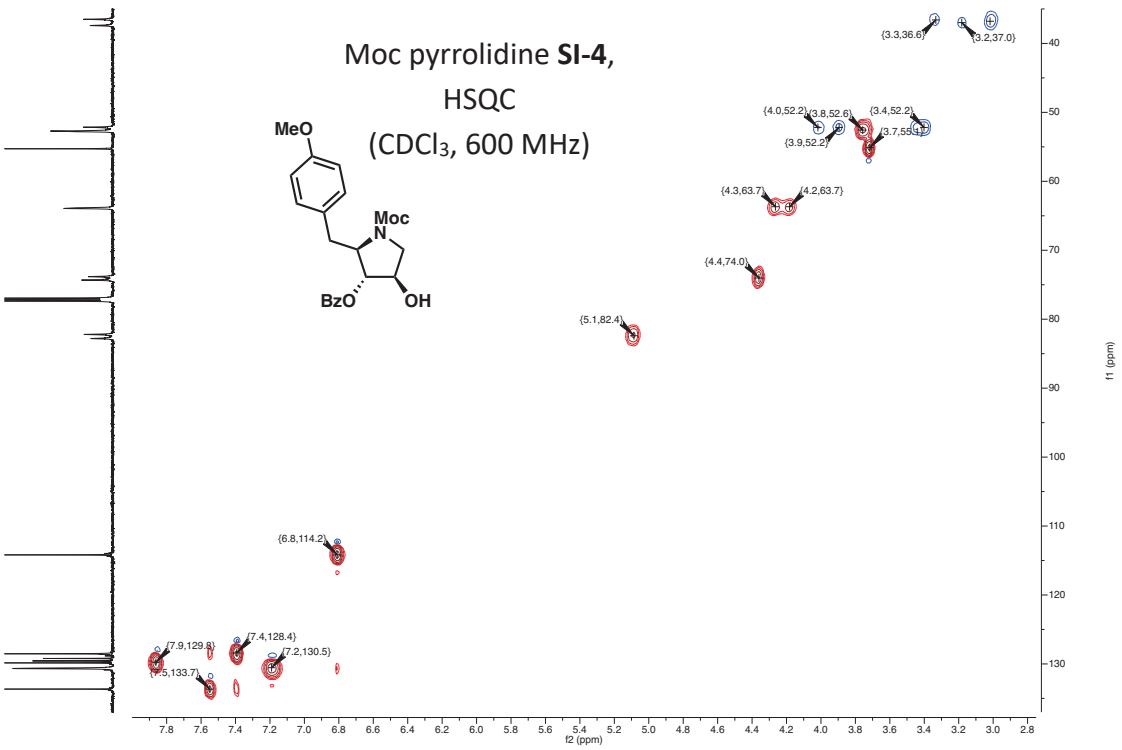

Moc pyrrolidine **5.26**, COSY
($CDCl_3$, 600 MHz)
MeO
Moc
N
HO
OBz
{4.3,3.0}
{3.4,3.0}
{5.0,3.7}
{5.0,4.3}
{7.2,6.8}
{7.9,7.4}
{7.6,7.4}
f2 (ppm)
f1 (ppm)

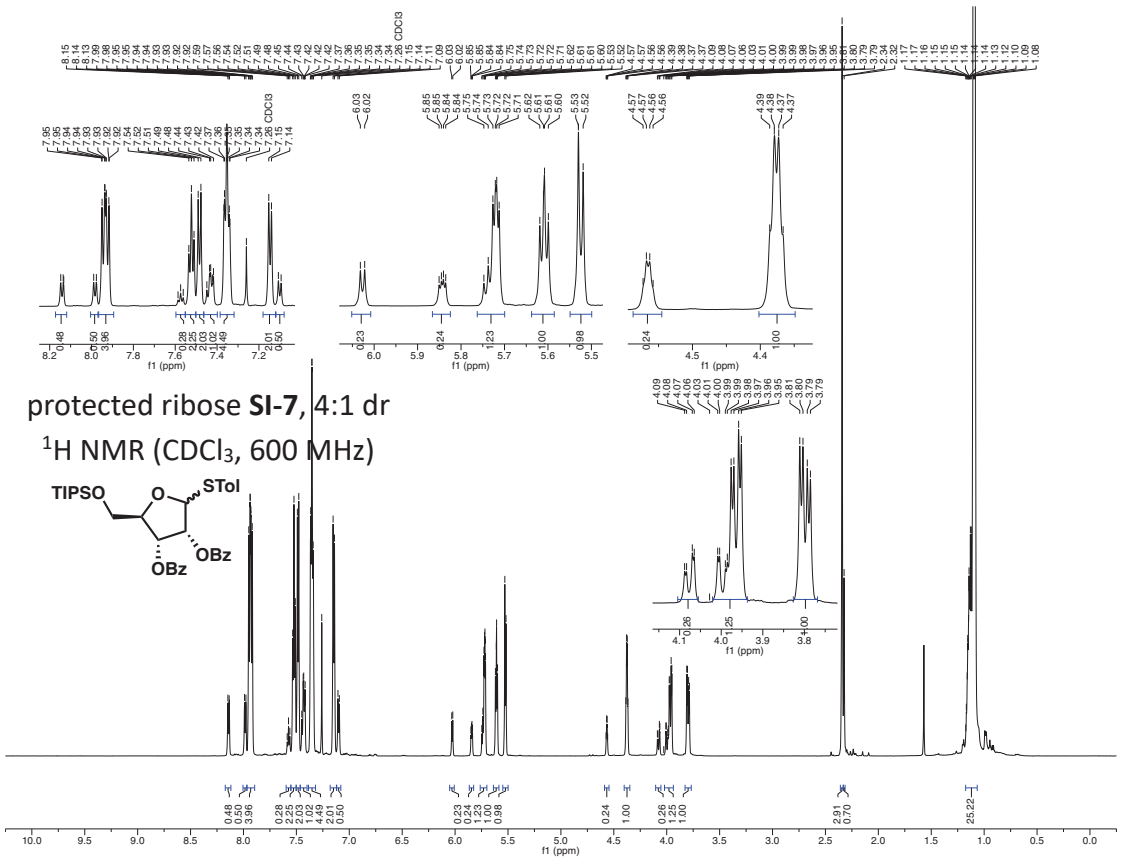

Moc pyrrolidine **5.26**, HSQC
($CDCl_3$, 600 MHz)
MeO
Moc
N
HO
OBz
{3.4,32.1}
{3.0,32.3}
{3.7,49.3}
{3.7,52.6}
{3.8,55.1}
{4.3,61.8}
{4.3,74.8}
{5.0,78.3}
{6.8,114.0}
{8.0,129.8}
{7.6,128.6}
{7.6,133.7}
{7.3,131.0}
{6.9,130.8}
{7.4,133.5}
{7.4,128.6}
f2 (ppm)
f1 (ppm)


Moc pyrrolidine **SI-4**, ^{1}H NMR
($CDCl_3$, 600 MHz)
MeO
Moc
N
BzO
OH


Moc pyrrolidine **SI-4**, ^{13}C NMR
($CDCl_3$, 151 MHz)
MeO
Moc
N
BzO
OH

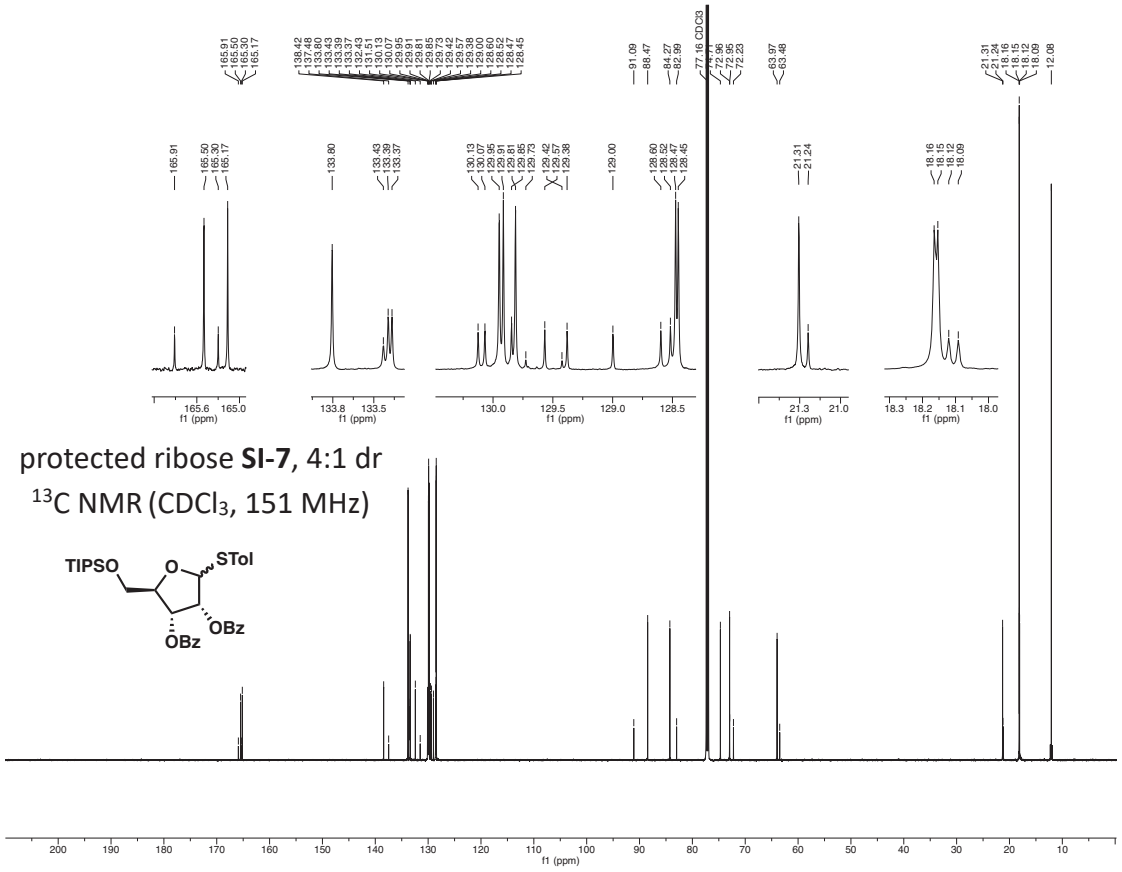

Moc pyrrolidine **SI-4**, COSY
($CDCl_3$, 600 MHz)
MeO
Moc
N
BzO
OH
{4.3,3.1}
{4.2,3.0}
{4.4,3.4}
{3.9,3.4}
{4.0,3.8}
{4.4,4.0}
{4.4,4.2}
{5.1,4.4}
{7.2,6.9}
{7.9,7.4}
{7.9,7.6}
f2 (ppm)
f1 (ppm)


Moc pyrrolidine **SI-4**,
HSQC
($CDCl_3$, 600 MHz)
MeO
Moc
N
BzO
OH
{3.3,36.6}
{3.2,37.0}
{4.0,52.2}
{3.8,52.6}
{3.4,52.2}
{3.9,52.2}
{3.7,55.1}
{4.3,63.7}
{4.2,63.7}
{4.4,74.0}
{5.1,82.4}
{6.8,114.2}
{7.9,129.8}
{7.4,128.4}
{7.2,130.5}
{7.5,133.7}
f2 (ppm)
f1 (ppm)



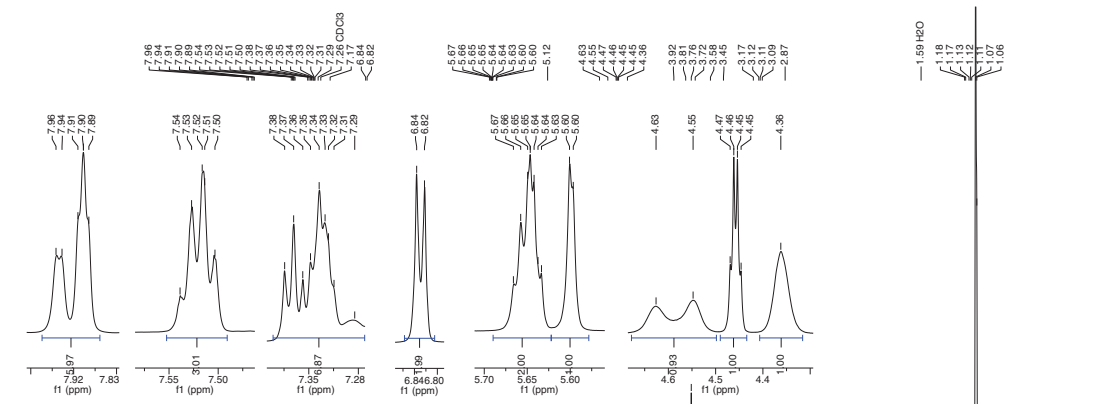
protected ribose **SI-7**, 4:1 dr

^{1}H NMR ($CDCl_3$, 600 MHz)



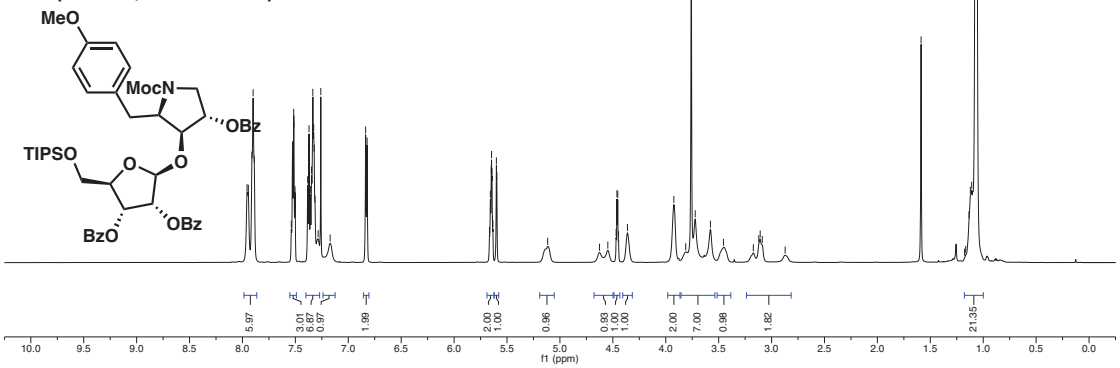
protected ribose **SI-7**, 4:1 dr

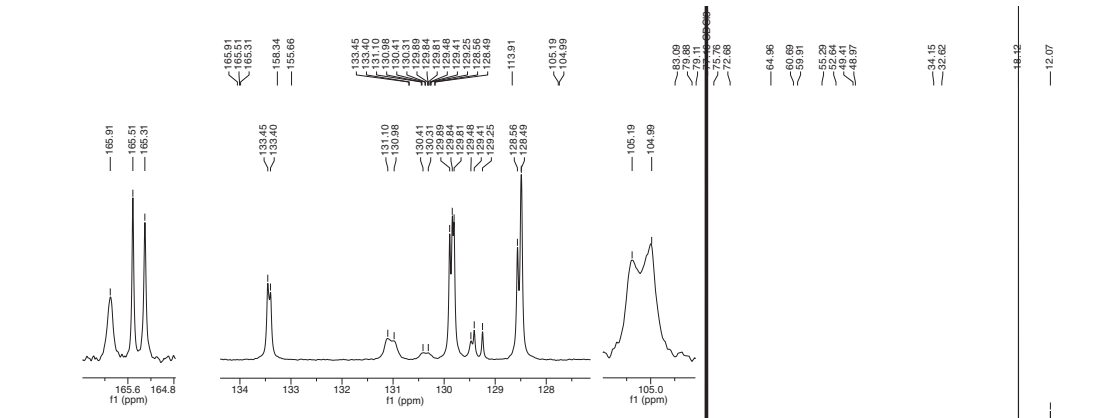
^{13}C NMR ($CDCl_3$, 151 MHz)



TIPS ether **SI-8**, ^{1}H NMR

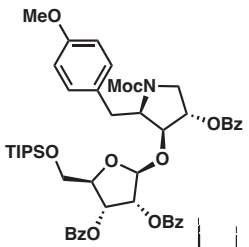
($CDCl_3$, 600 MHz)

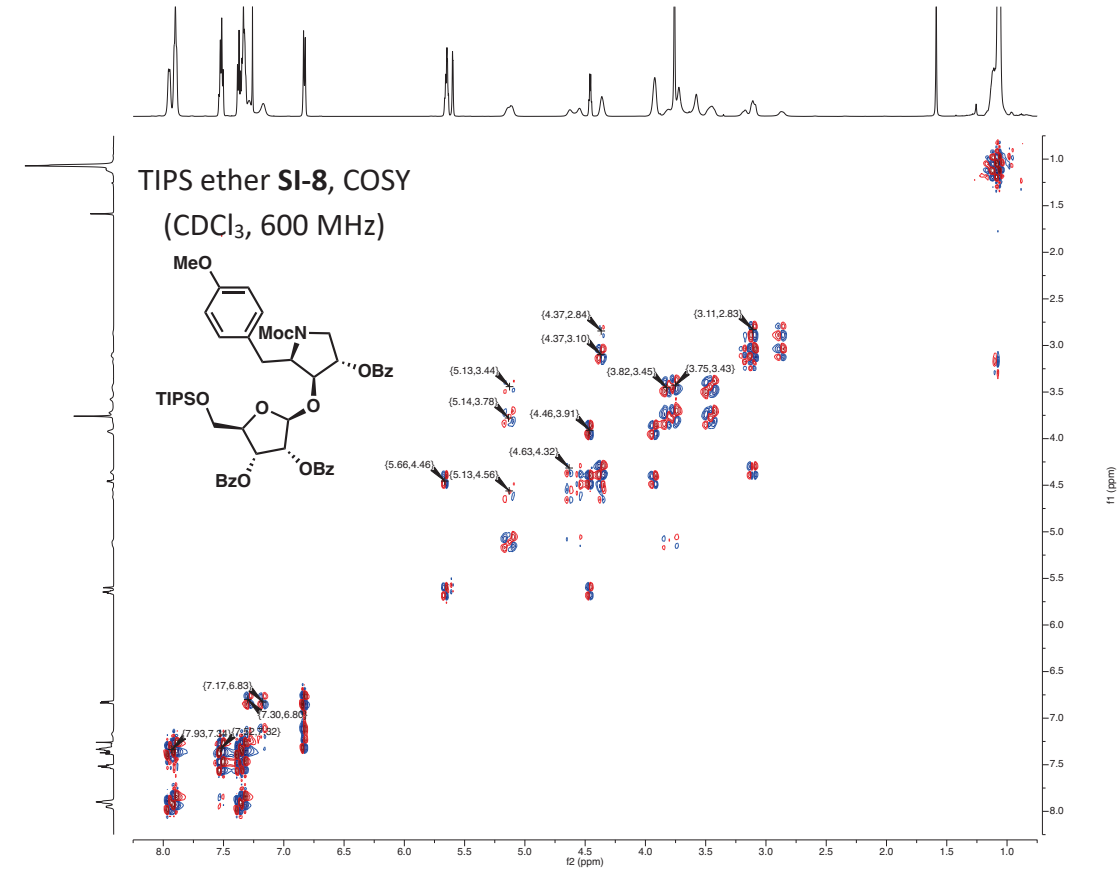


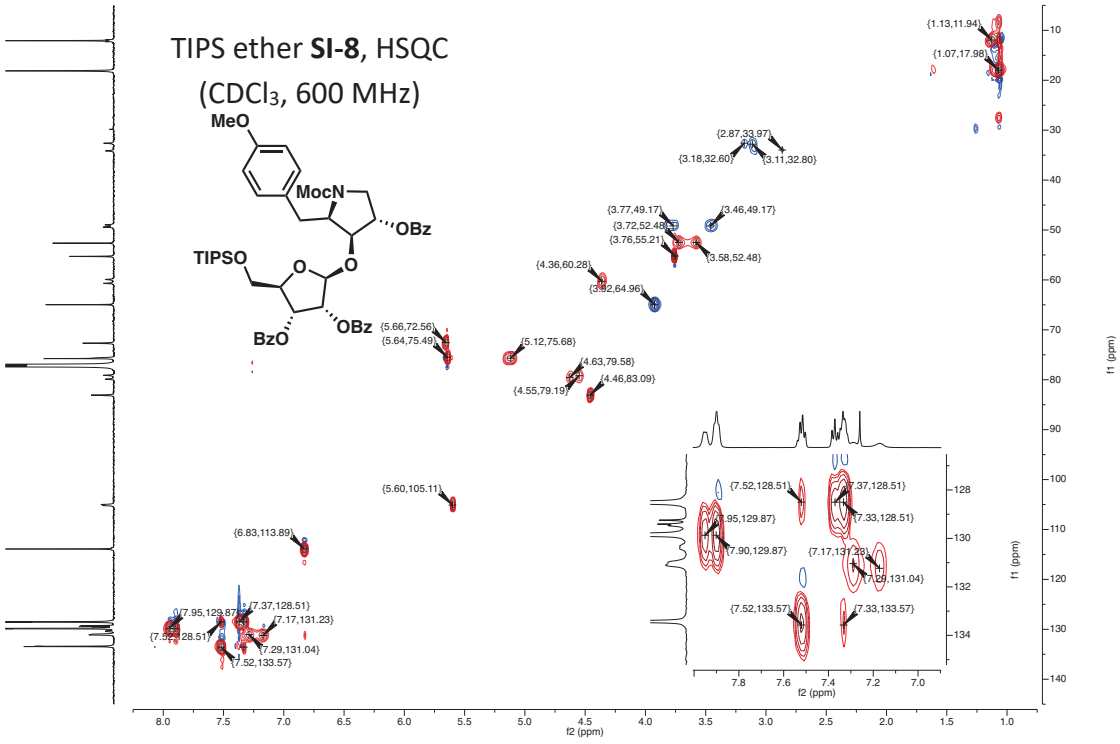


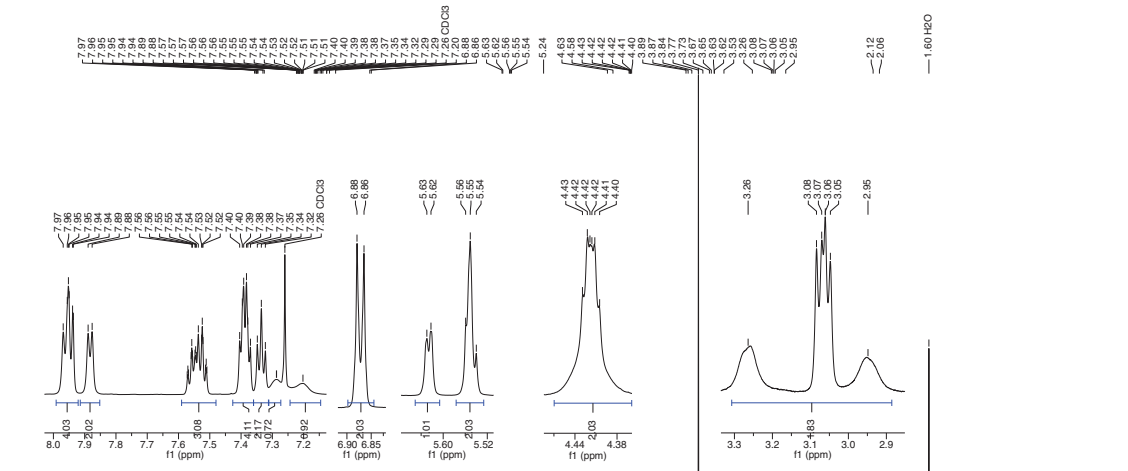
TIPS ether **SI-8**, ^{13}C NMR

($CDCl_3$, 151 MHz)



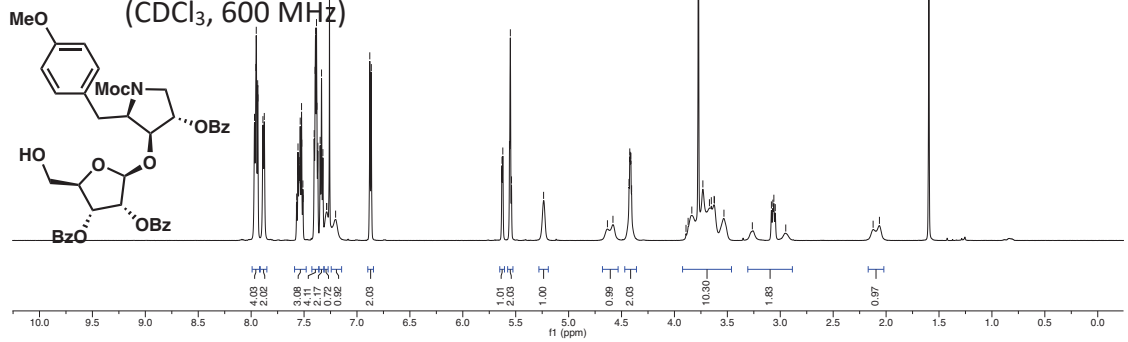

TIPS ether **SI-8**, COSY
(CDCl3, 600 MHz)
MeO
MocN
OBz
TIPSO
BzO
OBz
f2 (ppm)
f1 (ppm)

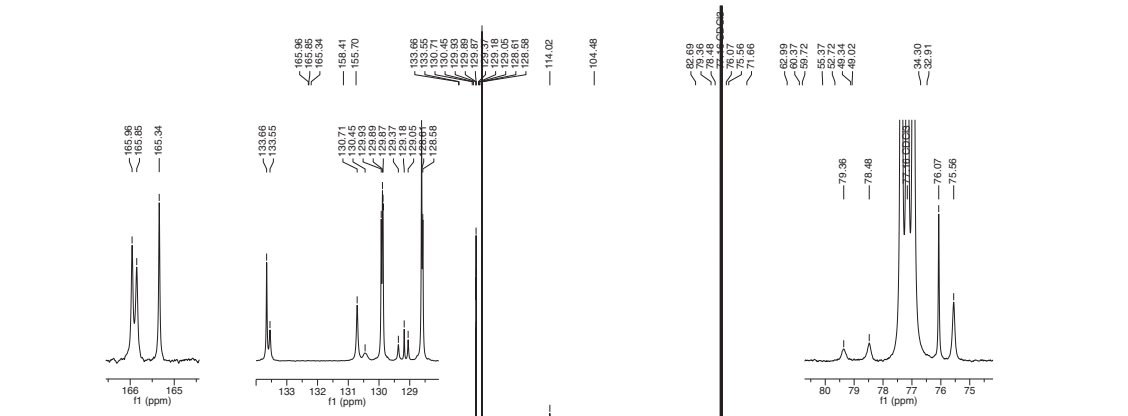

TIPS ether **SI-8**, HSQC
(CDCl3, 600 MHz)
MeO
MocN
OBz
TIPSO
BzO
OBz
f2 (ppm)
f1 (ppm)



primary alcohol **5.13**, ^{1}H NMR

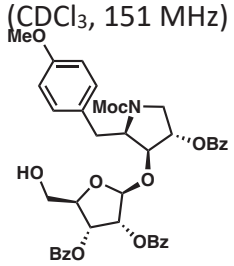
($CDCl_3$, 600 MHz)

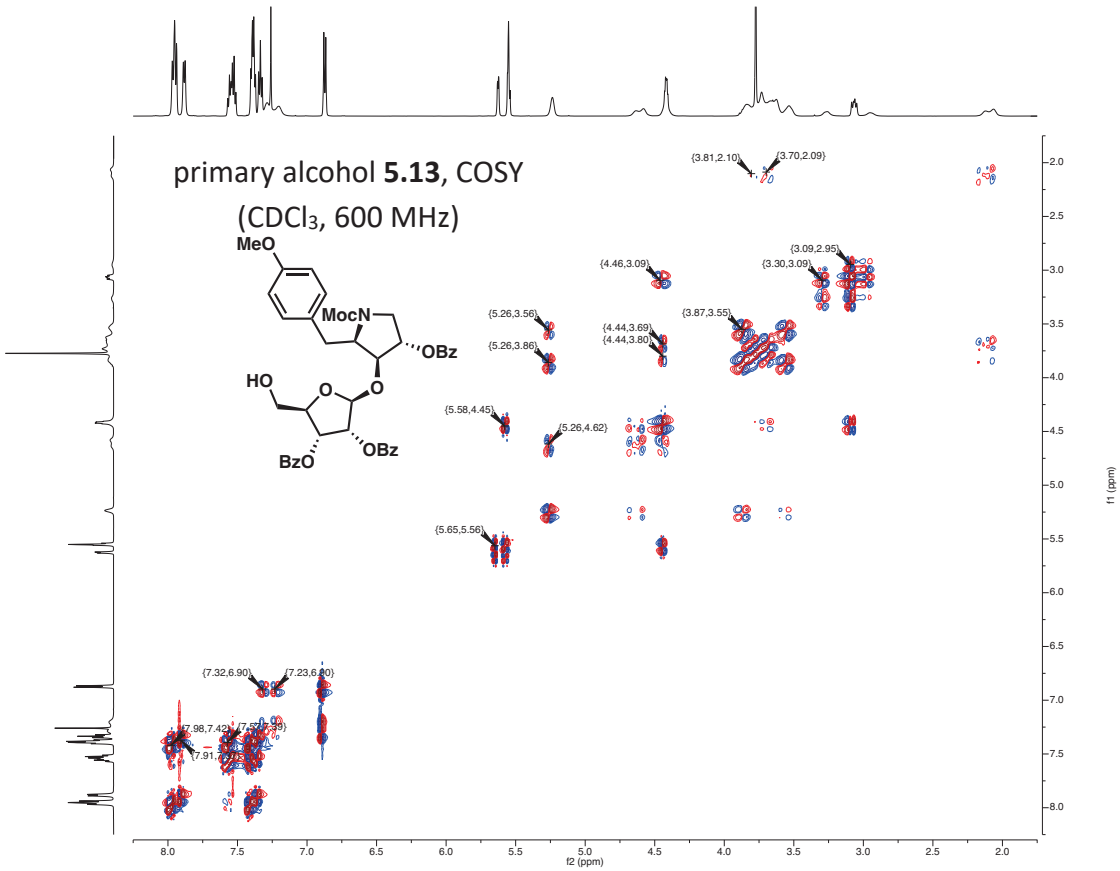


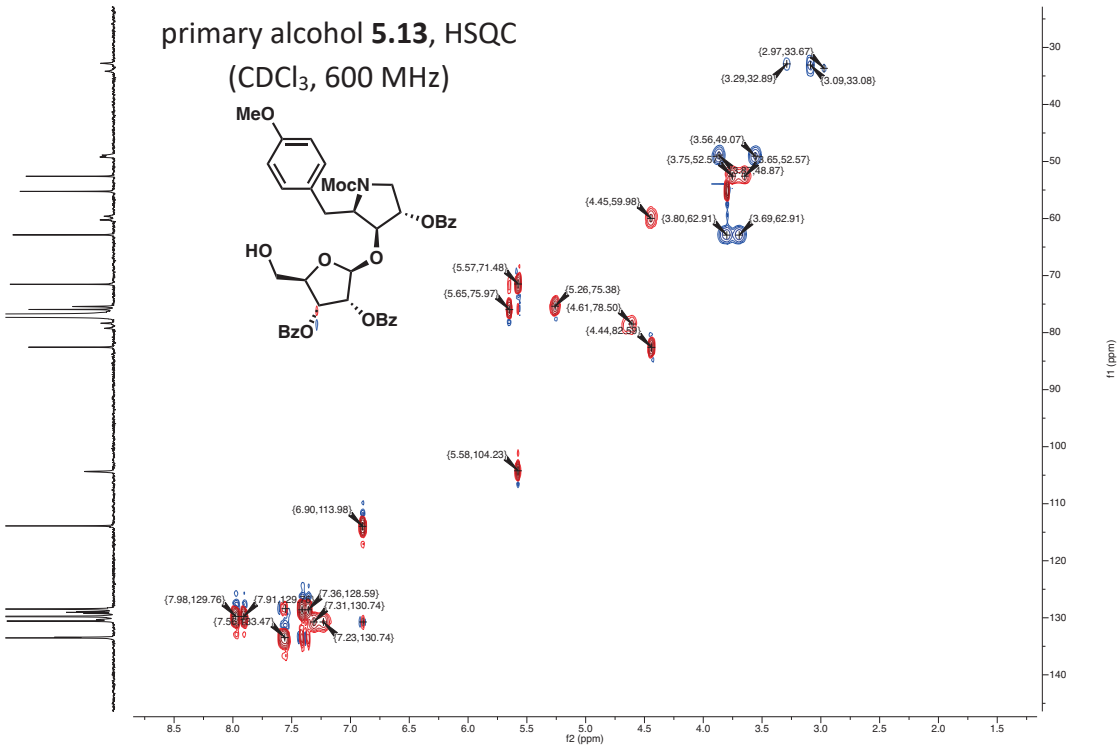


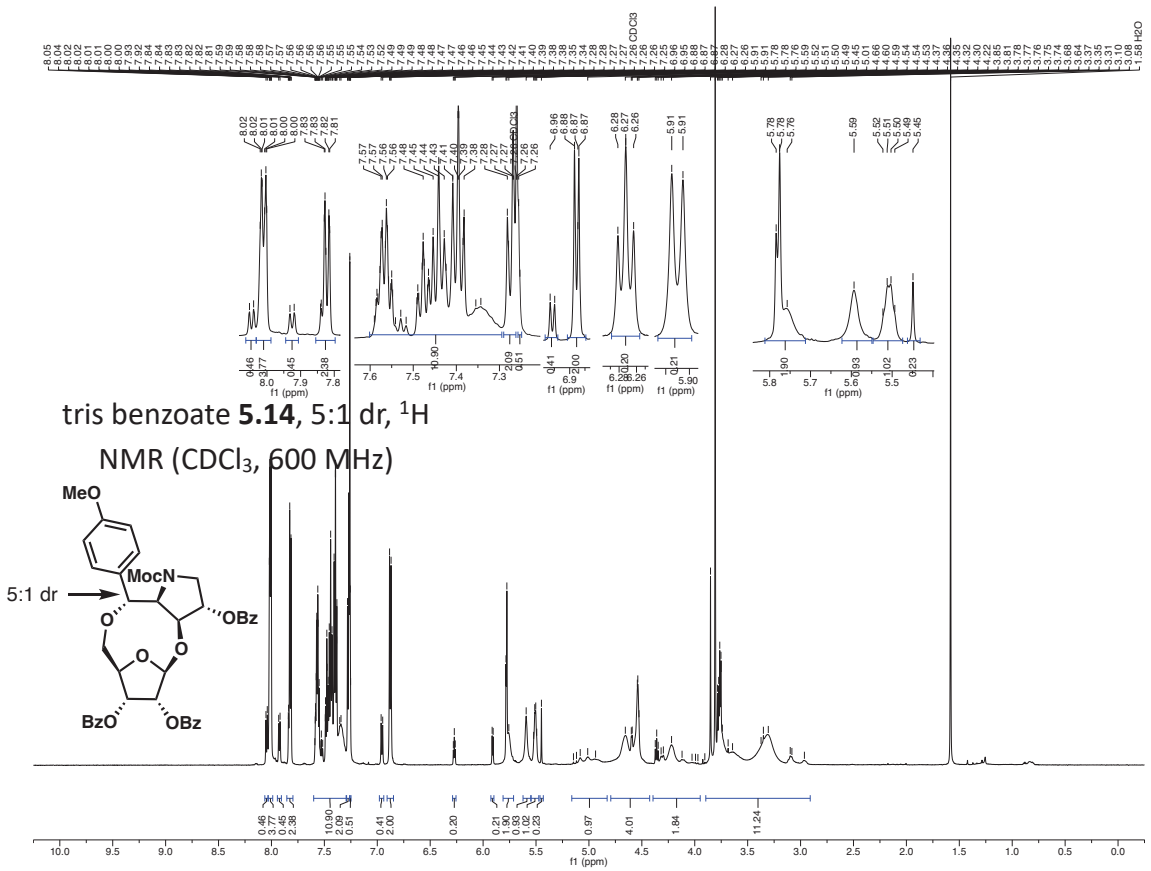
primary alcohol **5.13**, ^{13}C NMR

($CDCl_3$, 151 MHz)

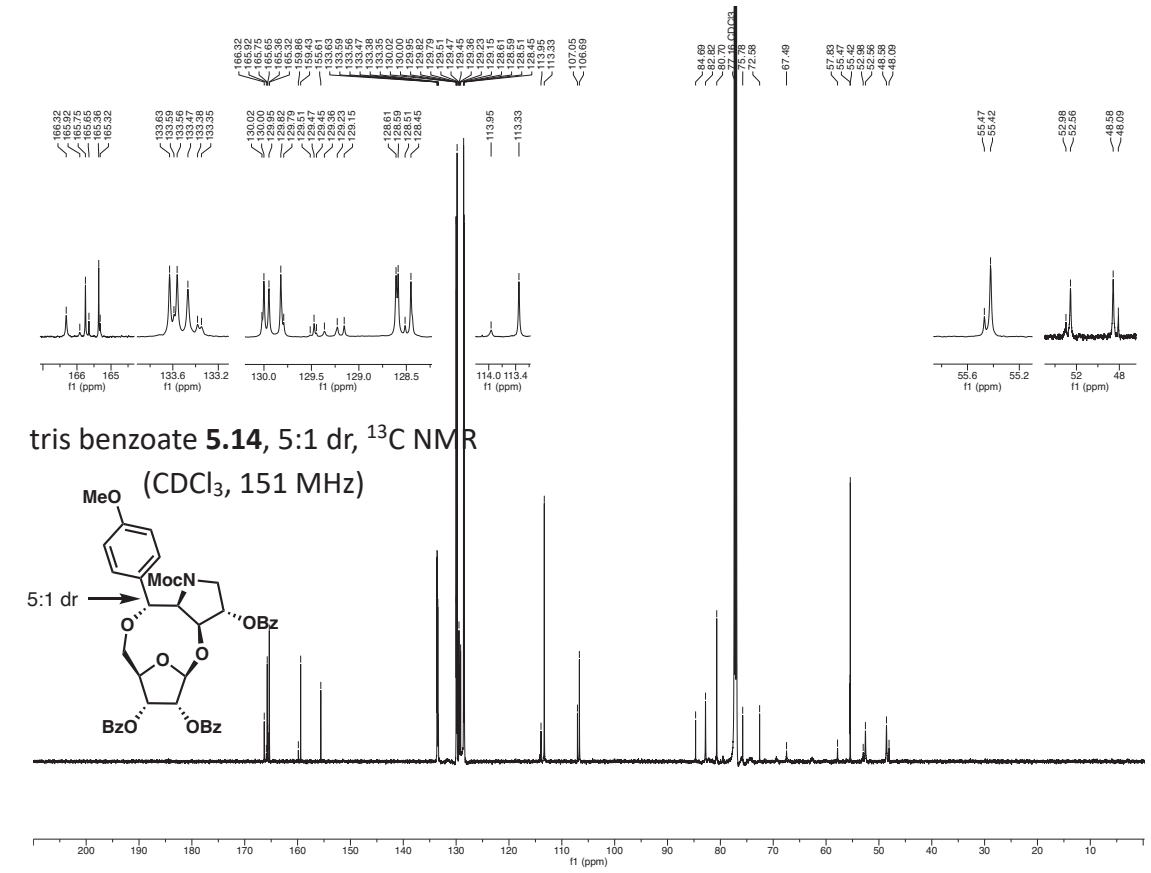



primary alcohol **5.13**, COSY
(CDCl3, 600 MHz)
MeO
MocN
OBz
HO
O
BzO
OBz
{3.81,2.10}
{3.70,2.09}
{4.46,3.09}
{3.09,2.95}
{3.30,3.09}
{5.26,3.56}
{5.26,3.86}
{4.44,3.69}
{4.44,3.80}
{3.87,3.55}
{5.58,4.45}
{5.26,4.62}
{5.65,5.56}
{7.32,6.90}
{7.23,6.90}
{7.98,7.42}
{7.91,7.73}
f2 (ppm)
f1 (ppm)

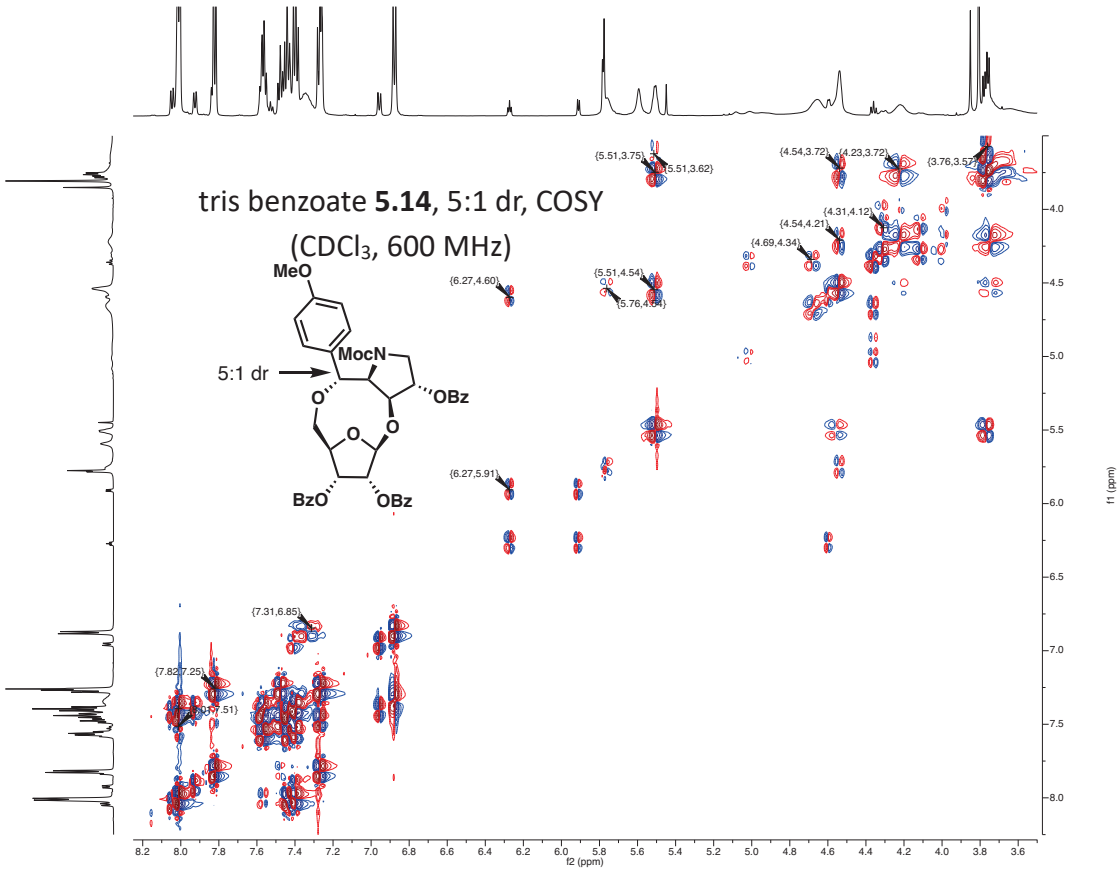

primary alcohol **5.13**, HSQC
(CDCl3, 600 MHz)
MeO
MocN
OBz
HO
O
BzO
OBz
{2.97,33.67}
{3.29,32.89}
{3.09,33.08}
{3.56,49.07}
{3.75,52.57}
{3.65,52.57}
{4.45,59.98}
{3.80,62.91}
{3.69,62.91}
{5.57,71.48}
{5.65,75.97}
{5.26,75.38}
{4.61,78.50}
{5.58,104.23}
{6.90,113.98}
{7.98,129.76}
{7.91,129.98}
{7.36,128.59}
{7.31,130.74}
{7.23,130.74}
f2 (ppm)
f1 (ppm)

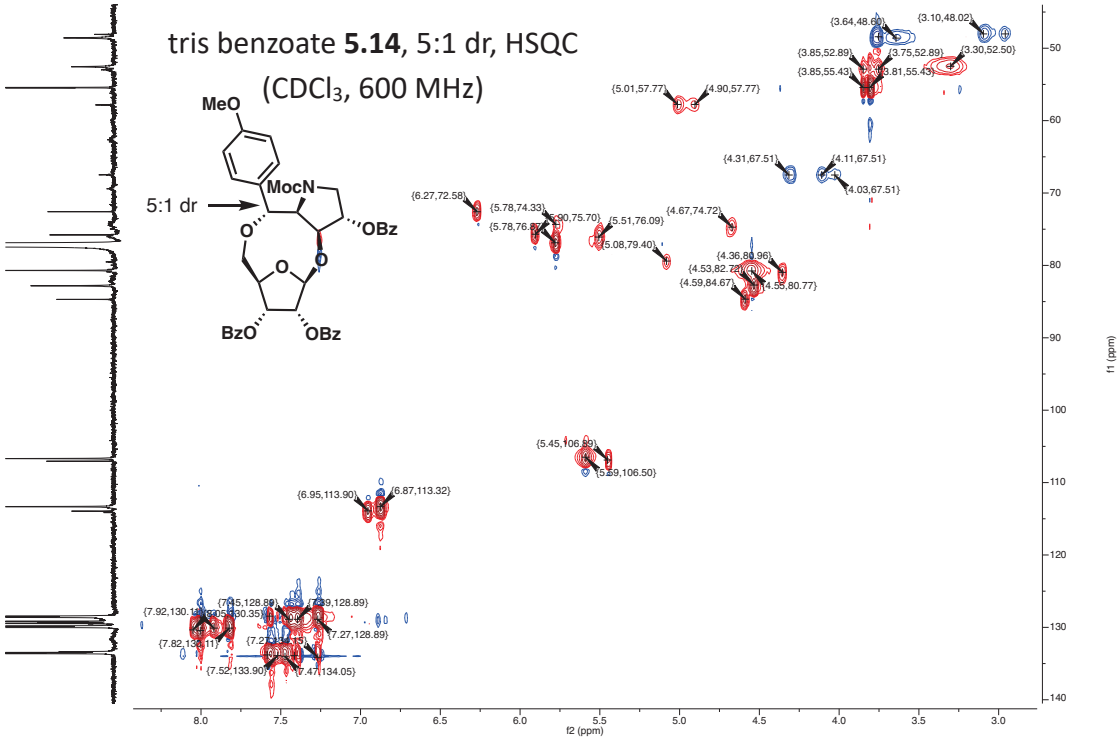


tris benzoate **5.14**, 5:1 dr, ^{1}H NMR ($CDCl_3$, 600 MHz)

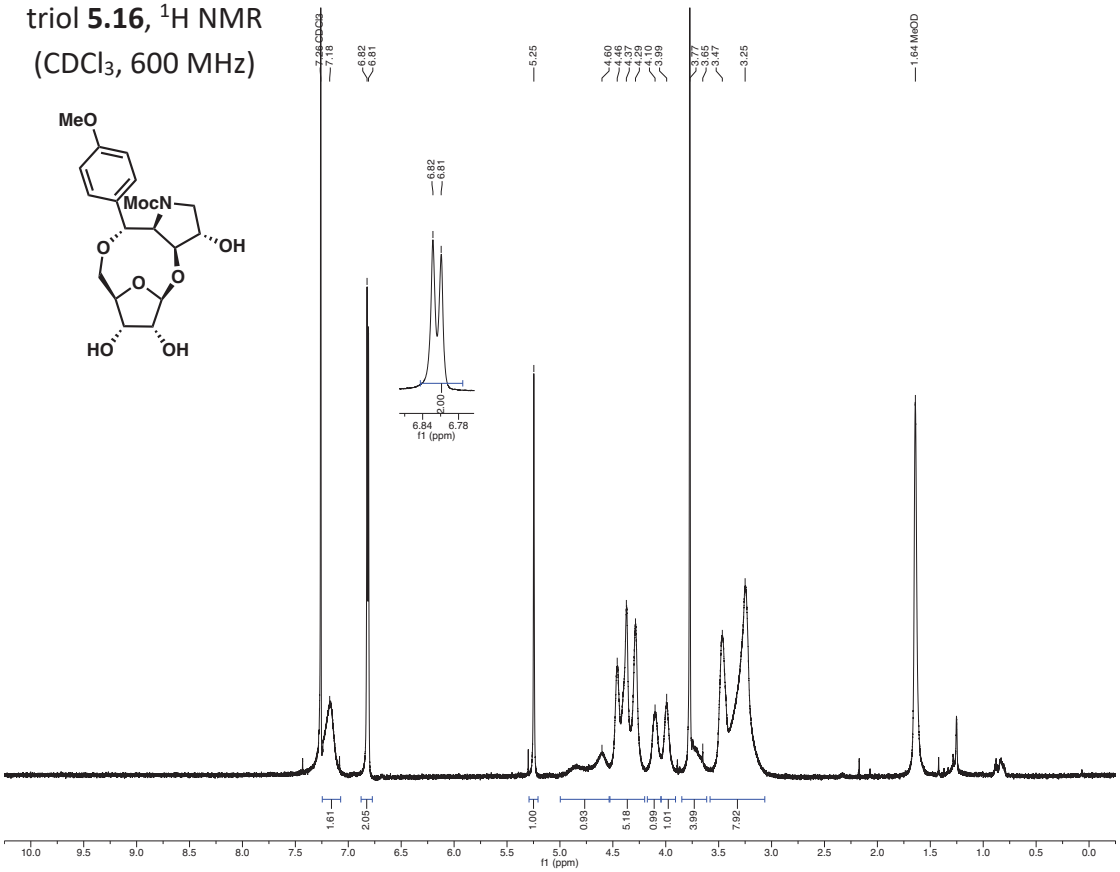


tris benzoate **5.14**, 5:1 dr, ^{13}C NMR ($CDCl_3$, 151 MHz)

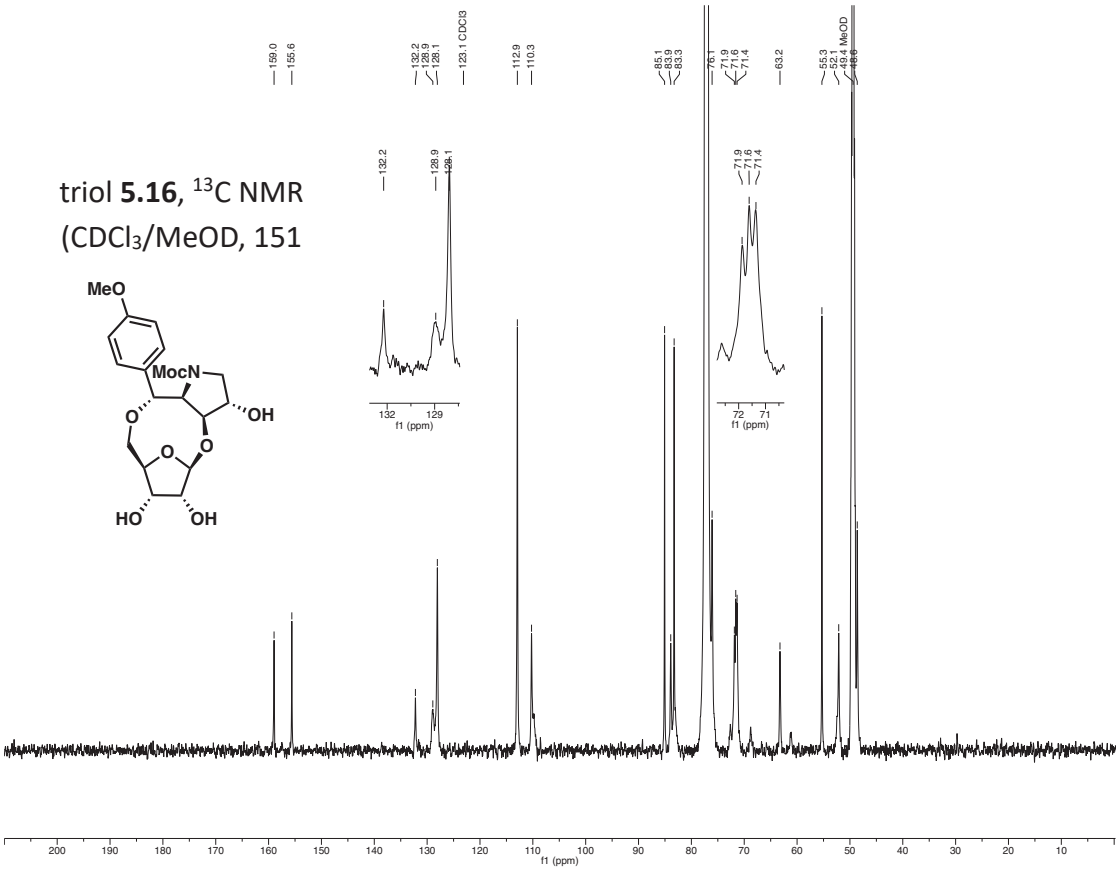

tris benzoate **5.14**, 5:1 dr, COSY
(CDCl3, 600 MHz)
MeO
MocN
5:1 dr
OBz
BzO
OBz
f2 (ppm)
f1 (ppm)

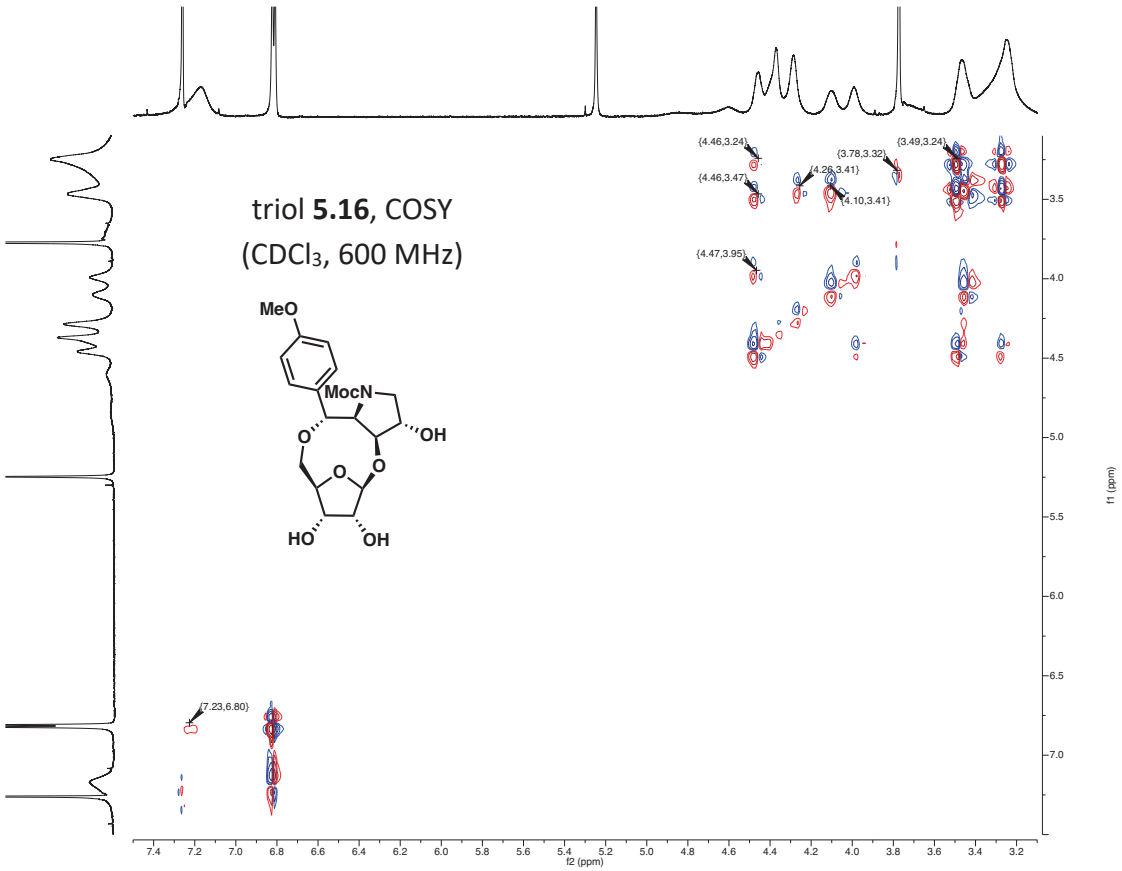

tris benzoate **5.14**, 5:1 dr, HSQC
(CDCl3, 600 MHz)
MeO
MocN
5:1 dr
OBz
BzO
OBz
f2 (ppm)
f1 (ppm)

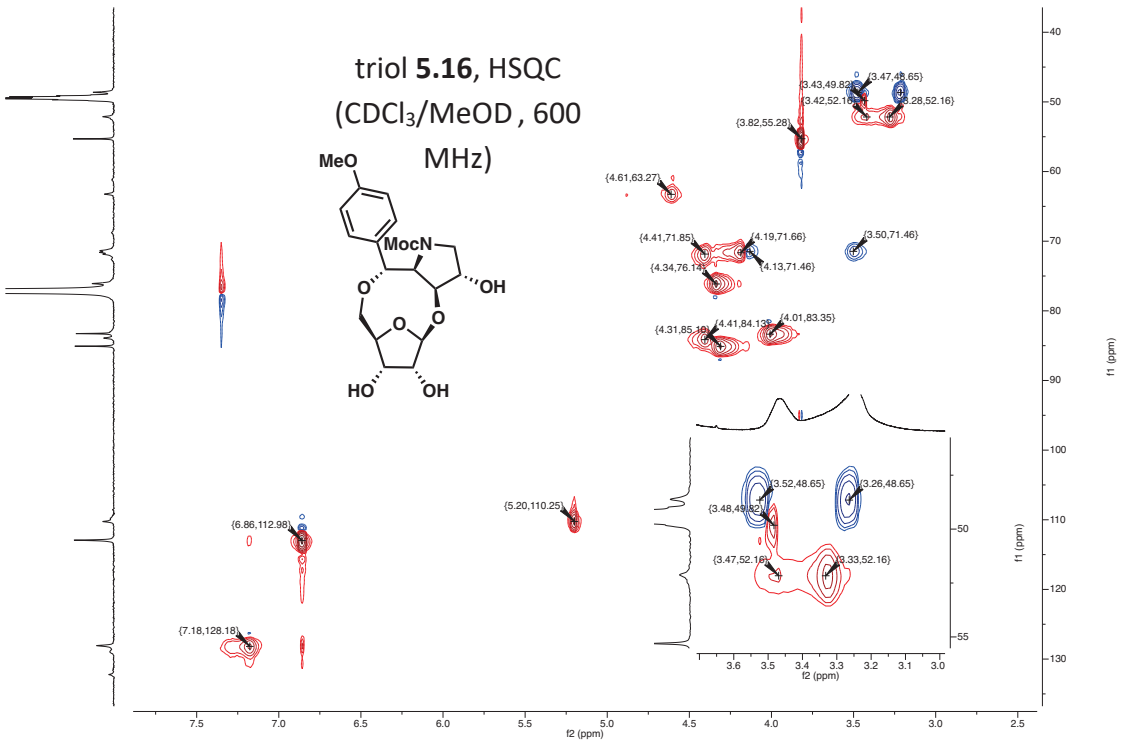
triol **5.16**, ^{1}H NMR ($CDCl_3$, 600 MHz)



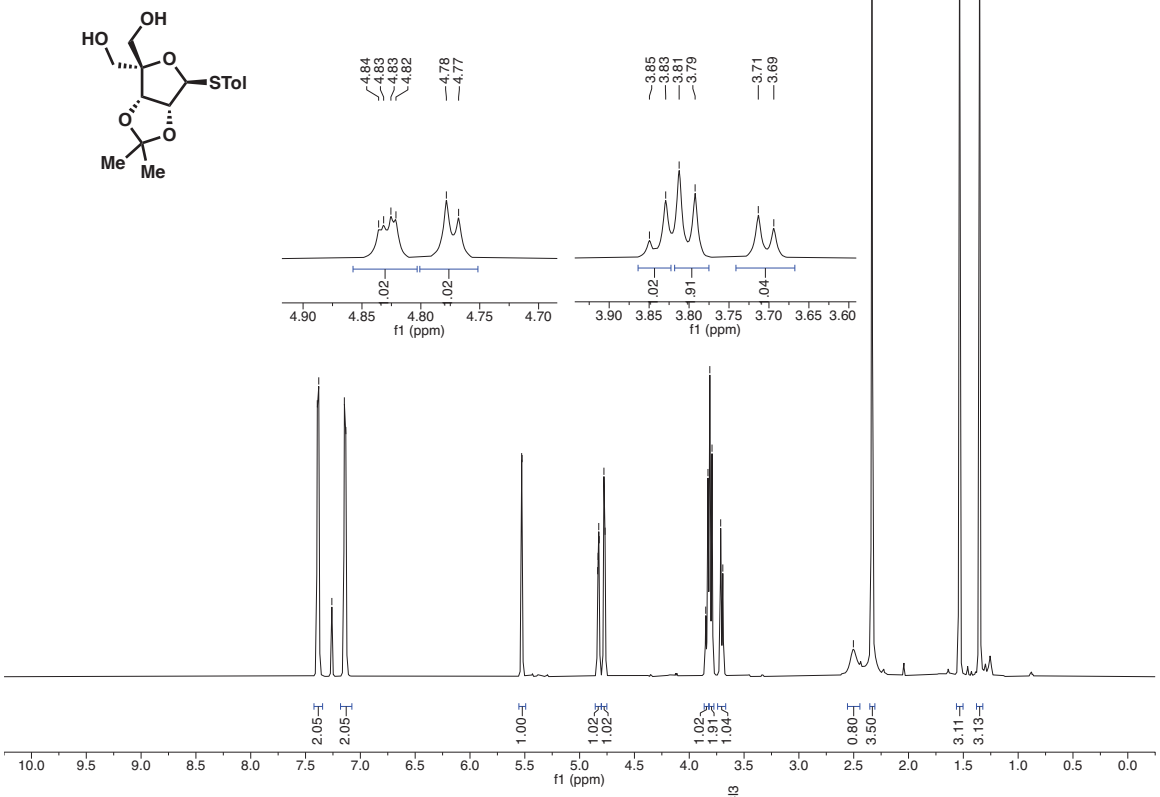
triol **5.16**, ^{13}C NMR ($CDCl_3$/MeOD, 151



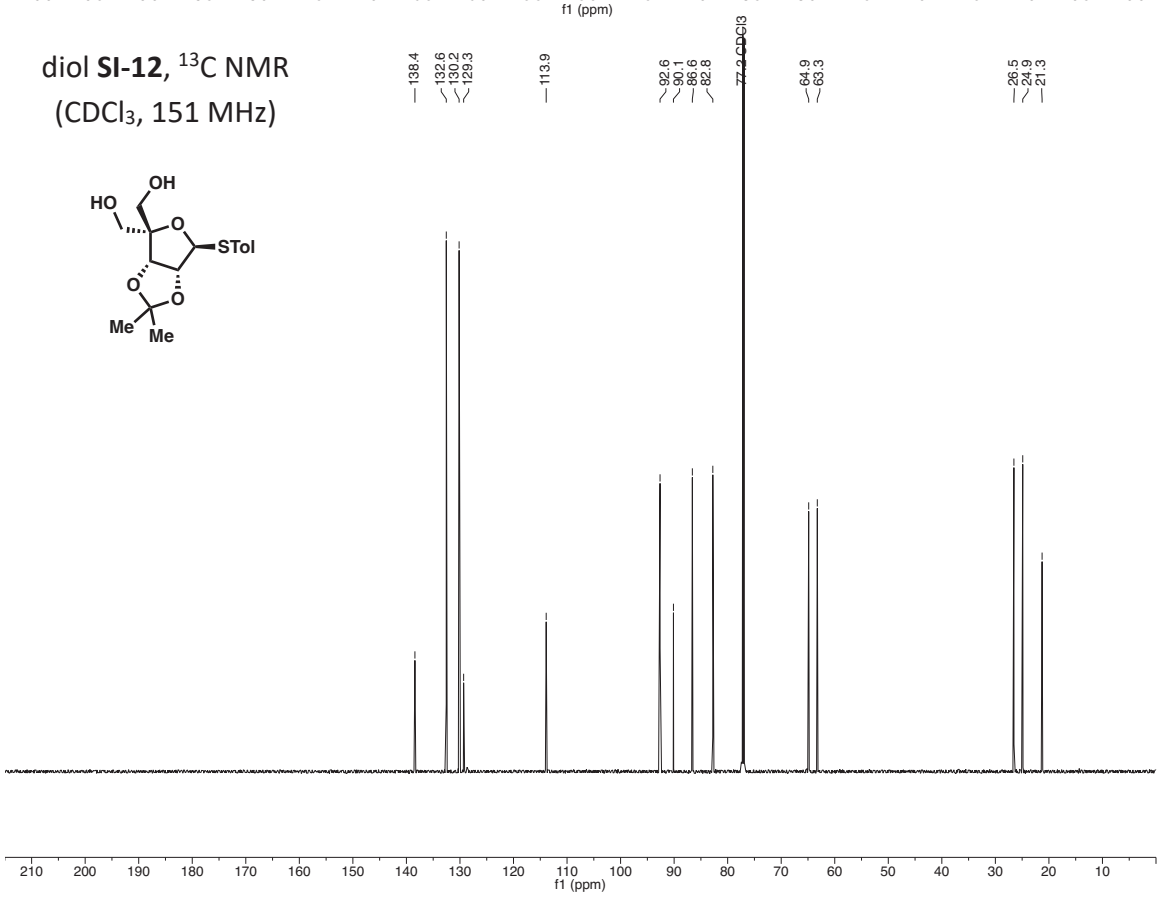

triol **5.16**, COSY
(CDCl3, 600 MHz)
MeO
MocN
OH
HO
OH
{4.46,3.24}
{4.46,3.47}
{3.78,3.32}
{4.26,3.41}
{4.10,3.41}
{3.49,3.24}
{4.47,3.95}
{7.23,6.80}
f2 (ppm)
f1 (ppm)


triol **5.16**, HSQC
(CDCl3/MeOD , 600
MHz)
MeO
MocN
OH
HO
OH
{3.43,49.82}
{3.47,48.65}
{3.42,52.16}
{3.28,52.16}
{3.82,55.28}
{4.61,63.27}
{4.41,71.85}
{4.19,71.66}
{3.50,71.46}
{4.34,76.14}
{4.13,71.46}
{4.31,85.16}
{4.41,84.13}
{4.01,83.35}
{5.20,110.25}
{6.86,112.98}
{7.18,128.18}
{3.52,48.65}
{3.26,48.65}
{3.48,49.82}
{3.47,52.16}
{3.33,52.16}
f2 (ppm)
f1 (ppm)

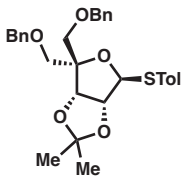
diol **SI-12**, ^{1}H NMR ($CDCl_3$, 600 MHz)



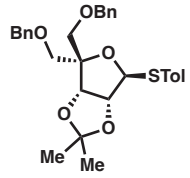
diol **SI-12**, ^{13}C NMR ($CDCl_3$, 151 MHz)

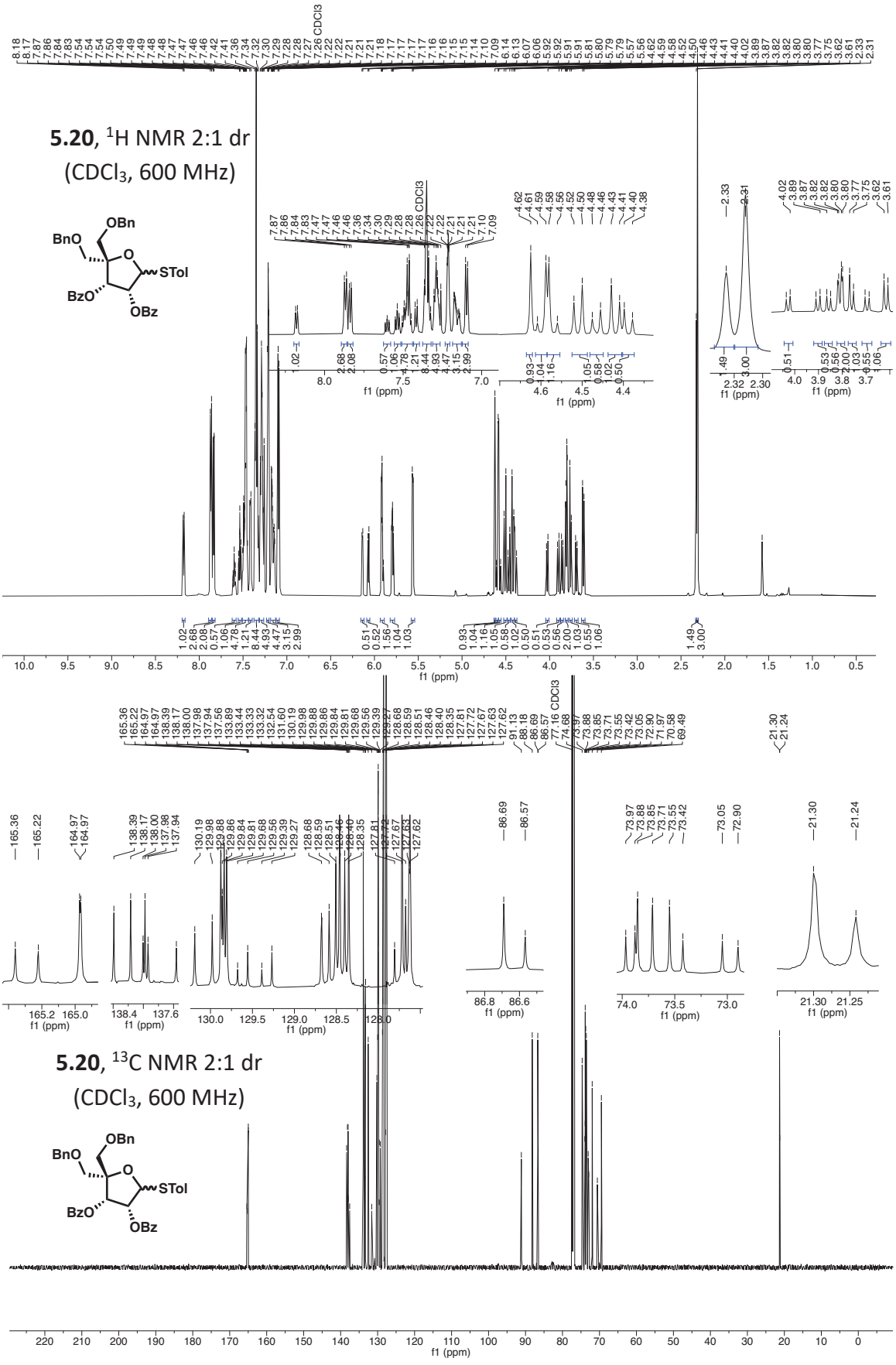


SI-13, ^{1}H NMR
($CDCl_3$, 600 MHz)

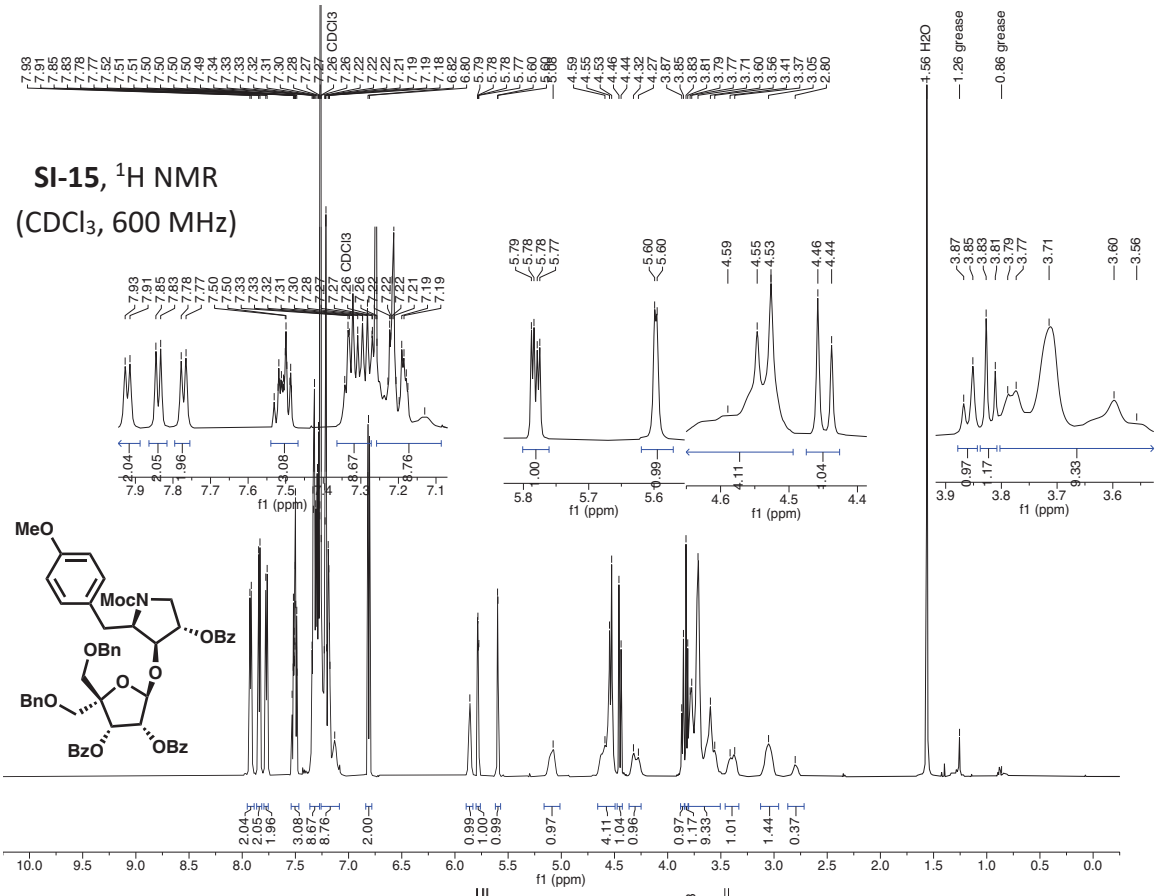


SI-13, ^{13}C NMR
($CDCl_3$, 151 MHz)

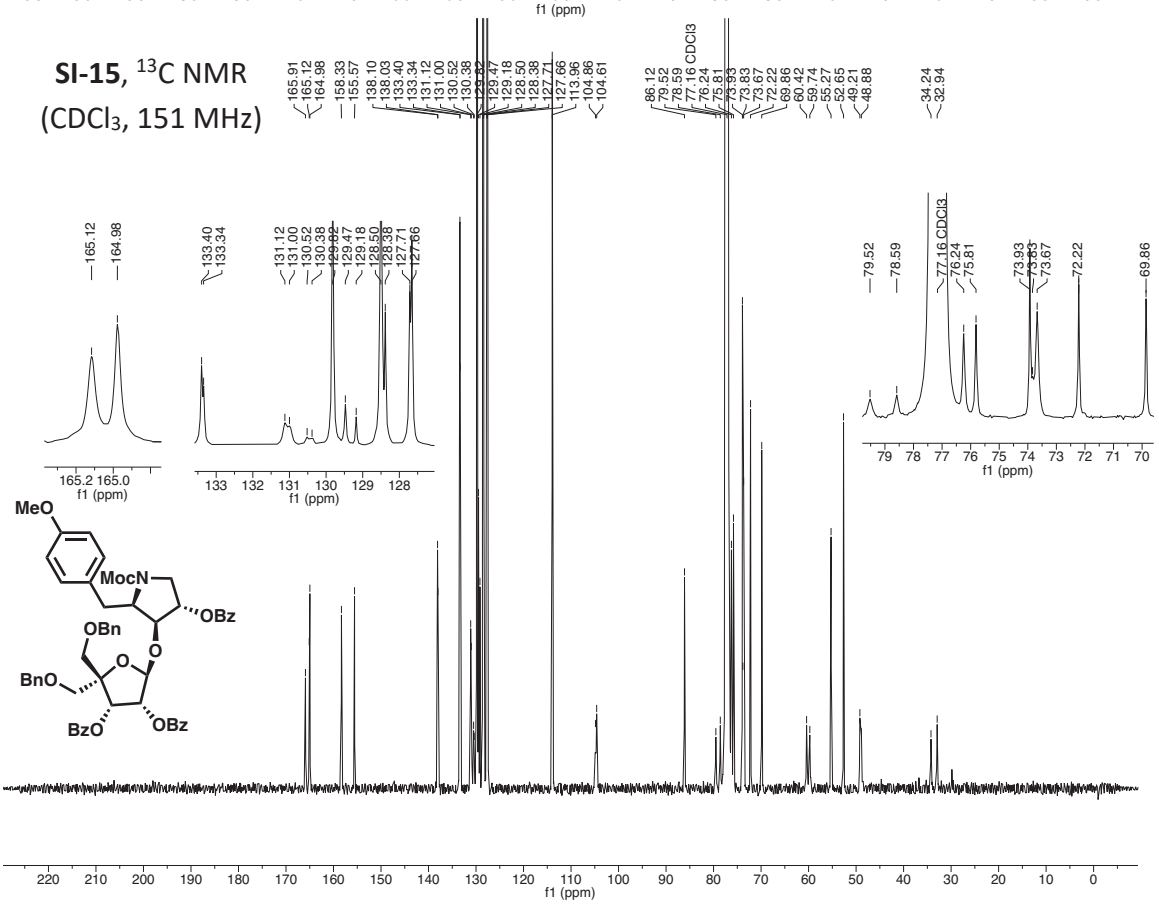


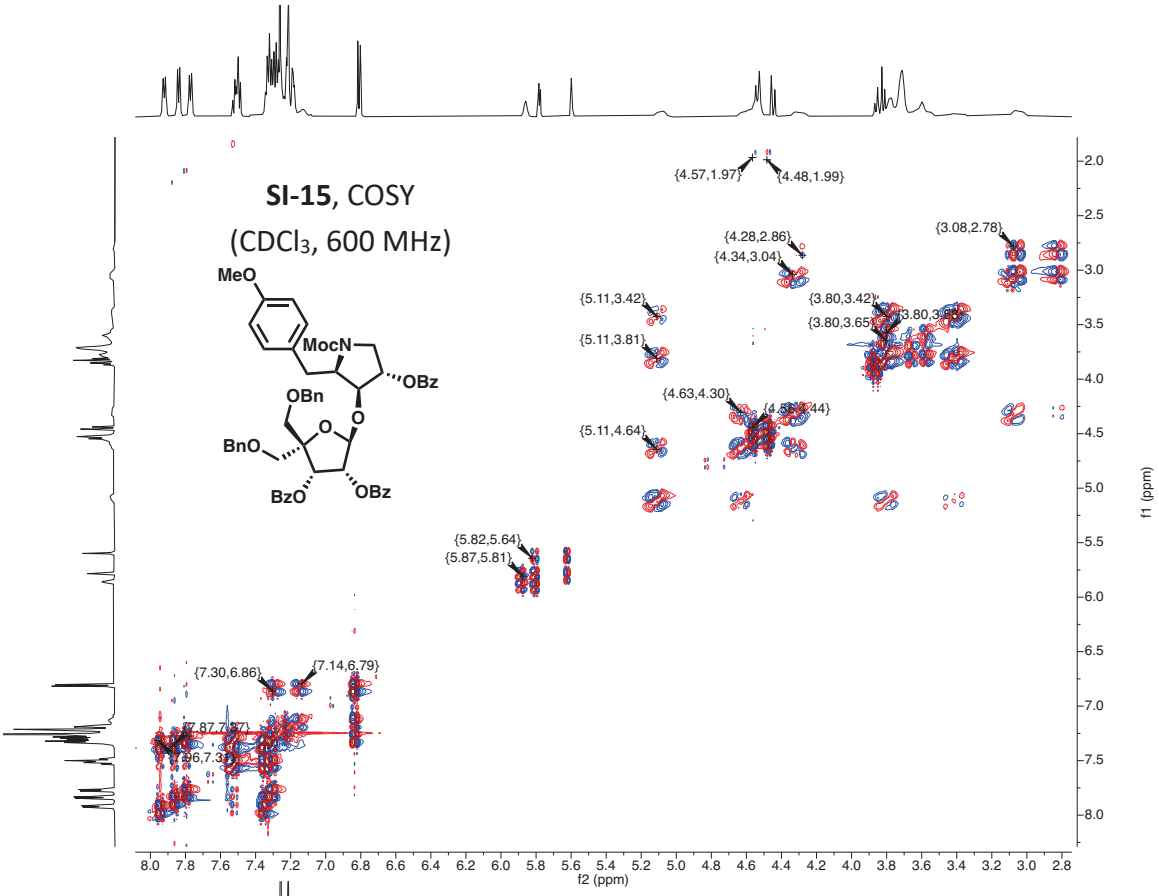

5.20, 1H NMR 2:1 dr
(CDCl3, 600 MHz)
OBn
BnO
STol
BzO
OBz
5.20, 13C NMR 2:1 dr
(CDCl3, 600 MHz)
OBn
BnO
STol
BzO
OBz

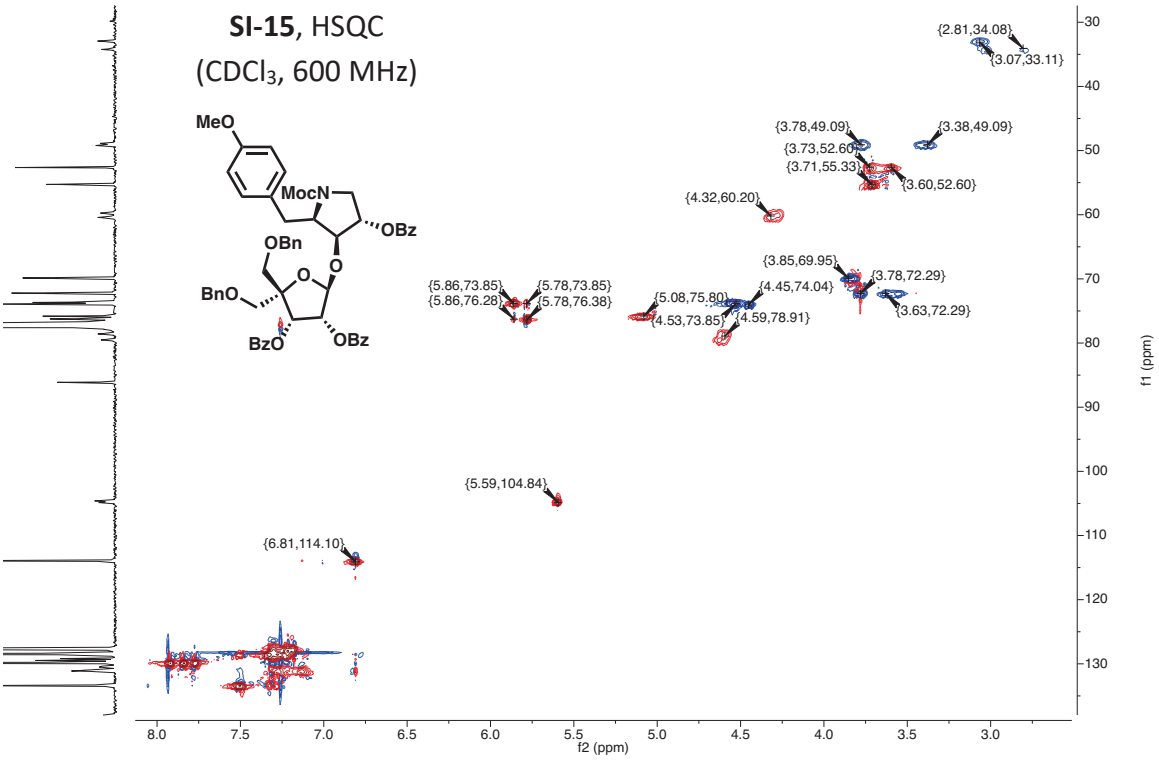
SI-15, ^{1}H NMR
($CDCl_3$, 600 MHz)

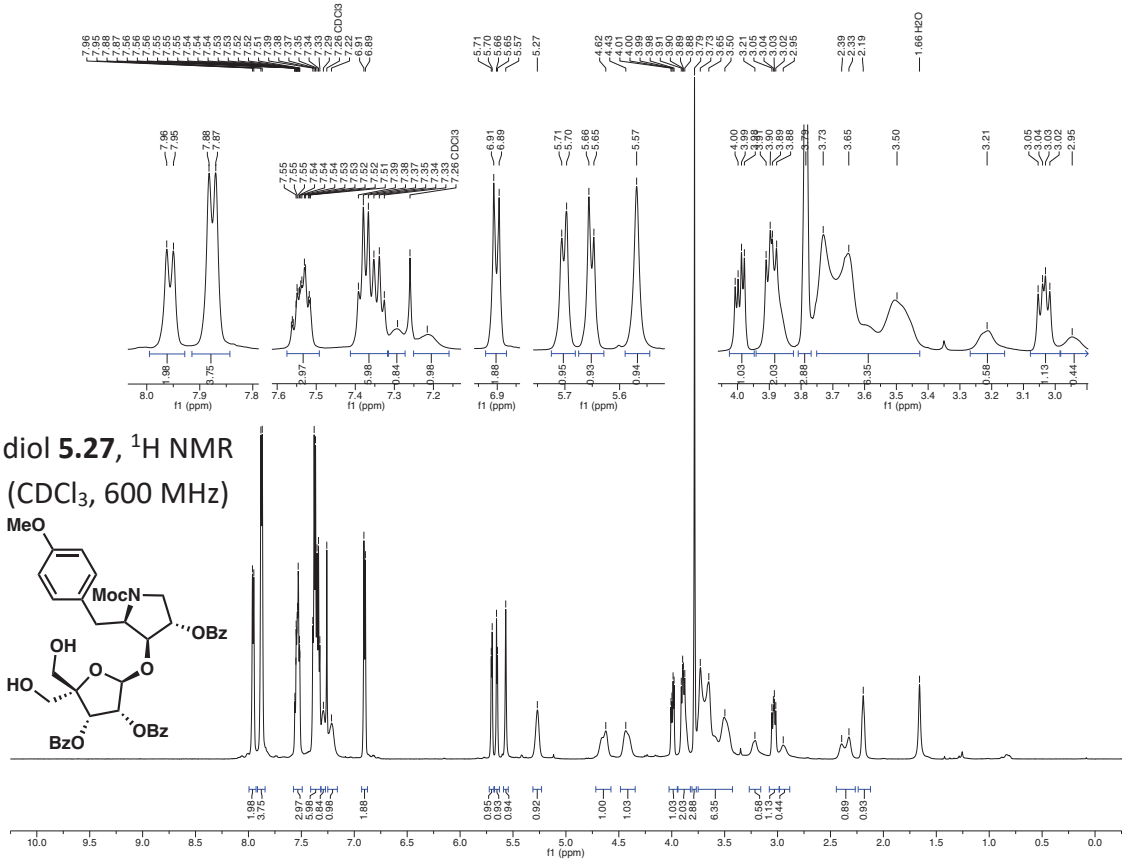


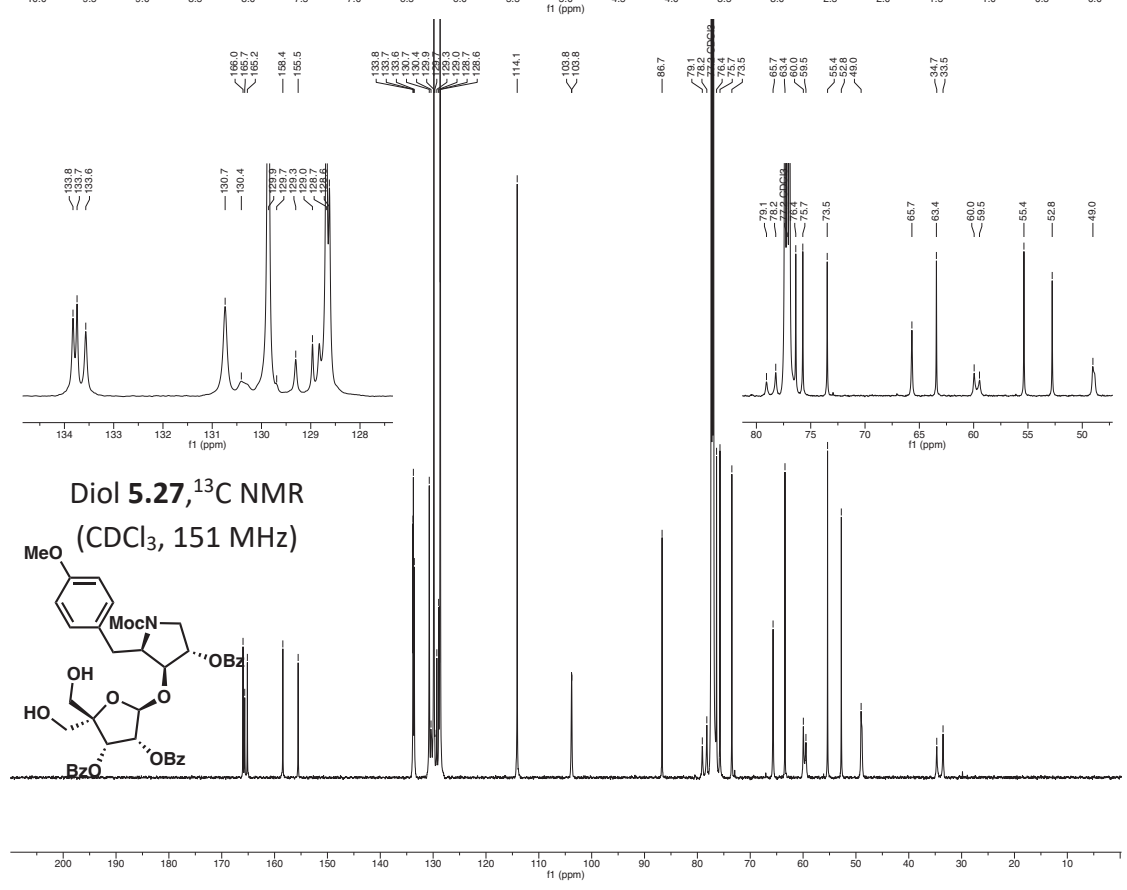
SI-15, ^{13}C NMR
($CDCl_3$, 151 MHz)

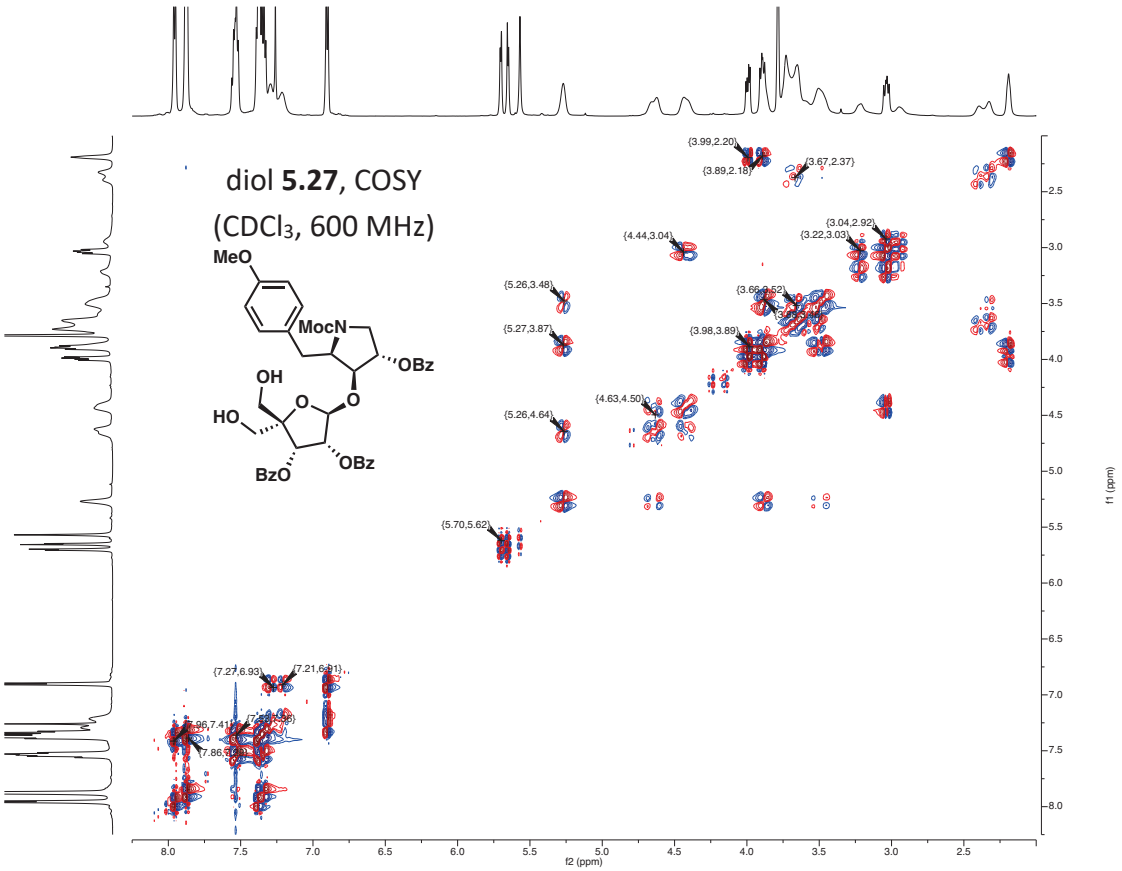


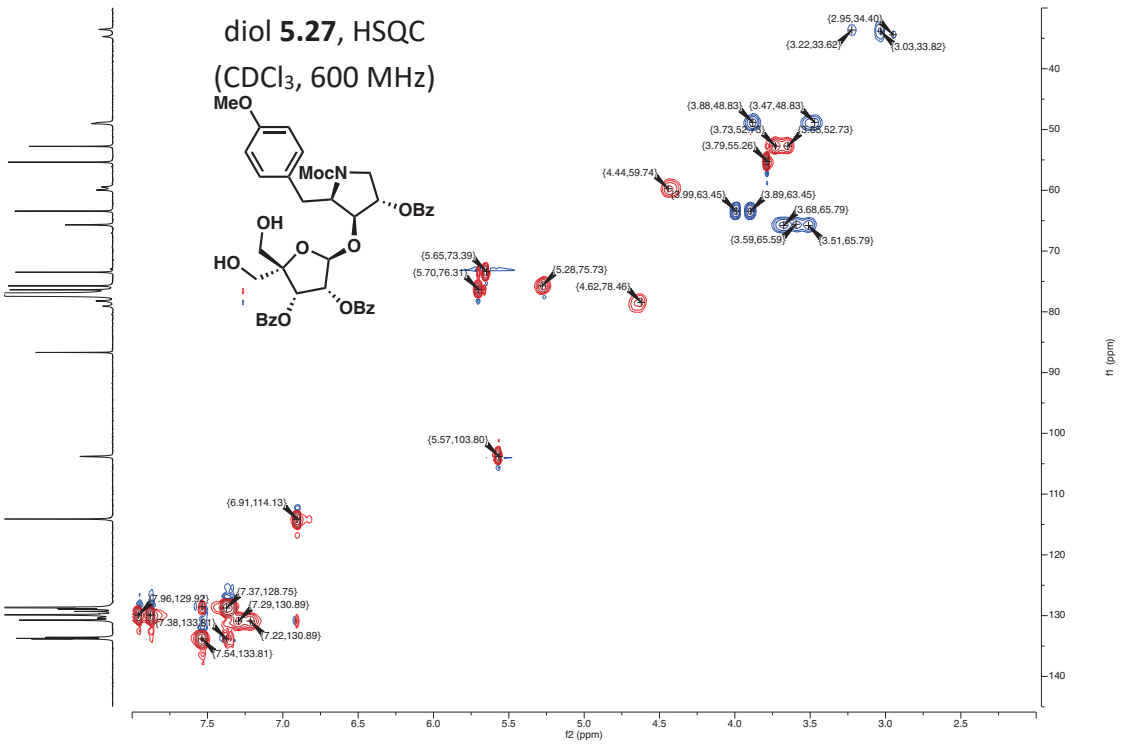

SI-15, COSY
(CDCl3, 600 MHz)
MeO
MocN
OBz
OBn
BnO
BzO
OBz
{4.57,1.97}
{4.48,1.99}
{4.28,2.86}
{4.34,3.04}
{3.08,2.78}
{5.11,3.42}
{3.80,3.42}
{3.80,3.65}
{5.11,3.81}
{4.63,4.30}
{5.11,4.64}
{5.82,5.64}
{5.87,5.81}
{7.30,6.86}
{7.14,6.79}
f2 (ppm)
f1 (ppm)

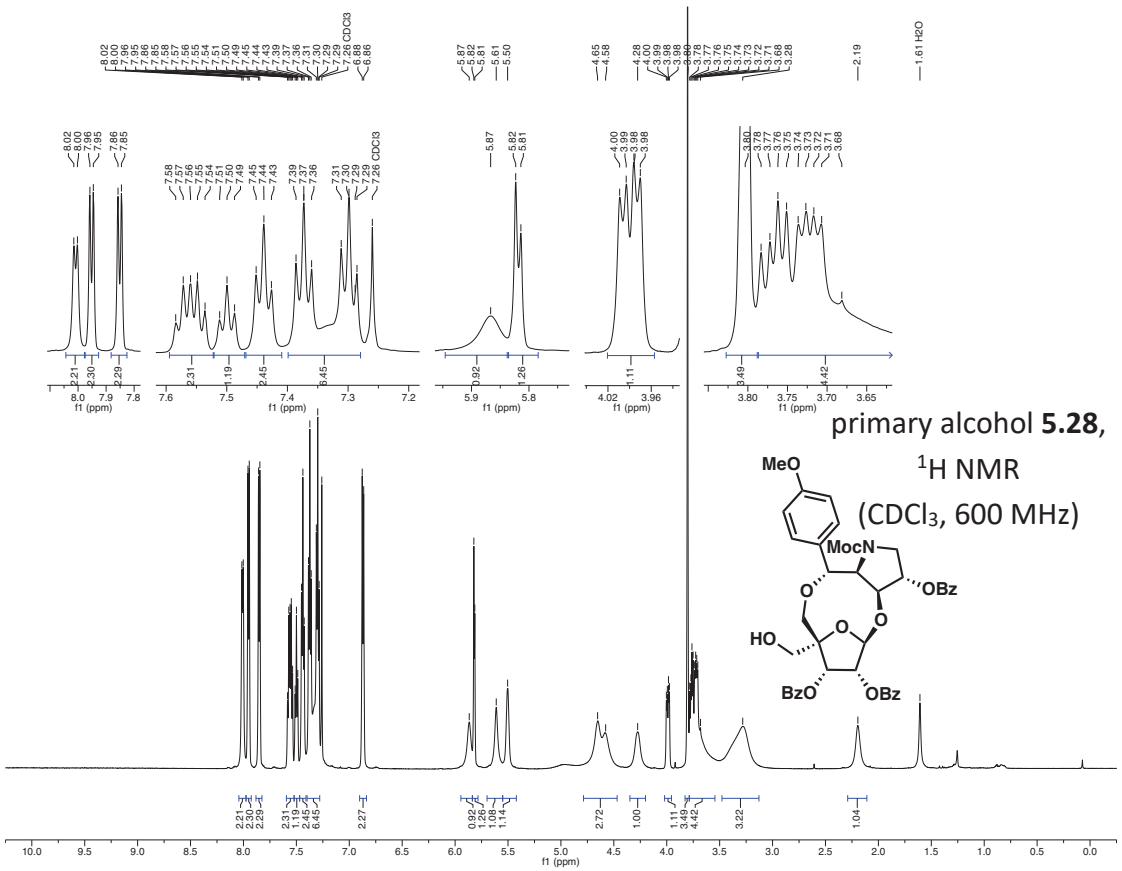

SI-15, HSQC
(CDCl3, 600 MHz)
MeO
MocN
OBz
OBn
BnO
BzO
OBz
{2.81,34.08}
{3.07,33.11}
{3.78,49.09}
{3.38,49.09}
{3.73,52.60}
{3.71,55.33}
{3.60,52.60}
{4.32,60.20}
{3.85,69.95}
{3.78,72.29}
{5.86,73.85}
{5.78,73.85}
{5.86,76.28}
{5.78,76.38}
{5.08,75.80}
{4.45,74.04}
{3.63,72.29}
{4.53,73.85}
{4.59,78.91}
{5.59,104.84}
{6.81,114.10}
f2 (ppm)
f1 (ppm)

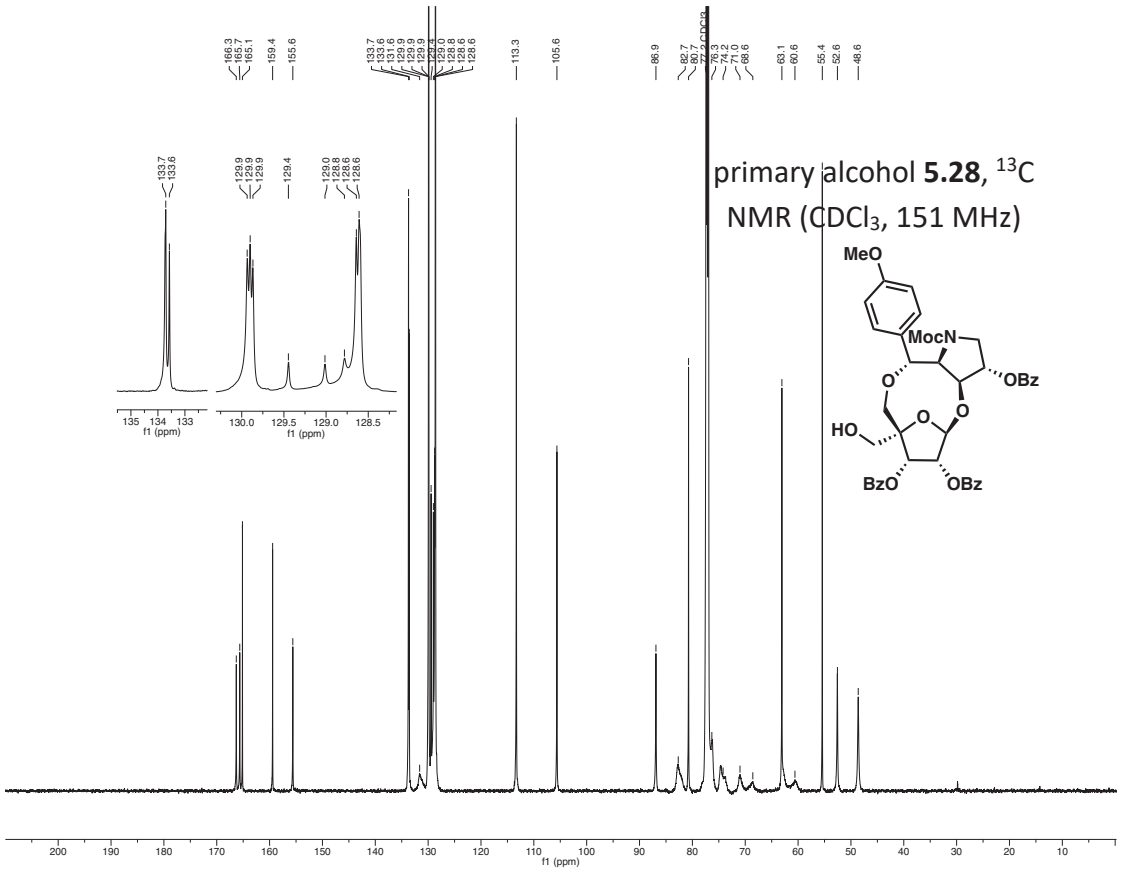

diol **5.27**, ^{1}H NMR
($CDCl_3$, 600 MHz)
MeO
MocN
OBz
OH
HO
O
O
BzO
OBz

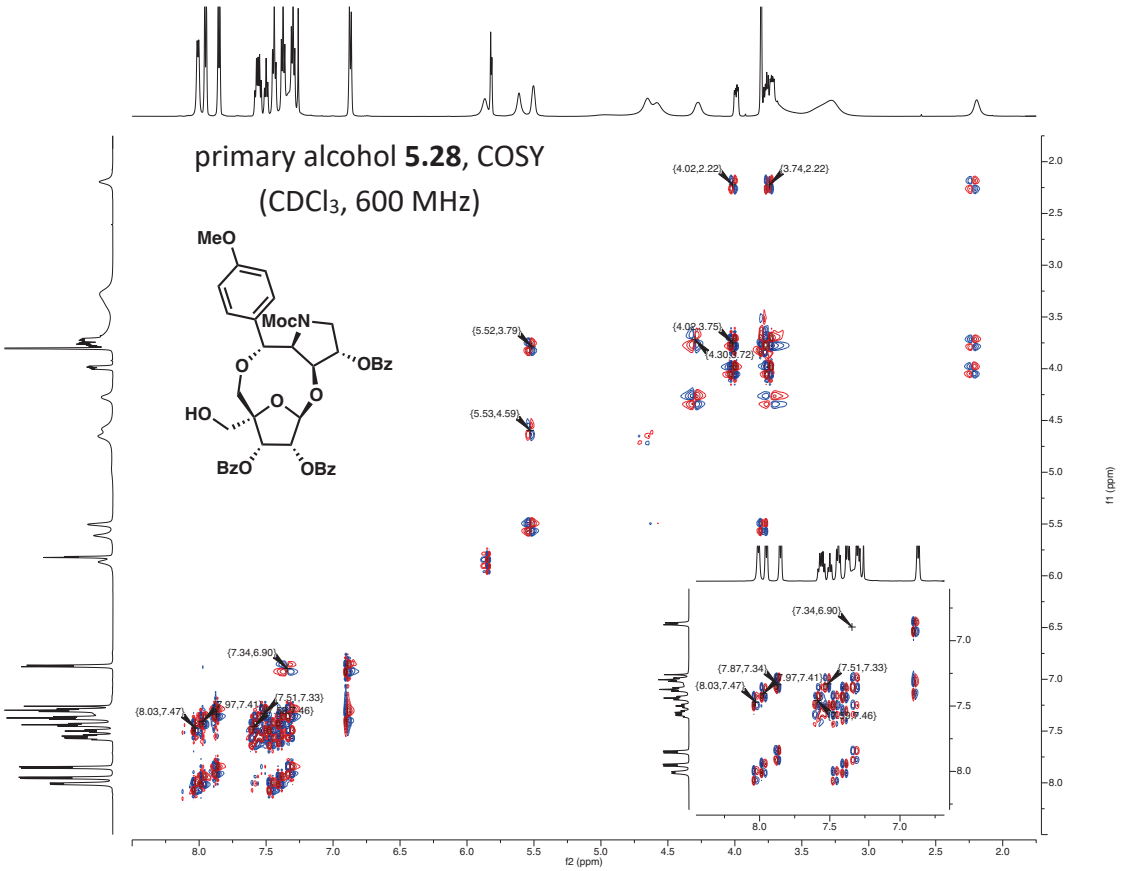

Diol **5.27**,^{13}C NMR
($CDCl_3$, 151 MHz)
MeO
MocN
OBz
OH
HO
O
O
BzO
OBz

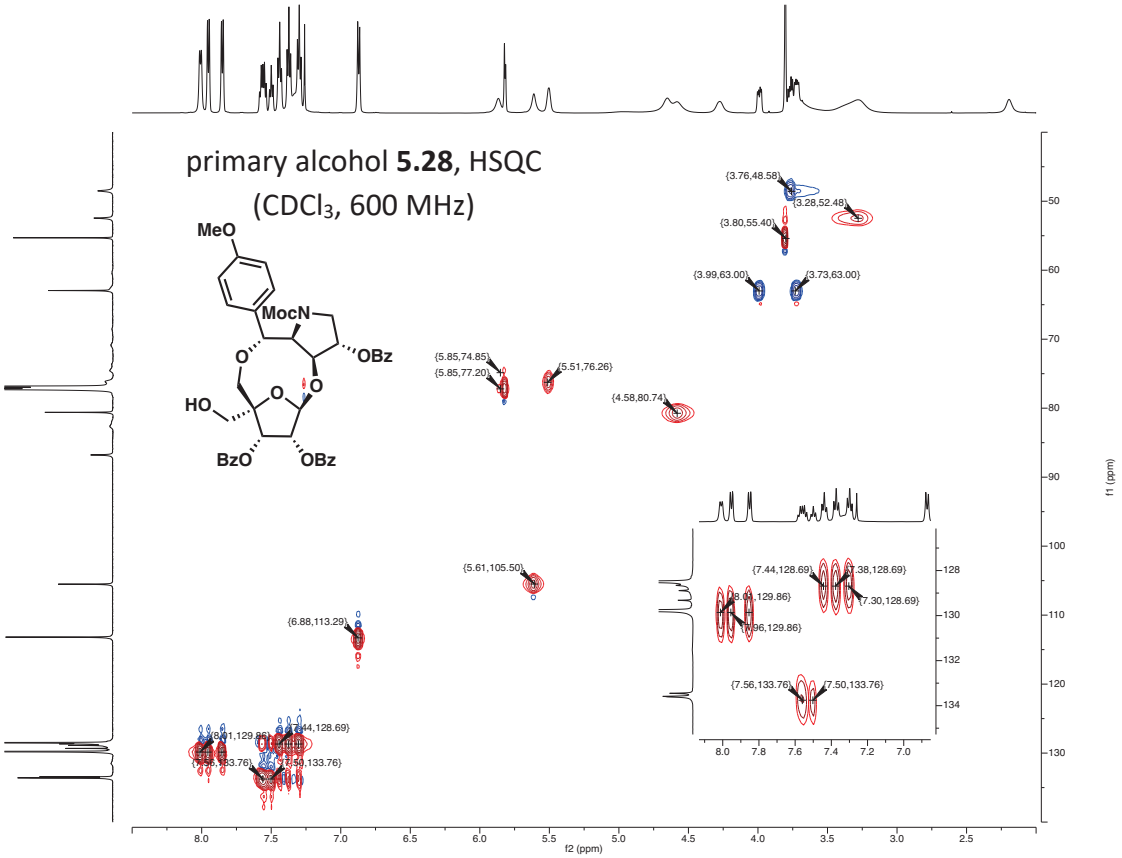

diol **5.27**, COSY
(CDCl3, 600 MHz)
MeO
MocN
OBz
OH
HO
O
BzO
OBz
f2 (ppm)
f1 (ppm)

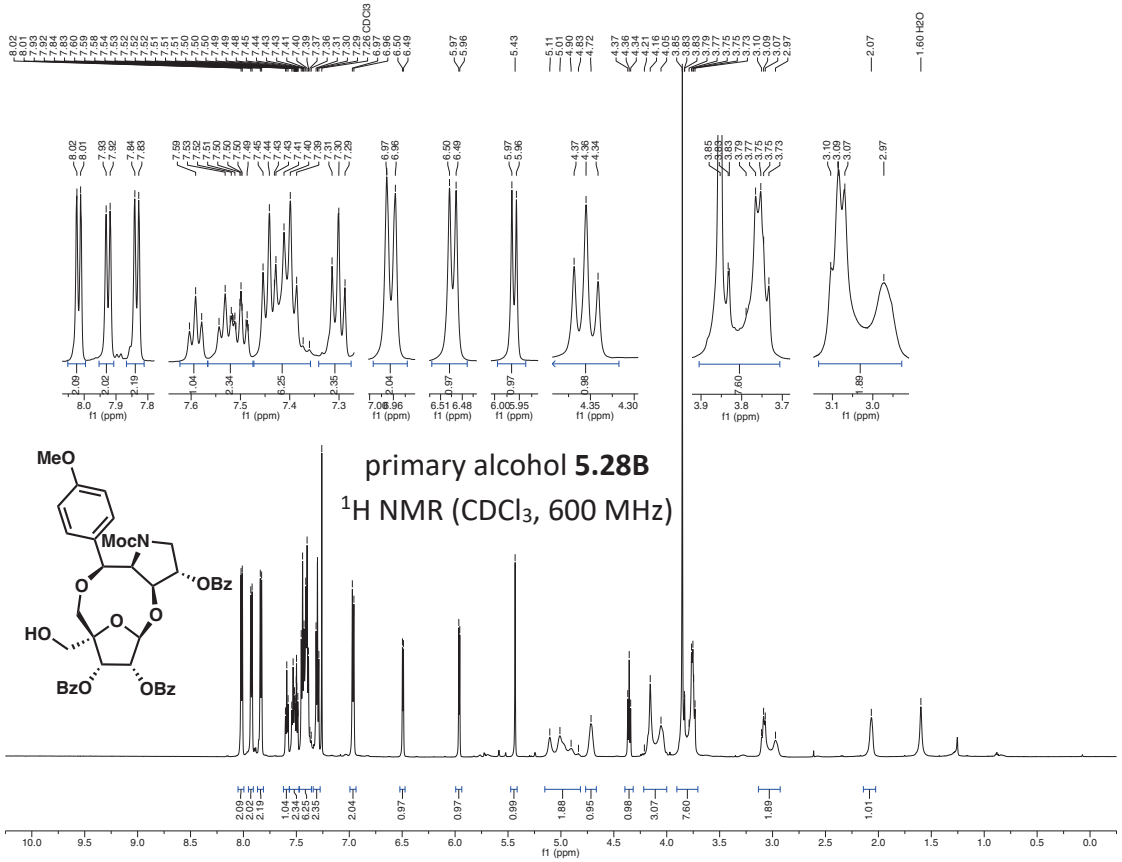

diol **5.27**, HSQC
(CDCl3, 600 MHz)
MeO
MocN
OBz
OH
HO
O
BzO
OBz
f2 (ppm)
f1 (ppm)

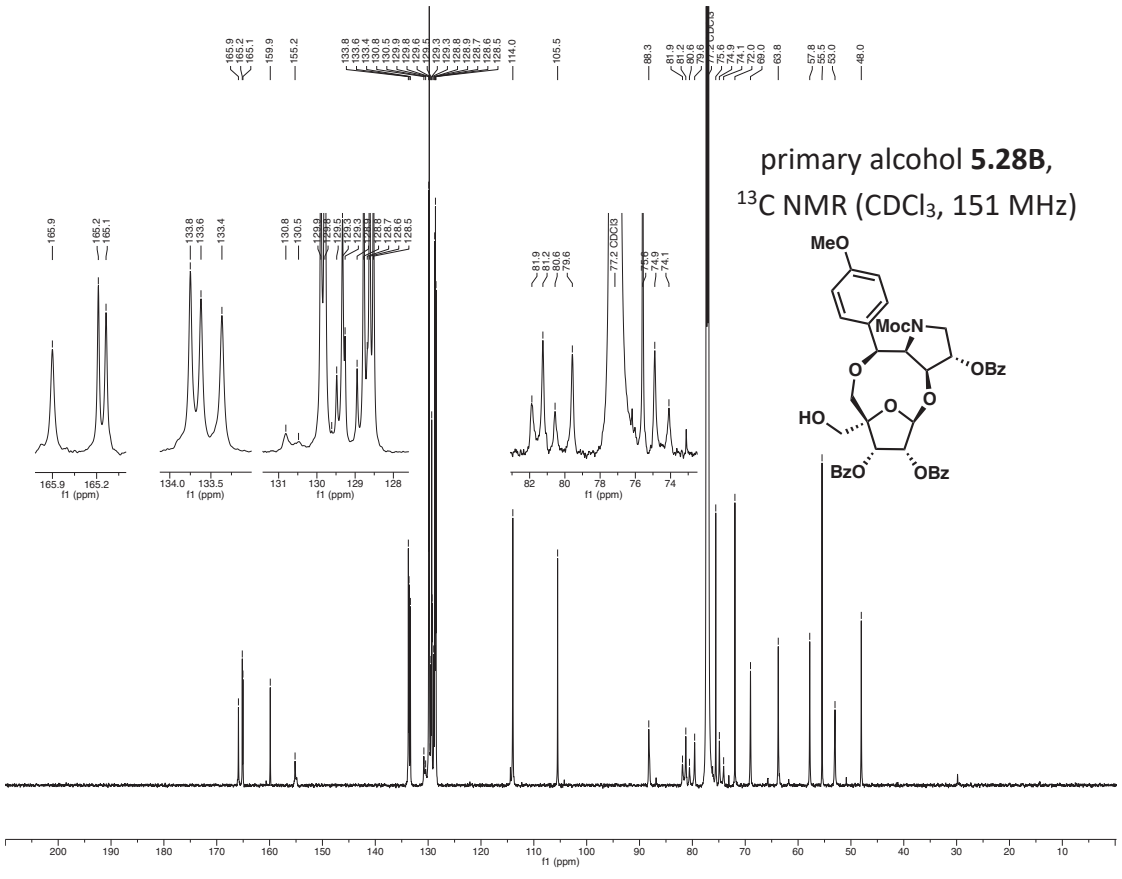

primary alcohol **5.28**, ^{1}H NMR (CDCl$_3$, 600 MHz)
MeO
MocN
OBz
HO
BzO
OBz
f1 (ppm)

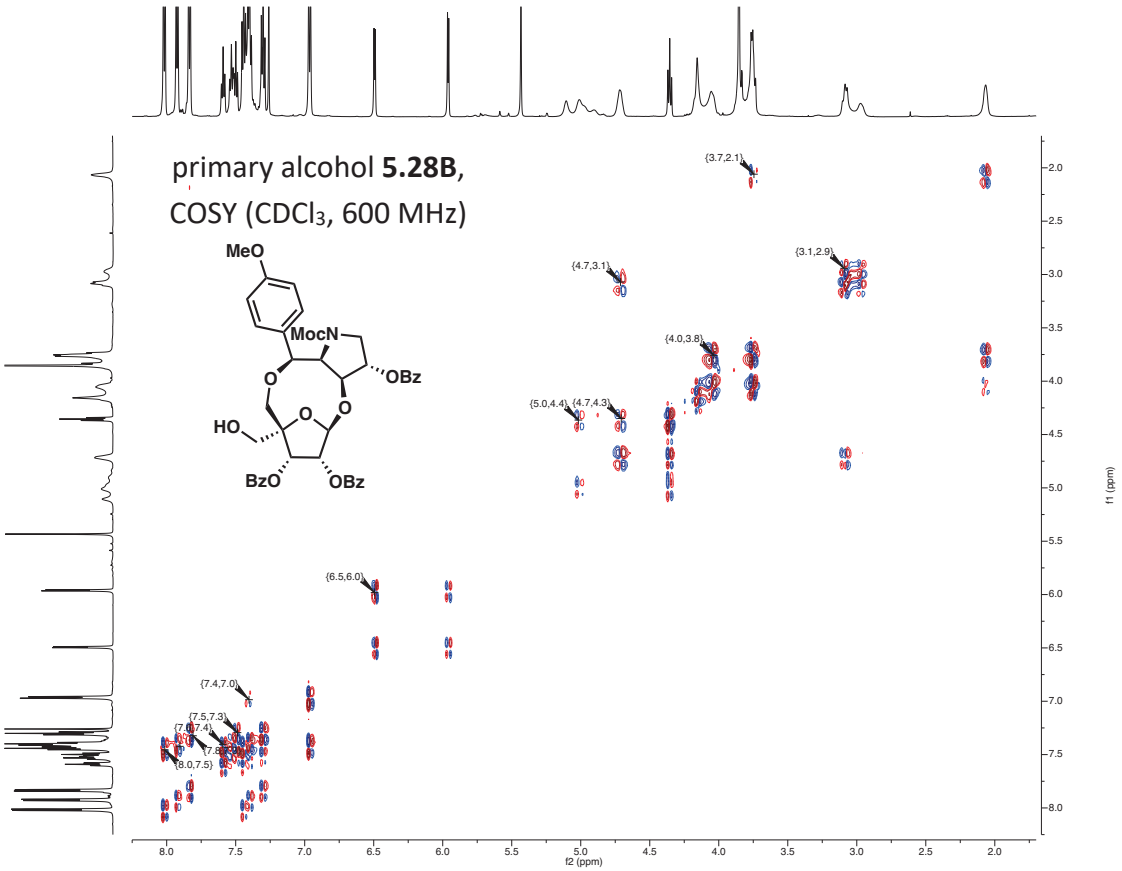

primary alcohol **5.28**, ^{13}C NMR (CDCl$_3$, 151 MHz)
MeO
MocN
OBz
HO
BzO
OBz
f1 (ppm)

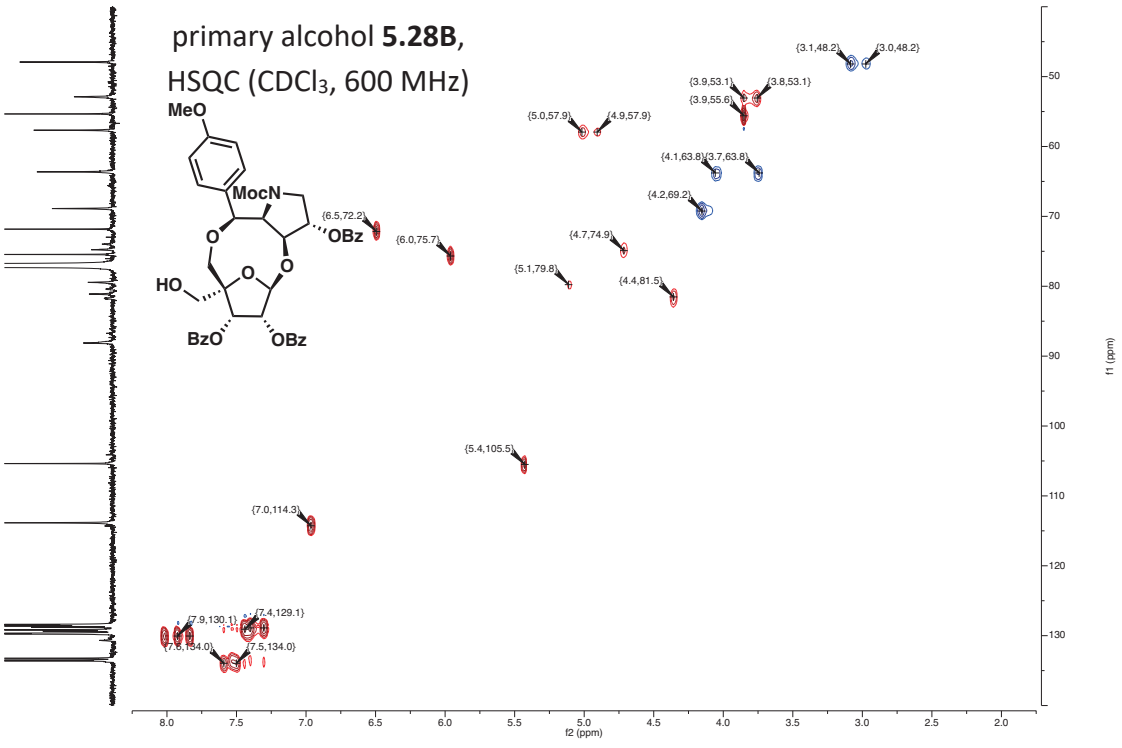

primary alcohol **5.28**, COSY
(CDCl3, 600 MHz)
MeO
MocN
OBz
HO
BzO
OBz
f2 (ppm)
f1 (ppm)

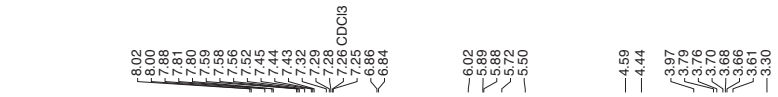

primary alcohol **5.28**, HSQC
(CDCl3, 600 MHz)
MeO
MocN
OBz
HO
BzO
OBz
f2 (ppm)
f1 (ppm)


primary alcohol **5.28B**
^{1}H NMR ($CDCl_3$, 600 MHz)
MeO
MocN
OBz
HO
BzO
OBz

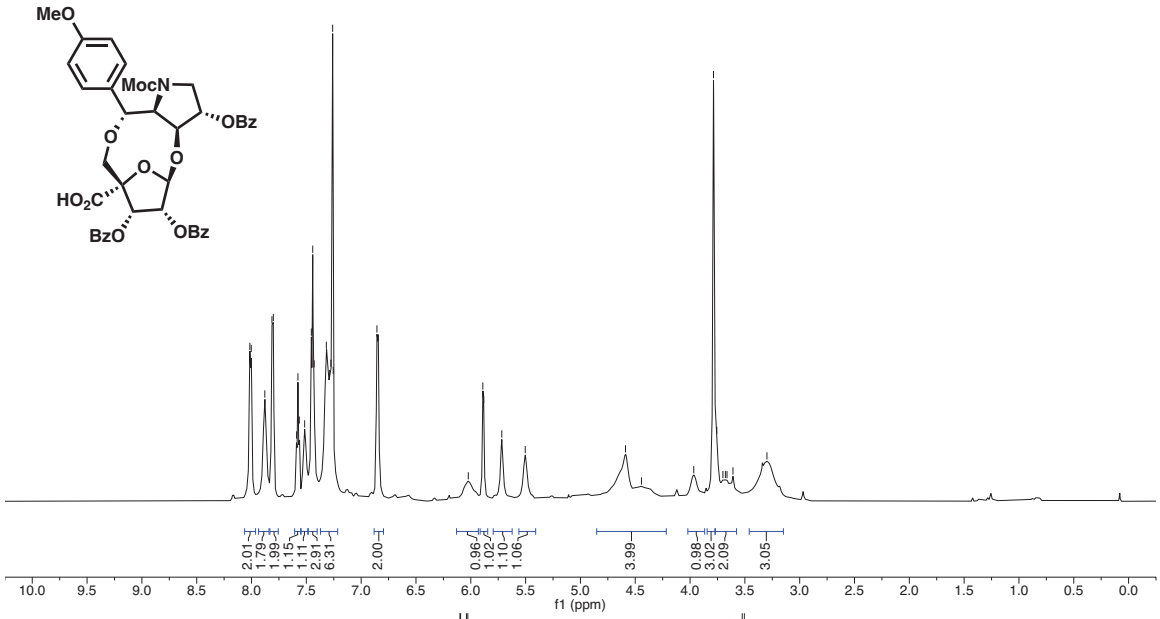

primary alcohol **5.28B**,
^{13}C NMR ($CDCl_3$, 151 MHz)
MeO
MocN
OBz
HO
BzO
OBz


primary alcohol **5.28B**,
COSY ($CDCl_3$, 600 MHz)
MeO
MocN
OBz
HO
BzO
OBz
f2 (ppm)
f1 (ppm)

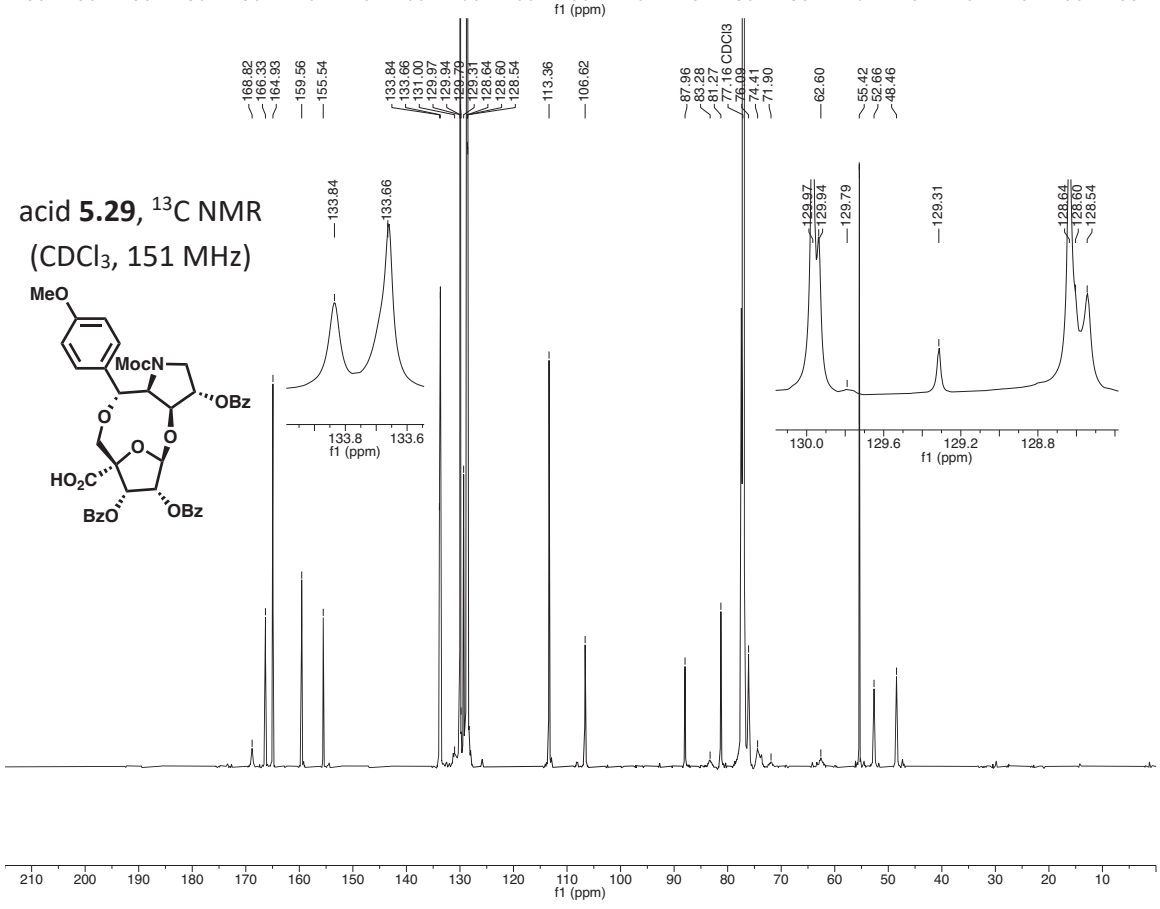

primary alcohol **5.28B**,
HSQC ($CDCl_3$, 600 MHz)
MeO
MocN
OBz
HO
BzO
OBz
f2 (ppm)
f1 (ppm)

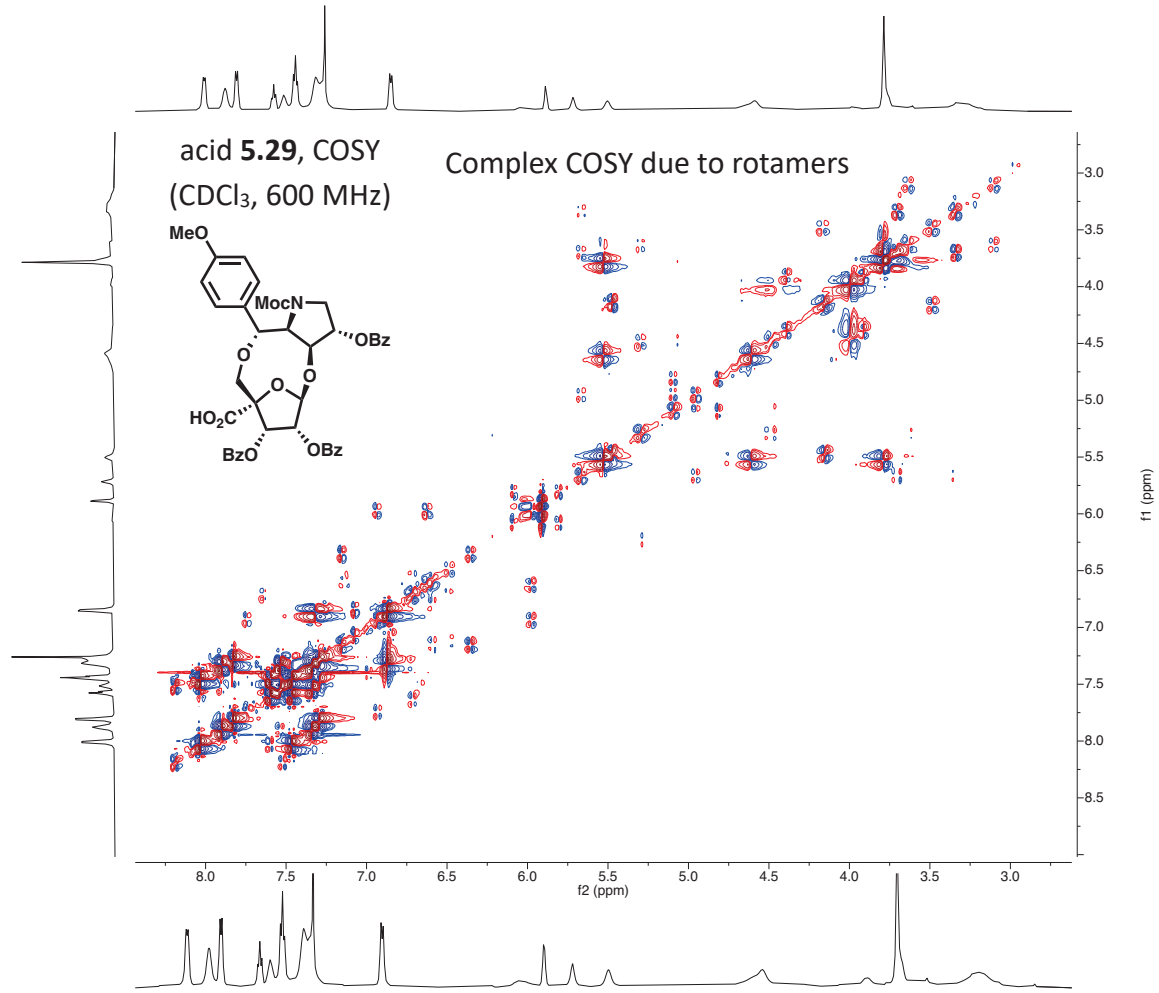


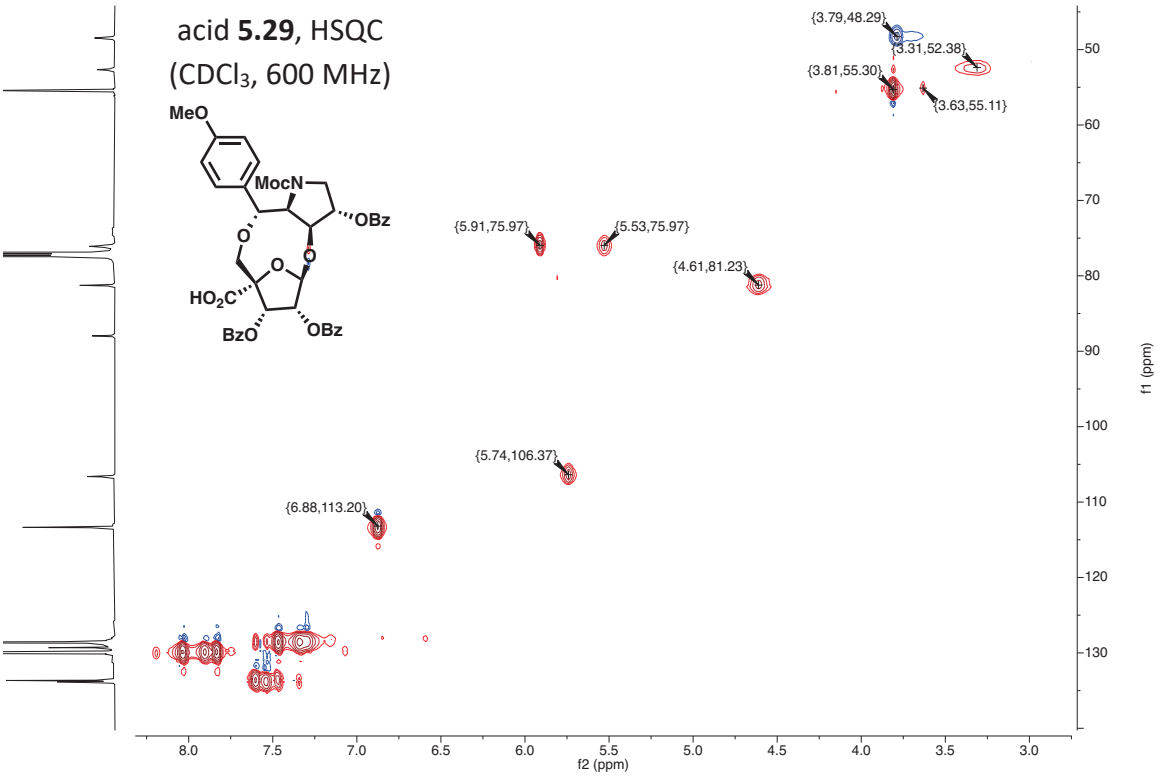
acid **5.29**, ^{1}H NMR
($CDCl_3$, 600 MHz)

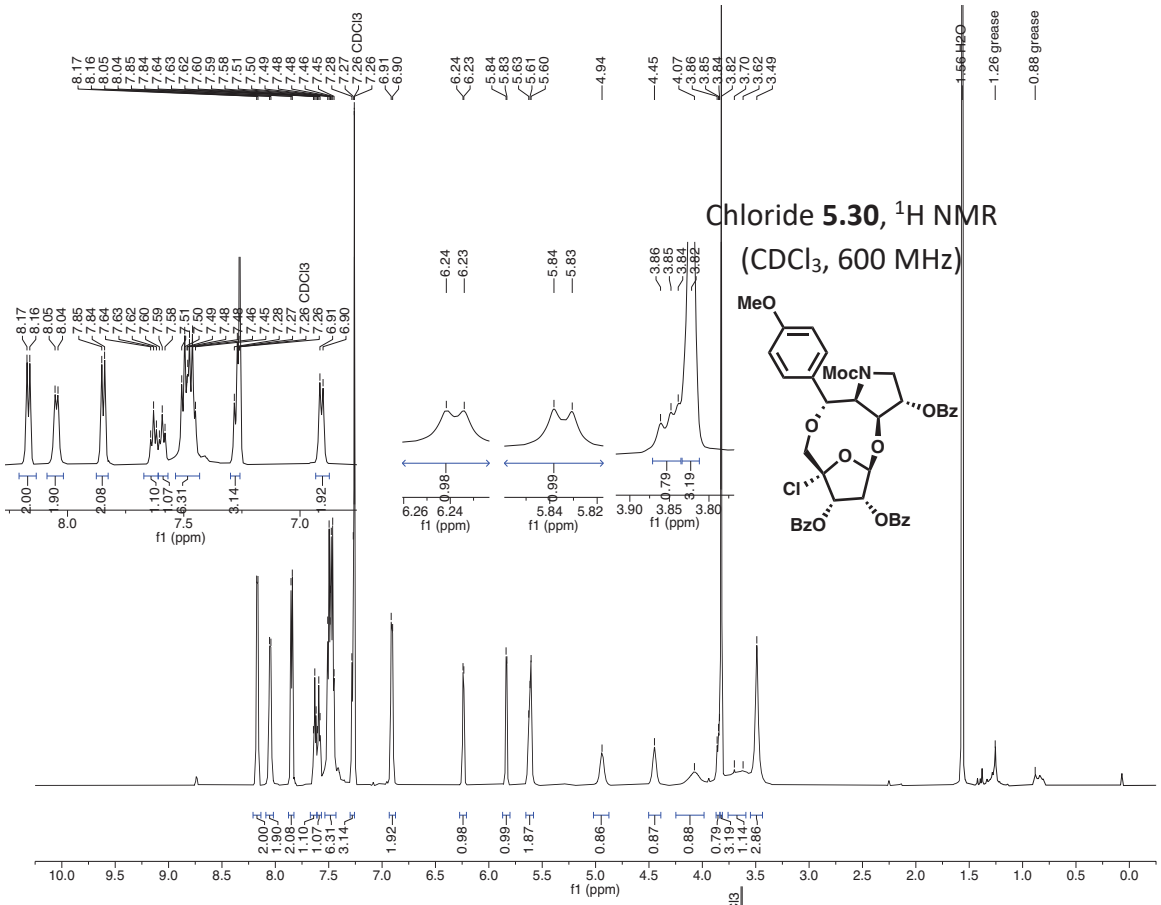


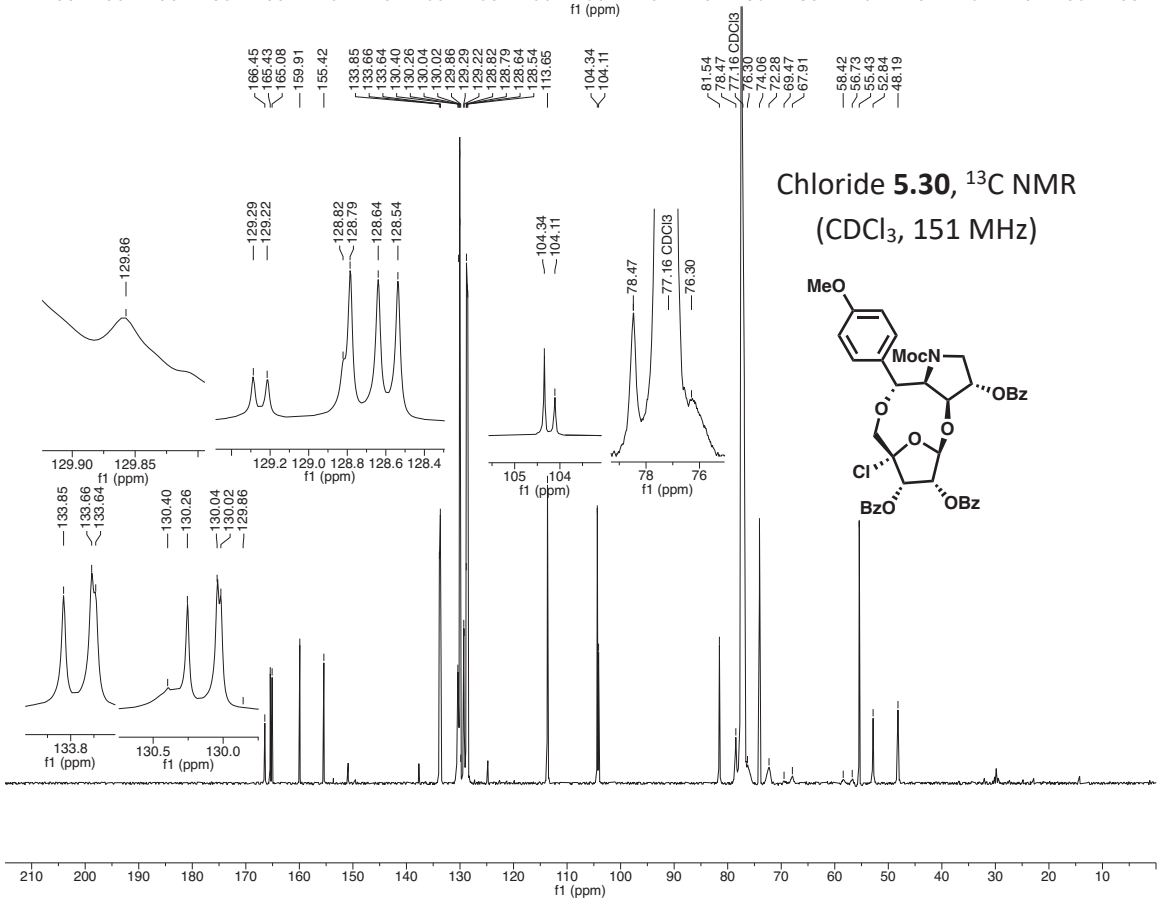
acid **5.29**, ^{13}C NMR
($CDCl_3$, 151 MHz)

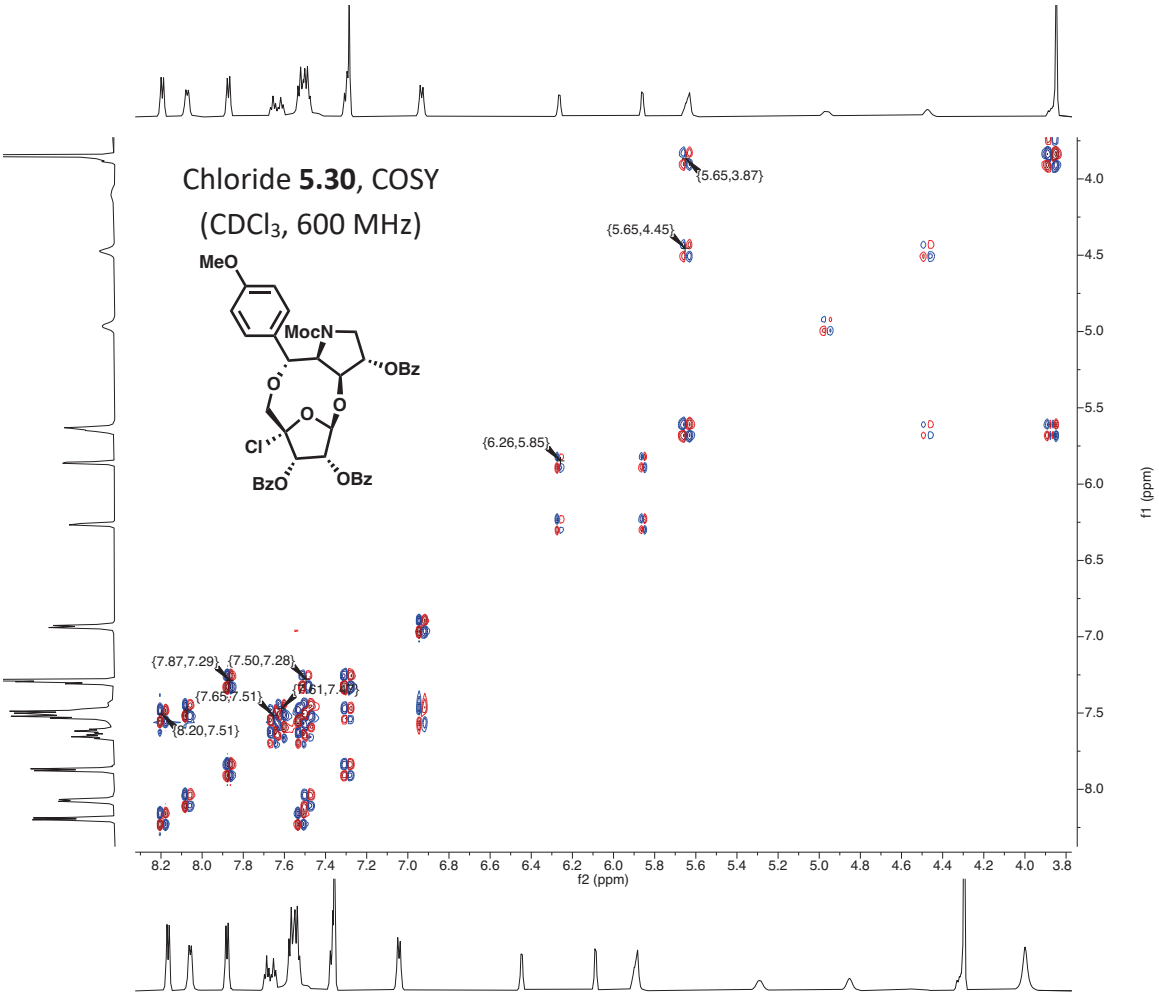


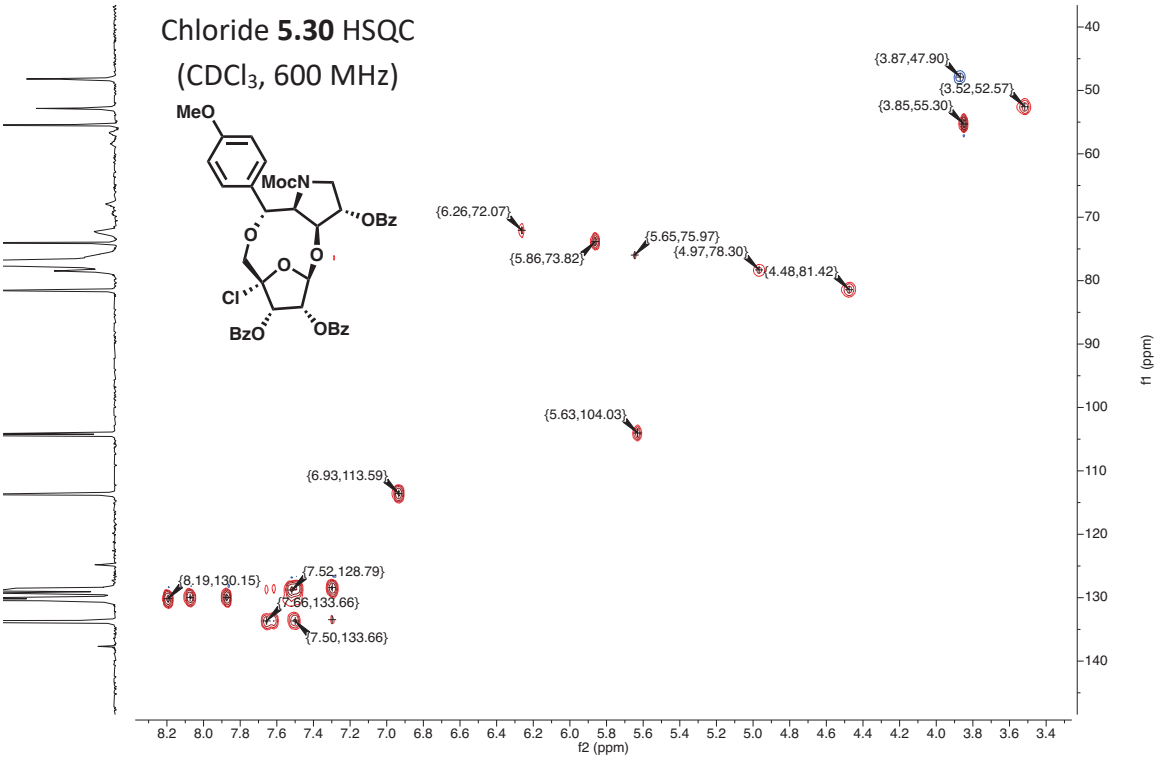

acid **5.29**, COSY
(CDCl3, 600 MHz)
Complex COSY due to rotamers
MeO
MocN
OBz
HO2C
BzO
OBz
f2 (ppm)
f1 (ppm)


acid **5.29**, HSQC
(CDCl3, 600 MHz)
MeO
MocN
OBz
HO2C
BzO
OBz
{3.79,48.29}
{3.31,52.38}
{3.81,55.30}
{3.63,55.11}
{5.91,75.97}
{5.53,75.97}
{4.61,81.23}
{5.74,106.37}
{6.88,113.20}
f2 (ppm)
f1 (ppm)

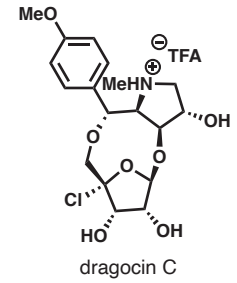

Chloride **5.30**, ^{1}H NMR
($CDCl_3$, 600 MHz)
MeO
MocN
OBz
O
O
O
Cl
BzO
OBz
f1 (ppm)


Chloride **5.30**, ^{13}C NMR
($CDCl_3$, 151 MHz)
MeO
MocN
OBz
O
O
O
Cl
BzO
OBz
f1 (ppm)


Chloride **5.30**, COSY
(CDCl3, 600 MHz)
MeO
MocN
OBz
O
O
O
Cl
BzO
OBz
{5.65,3.87}
{5.65,4.45}
{6.26,5.85}
{7.87,7.29}
{7.50,7.28}
{7.65,7.51}
{8.20,7.51}
f2 (ppm)
f1 (ppm)

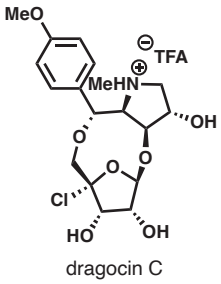

Chloride **5.30** HSQC
(CDCl3, 600 MHz)
MeO
MocN
OBz
O
O
O
Cl
BzO
OBz
{3.87,47.90}
{3.52,52.57}
{3.85,55.30}
{6.26,72.07}
{5.86,73.82}
{5.65,75.97}
{4.97,78.30}
{4.48,81.42}
{5.63,104.03}
{6.93,113.59}
{8.19,130.15}
{7.52,128.79}
{7.66,133.66}
{7.50,133.66}
f2 (ppm)
f1 (ppm)

dragocin C (**1.3**), ^{1}H NMR
(MeOD, 600 MHz)

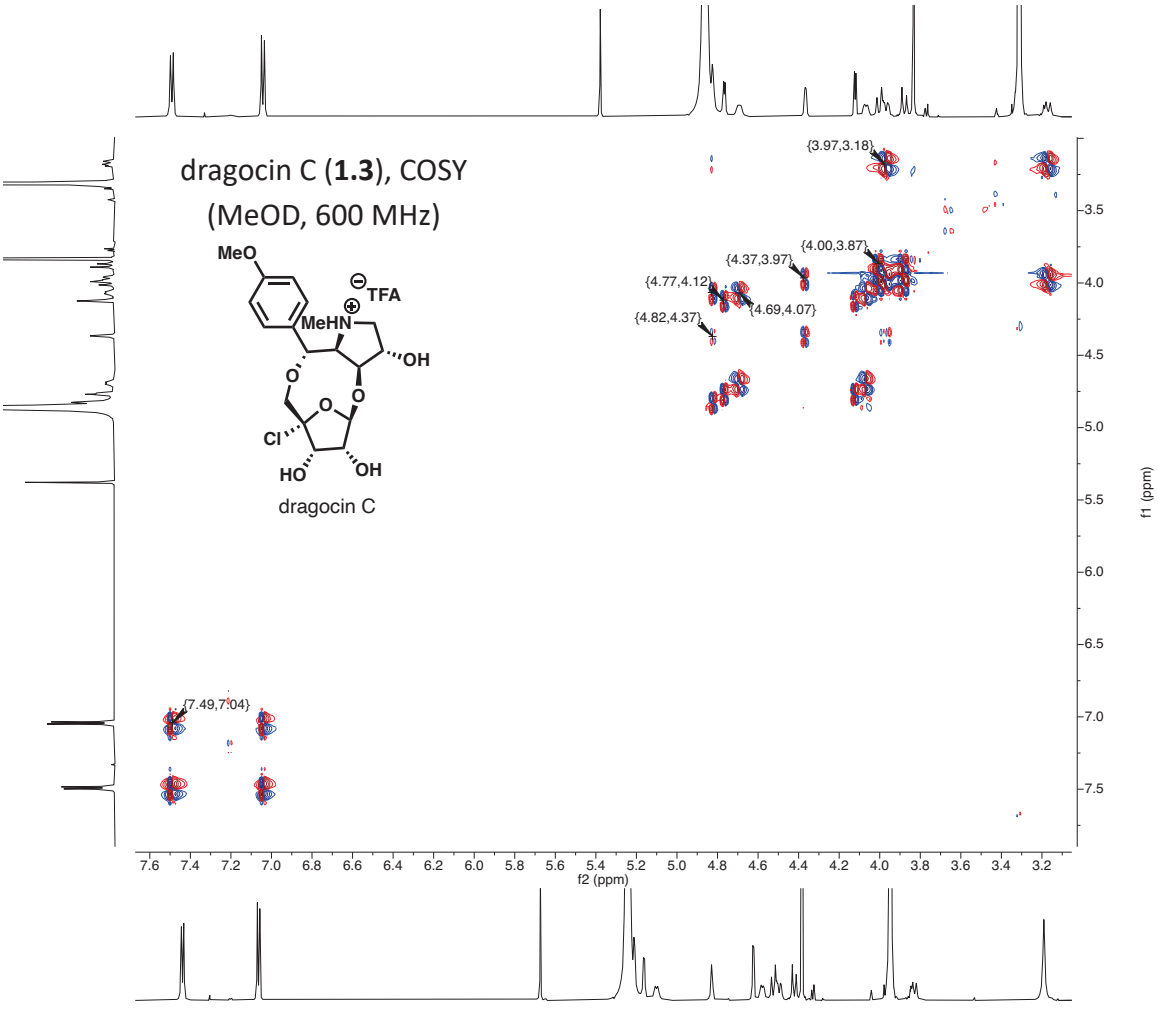


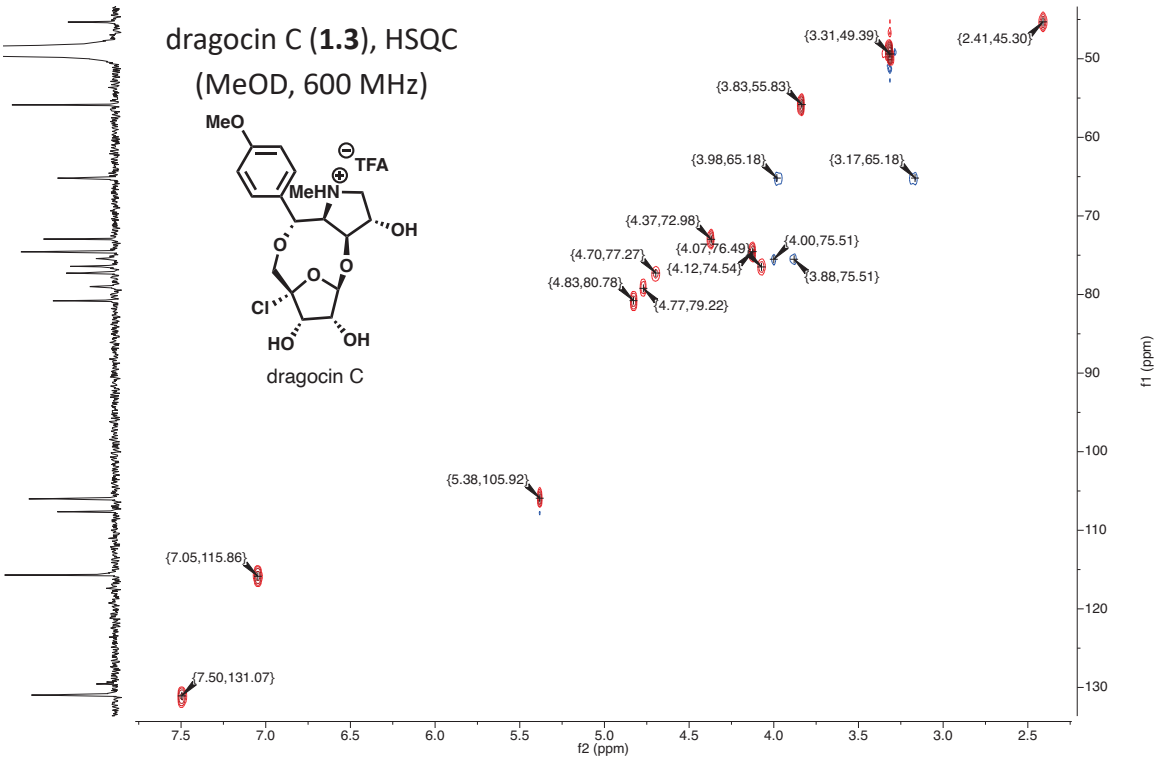
dragocin C

dragocin C (**1.3**), ^{13}C NMR
(MeOD, 151 MHz)

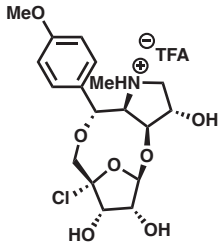


dragocin C


dragocin C (**1.3**), COSY
(MeOD, 600 MHz)
MeO
TFA
MeHN
OH
O
O
O
Cl
HO
OH
dragocin C
{3.97,3.18}
{4.37,3.97}
{4.00,3.87}
{4.77,4.12}
{4.69,4.07}
{4.82,4.37}
{7.49,7.04}
f1 (ppm)
f2 (ppm)


dragocin C (**1.3**), HSQC
(MeOD, 600 MHz)
MeO
TFA
MeHN
OH
O
O
O
Cl
HO
OH
dragocin C
{3.31,49.39}
{2.41,45.30}
{3.83,55.83}
{3.98,65.18}
{3.17,65.18}
{4.37,72.98}
{4.70,77.27}
{4.07,76.49}
{4.00,75.51}
{4.12,74.54}
{3.88,75.51}
{4.83,80.78}
{4.77,79.22}
{5.38,105.92}
{7.05,115.86}
{7.50,131.07}
f1 (ppm)
f2 (ppm)

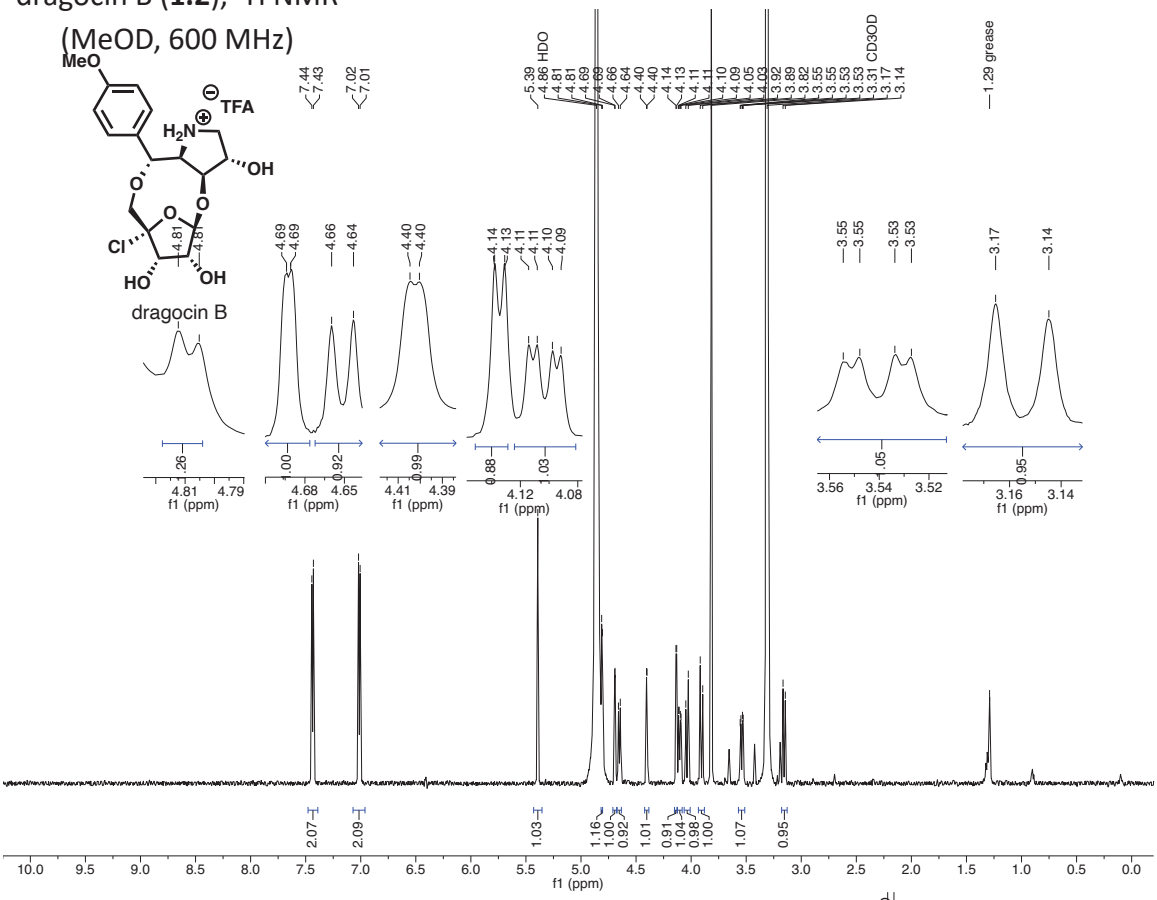
dragocin C (**1.3**), ^{19}F NMR



dragocin C

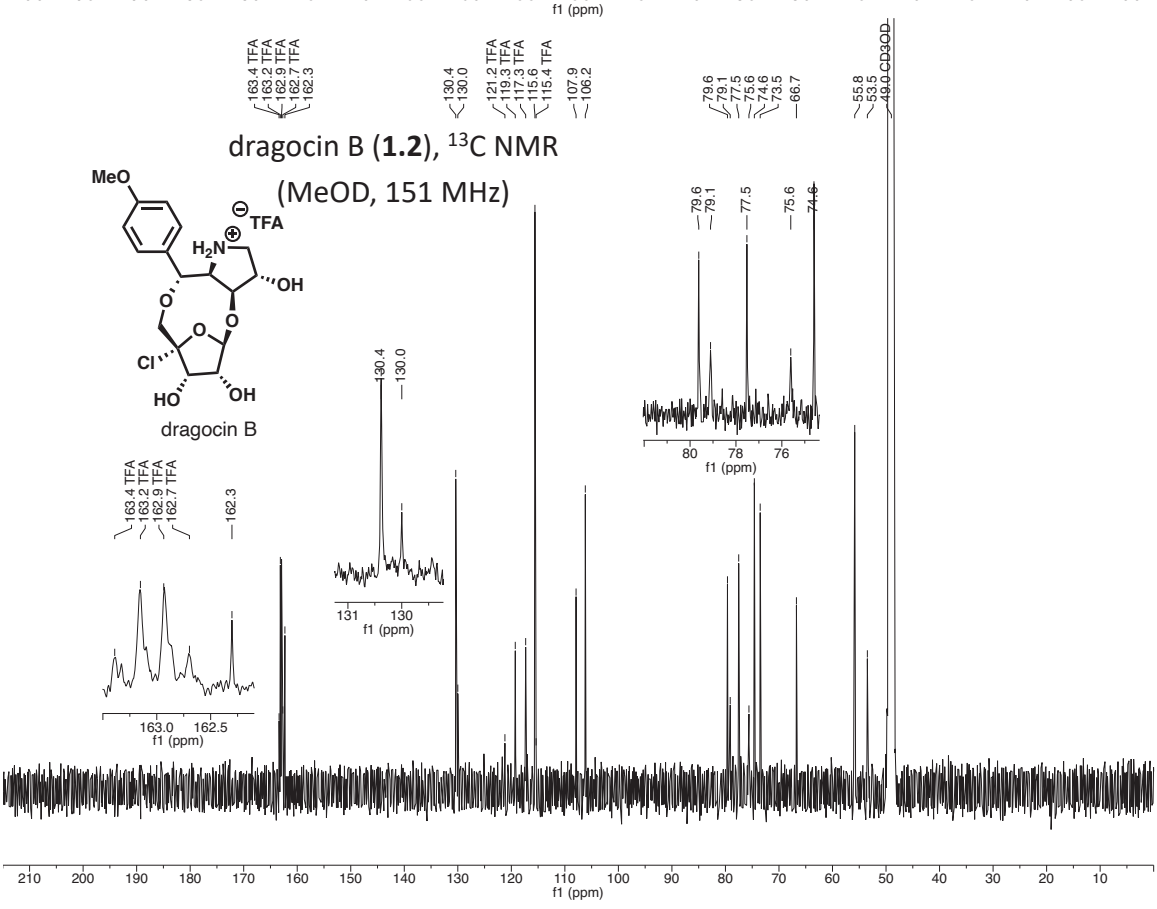
dragocin B (**1.2**), ^{1}H NMR

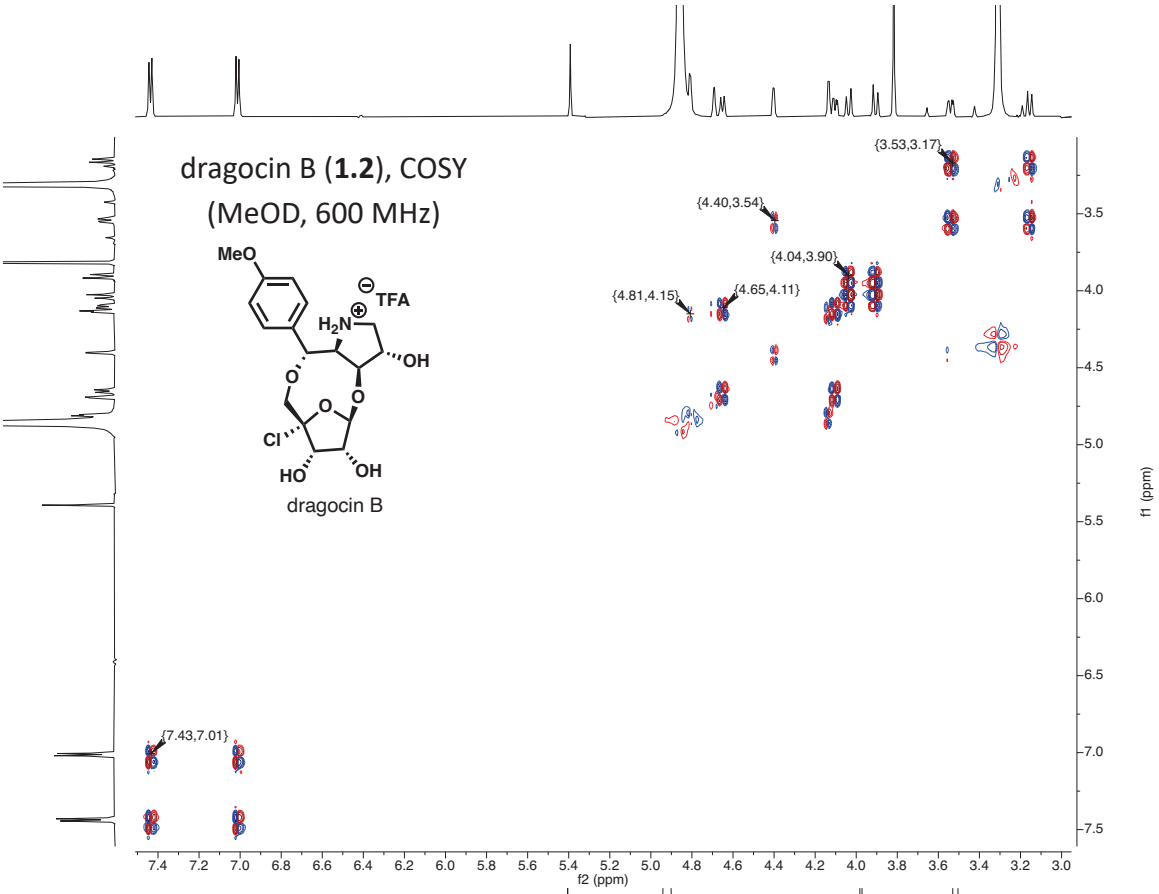
(MeOD, 600 MHz)

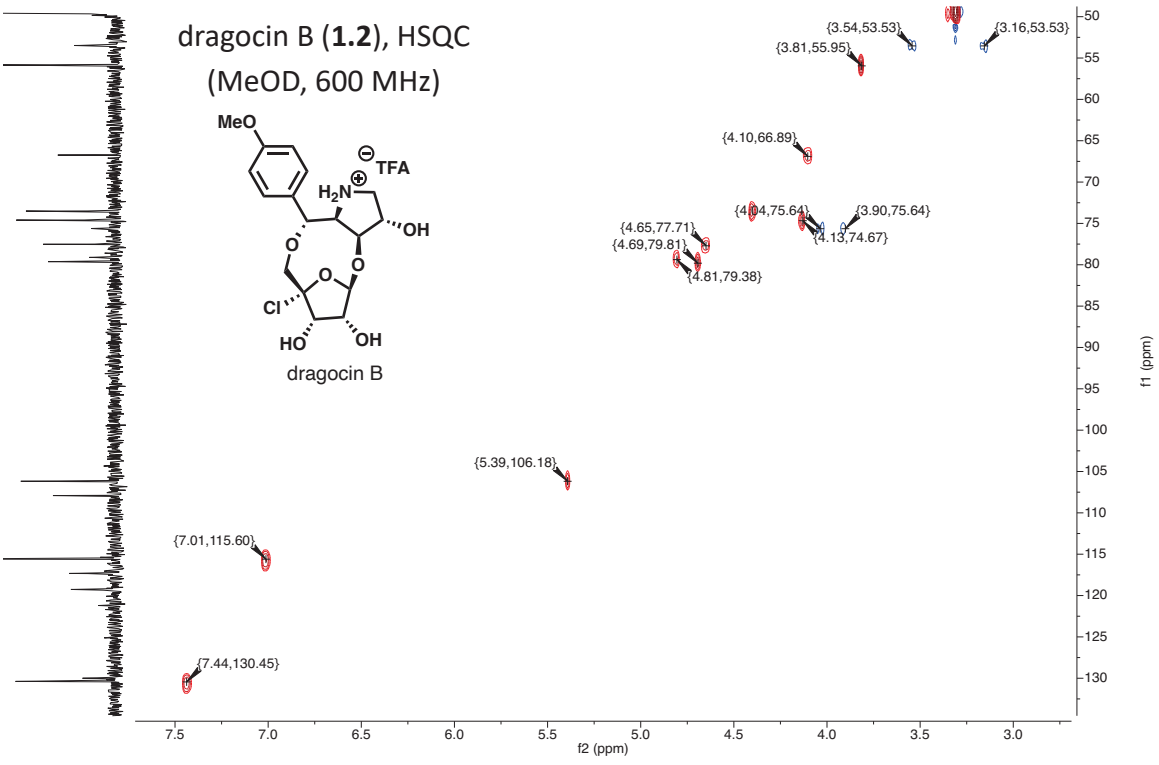


dragocin B (**1.2**), ^{13}C NMR

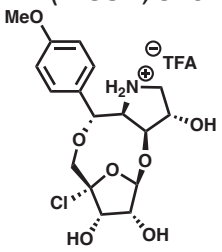
(MeOD, 151 MHz)



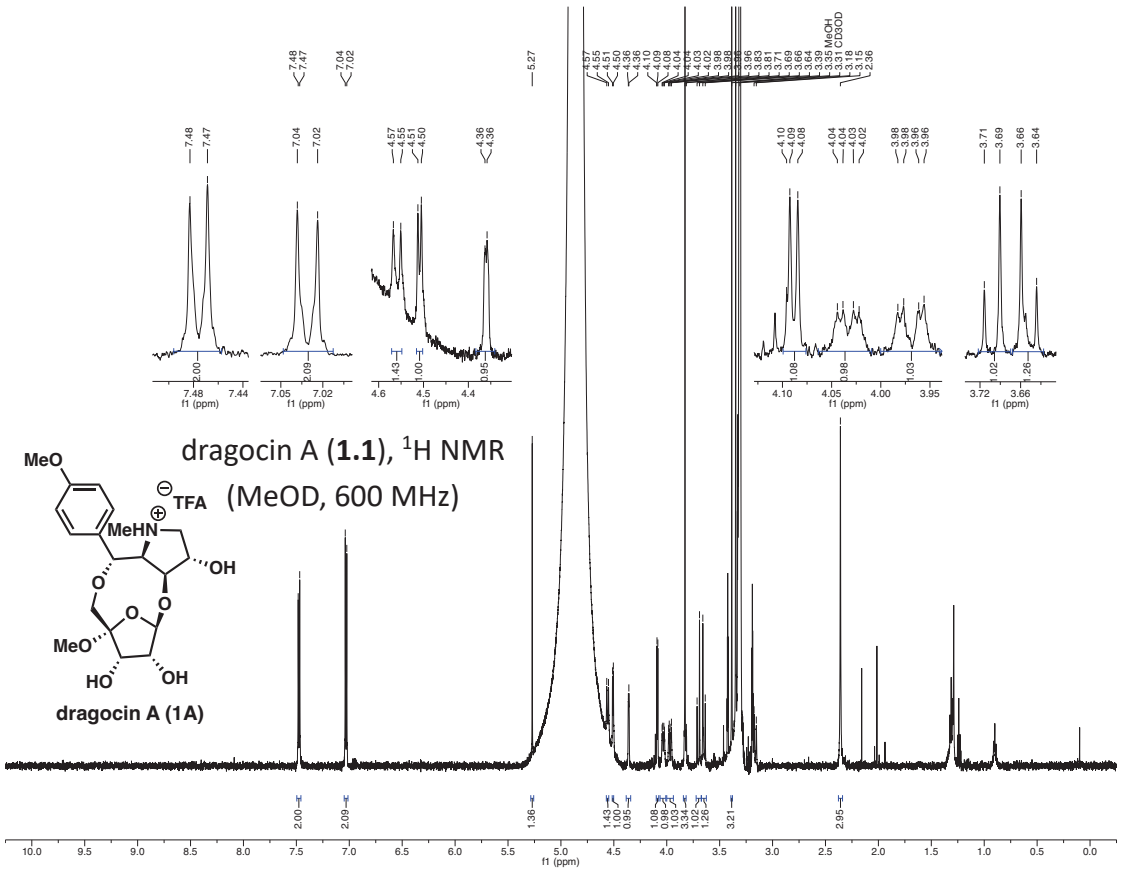

dragocin B (1.2), COSY
(MeOD, 600 MHz)
MeO
TFA
H2N
OH
O
O
O
Cl
HO
OH
dragocin B
{3.53,3.17}
{4.40,3.54}
{4.04,3.90}
{4.81,4.15}
{4.65,4.11}
{7.43,7.01}
f2 (ppm)
f1 (ppm)

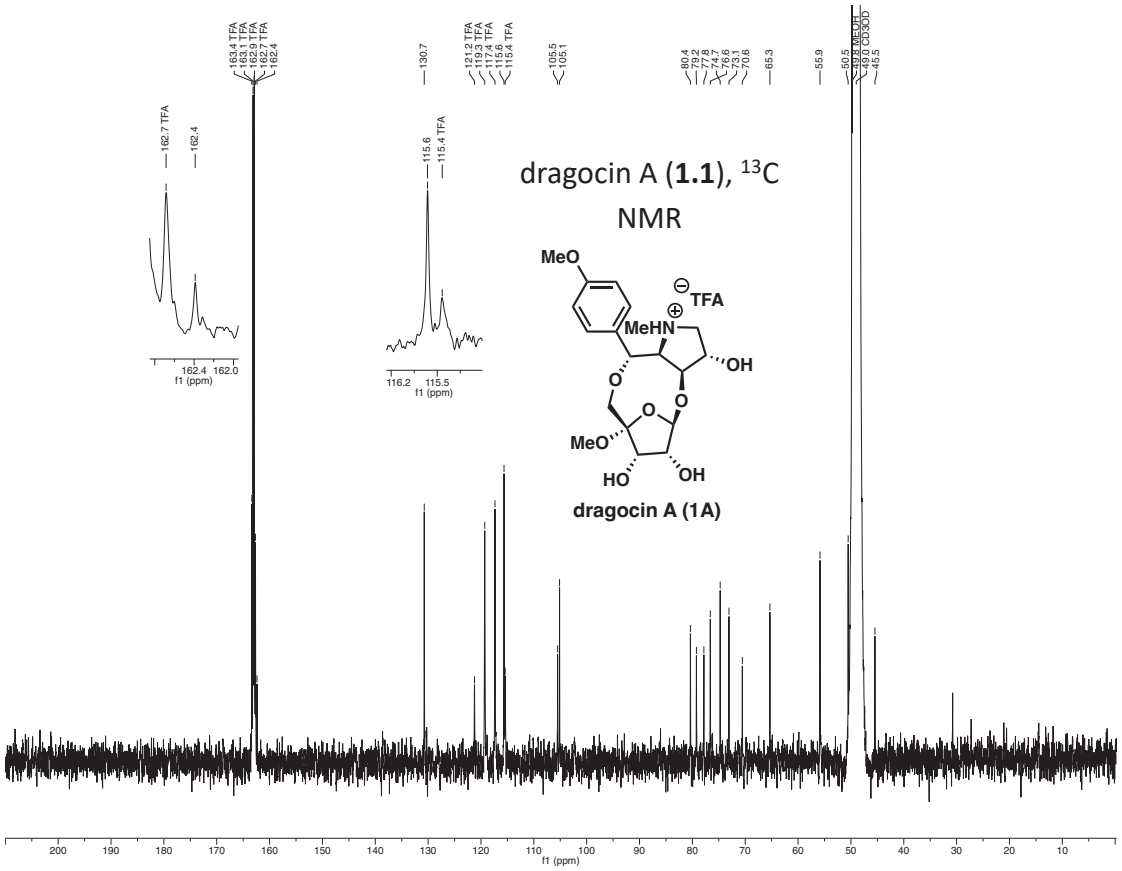

dragocin B (1.2), HSQC
(MeOD, 600 MHz)
MeO
TFA
H2N
OH
O
O
O
Cl
HO
OH
dragocin B
{3.54,53.53}
{3.16,53.53}
{3.81,55.95}
{4.10,66.89}
{4.04,75.64}
{3.90,75.64}
{4.65,77.71}
{4.69,79.81}
{4.13,74.67}
{4.81,79.38}
{5.39,106.18}
{7.01,115.60}
{7.44,130.45}
f2 (ppm)
f1 (ppm)

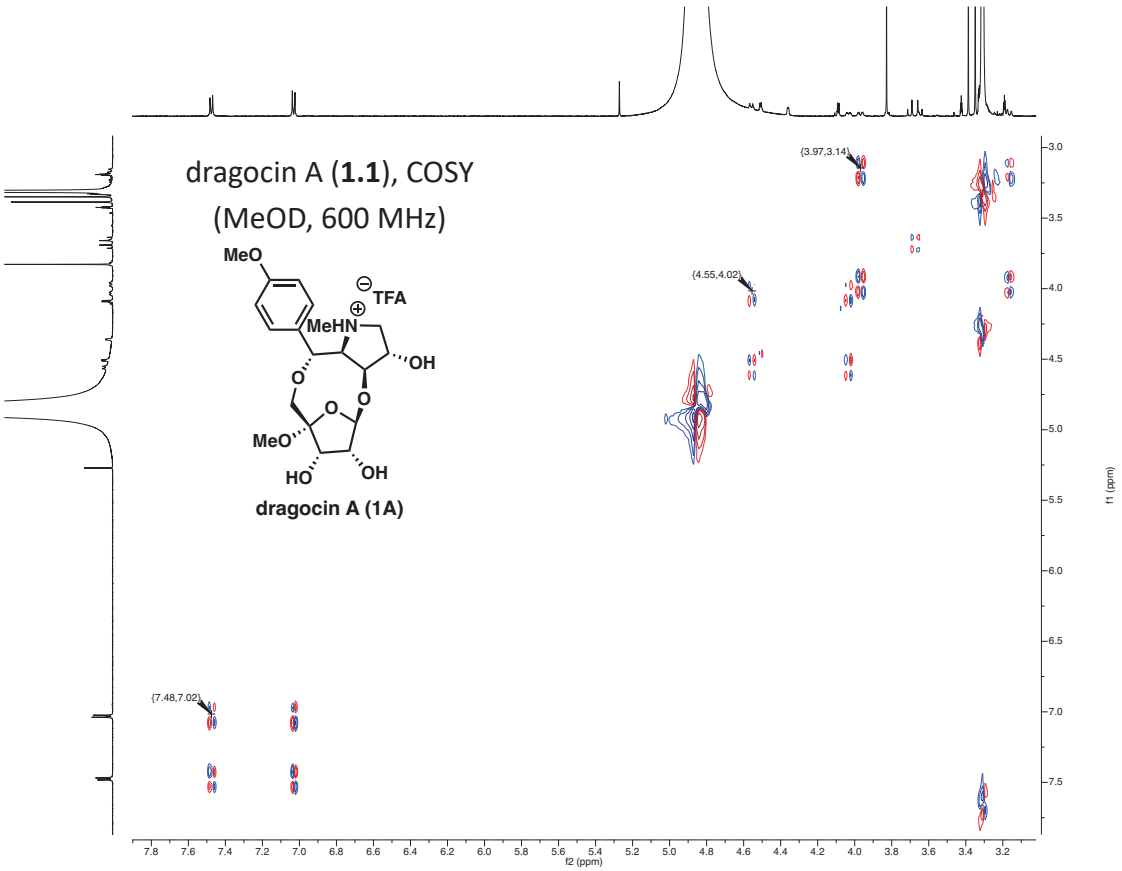
dragocin B (**1.2**), ^{19}F NMR (MeOD, 376 MHz)

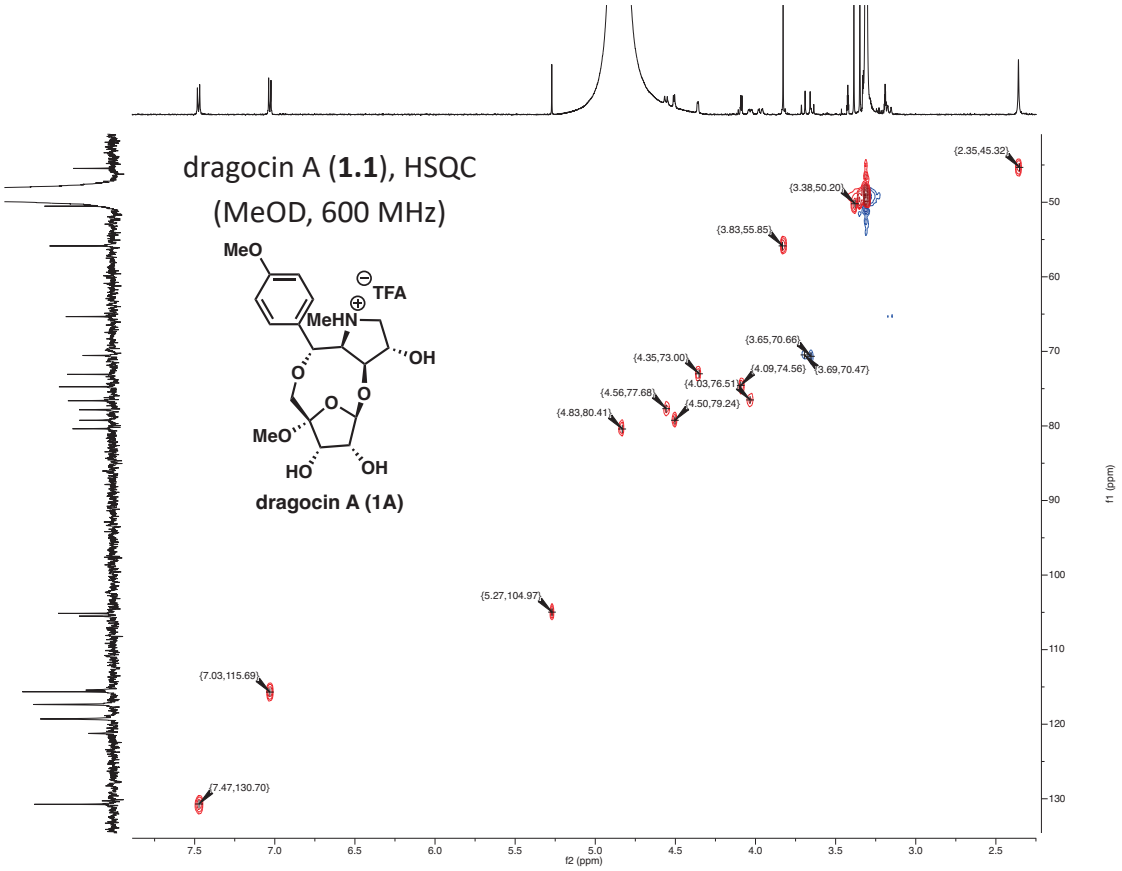


dragocin B

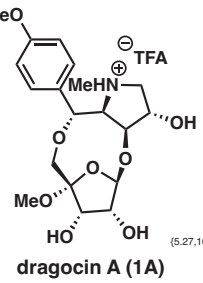

dragocin A (**1.1**), ^{1}H NMR
(MeOD, 600 MHz)
MeO
TFA
MeHN
OH
O
O
O
MeO
HO
OH
dragocin A (1A)
f1 (ppm)


dragocin A (**1.1**), ^{13}C
NMR
MeO
TFA
MeHN
OH
O
O
O
MeO
HO
OH
dragocin A (1A)
f1 (ppm)


dragocin A (**1.1**), COSY
(MeOD, 600 MHz)
MeO
TFA
MeHN
OH
O
O
O
MeO
HO
OH
dragocin A (1A)
{3.97,3.14}
{4.55,4.02}
{7.48,7.02}
f2 (ppm)
f1 (ppm)

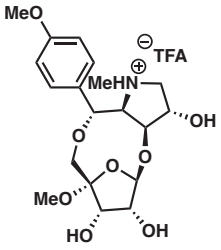

dragocin A (**1.1**), HSQC
(MeOD, 600 MHz)
MeO
TFA
MeHN
OH
O
O
O
MeO
HO
OH
dragocin A (1A)
{2.35,45.32}
{3.38,50.20}
{3.83,55.85}
{3.65,70.66}
{4.35,73.00}
{4.09,74.56}
{3.69,70.47}
{4.03,76.51}
{4.56,77.68}
{4.50,79.24}
{4.83,80.41}
{5.27,104.97}
{7.03,115.69}
{7.47,130.70}
f2 (ppm)
f1 (ppm)

dragocin A (**1.1**), HMBC
(MeOD, 600 MHz)



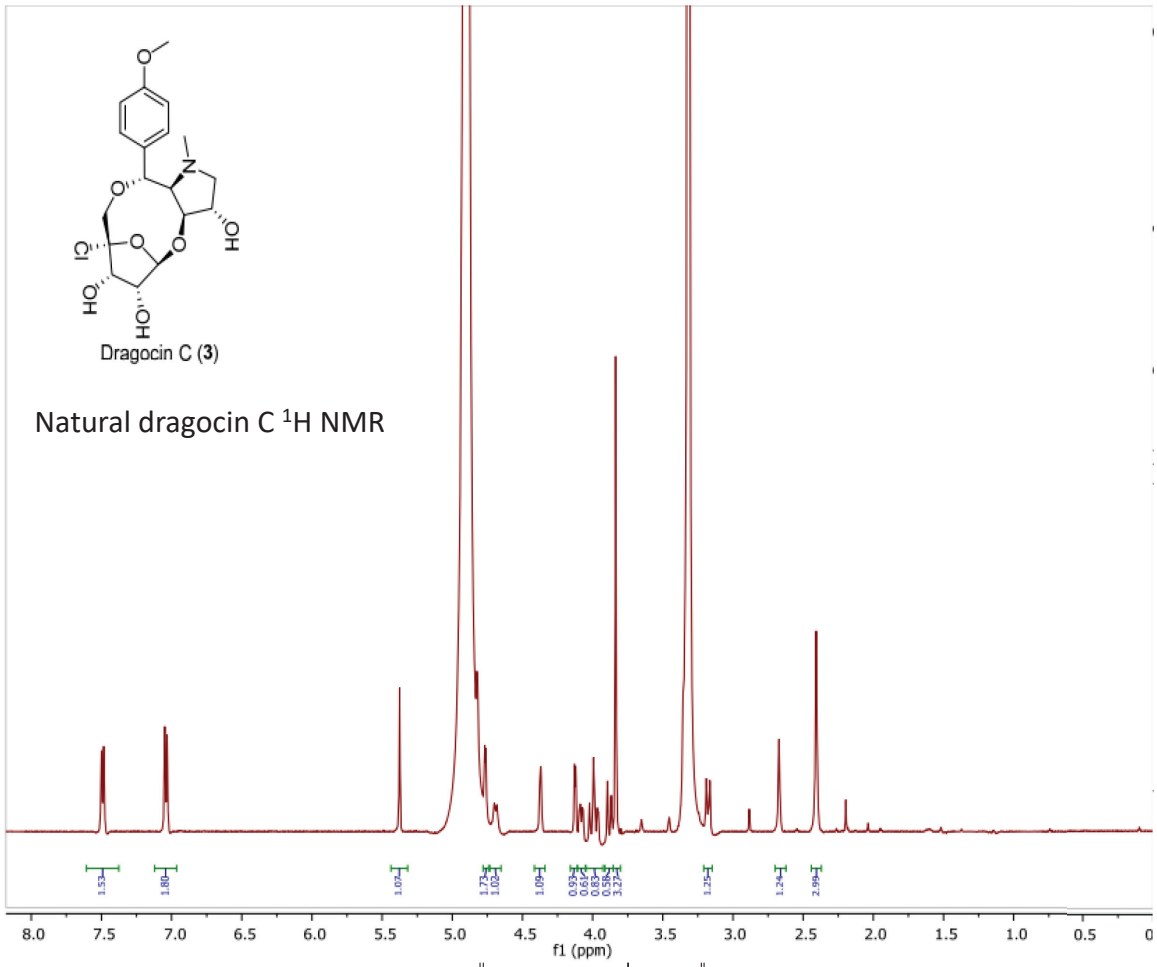
dragocin A (1A)

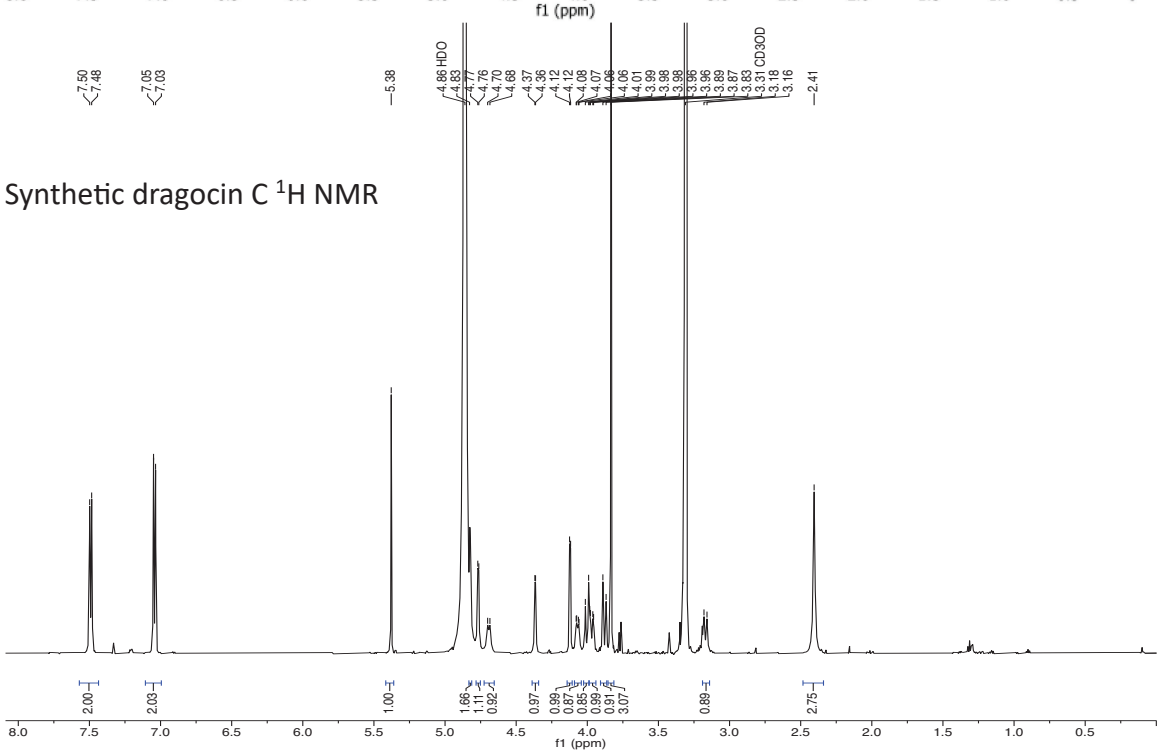
dragocin A (**1.1**), ^{19}F
NMR

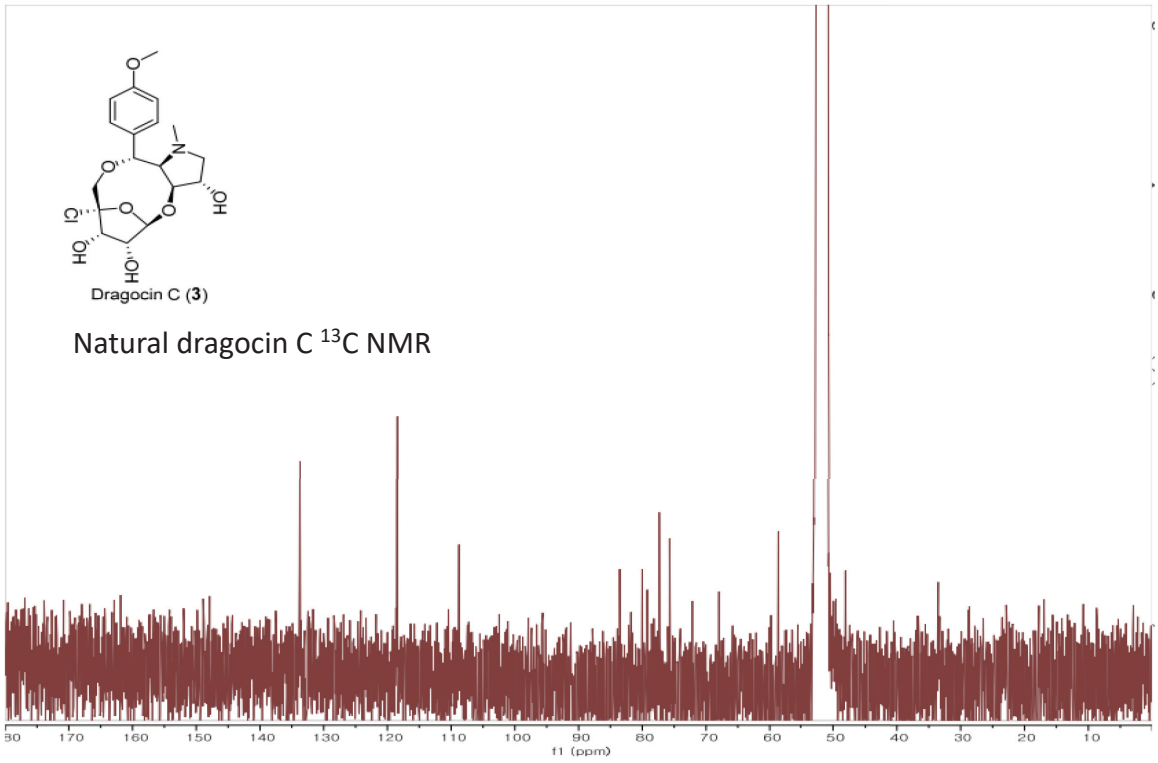


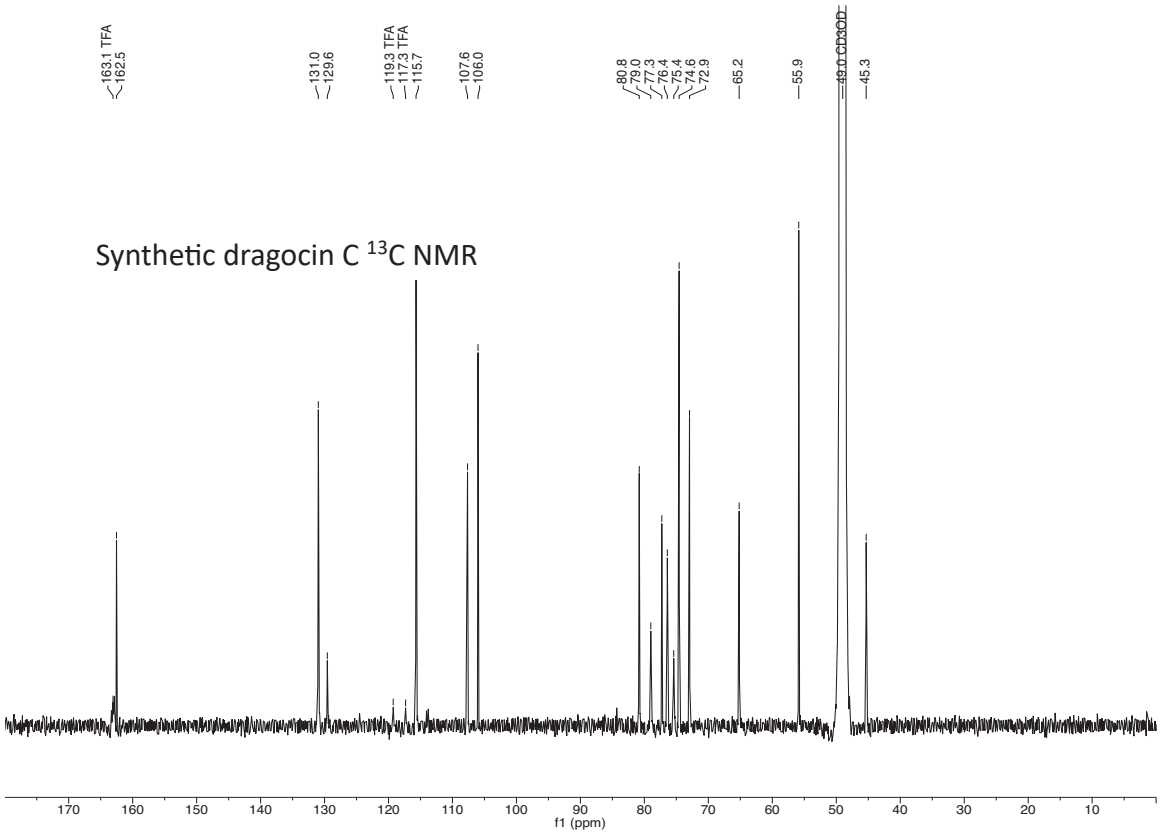
dragocin A (1A)

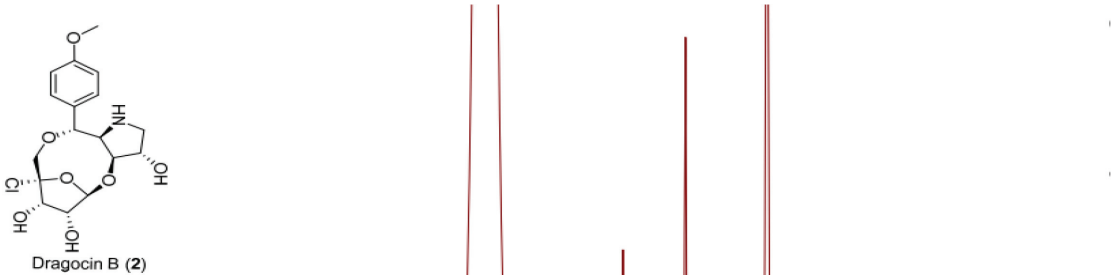
Natural and Synthetic Dragocins Stacked Spectra:





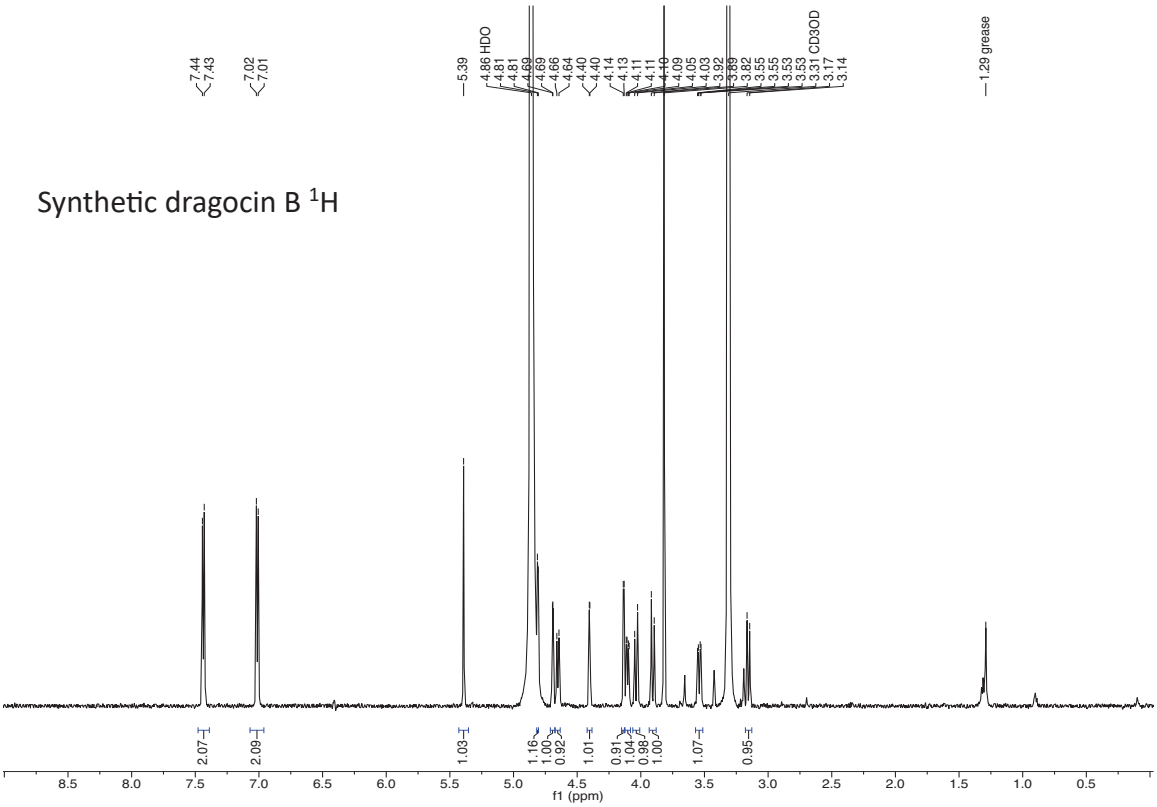

Dragocin C (3)
Natural dragocin C 13C NMR
f1 (ppm)


163.1 TFA
162.5
131.0
129.6
119.3 TFA
117.3 TFA
115.7
107.6
106.0
80.8
79.0
77.3
76.4
75.4
74.6
72.9
65.2
55.9
49.0 CD3OD
45.3
Synthetic dragocin C 13C NMR
f1 (ppm)



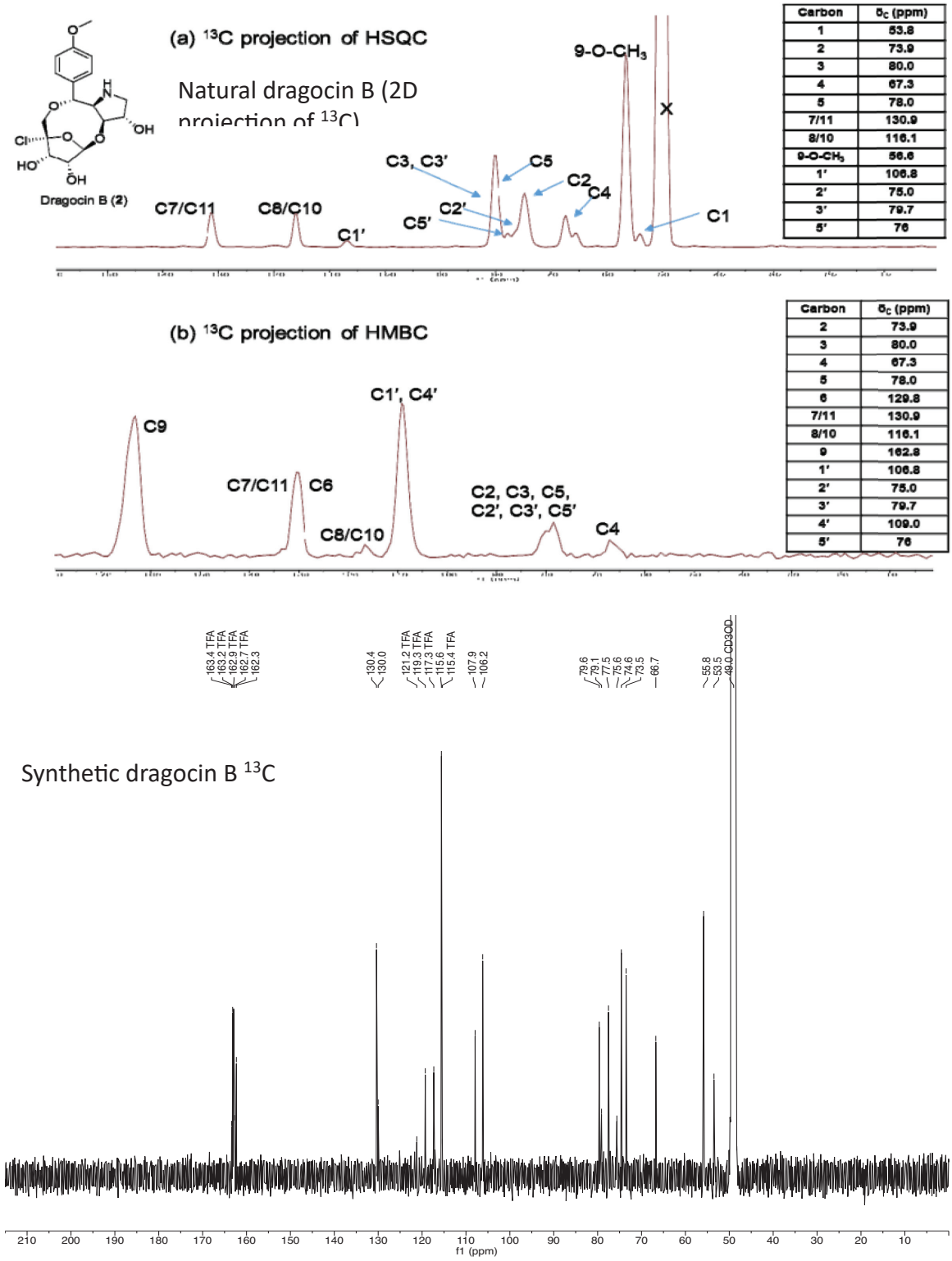
Natural dragocin B ^{1}H

Synthetic dragocin B ^{1}H

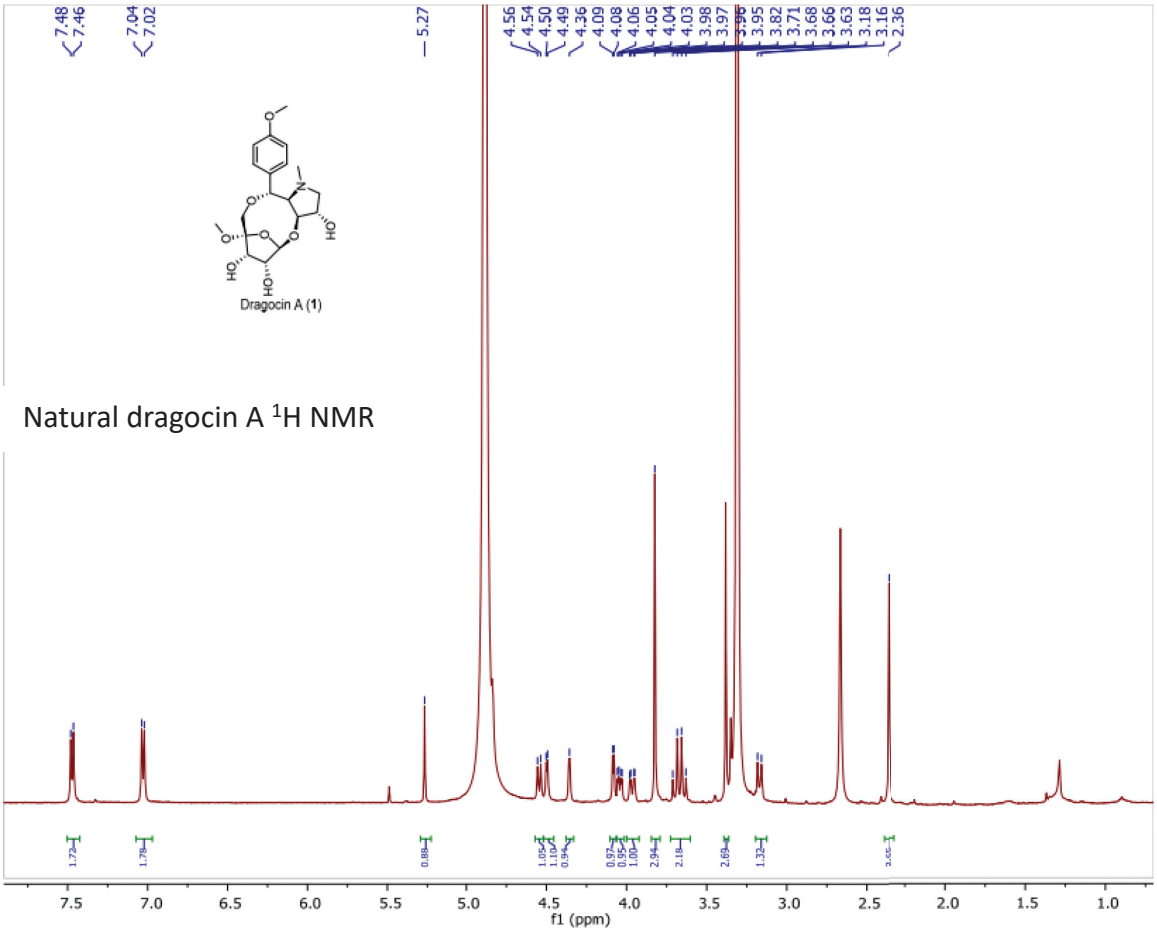


Synthetic vs. Natural Dragocin B (^{13}C NMR)

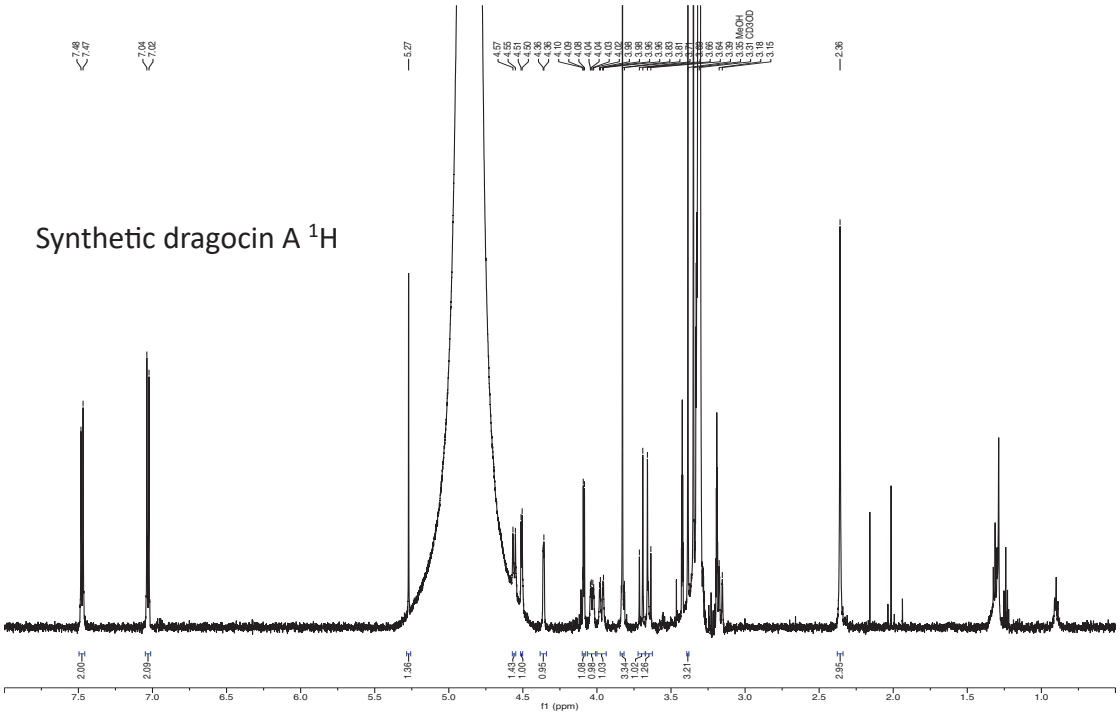
A 1D ^{13}C NMR spectra for this natural product was not provided in the original isolation



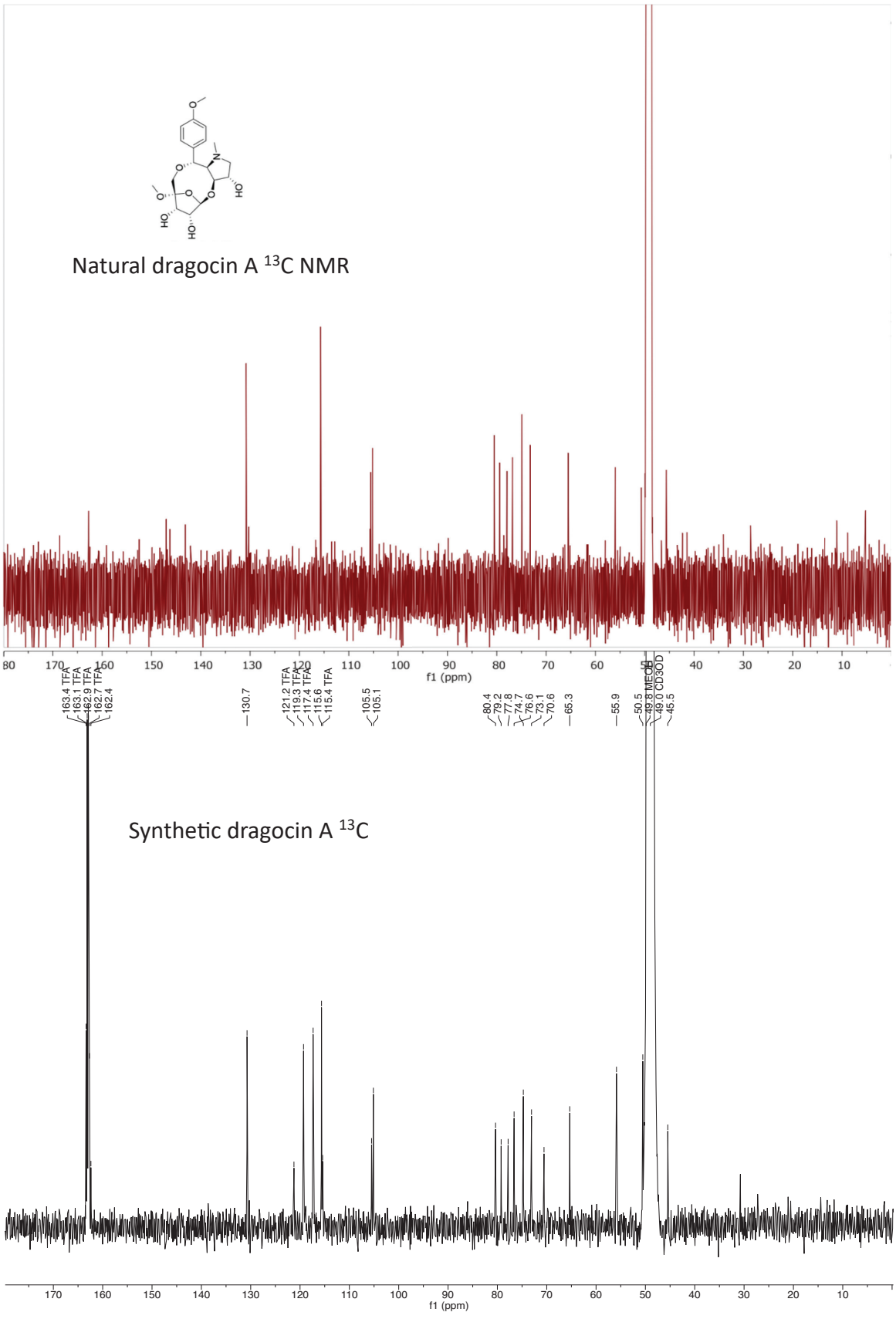
report. Signals for ^{13}C NMR were assigned by the isolation authors from 2D NMR projections (see below)



Natural dragocin A ^{1}H NMR



Synthetic dragocin A ^{1}H

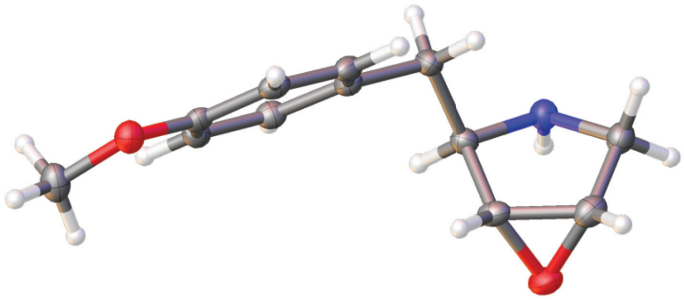

Natural dragocin A 13C NMR
f1 (ppm)
163.4 TFA
163.1 TFA
162.9 TFA
162.7 TFA
162.4
130.7
121.2 TFA
119.3 TFA
117.4 TFA
115.6
115.4 TFA
105.5
105.1
80.4
79.2
77.8
74.7
76.6
73.1
70.6
65.3
55.9
50.5
49.8 MEOH
49.0 CD3OD
45.5
Synthetic dragocin A 13C
f1 (ppm)

X-Ray Crystallography Data

Crystal Structure of anti-epoxide 5.8:

Experimental Summary: The single crystal X-ray diffraction studies were carried out on a Bruker SMART Pt 135 diffractometer equipped with Cu K□ radiation (λ=1.54178 Å).

Crystals of the subject compound were used as received (grow from MeOH / MTBE).
A 0.220 x 0.080 x 0.030mm colorless block crystal was mounted on a Cryoloop with Paratone oil. Data were collected in a nitrogen gas stream at 100(2) K using ϕ and □ scans. Crystal-to-detector distance was 45 mm and exposure time was 2.0, 5.0 and 8.0 seconds (depending on the 2 θ range) per frame using a scan width of 1.25°. Data collection was 99.5% complete to 67.679° in θ. A total of 9274 reflections were collected covering the indices, -9<=h<=8, -6<=k<=6, -13<=l<=16. 2035 reflections were found to be symmetry independent, with a R_{int} of 0.0385. Indexing and unit cell refinement indicated a **Primitive**, **Monoclinic** lattice. The space group was found to be **$P2_1$**. The data were integrated using the Bruker SAINT Software program and scaled using the SADABS software program. Solution by direct methods (SHELXT) produced a complete phasing model consistent with the proposed structure.
All nonhydrogen atoms were refined anisotropically by full-matrix least-squares (SHELXL-2014). All carbon bonded hydrogen atoms were placed using a riding model. Their positions were constrained relative to their parent atom using the appropriate HFIX command in SHELXL-2014. Crystallographic data are summarized in Table 1.



Notes: Excellent data and refinement,

Absolute structure parameter -0.02(11) conclusive

Table 1. Crystal data and structure refinement for Baran824.

Report date	2022-11-09	
Identification code	Baran824	
Empirical formula	C12 H15 N O2	
Molecular formula	C12 H15 N O2	
Formula weight	205.25	
Temperature	100.15 K	
Wavelength	1.54178 Å	
Crystal system	Monoclinic	
Space group	P 1 21 1	
Unit cell dimensions	a = 7.7646(5) Å	□= 90°.
	b = 5.2551(3) Å	□= 102.919(2)°.
	c = 13.4006(8) Å	□ = 90°.

Volume	532.95(6) $Å^3$
Z	2
Density (calculated)	1.279 Mg/m^3
Absorption coefficient	0.702 mm^{-1}
F(000)	220
Crystal size	0.22 x 0.08 x 0.03 mm^3
Crystal color, habit	colorless plank
Theta range for data collection	3.384 to 70.978°.
Index ranges	-9<=h<=8, -6<=k<=6, -13<=l<=16
Reflections collected	9274
Independent reflections	2035 [R(int) = 0.0385]
Completeness to theta = 67.679°	99.5 %
Absorption correction	Semi-empirical from equivalents
Max. and min. transmission	0.7534 and 0.6455
Refinement method	Full-matrix least-squares on F^2
Data / restraints / parameters	2035 / 1 / 141
Goodness-of-fit on F^2	1.093
Final R indices [I>2sigma(I)]	R1 = 0.0420, wR2 = 0.1146
R indices (all data)	R1 = 0.0424, wR2 = 0.1149
Absolute structure parameter	-0.02(11)
Extinction coefficient	0.011(3)
Largest diff. peak and hole	0.249 and -0.177 $e.Å^{-3}$

Table 2. Atomic coordinates (x 10^4) and equivalent isotropic displacement parameters ($Å^2$x 10^3)

for Baran824. U(eq) is defined as one third of the trace of the orthogonalized U^{ij} tensor.

	x	y	z	U(eq)
O(1)	5985(3)	1757(5)	8946(2)	28(1)
O(2)	6700(3)	6251(4)	3581(2)	23(1)
N(1)	9005(3)	4464(6)	9614(2)	22(1)
C(1)	7441(4)	5368(7)	9966(2)	25(1)
C(2)	5864(4)	4441(7)	9185(3)	27(1)
C(3)	6479(4)	3671(6)	8277(2)	22(1)
C(4)	8458(4)	4124(6)	8490(2)	20(1)
C(5)	8875(4)	6528(6)	7936(2)	23(1)
C(6)	8315(4)	6411(6)	6775(2)	21(1)
C(7)	7169(4)	8216(6)	6224(2)	22(1)
C(8)	6668(4)	8131(6)	5164(2)	21(1)
C(9)	7297(4)	6210(6)	4629(2)	19(1)
C(10)	8461(4)	4388(6)	5157(2)	21(1)
C(11)	8959(4)	4529(6)	6221(2)	21(1)
C(12)	7118(5)	4110(8)	3020(3)	30(1)

Table 3. Bond lengths [Å] and angles [°] for Baran824.

O(1)-C(2)	1.454(4)	C(8)-H(8)	0.9500
O(1)-C(3)	1.454(4)	C(8)-C(9)	1.389(4)
O(2)-C(9)	1.377(4)	C(9)-C(10)	1.395(4)
O(2)-C(12)	1.430(4)	C(10)-H(10)	0.9500
N(1)-H(1)	0.89(5)	C(10)-C(11)	1.394(4)
N(1)-C(1)	1.477(4)	C(11)-H(11)	0.9500
N(1)-C(4)	1.481(4)	C(12)-H(12A)	0.9800
C(1)-H(1A)	0.9900	C(12)-H(12B)	0.9800
C(1)-H(1B)	0.9900	C(12)-H(12C)	0.9800
C(1)-C(2)	1.503(5)		
C(2)-H(2)	1.0000	C(3)-O(1)-C(2)	60.2(2)
C(2)-C(3)	1.459(5)	C(9)-O(2)-C(12)	117.3(2)
C(3)-H(3)	1.0000	C(1)-N(1)-H(1)	111(3)
C(3)-C(4)	1.518(4)	C(1)-N(1)-C(4)	107.1(2)
C(4)-H(4)	1.0000	C(4)-N(1)-H(1)	107(3)
C(4)-C(5)	1.536(4)	N(1)-C(1)-H(1A)	110.6
C(5)-H(5A)	0.9900	N(1)-C(1)-H(1B)	110.6
C(5)-H(5B)	0.9900	N(1)-C(1)-C(2)	105.8(3)
C(5)-C(6)	1.520(4)	H(1A)-C(1)-H(1B)	108.7
C(6)-C(7)	1.394(5)	C(2)-C(1)-H(1A)	110.6
C(6)-C(11)	1.395(4)	C(2)-C(1)-H(1B)	110.6
C(7)-H(7)	0.9500	O(1)-C(2)-C(1)	112.7(3)
C(7)-C(8)	1.387(4)	O(1)-C(2)-H(2)	120.5

O(1)-C(2)-C(3)	59.9(2)	C(7)-C(6)-C(11)	117.6(3)
C(1)-C(2)-H(2)	120.5	C(11)-C(6)-C(5)	121.2(3)
C(3)-C(2)-C(1)	107.7(3)	C(6)-C(7)-H(7)	119.3
C(3)-C(2)-H(2)	120.5	C(8)-C(7)-C(6)	121.3(3)
O(1)-C(3)-C(2)	59.9(2)	C(8)-C(7)-H(7)	119.3
O(1)-C(3)-H(3)	120.4	C(7)-C(8)-H(8)	119.9
O(1)-C(3)-C(4)	112.8(3)	C(7)-C(8)-C(9)	120.1(3)
C(2)-C(3)-H(3)	120.4	C(9)-C(8)-H(8)	119.9
C(2)-C(3)-C(4)	107.8(3)	O(2)-C(9)-C(8)	115.9(3)
C(4)-C(3)-H(3)	120.4	O(2)-C(9)-C(10)	124.1(3)
N(1)-C(4)-C(3)	105.0(2)	C(8)-C(9)-C(10)	120.0(3)
N(1)-C(4)-H(4)	110.2	C(9)-C(10)-H(10)	120.6
N(1)-C(4)-C(5)	110.4(2)	C(11)-C(10)-C(9)	118.8(3)
C(3)-C(4)-H(4)	110.2	C(11)-C(10)-H(10)	120.6
C(3)-C(4)-C(5)	110.6(3)	C(6)-C(11)-H(11)	118.9
C(5)-C(4)-H(4)	110.2	C(10)-C(11)-C(6)	122.1(3)
C(4)-C(5)-H(5A)	108.6	C(10)-C(11)-H(11)	118.9
C(4)-C(5)-H(5B)	108.6	O(2)-C(12)-H(12A)	109.5
H(5A)-C(5)-H(5B)	107.5	O(2)-C(12)-H(12B)	109.5
C(6)-C(5)-C(4)	114.8(2)	O(2)-C(12)-H(12C)	109.5
C(6)-C(5)-H(5A)	108.6	H(12A)-C(12)-H(12B)	109.5
C(6)-C(5)-H(5B)	108.6	H(12A)-C(12)-H(12C)	109.5
C(7)-C(6)-C(5)	121.2(3)	H(12B)-C(12)-H(12C)	109.5

Table 4. Anisotropic displacement parameters ($Å^2 x 10^3$) for Baran824. The anisotropic displacement factor exponent takes the form: $-2\pi^2[h^2 a^{*2} U^{11} + ... + 2 h k a^* b^* U^{12}]$

	U^{11}	U^{22}	U^{33}	U^{23}	U^{13}	U^{12}
O(1)	30(1)	25(1)	29(1)	2(1)	9(1)	-7(1)
O(2)	22(1)	26(1)	22(1)	1(1)	4(1)	3(1)
N(1)	23(1)	22(1)	19(1)	2(1)	4(1)	2(1)
C(1)	27(2)	26(2)	24(2)	0(1)	10(1)	0(1)
C(2)	25(2)	26(2)	32(2)	4(2)	10(1)	1(1)
C(3)	21(2)	21(2)	23(2)	4(1)	2(1)	-4(1)
C(4)	20(2)	19(2)	21(2)	-1(1)	3(1)	-2(1)
C(5)	28(2)	21(2)	21(2)	-4(1)	7(1)	-6(1)
C(6)	23(2)	19(2)	22(2)	0(1)	8(1)	-4(1)
C(7)	21(2)	17(1)	30(2)	-2(1)	12(1)	-1(1)
C(8)	17(1)	18(1)	29(2)	3(1)	7(1)	-1(1)
C(9)	14(1)	21(2)	22(1)	1(1)	5(1)	-3(1)
C(10)	19(1)	19(2)	25(2)	-2(1)	7(1)	1(1)
C(11)	21(2)	19(2)	24(2)	3(1)	5(1)	1(1)
C(12)	29(2)	37(2)	23(2)	-4(2)	5(1)	5(2)

Table 5. Hydrogen coordinates (x 10^4) and isotropic displacement parameters ($Å^2$x 10^3) for Baran824.

	x	y	z	U(eq)
H(1)	9360(50)	2950(90)	9880(30)	32
H(1A)	7438	7249	10008	30
H(1B)	7433	4663	10650	30
H(2)	4686	5276	9116	32
H(3)	5726	3968	7578	27
H(4)	9068	2615	8272	24
H(5A)	8280	7996	8177	28
H(5B)	10164	6841	8131	28
H(7)	6722	9532	6581	26
H(8)	5893	9388	4803	25
H(10)	8906	3075	4797	25
H(11)	9763	3303	6581	26
H(12A)	6467	4234	2306	44
H(12B)	6784	2539	3322	44

H(12C)	8390	4091	3048	44

X-Ray Crystallography Data

Crystal Structure of triol 5.16:

Experimental Summary: The single crystal X-ray diffraction studies were carried out on a Bruker Microstar APEX II CCD diffractometer equipped with Cu K_α radiation (λ = 1.54178 Å).

Crystals of the subject compound were used as received. A 0.13 x 0.12 x 0.04 mm piece of a crystal was mounted on a Cryoloop with Paratone oil. Data were collected in a nitrogen gas stream at 100(2) K using ϕ and ω scans. Crystal-to-detector distance was 40 mm and exposure time was 5, 10, 15, or 20 seconds depending on the 2θ range per frame using a scan width of 1.25°. Data collection was 97.2% complete to 67.679° in θ. A total of 28145 reflections were collected covering the indices, −7<=h<=6, −30<=k<=30, −15<=l<=15. 6459 reflections were found to be symmetry independent, with a R_{int} of 0.0724. Indexing and unit cell refinement indicated a **P**rimitive, **Monoclinic** lattice. The space group was found to be $\boldsymbol{P2_1}$. The data were integrated using the Bruker SAINT Software program and scaled using the SADABS software program. Solution by direct methods (SHELXT) produced a complete phasing model consistent with the proposed structure.

All nonhydrogen atoms were refined anisotropically by full-matrix least-squares (SHELXL-2014). All carbon bonded hydrogen atoms were placed using a riding model. Their positions were constrained relative to their parent atom using the appropriate HFIX command in SHELXL-2014. Crystallographic data are summarized in Table 1.

Notes: The data quality was poor, but suitable for structural determination. Absolute stereochemistry was already known from a previous molecule. The crystal was refined as a twin with twin law -1 0 0 0 -1 0 0 0 1. There are two copies of the compound in the asymmetric unit. The chemical formula for the compound is: $C_{19}H_{25}NO_9$

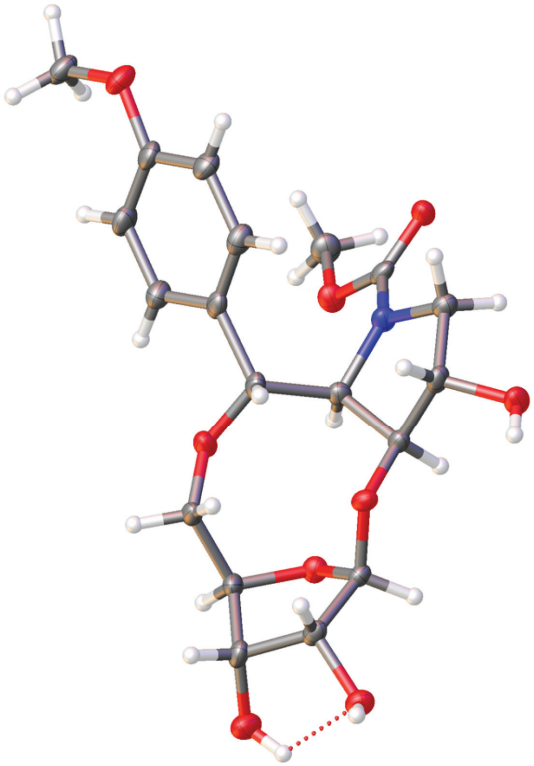


Table 1. Crystal data and structure refinement for Baran863.

Identification code	baran863_a	
Empirical formula	C19 H25 N O9	
Formula weight	411.40	
Temperature	100.15 K	
Wavelength	1.54178 Å	
Crystal system	Monoclinic	
Space group	P 1 21 1	
Unit cell dimensions	a = 5.8993(13) Å	□= 90°.
	b = 25.180(5) Å	□= 90.582(10)°.
	c = 12.615(3) Å	□ = 90°.
Volume	1873.8(7) $Å^3$	
Z	4	
Density (calculated)	1.458 Mg/m^3	
Absorption coefficient	0.989 mm^{-1}	
F(000)	872	
Crystal size	0.13 x 0.12 x 0.04 mm^3	
Theta range for data collection	1.754 to 68.501°.	
Index ranges	-7<=h<=6, -30<=k<=30, -15<=l<=15	
Reflections collected	28145	
Independent reflections	6459 [R(int) = 0.0724]	
Completeness to theta = 67.679°	97.2 %	
Absorption correction	Semi-empirical from equivalents	

Max. and min. transmission	0.5213 and 0.3976
Refinement method	Full-matrix least-squares on F^2
Data / restraints / parameters	6459 / 1 / 535
Goodness-of-fit on F^2	1.072
Final R indices [I>2sigma(I)]	R1 = 0.0490, wR2 = 0.1121
R indices (all data)	R1 = 0.0615, wR2 = 0.1230
Absolute structure parameter	-0.15(12)
Extinction coefficient	0.0024(3)
Largest diff. peak and hole	0.234 and -0.229 e.$Å^{-3}$

Table 2. Atomic coordinates (x 10^4) and equivalent isotropic displacement parameters ($Å^2$x 10^3)

for Baran863. U(eq) is defined as one third of the trace of the orthogonalized U^{ij} tensor.

	x	y	z	U(eq)
O(1)	-1259(8)	4041(2)	10712(4)	25(1)
O(1A)	9551(8)	6068(2)	5687(4)	25(1)
O(2)	2014(9)	4341(2)	11452(4)	24(1)
O(2A)	6621(9)	5677(2)	6520(4)	25(1)
O(3)	4752(10)	5100(2)	8127(4)	29(1)
O(3A)	3448(10)	4865(2)	3207(4)	28(1)
O(4A)	6484(9)	5624(2)	1894(4)	22(1)
O(4)	1562(8)	4319(2)	6839(4)	21(1)
O(5A)	8484(9)	5290(2)	-580(4)	28(1)
O(5)	-396(9)	4585(2)	4303(4)	30(1)
O(6A)	12083(10)	5901(2)	-392(5)	34(1)
O(6)	-4228(9)	4071(2)	4582(4)	31(1)
O(7A)	10383(9)	5737(2)	1769(4)	23(1)
O(7)	-2354(8)	4256(2)	6709(4)	21(1)
O(8)	-1363(9)	3329(2)	7852(4)	26(1)

O(8A)	9123(9)	6682(2)	2795(4)	27(1)
O(9A)	5128(10)	7906(2)	6729(4)	31(1)
O(9)	2477(9)	2022(2)	11670(4)	26(1)
N(1)	1712(10)	4221(2)	9679(4)	20(1)
N(1A)	6568(11)	5776(2)	4735(5)	22(1)
C(1A)	10635(14)	6151(3)	6713(6)	30(2)
C(1)	-2161(14)	3958(3)	11757(6)	30(2)
C(2A)	7509(13)	5831(2)	5700(6)	22(2)
C(2)	896(12)	4210(2)	10670(5)	20(2)
C(3A)	4520(13)	5451(3)	4614(6)	24(2)
C(3)	3828(12)	4501(3)	9510(6)	24(2)
C(4)	3928(12)	4579(3)	8323(6)	23(2)
C(4A)	4259(13)	5391(3)	3409(6)	23(2)
C(5A)	6648(13)	5485(3)	2984(5)	21(2)
C(5)	1505(13)	4491(3)	7918(5)	22(2)
C(6A)	8456(13)	5486(3)	1321(5)	21(1)
C(6)	-405(12)	4460(3)	6241(5)	22(2)
C(7)	-234(13)	4203(3)	5132(5)	24(2)
C(7A)	8194(13)	5701(3)	184(5)	22(2)
C(8)	-2324(13)	3827(3)	5071(6)	25(2)
C(8A)	10114(14)	6114(3)	86(6)	26(2)
C(9)	-2863(14)	3743(3)	6233(5)	23(2)
C(9A)	10649(14)	6241(3)	1247(6)	26(2)

C(10)	-1408(14)	3300(3)	6730(6)	27(2)
C(10A)	9056(15)	6664(3)	1666(6)	27(2)
C(11)	743(13)	3497(2)	8346(6)	23(2)
C(11A)	7132(14)	6498(2)	3331(6)	24(2)
C(12A)	7646(13)	5920(3)	3729(5)	22(2)
C(12)	460(13)	4089(3)	8698(6)	21(2)
C(13)	1285(12)	3115(2)	9240(5)	19(1)
C(13A)	6622(14)	6889(3)	4222(6)	24(2)
C(14A)	8239(14)	7243(3)	4580(6)	28(2)
C(14)	-384(13)	2960(3)	9948(6)	24(2)
C(15)	91(13)	2599(2)	10748(5)	22(2)
C(15A)	7786(14)	7590(3)	5412(6)	29(2)
C(16A)	5693(14)	7588(3)	5886(6)	27(2)
C(16)	2235(13)	2379(3)	10866(6)	22(2)
C(17A)	6865(14)	8253(3)	7125(6)	31(2)
C(17)	4621(14)	1766(3)	11795(6)	31(2)
C(18A)	4046(13)	7242(3)	5511(6)	27(2)
C(18)	3910(13)	2527(3)	10164(6)	25(2)
C(19)	3429(14)	2893(3)	9359(6)	26(2)
C(19A)	4497(13)	6898(3)	4686(6)	27(2)

Table 3. Bond lengths [Å] and angles [°] for Baran863.

O(1)-C(1)	1.442(9)	O(7A)-C(9A)	1.440(8)
O(1)-C(2)	1.341(9)	O(7)-C(6)	1.395(9)
O(1A)-C(1A)	1.453(8)	O(7)-C(9)	1.455(8)
O(1A)-C(2A)	1.344(9)	O(8)-C(10)	1.418(9)
O(2)-C(2)	1.226(8)	O(8)-C(11)	1.447(9)
O(2A)-C(2A)	1.227(9)	O(8A)-C(10A)	1.425(9)
O(3)-H(3)	0.8400	O(8A)-C(11A)	1.438(10)
O(3)-C(4)	1.420(8)	O(9A)-C(16A)	1.376(9)
O(3A)-H(3AA)	0.8400	O(9A)-C(17A)	1.432(9)
O(3A)-C(4A)	1.431(8)	O(9)-C(16)	1.363(8)
O(4A)-C(5A)	1.421(8)	O(9)-C(17)	1.426(9)
O(4A)-C(6A)	1.419(9)	N(1)-C(2)	1.345(9)
O(4)-C(5)	1.430(8)	N(1)-C(3)	1.451(9)
O(4)-C(6)	1.423(9)	N(1)-C(12)	1.472(9)
O(5A)-H(5AA)	0.8400	N(1A)-C(2A)	1.340(9)
O(5A)-C(7A)	1.426(8)	N(1A)-C(3A)	1.466(9)
O(5)-H(5)	0.8400	N(1A)-C(12A)	1.471(9)
O(5)-C(7)	1.424(8)	C(1A)-H(1AA)	0.9800
O(6A)-H(6AA)	0.8400	C(1A)-H(1AB)	0.9800
O(6A)-C(8A)	1.419(10)	C(1A)-H(1AC)	0.9800
O(6)-H(6)	0.8400	C(1)-H(1A)	0.9800
O(6)-C(8)	1.417(9)	C(1)-H(1B)	0.9800
O(7A)-C(6A)	1.413(9)	C(1)-H(1C)	0.9800

C(3A)-H(3AB)	0.9900	C(8)-C(9)	1.518(10)
C(3A)-H(3AC)	0.9900	C(8A)-H(8A)	1.0000
C(3A)-C(4A)	1.534(10)	C(8A)-C(9A)	1.529(10)
C(3)-H(3A)	0.9900	C(9)-H(9)	1.0000
C(3)-H(3B)	0.9900	C(9)-C(10)	1.537(10)
C(3)-C(4)	1.512(10)	C(9A)-H(9A)	1.0000
C(4)-H(4)	1.0000	C(9A)-C(10A)	1.519(10)
C(4)-C(5)	1.530(10)	C(10)-H(10A)	0.9900
C(4A)-H(4A)	1.0000	C(10)-H(10B)	0.9900
C(4A)-C(5A)	1.531(11)	C(10A)-H(10C)	0.9900
C(5A)-H(5AB)	1.0000	C(10A)-H(10D)	0.9900
C(5A)-C(12A)	1.555(9)	C(11)-H(11)	1.0000
C(5)-H(5A)	1.0000	C(11)-C(12)	1.564(9)
C(5)-C(12)	1.545(10)	C(11)-C(13)	1.514(9)
C(6A)-H(6AB)	1.0000	C(11A)-H(11A)	1.0000
C(6A)-C(7A)	1.540(9)	C(11A)-C(12A)	1.569(9)
C(6)-H(6A)	1.0000	C(11A)-C(13A)	1.525(10)
C(6)-C(7)	1.546(10)	C(12A)-H(12A)	1.0000
C(7)-H(7)	1.0000	C(12)-H(12)	1.0000
C(7)-C(8)	1.555(11)	C(13)-C(14)	1.391(11)
C(7A)-H(7A)	1.0000	C(13)-C(19)	1.390(11)
C(7A)-C(8A)	1.544(10)	C(13A)-C(14A)	1.378(10)
C(8)-H(8)	1.0000	C(13A)-C(19A)	1.389(11)

C(14A)-H(14A)	0.9500	C(2)-O(1)-C(1)	116.1(6)
C(14A)-C(15A)	1.394(10)	C(2A)-O(1A)-C(1A)	116.0(6)
C(14)-H(14)	0.9500	C(4)-O(3)-H(3)	109.5
C(14)-C(15)	1.386(10)	C(4A)-O(3A)-H(3AA)	109.5
C(15)-H(15)	0.9500	C(6A)-O(4A)-C(5A)	112.7(5)
C(15)-C(16)	1.387(10)	C(6)-O(4)-C(5)	113.7(5)
C(15A)-H(15A)	0.9500	C(7A)-O(5A)-H(5AA)	109.5
C(15A)-C(16A)	1.377(11)	C(7)-O(5)-H(5)	109.5
C(16A)-C(18A)	1.383(11)	C(8A)-O(6A)-H(6AA)	109.5
C(16)-C(18)	1.384(11)	C(8)-O(6)-H(6)	109.5
C(17A)-H(17D)	0.9800	C(6A)-O(7A)-C(9A)	107.5(5)
C(17A)-H(17E)	0.9800	C(6)-O(7)-C(9)	108.6(5)
C(17A)-H(17F)	0.9800	C(10)-O(8)-C(11)	116.8(6)
C(17)-H(17A)	0.9800	C(10A)-O(8A)-C(11A)	116.5(6)
C(17)-H(17B)	0.9800	C(16A)-O(9A)-C(17A)	116.5(6)
C(17)-H(17C)	0.9800	C(16)-O(9)-C(17)	117.8(6)
C(18A)-H(18A)	0.9500	C(2)-N(1)-C(3)	117.6(6)
C(18A)-C(19A)	1.383(10)	C(2)-N(1)-C(12)	126.6(6)
C(18)-H(18)	0.9500	C(3)-N(1)-C(12)	114.3(5)
C(18)-C(19)	1.398(10)	C(2A)-N(1A)-C(3A)	119.1(6)
C(19)-H(19)	0.9500	C(2A)-N(1A)-C(12A)	125.4(6)
C(19A)-H(19A)	0.9500	C(3A)-N(1A)-C(12A)	114.2(5)
		O(1A)-C(1A)-H(1AA)	109.5

O(1A)-C(1A)-H(1AB)	109.5	N(1)-C(3)-H(3A)	110.8
O(1A)-C(1A)-H(1AC)	109.5	N(1)-C(3)-H(3B)	110.8
H(1AA)-C(1A)-H(1AB)	109.5	N(1)-C(3)-C(4)	104.5(6)
H(1AA)-C(1A)-H(1AC)	109.5	H(3A)-C(3)-H(3B)	108.9
H(1AB)-C(1A)-H(1AC)	109.5	C(4)-C(3)-H(3A)	110.8
O(1)-C(1)-H(1A)	109.5	C(4)-C(3)-H(3B)	110.8
O(1)-C(1)-H(1B)	109.5	O(3)-C(4)-C(3)	108.1(6)
O(1)-C(1)-H(1C)	109.5	O(3)-C(4)-H(4)	109.9
H(1A)-C(1)-H(1B)	109.5	O(3)-C(4)-C(5)	113.3(6)
H(1A)-C(1)-H(1C)	109.5	C(3)-C(4)-H(4)	109.9
H(1B)-C(1)-H(1C)	109.5	C(3)-C(4)-C(5)	105.4(6)
O(2A)-C(2A)-O(1A)	122.7(6)	C(5)-C(4)-H(4)	109.9
O(2A)-C(2A)-N(1A)	123.8(7)	O(3A)-C(4A)-C(3A)	107.3(6)
N(1A)-C(2A)-O(1A)	113.4(6)	O(3A)-C(4A)-H(4A)	110.7
O(1)-C(2)-N(1)	113.0(6)	O(3A)-C(4A)-C(5A)	112.8(6)
O(2)-C(2)-O(1)	123.8(6)	C(3A)-C(4A)-H(4A)	110.7
O(2)-C(2)-N(1)	123.2(6)	C(5A)-C(4A)-C(3A)	104.4(6)
N(1A)-C(3A)-H(3AB)	111.1	C(5A)-C(4A)-H(4A)	110.7
N(1A)-C(3A)-H(3AC)	111.1	O(4A)-C(5A)-C(4A)	108.8(6)
N(1A)-C(3A)-C(4A)	103.5(6)	O(4A)-C(5A)-H(5AB)	109.4
H(3AB)-C(3A)-H(3AC)	109.0	O(4A)-C(5A)-C(12A)	115.7(5)
C(4A)-C(3A)-H(3AB)	111.1	C(4A)-C(5A)-H(5AB)	109.4
C(4A)-C(3A)-H(3AC)	111.1	C(4A)-C(5A)-C(12A)	104.0(6)

C(12A)-C(5A)-H(5AB)	109.4	C(6)-C(7)-C(8)	104.0(6)
O(4)-C(5)-C(4)	109.4(6)	C(8)-C(7)-H(7)	110.5
O(4)-C(5)-H(5A)	109.1	O(5A)-C(7A)-C(6A)	111.3(5)
O(4)-C(5)-C(12)	114.9(6)	O(5A)-C(7A)-H(7A)	110.4
C(4)-C(5)-H(5A)	109.1	O(5A)-C(7A)-C(8A)	110.0(6)
C(4)-C(5)-C(12)	105.1(6)	C(6A)-C(7A)-H(7A)	110.4
C(12)-C(5)-H(5A)	109.1	C(6A)-C(7A)-C(8A)	104.2(6)
O(4A)-C(6A)-H(6AB)	110.5	C(8A)-C(7A)-H(7A)	110.4
O(4A)-C(6A)-C(7A)	108.3(6)	O(6)-C(8)-C(7)	112.5(6)
O(7A)-C(6A)-O(4A)	110.3(5)	O(6)-C(8)-H(8)	111.3
O(7A)-C(6A)-H(6AB)	110.5	O(6)-C(8)-C(9)	107.9(6)
O(7A)-C(6A)-C(7A)	106.8(6)	C(7)-C(8)-H(8)	111.3
C(7A)-C(6A)-H(6AB)	110.5	C(9)-C(8)-C(7)	102.1(6)
O(4)-C(6)-H(6A)	110.3	C(9)-C(8)-H(8)	111.3
O(4)-C(6)-C(7)	108.3(6)	O(6A)-C(8A)-C(7A)	112.6(6)
O(7)-C(6)-O(4)	110.8(5)	O(6A)-C(8A)-H(8A)	111.0
O(7)-C(6)-H(6A)	110.3	O(6A)-C(8A)-C(9A)	108.9(6)
O(7)-C(6)-C(7)	106.9(5)	C(7A)-C(8A)-H(8A)	111.0
C(7)-C(6)-H(6A)	110.3	C(9A)-C(8A)-C(7A)	102.0(6)
O(5)-C(7)-C(6)	112.1(6)	C(9A)-C(8A)-H(8A)	111.0
O(5)-C(7)-H(7)	110.5	O(7)-C(9)-C(8)	103.4(6)
O(5)-C(7)-C(8)	109.1(6)	O(7)-C(9)-H(9)	110.0
C(6)-C(7)-H(7)	110.5	O(7)-C(9)-C(10)	111.3(6)

C(8)-C(9)-H(9)	110.0	O(8)-C(11)-C(13)	108.0(5)
C(8)-C(9)-C(10)	111.9(6)	C(12)-C(11)-H(11)	108.8
C(10)-C(9)-H(9)	110.0	C(13)-C(11)-H(11)	108.8
O(7A)-C(9A)-C(8A)	103.4(5)	C(13)-C(11)-C(12)	114.5(6)
O(7A)-C(9A)-H(9A)	109.8	O(8A)-C(11A)-H(11A)	109.4
O(7A)-C(9A)-C(10A)	112.9(6)	O(8A)-C(11A)-C(12A)	107.0(6)
C(8A)-C(9A)-H(9A)	109.8	O(8A)-C(11A)-C(13A)	107.9(6)
C(10A)-C(9A)-C(8A)	111.0(7)	C(12A)-C(11A)-H(11A)	109.4
C(10A)-C(9A)-H(9A)	109.8	C(13A)-C(11A)-H(11A)	109.4
O(8)-C(10)-C(9)	112.1(6)	C(13A)-C(11A)-C(12A)	113.7(6)
O(8)-C(10)-H(10A)	109.2	N(1A)-C(12A)-C(5A)	100.6(5)
O(8)-C(10)-H(10B)	109.2	N(1A)-C(12A)-C(11A)	114.9(6)
C(9)-C(10)-H(10A)	109.2	N(1A)-C(12A)-H(12A)	109.4
C(9)-C(10)-H(10B)	109.2	C(5A)-C(12A)-C(11A)	112.9(6)
H(10A)-C(10)-H(10B)	107.9	C(5A)-C(12A)-H(12A)	109.4
O(8A)-C(10A)-C(9A)	111.0(6)	C(11A)-C(12A)-H(12A)	109.4
O(8A)-C(10A)-H(10C)	109.4	N(1)-C(12)-C(5)	100.8(5)
O(8A)-C(10A)-H(10D)	109.4	N(1)-C(12)-C(11)	113.6(5)
C(9A)-C(10A)-H(10C)	109.4	N(1)-C(12)-H(12)	109.5
C(9A)-C(10A)-H(10D)	109.4	C(5)-C(12)-C(11)	113.6(6)
H(10C)-C(10A)-H(10D)	108.0	C(5)-C(12)-H(12)	109.5
O(8)-C(11)-H(11)	108.8	C(11)-C(12)-H(12)	109.5
O(8)-C(11)-C(12)	107.9(5)	C(14)-C(13)-C(11)	120.7(6)

C(19)-C(13)-C(11)	121.4(7)	O(9A)-C(17A)-H(17D)	109.5
C(19)-C(13)-C(14)	117.8(6)	O(9A)-C(17A)-H(17E)	109.5
C(14A)-C(13A)-C(11A)	121.1(7)	O(9A)-C(17A)-H(17F)	109.5
C(14A)-C(13A)-C(19A)	118.4(7)	H(17D)-C(17A)-H(17E)	109.5
C(19A)-C(13A)-C(11A)	120.4(7)	H(17D)-C(17A)-H(17F)	109.5
C(13A)-C(14A)-H(14A)	119.5	H(17E)-C(17A)-H(17F)	109.5
C(13A)-C(14A)-C(15A)	121.0(7)	O(9)-C(17)-H(17A)	109.5
C(15A)-C(14A)-H(14A)	119.5	O(9)-C(17)-H(17B)	109.5
C(13)-C(14)-H(14)	119.6	O(9)-C(17)-H(17C)	109.5
C(15)-C(14)-C(13)	120.8(7)	H(17A)-C(17)-H(17B)	109.5
C(15)-C(14)-H(14)	119.6	H(17A)-C(17)-H(17C)	109.5
C(14)-C(15)-H(15)	119.4	H(17B)-C(17)-H(17C)	109.5
C(14)-C(15)-C(16)	121.1(7)	C(16A)-C(18A)-H(18A)	119.6
C(16)-C(15)-H(15)	119.4	C(16A)-C(18A)-C(19A)	120.8(7)
C(14A)-C(15A)-H(15A)	119.9	C(19A)-C(18A)-H(18A)	119.6
C(16A)-C(15A)-C(14A)	120.2(7)	C(16)-C(18)-H(18)	120.0
C(16A)-C(15A)-H(15A)	119.9	C(16)-C(18)-C(19)	120.1(7)
O(9A)-C(16A)-C(15A)	123.9(7)	C(19)-C(18)-H(18)	120.0
O(9A)-C(16A)-C(18A)	117.1(7)	C(13)-C(19)-C(18)	121.4(7)
C(15A)-C(16A)-C(18A)	119.0(7)	C(13)-C(19)-H(19)	119.3
O(9)-C(16)-C(15)	115.6(7)	C(18)-C(19)-H(19)	119.3
O(9)-C(16)-C(18)	125.7(7)	C(13A)-C(19A)-H(19A)	119.7
C(18)-C(16)-C(15)	118.7(6)	C(18A)-C(19A)-C(13A)	120.6(7)

C(18A)-C(19A)-H(19A) 119.7

Symmetry transformations used to generate equivalent atoms:

Table 4. Anisotropic displacement parameters ($Å^2 x\ 10^3$) for Baran863. The anisotropic displacement factor exponent takes the form: $-2\pi^2[h^2 a^{*2} U^{11} + ... + 2 h k a^* b^* U^{12}]$

	U^{11}	U^{22}	U^{33}	U^{23}	U^{13}	U^{12}
O(1)	31(3)	24(2)	20(3)	2(2)	-1(2)	-2(2)
O(1A)	30(3)	26(2)	19(2)	-1(2)	-3(2)	-6(2)
O(2)	36(3)	19(2)	17(2)	-4(2)	-2(2)	-1(2)
O(2A)	40(3)	19(2)	17(2)	0(2)	5(2)	-5(2)
O(3)	41(3)	31(3)	16(3)	1(2)	0(2)	-15(3)
O(3A)	42(3)	23(2)	18(2)	-4(2)	1(3)	-10(2)
O(4A)	30(3)	20(2)	16(2)	-2(2)	3(2)	3(2)
O(4)	28(3)	19(2)	16(2)	-2(2)	3(2)	2(2)
O(5A)	38(3)	25(2)	20(3)	-4(2)	1(2)	-2(2)
O(5)	34(3)	35(3)	19(2)	10(2)	2(2)	-3(3)
O(6A)	43(3)	28(3)	31(3)	-9(2)	11(3)	-5(3)
O(6)	40(3)	23(3)	29(3)	5(2)	-6(2)	-2(2)
O(7A)	30(3)	20(2)	18(2)	0(2)	-1(2)	-1(2)

O(7)	26(3)	17(2)	19(2)	-3(2)	3(2)	-1(2)
O(8)	35(3)	21(2)	22(3)	4(2)	-5(2)	-4(2)
O(8A)	42(3)	20(2)	19(3)	0(2)	7(2)	-8(2)
O(9A)	38(3)	21(2)	33(3)	-10(2)	2(3)	2(2)
O(9)	32(3)	22(2)	24(3)	7(2)	-2(2)	0(2)
N(1)	28(3)	17(3)	15(3)	-2(2)	3(2)	-1(2)
N(1A)	31(3)	19(3)	15(3)	-2(2)	0(3)	-4(3)
C(1A)	38(4)	29(4)	22(4)	-3(3)	-4(3)	-5(4)
C(1)	41(5)	26(4)	22(4)	5(3)	2(3)	0(3)
C(2A)	37(4)	13(3)	17(3)	-4(3)	1(3)	5(3)
C(2)	35(4)	9(3)	16(3)	-2(3)	1(3)	0(3)
C(3A)	34(4)	20(3)	20(3)	-2(3)	3(3)	-1(3)
C(3)	27(4)	23(3)	24(4)	3(3)	-2(3)	-8(3)
C(4)	26(4)	19(3)	23(4)	-1(3)	4(3)	-3(3)
C(4A)	34(4)	15(3)	20(4)	-4(3)	-2(3)	-5(3)
C(5A)	33(4)	14(3)	15(3)	-1(3)	3(3)	-1(3)
C(5)	33(4)	15(3)	18(3)	0(3)	4(3)	-2(3)
C(6A)	27(4)	14(3)	20(3)	-4(3)	5(3)	-2(3)
C(6)	32(4)	15(3)	20(4)	2(3)	0(3)	-1(3)
C(7)	37(4)	24(3)	11(3)	3(3)	3(3)	3(3)
C(7A)	34(4)	16(3)	16(3)	-2(3)	-1(3)	1(3)
C(8)	34(4)	18(3)	23(4)	2(3)	-1(3)	0(3)
C(8A)	42(5)	12(3)	24(4)	-1(3)	4(3)	-2(3)

C(9)	30(4)	21(3)	19(3)	-1(3)	4(3)	-3(3)
C(9A)	37(4)	15(3)	25(4)	-2(3)	12(3)	-5(3)
C(10)	42(4)	19(3)	20(4)	-1(3)	-1(4)	-2(3)
C(10A)	50(5)	15(3)	17(4)	1(3)	10(3)	-3(3)
C(11)	30(4)	17(3)	22(4)	-1(3)	-2(3)	-3(3)
C(11A)	38(4)	13(3)	22(4)	1(3)	3(3)	-1(3)
C(12A)	30(4)	20(3)	15(3)	-1(3)	2(3)	-5(3)
C(12)	28(4)	16(3)	21(3)	1(3)	1(3)	0(3)
C(13)	28(4)	13(3)	16(3)	-1(3)	-3(3)	0(3)
C(13A)	41(4)	13(3)	18(3)	2(3)	0(3)	-1(3)
C(14A)	33(4)	19(3)	31(4)	-4(3)	5(4)	-3(3)
C(14)	33(4)	16(3)	23(4)	-1(3)	-3(3)	-3(3)
C(15)	32(4)	15(3)	19(3)	1(3)	2(3)	-3(3)
C(15A)	41(5)	18(3)	29(4)	-6(3)	0(4)	-6(3)
C(16A)	41(5)	12(3)	28(4)	-2(3)	3(4)	2(3)
C(16)	35(4)	12(3)	18(3)	2(3)	-2(3)	-3(3)
C(17A)	42(5)	20(4)	30(4)	-10(3)	0(4)	3(3)
C(17)	37(4)	24(4)	33(4)	11(3)	-3(4)	3(3)
C(18A)	34(4)	18(3)	29(4)	-3(3)	3(3)	3(3)
C(18)	24(4)	20(3)	31(4)	1(3)	-3(3)	2(3)
C(19)	35(4)	18(3)	26(4)	3(3)	-2(3)	-7(3)
C(19A)	34(4)	19(3)	28(4)	-4(3)	-4(3)	-2(3)

Table 5. Hydrogen coordinates (x 10^4) and isotropic displacement parameters ($Å^2$x 10^3) for Baran863.

	x	y	z	U(eq)
H(3)	5204	5120	7499	44
H(3AA)	3081	4837	2565	41
H(5AA)	7496	5321	-1061	41
H(5)	910	4688	4142	44
H(6AA)	11736	5627	-735	51
H(6)	-3804	4339	4239	46
H(1AA)	12213	6259	6611	45
H(1AB)	10595	5820	7122	45
H(1AC)	9827	6430	7098	45
H(1A)	-2028	3582	11946	44
H(1B)	-3761	4063	11764	44
H(1C)	-1308	4173	12271	44
H(3AB)	3188	5632	4920	29
H(3AC)	4714	5101	4960	29
H(3A)	5133	4287	9766	29

H(3B)	3833	4846	9884	29
H(4)	4967	4311	8003	27
H(4A)	3176	5662	3119	28
H(5AB)	7558	5152	3062	25
H(5A)	650	4833	7959	26
H(6AB)	8664	5092	1312	25
H(6A)	-518	4855	6175	27
H(7)	1203	3994	5074	29
H(7A)	6682	5875	87	26
H(8)	-1937	3484	4716	30
H(8A)	9575	6438	-301	31
H(9)	-4508	3659	6315	28
H(9A)	12254	6364	1319	31
H(10A)	-2020	2951	6509	32
H(10B)	160	3329	6463	32
H(10C)	9497	7015	1379	33
H(10D)	7490	6587	1422	33
H(11)	1977	3476	7809	28
H(11A)	5825	6490	2820	29
H(12A)	9323	5870	3797	26
H(12)	-1185	4170	8791	26
H(14A)	9684	7250	4254	33
H(14)	-1867	3104	9882	29

H(15)	-1072	2500	11225	27
H(15A)	8924	7830	5652	35
H(17D)	6355	8421	7781	46
H(17E)	7184	8527	6595	46
H(17F)	8245	8047	7269	46
H(17A)	4543	1508	12376	47
H(17B)	5785	2032	11959	47
H(17C)	5007	1582	11137	47
H(18A)	2588	7242	5825	32
H(18)	5387	2380	10230	30
H(19)	4593	2992	8883	32
H(19A)	3343	6665	4435	33

ProQuest Number: 30994491

INFORMATION TO ALL USERS
The quality and completeness of this reproduction is dependent on the quality
and completeness of the copy made available to ProQuest.



Distributed by ProQuest LLC (2024).
Copyright of the Dissertation is held by the Author unless otherwise noted.

This work may be used in accordance with the terms of the Creative Commons license
or other rights statement, as indicated in the copyright statement or in the metadata
associated with this work. Unless otherwise specified in the copyright statement
or the metadata, all rights are reserved by the copyright holder.

This work is protected against unauthorized copying under Title 17,
United States Code and other applicable copyright laws.

Microform Edition where available © ProQuest LLC. No reproduction or digitization
of the Microform Edition is authorized without permission of ProQuest LLC.

ProQuest LLC
789 East Eisenhower Parkway
P.O. Box 1346
Ann Arbor, MI 48106 - 1346 USA